2010-12-13

Braided Collagen Microthreads as a Cell Delivery System in Bioengineered Muscle Regeneration

Jennifer Lynn Makridakis
Worcester Polytechnic Institute

Braided Collagen Microthreads as a Cell Delivery System in Bioengineered Muscle Regeneration

Jennifer Lynn Makridakis

A thesis to be submitted to the faculty of Worcester Polytechnic Institute in partial fulfillment of the requirements for the Degree of Master of Science

Submitted by:

Jennifer Makridakis
Department of Biomedical Engineering

_____

Approved by:

George Pins, PhD
Associate Professor
Department of Biomedical Engineering

_____

Raymond Page, PhD
Assistant Professor
Department of Biology and Biotechnology
Department of Biomedical Engineering
Cellthera, Inc.

_____

Marsha Rolle, PhD
Assistant Professor
Department of Biomedical Engineering

_____

November 2010

Acknowledgements

I would like to thank my advisors, George Pins, Ray Page, Marsha Rolle, and Tanja Dominko, for guiding me throughout the process of working on this thesis. Your patience and willingness to answer questions was appreciated greatly.

Much appreciation to the following individuals whose assistance was vital to the completion of this project:

Deepti Kalluri

Kushal Palkhiwala

Sharon Shaw

Katie Bush

Tracy Gwyther

Jon Grasman

Lucy Vilner

Victoria Huntress

Cellthera, Inc.

Funding for this project was provided from:

DoD – DARPA (Ray Page, Tanja Dominko)

Army (Ray Page, Tanja Dominko)

NIH (EB-005645) (George Pins)

Abstract

Engineered muscle tissue offers a promising solution for the treatment of large muscle defects. Three-dimensional tissue engineered matrices, such as microthreads, can be used to grow new myofibers that will reduce scar formation and integrate easily into native myofibers. We hypothesize that adsorbing growth factors to the surface of braided collagen scaffolds using crosslinking strategies will promote muscle derived fibroblastic cell (MDFC) attachment and growth, which will serve as a platform for delivering cells to large muscle defects for muscle regeneration. To test this hypothesis, self-assembled type I collagen threads were braided and crosslinked using 1-ethyl-3-(3-dimethylaminopropyl) carbodiimide hydrochloride (EDC) with and without heparin and 5 ng/mL, 10 ng/mL, or 50 ng/mL fibroblast growth factor (FGF-2) bound to the surface. Using immunhistochemistry, braided collagen scaffolds showed the presence of FGF-2 on the surface, and braiding the microthreads increased the mechanical properties compared to single threads. To determine the effect of FGF-2 on MDFC attachment, growth, and alignment, scaffolds were seeded with a MDFC cell suspension for 4 hours using a PDMS mold with a sealed 1 mm by 12 mm channel and cultured for 1, 5, or 7 days. After 1 day of culture, the results show a significant increase in cell attachment on braids crosslinked with EDC/NHS with heparin and no significant difference in attachment between the different concentrations of FGF-2 and EDC/NHS crosslinked scaffolds. After 7 days in culture, the MDFCs responded to FGF-2 with a positive linear correlation between growth rate and concentration of FGF-2 on the surface. Additionally, all control scaffolds showed cellular alignment after 7 days, while MDFCs on FGF-2 modified scaffolds showed limited alignment. These results show braided collagen scaffolds crosslinked with EDC/NHS with heparin delivering a controlled quantity of FGF-2 can support MDFC attachment and growth, which may serve as an exciting new approach to facilitate the growth and ultimately the delivery of cells to large defects in muscle regeneration.

Table of Contents

Table of Figures

Table of Tables

Table of Abbreviations

Abbreviations	Meaning
BAM	Bioartificial muscle
BSA	Bovine serum albumin
DMD	Duchenne Muscular Dystrophy
DPBS	Dulbecco's phosphate buffered saline
EDC	1-ethyl-3-(3-dimenthylaminopropyl) carbodiimide hydrochloride
EDC/NHS	1-ethyl-3-(3-dimenthylaminopropyl) carbodiimide hydrochloride with N-hydroxysuccinimide
EGF	Epidermal growth factor
FGF-2	Fibroblast growth factor-2
FGFR	Fibroblast growth factor receptor
GDF-8	Myostatin (also known as growth differentiation factor 8)
HGF	Hepatocyte growth factor
IGF	Insulin-like growth factor
IL-6	Interleukin-6
iPS cells	Induced pluripotent stem cells
LIF	Leukemia inhibitory factor
MDFC	Muscle-derived fibroblastic cell
MES	2-morpholinoethane sulphonic acid
MTM	Maximum tangent modulus
Myf5	Myogenic factor 5
Myf6	Myogenic factor 6
MyoD	Myogenic differentiation factor-1
NHS	N-hydroxysuccinimide
OCT4	Octamer-binding transcription factor 4
Pax3	Paired box gene 3
Pax7	Paired box gene 7
PBS	Phosphate buffered saline
PCL	Poly(ε-caprolactone)
PDMS	polydimethylsiloxane
PEG	Polyethylene glycol
PGA	Polyglycolic acid
PLAGA	Polylactic-co-glycolic acid
PLL/HA	Poly(L-lysine)/hyaluronan
PLLA	Poly-L-lactic acid
rhGH	Recombinant human growth hormone
RICE	Rest, ice, compression, and elevation
SAF	Strain at failure
SOX2	(Sex determining region Y)-box 2
TGF-β	Transforming growth factor-β
UTS	Ultimate tensile strength
VEGF	Vascular endothelial growth factor
ε	Tensile strain
σ	Tensile stress

Chapter 1: Introduction

Skeletal muscle, which makes up nearly half the tissue in the human body, is composed of highly vascularized and innervated bundles of myofibers, which are responsible for the contraction and movement of the body.[1-4] When skeletal muscle is injured by trauma, it has the ability to self-regenerate, which occurs in four wound healing phases, degeneration, inflammation, tissue formation, and tissue remodeling.[1] At the backbone of regeneration are satellite cells, which are undifferentiated progenitor cells located beneath the basal lamina of the myofibers. They are activated from their quiescent state during the tissue formation phase after the onset of an injury to proliferate, self-renew, differentiate into myoblasts, or muscle precursor cells, and fuse into new myofibers.[3,5] Research has found that the controlled expression of certain trophic factors, such as the families of fibroblast growth factors (FGFs), transforming growth factors-β (TGFs-β), insulin-like growth factors (IGFs), hepatocyte growth factor (HGF), and interleukin-6 (IL-6), regulate the activation, proliferation, and differentiation of satellite cells as well as the initiation of vascularization and reinnervation.[1] During tissue remodeling, fibrosis within the defect area causes the formation of scar tissue due to an excessive amount of type I collagen present.[6] Muscle defects caused by trauma are classified as ranging from first-degree defects, defined as minimal myofiber damage with slight swelling, to third-degree defects, defined as a defect spanning the entire depth of the muscle. During the regeneration of minor injuries, capillaries and myofibers are able to regenerate with limited scar tissue formation allowing for almost complete tissue regeneration. However, in full thickness defects, the increased scar formation and lack of satellite cell availability limits the regeneration and revascularization of the skeletal muscle resulting in the loss of some or all of the muscle function.[7]

Skeletal muscle injuries are caused by a variety of mechanisms, including varying degrees of direct trauma, indirect causes, and genetic diseases.[2] Injuries caused by direct trauma, like contusions or lacerations, occur predominately in athletes and soldiers in combat.[6,8-13] The major concern with substantial muscle loss related to large muscle defects is that it causes deformities, persistent muscle weakness, and loss of function. Skeletal muscle degradation associated with innate genetic diseases causes the muscles eventually to become completely atrophied leading to extensive long-term care and death of the afflicted.[2,6,14-16] Clinically, first and second-degree muscle defects are treated using a combination of rest, ice, compression, and elevation, but this method does not eliminate the formation of scar tissue and is sometimes associated with injury reoccurrence.[6,7,17,18] Plastic and reconstructive surgeries, such as the transplantation of autologous muscle grafts or myogenic cell injections, are performed as treatments for third degree injuries to bridge the gap and help initiate muscle regeneration.[18] Limitations associated with surgical procedures are scar formation, limited cell incorporation, weakness, morbidity, and mortality.[19,20]

In order to overcome limitations associated with the sub-optimal clinical treatments, research is being performed on implanting biomaterials into muscle defects. Three dimensional tissue engineered muscle needs to be biocompatible, biodegradable, biologically and mechanically stable, and induce host cell migration, regeneration, and revascularization.[1,8,16] *In vitro* and *in vivo* studies using synthetic materials and natural polymers, like polyglycolic acid (PGA), poly(ε-caprolactone) (PCL), hyaluronic acid, alginate, fibrin, and acellular matrix, have shown to support myoblast migration, differentiation, fusion, and in some cases promote revascularization.[21-24] However, due to limitations in scaffold design including biodegradability, which affects myofiber maturity, density, and population homogeneity; and stiffness, which

affects myofiber length and the force generated, these biomaterials still do not meet the conditions needed for clinical studies.[8]

Another biomaterial investigated for muscle regeneration is collagen since it possesses strong mechanical properties, suitable cell-matrix binding efficiencies, weak immunogenic responses, and high biodegradability.[25-29] Another advantage of using collagen is that it can be manipulated into different structures, such as gels, microthreads, and porous sponges, making it a good candidate for many different tissue-engineering applications. By incorporating chemical, mechanical, or extracellular matrix modifications on the surface of collagen scaffolds, myoblasts can be differentiated to form mature myofibers.[30-34] Cornwell et al. has shown that collagen microthreads seeded with fibroblast cells promoted cell migration and alignment, which suggests the potential for microthreads to be used for muscle regeneration.[35,36] In addition, by manipulating the structure of microthreads through bundling, twisting, weaving, or braiding, the scaffolds shows structurally similar properties compared to native myofibers, as well as increased surface area and mechanical strength.[37] By chemical crosslinking, the biostability and mechanical strength of the scaffold can be increased, and it promotes cell migration, viability, differentiation, and myofiber formation.[28,38-40] Another way to optimize collagen scaffolds for muscle regeneration is by binding heparin and FGF-2 to the surface. Studies show that in the presence of FGF-2, cellular proliferation and migration increase, and by binding it to heparin, FGF-2 is stabilized and protected from denaturation and proteolytic degradation.[41-43]

In addition to the studies of different biomaterials for muscle regeneration, the benefits of using certain cell types, such as myoblasts and satellite cells, has been investigated, which showed that myoblasts and satellite cells remain viable and active on three dimensional scaffolds.[44,45] The limitations associated with using these cells clinically are loss of myogenicity,

low cell survival and incorporation, and they are not self renewing satellite cells.[11] A potential way to overcome these limitations is by using fibroblast cells that have been programmed to express a stem cell phenotype. Research shows that exposing fibroblasts to FGF-2 in a low oxygen environment induces them to express stem cell related genes, suggesting this treatment may lead to cell dedifferentiation.[46]

In summary, we hypothesize that chemically conjugating heparin to the surface of braided collagen scaffolds will serve as an effective method to load heparan sulfate binding growth factors, such as FGF-2, to promote cell attachment and growth. This technology could serve as a platform for delivering cells to promote regeneration of large muscle defects.

Chapter 2: Background

This project investigates a novel scaffold for muscle cell attachment and growth that could be used as a method for delivering muscle derived fibroblastic cells to a large muscle defect related to trauma or muscle diseases in the future. The development of a novel cell delivery system for muscle regeneration requires an understanding of skeletal muscle anatomy, specifically how it responds to injuries naturally. During the preliminary stages of scaffold development, an understanding of how the surface of collagen microthreads can be altered chemically to control the cells delivered and the interactions it has with the native muscle tissue also needs to be examined. In addition, this section will summarize the current approaches and limitations in treating large muscle defects, both surgically and with tissue engineered methods.

2.1. Skeletal Muscle

Skeletal muscle is the most abundant tissue in the human body, accounting for nearly 45% of the total body mass.[1,4] Skeletal muscles are highly vascularized and innervated bundles of myofibers attached to the skeleton allowing for joint movement.[2,3] A single myofiber, which ranges from 20 μm to 100 μm in diameter, is composed of fused myoblasts, which create many myofibrils.[7,17] A myofibril is derived from repeating sarcomeres, which are made of contractile proteins of thin actin filaments and thick myosin filaments (*Figure 1*).[1] Surrounding each myofiber is a plasma membrane called the sarcolemma and a basement membrane called the basal lamina, consisting of an inner layer, an intermediate layer, and an outer lamina densa.[3,4] Located between the sarcolemma and the basal lamina are the muscle mononuclear undifferentiated progenitor cells called satellite cells, which are quiescent in mature healthy myofibers. Satellite cells make up 2-7% of all myofiber related nuclei.[47] They are the key to the

self-regeneration of skeletal muscles when they are activated, proliferate, self-renew, and differentiate into myoblasts.[3,4,12] This process will be described in detail in the following section.

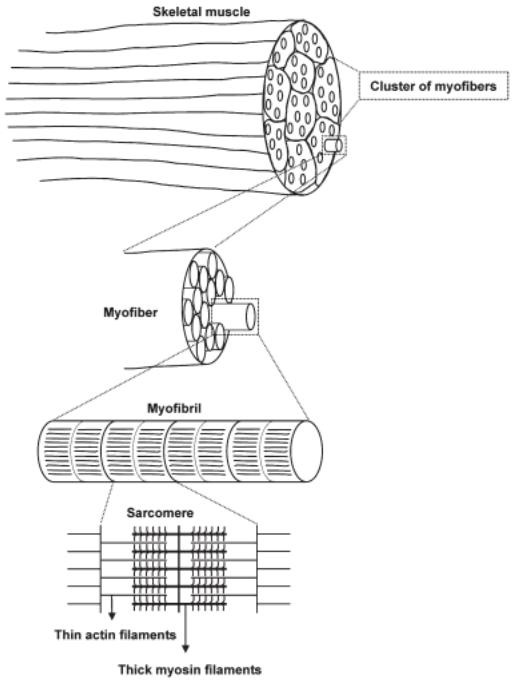

Figure 1: Structure of the skeletal muscle

A single myofiber is composed of fused myoblasts, which create many myofibrils. A myofibril is derived from repeating sarcomeres, which are made of contractile proteins of thin actin filaments and thick myosin filaments (Figure adapted from[1]).

Nerves that are in contact with the skeletal muscles are responsible for the functional control of contraction and movement of myofibers.[2] A motor unit consists of a single nerve axon and all the myofibers it connects to, which ranges from ten to up to a thousand myofibers depending on the type of movement the muscle must perform.[4] The three types of myofibers that make up the human skeletal muscles are classified by their contractile properties. Type 1 myofibers are slow twitch and fatigue resistant and type 2A and 2B myofibers are fast twitch and moderately fatigue resistant or not fatigue resistant respectively.[1,4,48] The arrangement of the different types of myofibers in the muscle is determined by its function. Muscle contraction is initiated by the release of acetylcholine from the presynaptic axons, which binds to the myofibers

and depolarizes the myoblasts. This results in an action potential across the length of the myofiber resulting in contraction.[4,48] Subsequently, the myosin and actin filaments bind and contract due to the release of intracellular calcium. Muscle relaxation occurs when acetylcholine deactivates.[4,48]

2.1.2. Native Skeletal Muscle Regeneration

Following traumatic injury, the wound healing process for skeletal muscle occurs in four phases, degeneration, inflammation, tissue formation, and tissue remodeling resulting in fibrosis of the tissue.[1,6,7,18,49] Degeneration and inflammation occur immediately following the injury and continue for up to two weeks. Tissue formation begins about one week after the injury occurs and peaks two weeks after onset. Tissue remodeling is initiated at week two and scar tissue can continue to form for up to a month (*Figure 2*).[4,6,13,50]

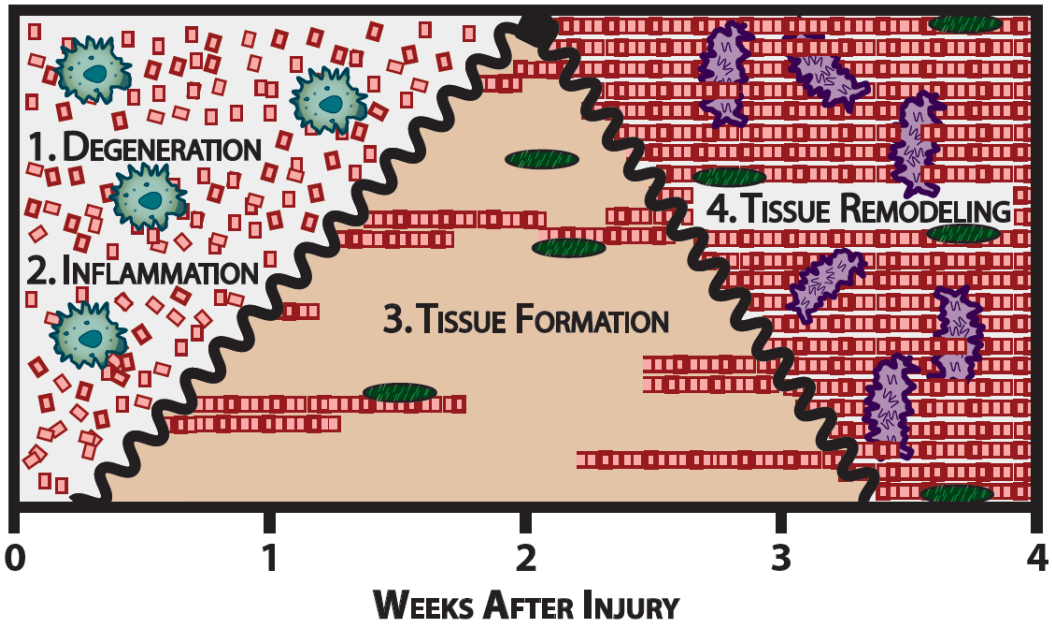

Figure 2: Four phases of wound healing

Following traumatic injury, the wound healing process for skeletal muscle occurs in four phases, degeneration, inflammation, tissue formation, and tissue remodeling. Wound healing can last for up to 4 weeks after the injury occurs.

When the muscle is injured by trauma, the first stage of wound healing begins with the sarcolemma releasing extracellular calcium into the damaged site and proteolysis of the damaged tissue.[13] The degeneration of the injured location is contained within a contraction band surrounding the defect.[51] Blood vessels are injured at the site of the defect causing the release of chemotactic factors to activate the inflammatory cells such as neutrophils and later macrophages.[1,6,52] Macrophages, which phagocytose or digest muscle debris, amplify the inflammatory response within the injured site.[7,51,52] In addition, macrophages enhance the inflammatory response and support satellite cell survival, proliferation, and differentiation through the release of growth factors.[1,2,52] The extent to which the damaged area revascularizes is dependent on the extent of the injury with limited revascularization in larger defects due to increased scar formation.[51] As new capillaries form and migrate to the center of the defect, they provide the oxygen needed for aerobic metabolism, which is needed for myofiber formation.[18]

Once the inflammatory response phase has ceased, tissue formation begins to occur. At the backbone of skeletal muscle regeneration are satellite cells, which are activated by several trophic factors triggered during self-regeneration, such as FGFs, TGFs-β, IGFs, HGF, and IL-6.[1,2,17,53] The specific role each of these growth factors play in the regeneration process will be described in detail in the following section. In healthy skeletal muscle, satellite cells, also known as the skeletal muscle stem cell, remain in a quiescent state between the basal lamina and the sarcolemma *(Figure 3A*).[11,53,54] Typically, there are two different types of satellite cells present in skeletal muscle, committed satellite cells, which are programmed to differentiate and proliferate into myoblasts, and self renewing satellite cells, which divide before differentiation in order to renew the population.[18,54-56] When a defect occurs, satellite cells expressing the paired box gene 7 (Pax7) protein are activated and migrate along the damaged myofiber to the defect

area.[1,2,53,57] Although less common, satellite cells can migrate from adjacent myofibers if the connective tissue separating the myofibers is not damaged. After the up-regulation of the myogenic differentiation factors, myogenic differentiation factor-1 (MyoD) and myogenic factor 5 (Myf5), satellite cells begin to proliferate and differentiate into myoblasts. Adult myoblasts are the mononuclear myogenic precursor cells to myofibers.[2,5] The activated satellite cells become mature myoblasts with the decreased expression of paired box gene 3 (Pax3) and Pax7 and increased expression of myogenin and myogenic factor 6 (Myf6) (*Figure 3B*).[1,2,50,58] In the next stage of regeneration, the newly differentiated myoblasts begin to fuse to one another or to the existing damaged myofibers to create new myofibers (*Figure 3C*).[6] The process is complete when the newly formed myofibers thicken and the nuclei move from the center of the myofiber to the periphery (*Figure 3D*).[53]

Scar tissue can form within the damaged area due to fibrosis during tissue remodeling. This is caused by an influx of TGF-β1 in the defect, which induces myogenic cells to differentiate into myofibroblasts that produces a surplus of type I collagen.[1,6] The collagen synthesized by fibroblast cells is important during healing as it is repairs myofiber-tendon junctions and the muscle tensile strength.[59] The connective tissue formed after muscle damage produces contractile forces, which makes it possible for the injury to maintain some limited mobility during the healing process.[18] In contrast to minor injuries, in large muscle defects the scar tissue formation can be extensive, limiting the regeneration of the skeletal muscle resulting in loss of some or all of the muscle function.[7]

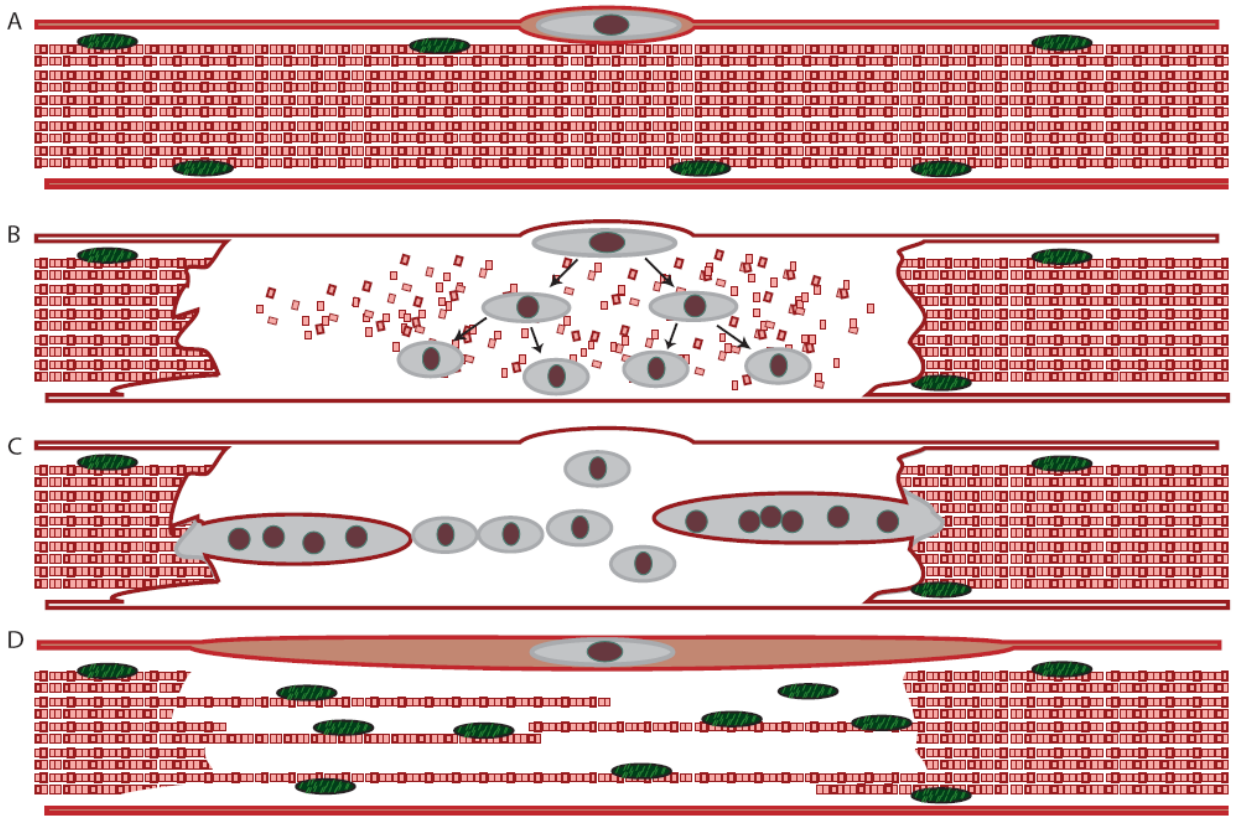

Figure 3: Native skeletal muscle regeneration

Once the inflammatory response phase has ceased, tissue formation begins to occur. In healthy skeletal muscle, satellite cells remain in a quiescent state between the basal lamina and the sarcolemma (A). When a defect occurs, satellite cells are activated and migrate along the damaged myofiber to the defect area. They begin to proliferate and differentiate into mature myoblast cells (B). Next, the newly differentiated myoblast begin to fuse to one another or to the existing damaged myofibers to create new myotubes (C). The process is complete when the newly formed myofibers thicken and the nuclei move from the center of the myofiber to the periphery (D).

2.1.2.1. Growth Factors

An important aspect in native muscle regeneration is to investigate the role of growth factors in skeletal muscle wound healing. Research has shown that trophic factors, which have the greatest influence over the regeneration process, are within the families of FGF, TGF-β, HGF, IGF, and IL-6.[4,53,60] *In vivo* and *in vitro* studies found that the controlled regulation of these factors within the muscle defect greatly affects the activation, proliferation, and differentiation of satellite cells, as well as revascularization. During the initial stages of skeletal muscle regeneration, HGF is upregulated in proportion to the size of the defect and plays a vital

role in the regulation of satellite cells.[2,13] At the point when the injury occurs, HGF increases, inducing satellite cells out of the quiescent state.[12,58,60] Further, studies found that HGF acts directly on the satellite cells to promote both proliferation and differentiation at the wound site.[2,4,60,61] Once the satellite cells have differentiated into myoblasts and begun to fuse to form new myofibers, the amount of HGF present in the defect decreases.[60]

In addition to HGF playing a vital role in the regulation of satellite cells, factors in the FGF family activate proliferation, differentiation, and revascularization during wound healing.[4,62] Studies using mice with a knockout of FGF-6, which is upregulated during muscle regeneration, have shown a decrease in new myofiber formation with increased scar tissue.[12,51,60] In contrast, some studies showed no difference in the regeneration process with the deletion of FGF-6, suggesting a different FGF isoform may induce regeneration in a similar manner.[2] The FGFs found in the basal lamina surrounding myotubes, specifically FGF-2, influences both proliferation and fusion of newly differentiated myoblasts.[49] The FGF receptors (FGFRs) have an effect on the activation and regulation of satellite cells.[62] Specifically, FGFR-1 increases drastically during the beginning stages of tissue formation, and it has been found during *in vitro* studies that its expression increases myoblast proliferation and decreases differentiation.[2] The FGFs play a greater role in the regulation of revascularization of the defect area by stimulating angiogenesis.[2]

The members of the TGF-β family, TGF-β1, TGF-β2, and TGF-β3, are involved in a variety of aspects of the muscle regeneration process including myoblast fusion, inflammatory responses, and motor neuron survival.[61] An upregulation of TGF-β1 is present during muscle remodeling, which has been shown to induce fibrosis.[6,12,50,51] Studies suggest that myostatin (GDF-8), which has been detected in both satellite cells and myoblasts, regulates the number of

myofibers formed and the myoblast density within each by inhibiting satellite cell proliferation.[2] During degeneration, the damaged muscle fibers have increased levels of GDF-8 and decreased satellite cell activity, while during the early stages of tissue formation, GDF-8 is reduced with the onset of satellite cell differentiation and proliferation. These studies suggest GDF-8 blocks satellite cell activation during degeneration in order to limit the number of regenerated myofibers.[2,50]

During tissue formation, the ligands in the IGF family, IGF-I and IGF-II, are upregulated stimulating proliferation, differentiation, and fusion of myoblasts.[60,61] Studies involving the addition of increased levels of IGF-I to satellite cells during regeneration leads to dense myofiber formation, proving further IGFs play a role in the regulation of myoblasts.[49,51,63] Studies using mice found IGF to be involved in inflammatory regulation and limiting the amount of scar tissue formed within the wound.[50,60,64] In addition to promoting myoblast growth, IGFs may contribute to the regeneration process by encouraging cell survival and reinnervation.[12,13,64] Lastly, members of the IL-6 family of cytokines, IL-6 and leukemia inhibitory factor (LIF), are present during the phases of degeneration, inflammation, and tissue formation.[6,58] Immediately following the onset of the injury, IL-6 stimulates the degeneration of the injured myofibers.[2] In addition, it controls the synchronization of satellite cell proliferation and induces apoptosis of macrophages.[60] The LIF influence myoblast proliferation during the tissue formation phase. Studies also suggest LIF is present within the defect prior to inflammation.[58]

2.2. Motivation for Tissue Engineered Skeletal Muscle Regeneration

Skeletal muscle injuries can occur from an array of mechanisms, in the form of direct trauma, indirect causes, and genetic diseases.[2,4,8,10,14,16,34,65,66] Skeletal muscle injuries resulting from direct trauma, as from excessive exercise, contusions, strain, or lacerations, are classified

clinically as either first, second, or third degree injuries.[2,6,8,10-13] First-degree injuries signify minimal myofiber damage with slight swelling, which results in little or no loss of skeletal muscle function.[17,18] Second-degree injuries represent a defect with moderate myofiber damage resulting in restricted skeletal muscle contraction due to scar tissue formation.[17,18] Lastly, a third-degree injury results in the greatest loss of function and extensive scar formation due to a severe injury spanning the entire depth of the muscle.[17,18] Skeletal muscle injuries occurring during sport activities, which result from shearing of both the myofiber and the connective tissue, account for approximately 35-55% of all sports injuries. These injuries result in billions of dollars in health care expenses to repair them.[6,7,10,17,49,67]

Besides sports related injuries, skeletal muscle loss is a substantial concern during combat. Military injuries resulting in muscle loss can cause acute cosmetic deformities, chronic muscle weakness, and devastating loss of function.[9] On the battlefield, extremity injuries account for 63% of the soldiers diagnosed and 69% of the disabled veterans.[68] Although not all extremity injuries are caused by large muscle defects, it is not uncommon. In addition, skeletal muscle injuries occur due to indirect causes, such with ischemia and neurological disorders, which is caused by exercise-induced or traumatic compartment syndromes stemming from direct trauma or over-exertion.[2,4,6,10,11,13,16,50] In severe injuries, the slow recovery process can be accompanied with intense pain, muscle atrophy, and risk of a recurrent injury.[11,16]

With innate genetic diseases, such as muscular dystrophies, inflammatory myopathies, congenital myopathies, and spinal muscular atrophy, the myofibers eventually become inert due to an increase in degeneration of the fibers.[2,6,14-16,20] One in every 3,500 males is diagnosed with Duchenne Muscular Dystrophy (DMD) each year, which causes striated muscles to weaken due to the absence of the structurally stabilizing protein, dystrophin.[15,69] Males afflicted with this

disease have decreased mobility over time eventually leading to confinement to a wheelchair at 8-10 years old and a life expectancy between 20 and 30 years after suffering respiratory or cardiac failure.[69] In 2000, due to the long-term care required, it cost an estimated 254 billion dollars to treat the symptoms of musculoskeletal diseases in the United States.[70,71] Since mobility and function cannot be restored fully in skeletal muscle with extreme trauma due to limited satellite cell availability in large defects and scar formation, there is a need for alternative methods of regeneration.[65,70]

2.2.1. Clinical Treatment for Large Muscle Defects

Currently, clinical treatment of muscle defects depends on the severity of the injury, but due to scar formation, loss of mobility, and length of recovery period, these methods remain sub-optimal.[6] When skeletal muscle injury occurs, the first step in treatment is by resting the wound with a combination of ice, compression, and elevation, or RICE, which limits pain, inflammation, and blood loss.[6,7,17,18,72] Immediately following the injury, studies suggest the wound needs to be mobilized to ensure maximal vascularization and regeneration, but the disadvantages associated with this practice are greater scar tissue formation as well as a higher probability of injury reoccurrence.[7,17,18,72] Although immobilization has been shown to limit the negative effects of muscle activity, if this process is performed after the first few days of the initial injury, it can cause atrophy of the healthy muscle.[7,17,18,72] Other treatments aid in the natural muscle regenerative process, including heat, physical therapy exercises, and anti-inflammatory drugs, but none of the methods fully repair the skeletal muscle to its pre-injury state due to the formation of scar tissue.[6,7,17,18]

Typically, operative procedures are performed only when all other options have been considered, but third-degree muscle injury, or full thickness defect, cannot regenerate itself

without surgical intervention.[73] In full thickness defects where the damaged area leaves a gap in the myofibers, surgery can be used to aid in the bridging of the gap and help initiate reinnervation of the truncated myofiber ends.[7,17,18,65] The success of these surgeries is extremely limited. Although it limits scar tissue formation, it does not eliminate it.[8,19,65] Through plastic and reconstructive surgery, surgeons transplant local and distant autologous muscle grafts into the defect location. Using muscular flaps is not ideal treatment with limited success due to limited donor site availability, and after the surgery, it has a high risk of donor site morbidity and mortality.[8,9,19,20] When successful, the muscle flaps only work to restore the muscle coverage in the gap created by the injury, but does not restore the strength.[9,20,73] Clinical studies using myogenic cell injections, such as with myoblast or satellite cells, resulted in rapid cell death, rejection, and limited cell incorporation, with less than 5% integration into healthy myofibers after 48 hours.[8,74,75] In addition, transplanting prosthetic patches made of Teflon™ or Marlex™ has been used to repair muscle defects, but this has the risk of a negative foreign body response.[73,76]

2.3. Biomaterials for Skeletal Muscle Regeneration

In order to overcome the limitations involved in the clinical treatment of skeletal muscle injuries, the use of synthetic and natural biomaterials has been investigated to decrease the recovery period and scar tissue formation during muscle regeneration.[1] When considering the appropriate biomaterial for scaffold implantation, a number of conditions need to be considered to meet the criteria for functional tissue engineered skeletal muscle. Primarily, the material needs to be biocompatible and biodegradable in order to integrate into the skeletal native muscle without rejection, and to stimulate native tissue ingrowth, which eventually will replace the scaffold in the wound.[1,8,16,21,77] Using a three-dimensional matrix for implantation, a large

number of cells can be transplanted in aligned myotubes, which gives a greater probability to restore function in the damaged area.[65,78] In addition, the three-dimensional matrix should induce satellite cell migration, proliferation, and differentiation as well as fusion and alignment with host myofibers.[1,16,79] The materials can be manipulated using crosslinking to control the rate of biodegradability, which can be used to ensure the fully regenerated muscle only contains natural muscle tissue.[1,16,65] In addition, the scaffold needs to allow for the tissue to regenerate into a three dimensional matrix without losing the mechanical stability of the newly formed tissue.[1,8,21,23] In order to ensure the healthy skeletal muscle will bind and grow into the biomaterial, the material needs to have a high affinity for the myotube surface.[16,21] In large muscle defects, scar tissue formation early in the regeneration process prevents ample revascularization of the new tissue, so the biomaterial implant needs to be porous to promote the flow of blood, nutrient exchange, cell migration, and new vessel formation thorough the scaffold.[1,21,66,77,78] Finally, the ideal material will not provoke a cytotoxic response, which includes not releasing toxins into the muscle.[16,21]

2.3.1. Current Methods and Limitations

Researchers have investigated the effects of using scaffolds made of synthetic and natural biomaterials to induce muscle regeneration. Through *in vitro* and *in vivo* studies, biomaterials were manipulated into three-dimensional matrices or gel solutions to seed with different cell types and to determine the optimal environment to promote muscle regeneration.[80] Engineered muscle can be created from both synthetic materials, such as PGA and PCL as well as natural polymers, such as hyaluronic acid, alginate, fibrin, acellular matrices, and collagen.[21-24] In addition to the different biomaterials being considered to optimize muscle regeneration, much research has emphasized the effect of how the implantation of different cell types, like

myoblasts, satellite cells, and fibroblasts, on stimulating native muscle growth.[77,81,82] Currently, bioengineered scaffolds do not meet the criteria needed for human clinical studies since they do not match native muscle tissue in length, diameter, maturity, density, or mechanical properties.[8] Table 1 summarizes the benefits and limitations of each of these methods.

Three-dimensional scaffolds fabricated out of PGA have been studied in tissue-engineered muscle since the geometry of the polymer can be altered to contain varying pore sizes, which allows nutrition, cells, and blood to flow through the scaffold.[20,65,83] This material is also beneficial due to its stiffness and degradation properties, which can be controlled and programmed to degrade using hydrolysis.[65,77] Six weeks after implantation into the peritoneal cavity, Saxena et al. provided evidence that implanting a non-woven PGA mesh seeded with myoblasts initially supported myofiber attachment, formation, and survival through diffusion of nutrients through the porous mesh. Implanted myoblasts show the ability to fuse with the existing myofiber ends as they regenerate to bridge the gap in the damaged muscle quicker.[20] However, once the PGA mesh has degraded, the engineered muscle needs vascularization to remain viable, integrate into the native muscle, and form a full thickness myofiber.[20,65] The studies performed by Kamelger et al. indicated that by providing the scaffold with a highly vascularized environment, myoblasts were able to form myotubes and remain viable outside the native skeletal muscle.[21] This suggests the possibility of implanting a fully vascularized engineered skeletal muscle into large muscle defect to promote muscle regeneration.

Polyesters, such as PCL, has been used in tissue engineering because their properties, including biocompatibility, biodegradability, and elasticity, can be controlled in order to provide the appropriate structure for myoblast growth and contraction.[23,24] The disadvantage of using PCL alone to regenerate skeletal muscle is that the material does not promote cellular adhesion

or myoblast fusion.[84] In order to mimic the extracellular matrix, biocompatible polymer nanofibers have been electrospun into controlled patterns to promote alignment and cell growth.[85] Researchers have investigated how to create composite polymers using gelatin or collagen with PCL to promote muscle regeneration.[24,84,86] Gravity spun nanofibers composed of PCL and gelatin seeded with myoblasts promoted attachment, proliferation, differentiation, and myoblast fusion into myofibers.[84,86] When PCL is electrospun with type I collagen into a mesh scaffold and seeded with human myoblasts, the collagen creates a hydrophilic surface allowing the myoblasts to adhere, proliferate, fuse into myofibers, and align with the nanofibers of the scaffold.[24]

Other scaffolds used to regenerate muscle are constructed out of hyaluronic acid, in the form of films and hydrogels. The advantage of using hyaluronan, which is a glycosaminoglycan extracted from rooster combs, in tissue engineering is that it is combined easily with other biomaterials to increase the thickness using layers. The surface chemistry of the scaffold can be altered to increase the seeding efficiency, and the mechanical properties can be controlled depending on the application.[87] In addition, the advantages of hyaluronan as a tissue engineering scaffold are that it is non-toxic, biocompatible, and biodegradable.[88] Ren et al. seeded rat myoblasts onto a polyelectrolyte multilayer film consisting of poly(L-lysine)/hyaluronan (PLL/HA), and the results showed that cell attachment, proliferation, and spreading increased with increased stiffness.[87,89] On stiff films, the myoblasts differentiated and fused into long, thin, striated myotubes that detached due to the contractile properties of skeletal muscles, but myoblasts on soft films detach rapidly fusing into short and thick myotubes due to weak adhesion between the cells and the scaffold.[87] Implanting a hyaluronic acid hydrogel seeded with rat myoblasts into a vascularized capsule within a rat model resulted in honeycombed

structures surrounded by multinucleated myotubes. Although none of the seeded myoblasts migrated out of the wound site, the scaffold induced an inflammatory response, which could increase scar formation.[21]

Alginate, which is derived from seaweed, has been used in tissue engineering due to its structural and chemical stability, biocompatibility, and ability to support cell survival in culture by controlling the porosity of the scaffold.[70,90,91] Alginate hydrogels can be chemically altered using crosslinking to promote cellular adhesion and control the degradation *in vivo*, which are beneficial in engineering muscle tissue.[70,92] *In vitro* studies using porous alginate hydrogels, suggested that modifying the surface with adhesion proteins enhanced myoblast attachment, proliferation, and fusion into mature myofibers.[70,93] Boontheekul et al. found that with increased stiffness and increased degradation of the hydrogel, the adhesion, proliferation, and differentiation of the myoblasts increased, but the hydrogels did not support migration and spreading.[92,93] When implanted subcutaneously into a vascularized capsule in a rat model, the alginate solution allowed for myotube fusion adjacent to the capsule wall, but alginate hydrogel elicited an inflammatory response from the surrounding native tissue.[21]

The use of fibrin gels has been beneficial in skeletal muscle tissue engineering since cells readily proliferate and migrate while producing proteases and extracellular matrix proteins that degrade and remodel the scaffold, respectively.[94] The attributes of fibrin, which is a mixture of fibrinogen and thrombin that are advantageous in tissue engineering, are it is biocompatible, biodegradable, non-toxic, and not immunogenic.[16,19,95-97] Three dimensional fibrin matrices bind to native muscle tissue making it an ideal candidate for bridging the gap in large muscle defects.[19,95] In addition, growth factors which facilitate muscle repair, such as FGF-2 or IGF-I, can be mixed into the fibrin solution, which allows it to bind to the scaffold matrix and aid in the

regeneration process.[94] Huang et al. improved their previous research by seeding myoblasts onto a fibrin gel instead of fibroblasts and laminin to create their cylindrical muscle constructs, or myooids, which decreased the maturation time from thirty days to ten days.[94,98] The fibrin myooids produced similar contractile and force production properties as their previous studies, but the constructs remained 10 times in smaller cross sectional area than adult human myotubes meaning it does not meet requirements for clinical use.[94,98] Using mechanical stimulus and patterned models, studies have found that myoblasts can be conditioned to align and proliferate in linear patterns mimicking native skeletal muscle tissue.[96-98]

In vivo studies showed that fibrin gel scaffolds completely degrades within 3 to 4 weeks leaving behind myoblasts, which have fused to form myofibers and are partially attached to the native tissue.[19,94,95] Fibrin gel injections filled the entire defect volume without eliciting a foreign body reaction, but the scaffolds were fragile and difficult to keep sterile.[19,95] In an effort to innervate the tissue-engineered muscle, Dhawan et al. mixed satellite cells with a fibrin gel and wrapped it around a truncated femoral nerve. The results of this study showed that after 4 weeks, the femoral pedicle had completely incorporated into the fibrin scaffold with the differentiated satellite cells showing characteristic skeletal muscle striations as well as capillary formation.[80,99] Although this method increased the contractile forces, there was no strong evidence of neuromuscular junctions present.[80]

In an attempt to avoid adverse foreign body responses when implanting a biomaterial into a defect, research has been performed to develop an acellular scaffold, which is created through a detergent-enzymatic treatment of mammalian muscle, for muscle regeneration.[77,100,101] An advantage of using an acellular scaffold is it contains residual neural pathways that could initiate innervation. The existing extracellular matrix containing proteins may help revascularize the

scaffold, maintain the shape and structure, and help integrate the scaffold into the defect environment.[16,100] The results of experiments performed by attaching myoblasts to acellular matrices showed the ability to support myoblast proliferation, differentiation, and fusion of myoblasts as well as myofiber mechanical properties.[100,101] However, absent of vascularization or a nerve supply, the scaffolds lacked neuromuscular interfaces and capillary formation, which had been found to be imperative in the muscle regeneration process.[100,101] Seeding with satellite cells instead of myoblasts, research has demonstrated a high muscle construct survival rate, and with the addition of neural and fibroblast cells, the constructs had muscle-like alignment, excitability, contractility, and neuromuscular junction formation.[102-104] These scaffolds are still not optimal for clinical use since they do not express mature adult skeletal muscle characteristics, like any myosin heavy chain formation, and produce only 1% of the isometric titanic force created by human myoblasts.[102,103] After implantation of the acellular muscle constructs seeded with myoblasts into rat defects, the results demonstrated that in developing muscle, the scaffolds were able to initiate the formation of aligned skeletal muscle fibers, neovascularization, and innervations after 9 months.[73,101] However, when implanted into adult rat muscle, the engineered muscle experienced a loss of contractile muscle fibers suggesting the regenerative capacity of the native muscle is not as successful when the myotubes are mature.[101] Another disadvantage of using an acellular matrix for muscle regeneration is they are fragile, making them a non-optimal choice clinically.[77]

Biomaterial	Research Method	Cell Type	Functional Outcome	Limitations
PGA[20,21,65]	*In vivo*	Rat myoblast	• formation of multinucleated myotubes • no implanted cell migration • supportive capillary network growth	• vascularization not sufficient enough for thick tissue formation
PCL[24,84,86]	*In vitro*	Human and mouse myoblast	• Gelatin increases adhesion, proliferation, fusion, and differentiation • Collagen increases adhesion, fusion, alignment, and proliferation	• PCL alone does not form myofibers
PLL/HA[87,89]	*In vitro*	Mouse myoblast	• Stiff films (elastic modulus > 350 kPa) increase attachment, proliferation, differentiation, and spreading • Stiff films produce long, thin, striated myotubes detaching due to contractile properties	• Flexible films produce short and thick myotubes
Hyaluronic acid[21]	*In vivo*	Rat myoblast	• Honeycombed structures surrounded by multinucleated myotubes • No implanted cell migration	• Inflammatory response
Alginate[70,92,93]	*In vitro*	Mouse myoblast	• Surface modifications enhance attachment, proliferation, and fusion • Porosity increases cell survival and migration • Stiffness promotes adhesion, proliferation, and differentiation • Increased degradation increases proliferation	• No cell spreading or migration
Alginate[21]	*In vivo*	Rat myoblast	• Myotubes fusion adjacent to capsule wall • No implanted cell migration • Inflammatory response	• Inflammatory response
Fibrin[94,96-98]	*In vitro*	Mouse and rat myoblast	• Electrical stimulus alters the contractility • Cylinder muscle structure forms in 10 days • Positive force frequency • Twitch-to-tetanus ratio in human range • Aligned myotubes achieved through continuous strain and micropatterns • stable cell contraction	• Specific force 7 times less than human skeletal muscle • Cross sectional area 10 times less than human myotube

Biomaterial	Research Method	Cell Type	Functional Outcome	Limitations
Fibrin[19,95,99]	*In vivo*	Rat myoblast	• Gel injection remained in the implantation site with no migration • Liquid characteristic in situ allowed to completely fill the defect • No inflammation, rejection, or foreign body reaction • Partial fusion to host myofibers after 25 days • Remain in myogenic phenotype • Capillary formation within the construct	• Scaffold has predefined shape not identical to wound dimensions • Fragile • Difficult to maintain sterility clinically
Fibrin[80]	*In vivo*	Rat satellite cell	• Femoral artery, vein, and nerve incorporated into the construct after 4 weeks • Satellite cells differentiated into myoblasts to form myotubes • Striated banding pattern • Neurotized increases contractile forces	• Few neuromuscular junctions formed
Acellular[100,101]	*In vitro*	Mouse and rat myoblast	• Able to support myoblast proliferation, differentiation, and fusion • Contractile and force production	• No neuromuscular interfaces • No blood supply
Acellular[102-104]	*In vitro*	Rat satellite cell	• 95% formation success rate • Introduction of neural cells formed neuromuscular junctions • Introduction of fibroblast cells created constructs muscle-like in appearance, excitability, and contractile function	• No expression of myosin heavy chains • 1% isometric titanic force of human myoblasts
Acellular[73,101]	*In vivo*	Rat myoblast	• FGF-2 and TGF-β1 present in matrix promotes capillary formation • Formation of skeletal muscle fibers, neovascularization, and innervations • Survived 9 months *in vivo* in developing muscle • Myotubes aligned in the longitudinal direction	• After 3 months in mature skeletal muscle loss of contractile muscle fibers

Table 1: Current research on muscle regeneration using biomaterials

Summary of the current research techniques used for skeletal muscle regeneration using different biomaterials.

2.3.2. Collagen

Collagen, particularly types I, II, and III collagen, belong to a family of extracellular matrix proteins found in the connective tissues of the human body, specifically the dermis, tendons, and blood vessels.[25] Collagen scaffolds are used in a wide range of tissue engineering applications including skin, cartilage, bone, and nerve.[26] These scaffolds possess strong mechanical properties similar to those of skeletal muscle and satisfactory cell-matrix binding efficiencies.[27,28] Collagen can be molded into many different matrix compositions, such as gels, microthreads, and porous sponges, making it ideal for many different applications. Collagen scaffolds produce weak immunogenic responses and are highly biodegradable.[29] When implanted into the body, an inflammatory response sends macrophages and fibroblasts to the site of the wound. This activation causes natural enzymes to break down the scaffolds at a faster rate.[32] A way to overcome the biodegradable limitations *in vivo* is to crosslink the collagen matrix, creating bonds between the different chains to increase its stability. Collagen has been crosslinked using both physical and chemical crosslinking agents. Crosslinking collagen results in scaffolds with stronger mechanical stability, resistance to swelling, and slower degradation rate.[32] Crosslinking mechanisms will be described in more detail in later in the chapter.

Tissue engineered collagen scaffolds have been used extensively in researching ways to optimize muscle regeneration. Table 2 summarizes the benefits and limitations of using each type of collagen matrix composition. Vandenburgh et al. developed bioartificial muscles (BAMs), which are created by casting a cell-collagen solution around two posts. As the myoblasts fuse and differentiate into myofibers, the gel solution contracts aligning the myofibers along the long axis between the two posts.[105] Research using mechanical stimulation on BAMs has shown that it can increase the myofiber diameter. These constructs can withstand a constant

40% strain rate for up to five hours, and increased cell death occurs under static loading over time.[105-108] In addition to the regenerative capacity of tissue engineering in large muscle defects, BAMs have also been used to deliver proteins to the wound site to reverse the effects of muscle wasting due to disease or aging.[30] Researchers showed that controlled release of recombinant human growth factor from a BAM scaffold obtains a more consistent host response upon implantation than directly injecting the hormone into the muscle.[30] Although studies show BAMs to be beneficial as a drug delivery system, several characteristics limit its potential for muscle regeneration at this time, such having a myotube diameter that is twenty times smaller than human myotubes and a low muscle fiber to biomaterial ratio.[30,105,106,109,110]

In addition to using collagen gels as a means to help create an engineered muscle, it can be used as a platform to help promote muscle regeneration in the form of nanofibers, fibril matrices, and films.[31,33,34] When seeded onto collagen electrospun nanofibers, myoblasts showed increased proliferation, maintenance of myogenic properties, and myotube formation. Analysis of myotube orientation showed alignment of the fibers, which was influenced by the orientation of the nanofiber scaffold.[31] In an attempt to create a thicker muscle scaffold, Yan et al. attached a thin collagen matrix with parallel-aligned fibrils along the bottom of a culture dish and seeded satellite cells to this surface. Once attached, a second collagen-cell layer was spread over the construct in order to make a multilayer scaffold.[34] The results proved that after five days, the first layer of cells fused in the direction of the collagen fibrils with the second layer of cells having less structured alignment. However, the model is not reproducible since the hypercontraction of the gel caused by contracting myotubes causes the substrate to detach from the culture dish resulting in poorly formed myotubes. When this model successfully binds to the underlying substrate, there is decreased cell viability after 21 days.[34] Another matrix studied for

muscle regeneration is collagen film scaffolds, which promotes skeletal muscle cell attachment, proliferation, fusion, and alignment. This scaffold is not suitable for muscle regeneration due to insignificant mechanical properties and sporadic myotube formation and maturation.[33]

A prominently used scaffold method is suspending cells into a collagen gel, which is attractive for research since the gel biodegradability resembles a native wound healing response, and there is a high density of cellular attachment sites on and within the matrix.[8,111] An advantage of using gel matrices in tissue engineering is that the cellular contraction, differentiation, and alignment within a gel can be controlled through electrical stimulation by adjusting the frequency, duration and direction of the electrical pulses.[112] In addition, applying a uniaxial load to cell seeded gels induces myoblasts to elongate in the direction of the load, and over time, the myoblasts fuse, align, and mature into multinucleated myotubes.[113] However, the results showed a heterogeneous population of mature myotubes formed, and there was a decrease in the number of myotubes present with time due to cell death within the gel scaffold.[112,113] Collagen gels can also be modified easily using growth factors and other polymers to create the optimal environment for muscle regeneration.[22,31,114] Gawlitta et al. studied the effects of adding IGF, which has been shown to regulate myoblast activity during native muscle regeneration, to the gel scaffold and found that it caused myoblast differentiation *in vitro*, which suggests that it could aid in creating tissue-engineered myotubes.[114] Mixing vascular endothelial growth factor (VEGF) within the gel solution showed an increase in engineered muscle density, contractibility, and capillary formation *in vivo*, but the influence of VEGF on the host environment decreased in aged mouse models.[22] Furthermore, creating copolymer solutions with fibrin allows for a significant increase in myoblast proliferation, differentiation, and fusion, but the myotubes on this substrate did not produce contractile forces, which shows a lack of maturity in the myotube

formation.[31] Huang et al. created a micropatterened substrate using a polydimethylsiloxane (PDMS) mold to regulate organization, F-actin assembly, and alignment of myotube formation before transferring the cell sheet to a collagen gel. By varying the width of the microgrooves, they could control how well the myotubes aligned.[115]

Creating a porous collagen sponge for muscle regeneration shows promise since the dimension and variability of the pores can be controlled through lyophilizing techniques, which allows for diffusion of nutrients throughout the scaffold.[8] Myoblasts seeded onto porous collagen sponges exhibit myotube formation in alignment with the pore structure, which suggests that by fabricating a scaffold with long, parallel pores, the myotubes will form with skeletal muscle characteristics.[76,116] Studies have shown that increasing the pore size within the sponge increases myotube viability and myoblast matrix production.[76,116] In high-density scaffolds, there was a 45% apoptosis rate after 4 weeks with no significant myoblast proliferation.[31] When sponges seeded with satellite cells are electrically stimulated the expression of MyoD and desmin, which are expressed during native muscle regeneration, is enhanced, and the myogenicity of the cells can be controlled.[27,45,117] In addition, seeding the scaffolds under dynamic culture conditions increases seeding efficiency and cell viability with very little cell death after 24 hours.[27,45,117]

In order to determine the effects of using a porous collagen sponge for muscle repair, Grefte et al. implanted an acellular scaffold into a rat model. The results showed that in the presence of a fibrotic discontinuity, the native muscle tissue still has the ability to activate satellite cells from the adjacent myotubes, but the satellite cells were unable to migrate onto the scaffold without donor cell signaling, which blocks proper muscle regeneration properties.[118,119] When implanting a collagen sponge seeded with myoblasts or satellite cells into a wound defect,

the construct was able to produce contractile forces and signal host cell migration, but it provoked a large inflammatory response.[27,45,76,116] Although mature myofiber formation was present after six weeks, the maturation of the myofibers was not consistent throughout the scaffold, and little evidence of muscle striations was observed.[76,116] Carnio et al. used a collagen sponge seeded with satellite cells in attempts to reverse muscle wasting in dystrophin deficient mice, and although the cells remained viable after implantation, the dystrophin restoration was not significant enough to be functionally relevant.[27] Since the collagen structure can be altered easily depending on the tissue-engineered application, it makes it an attractive biomaterial platform for muscle regeneration scaffolds.[30,31,33,34]

Scaffold Type	Research Method	Cell Type	Functional Outcome / Limitations
BAMs [105-108]	*In vitro*	Human and mouse myoblast	• Mechanical stimulation for 8 days increased myofibers diameter by 12% • Higher collagen concentration and fewer seeded myoblasts improves anchor attachment in BAM development • Cells can withstand a constant application of strains below 0.35 for up to 5 hours • Static muscle fiber diameter 20 times smaller than human skeletal muscle • Hypertrophy did not increase myofibers diameter great enough for clinical relevance • 2-15% of construct occupied by muscle fibers • Increased cell death with time under static loading • 40% strain compression for 24 hours causes higher cell death in increasingly acidic solutions
BAMs[30]	*In vivo*	Mouse myoblast	• Controlled release of recombinant human growth hormone (rhGH) obtains a more consistent host response
Electrospun nanofibers [31]	*In vitro*	Rat myoblast	• Promoted proliferation, maintenance of myogenic properties, and myotubes fusion • Alignment of fibers influenced by orientation of fibers
Fibril matrix[34]	*In vitro*	Rat satellite cell	• Attachment, cell elongation, differentiation, and fusion in the direction of collagen fibrils after 5 days • Thicker construct achieved through collagen gel layering • Embryonic and adult myosin heavy chain expression suggest maturation between day 14 and 21 • Decreased cell viability at day 21 • Model not easily reproduced due to hypercontraction detaching the substrate from the culture dish
Film[33]	*In vitro*	Mouse myoblast	• Promoted attachment, proliferation, and fusion • Alignment not parallel with longitudinal axis of film • Myotube formation and maturation varies throughout structure • Properties not suitable for muscle regeneration
Gel[31,112-115]	*In vitro*	Mouse and rat myoblast	• Differentiated myoblasts formed myotubes after 2 days • Myotubes contraction causes detachment after 8 days • Myotube contraction may be controllable by adjusting the frequency, duration, and direction of electrical pulses • Uniaxial loading induced fusion, maturation, and alignment of myotubes after 6 days • Uniaxial loading induces cell elongation • IGF causes differentiation • Seeding on fibrin copolymer allows for significant proliferation, differentiation, and fusion • Fibrin copolymer does not provoke myofibers contraction • Micropatterned substrates regulates organization, formation, F-actin assembly, and alignment • Myotube death after 12 days in culture • Collagen-fiber copolymer not stable enough for *in vivo* analysis • Gels contain a mixture of myotubes and myoblasts after 6 days • Myoblast alignment decreases with increase micropattern groove widths

Scaffold Type	Research Method	Cell Type	Functional Outcome / Limitations
Gel[22]	*In vivo*	Mouse myoblast	• VEGF increases muscle density, contractibility, and capillary formation • Older host environments reduce the implant's regenerative influence
Sponge[31,76,116]	*In vitro*	Mouse and rat myoblast	• Cells seed in small clusters centrally between collagen bundles • Myotubes formation in alignment with pore structure • Formation of extracellular matrix in low density scaffolds • Viable myotubes for 30 days in low density scaffolds • No significant myoblast proliferation after 4 weeks in high density scaffolds • High density of scaffold causes 45% apoptosis rate after 4 days
Sponge[27,45,117]	*In vitro*	Mouse satellite cell	• Dynamic culture conditions increase seeding efficiency and viability • Electrical stimulation enhances the expression of MyoD and desmin • Electrical stimulation controls cell myogenicity • Very little cell death throughout seeded sponge after 24 hours
Sponge[118,119]	*In vivo*	Acellular	• Uninterrupted satellite cell activation in adjacent muscle tissue • Reduced bleeding at the wound site • No evidence of satellite cells on or within sponge • Sponge blocks proper muscle regeneration properties
Sponge[76,116]	*In vivo*	Mouse and rat myoblast	• Able to produce contractile force • Host cell migration onto sponge • After 6 weeks giant cell formations were present • Mixture of mature and immature myofibers • No vascularization • No striated muscle • High inflammatory response
Sponge[27,45]	*In vivo*	Mouse satellite cells	• Shape easily manipulated to fit defect • Small myotubes formation within electrically stimulated scaffold after 10 days • Low cell death post implantation • Host cell colonization inside scaffold • Inflammatory response • Dystrophin restoration in dystrophin deficient mice too low to be functionally relevant

Table 2: Current research on muscle regeneration using collagen scaffolds

Summary of the current research techniques using collagen for skeletal muscle regeneration.

2.3.2.1. Self Assembly of Type I Collagen Microthreads

The regenerative capacity of self-assembled type I collagen microthreads has been researched extensively in the field of tendon and ligament regeneration.[120-122] By extruding soluble collagen through small diameter tubing, the collagen molecules are able to self assemble by growing linearly and laterally into fibrils which fuse, possessing characteristic type I collagen structure.[123] Cornwell et al. investigated the cell-matrix interactions and the mechanical properties of single collagen microthreads.[35,36] Fibroblasts readily migrate onto collagen microthreads suggesting the potential of collagen microthreads to elicit host cells to migrate into the wound site for enhanced regeneration.[35] In addition, through crosslinking, the mechanical properties of the threads, such as tensile strength and stiffness, can be increased, as well as decrease the rate of degradation to ensure the scaffolds remains in the defect long enough to support regeneration.[36]

The long cylindrical structure of the fibers acts as a guide to better align and orient the cells into a native myotube formation.[124] Studies have shown that using microthread based scaffolds for ligament regeneration is beneficial since the structure can be easily manipulated through twisting, weaving, or braiding, which increases the surface area and mechanical strength of the scaffold, which are attributes important in muscle regeneration as well.[37] Braiding thread scaffolds are structurally similar to the composition of native skeletal muscle in that they are an arrangement of bundles. Although the braids lack parallel fiber alignment, by weaving each thread throughout the entire length and width of the scaffold, it prevents catastrophic failure if one thread is damaged.[37,125] Braiding threads also allow for controlled and integrated pores, which allow for diffusion of nutrients and waste.[37,125,126]

2.3.2.2. Crosslinking using Carbodiimides

In order to form an irreversible bond between two collagen molecules at different locations, bifunctional chemicals are used to chemically crosslink them to one another by incorporating the chemical into the collagen structure.[127] The benefits of using a chemical crosslinker, such as glutaraldehyde, formaldehyde, or carbodiimides, are that they are stable. The strength of the bond is controlled easily by manipulating the crosslinking environment, and the residual chemicals can be washed away by rinsing the scaffolds.[127] Although the majority of chemical crosslinkers are integrated into the chemical bond, the advantage of crosslinking collagen based scaffolds using 1-ethyl-3-(3-dimethylaminopropyl) carbodiimide hydrochloride (EDC) is that it initiates the bond between collagen molecules without become a part of the structure.[127,128] Using EDC increases the biostability and mechanical strength without leaving a toxic residue within the structure.[38,39]

The EDC chemical, which is a zero-length agent, crosslinks collagen by initiating a nucleophilic reaction between the carboxylic groups of aspartic and glutamic acids with the amine groups of lysine and hydroxylysine amino acids to form a covalent bond between them (*Figure 4*).[28,29,40,129] After this amide bond between adjacent polypeptide chains forms, the crosslink reaction releases urea, a highly soluble waste product, from the scaffold.[29] This biproduct is nontoxic to the body and removed by simply rinsing the scaffold.[130] Studies show that the optimal environment to EDC crosslink collagen based scaffolds is in a solution having a pH between 5.0 and 5.5, which helps to initiate the reaction.[131] Crosslinking using EDC does not produce a stable reaction when used to crosslink alone since the unstable amine intermediate reaction causes the hydrolysis of the ester bond, reversing the crosslink effects. To stabilize the reaction, N-hydroxysuccinimide (NHS) is added to EDC, which prevents the hydrolysis by

activating the ester bond and eliminating the formation of intermediate reactions.[131,132] Cornwell et al. showed that by crosslinking collagen microthreads using EDC/NHS, it increased the mechanical stability of the collagen threads, increased the hydrophilicity of the surface compared to physical crosslinkers, and promoted cell migration.[36] Pieper et al. found that EDC crosslinked porous sponges maintained their structure after implantation, supported cell survival, and promoted cell differentiation and fusion of myoblasts into myotubes.[28,133]

2.3.2.3. Surface Modification

Another advantage of using EDC to crosslink collagen scaffolds is that it can aid in the further alteration of the collagen surface to improve the biocompatibility of the structure. Heparin is associated with cell surfaces and the extracellular matrix, and can be immobilized onto the collagen surface covalently by mixing it into the EDC/NHS solution (*Figure 4*).[38,40,129] Studies have shown that heparin increases blood compatibility and decreases the foreign body response of the scaffolds. It also reduces platelet adhesion and aggregation when implanted into an animal model.[39,129] Other studies show an increase in vascularization when collagen gels crosslinked with heparin are implanted into a wound site.[133]

In addition, by immobilizing heparin to the surface it can be used to bind and regulate proteins, such as growth factors known to improve adhesion, migration, proliferation, and differentiation to enhance regeneration.[38,40] Growth factors associated with wound healing, such as FGF-2, have a high affinity for heparin, and they are known as heparin-binding growth factors.[41,42] Activated FGF-2 denatures quickly, so by electrostatically binding it to heparin, the scaffold can act as a storage unit until the FGF-2 is needed in the wound.[38,132] Heparin will stabilize the FGF-2, prevent denaturation and proteolytic degradation, and aid in cell membrane receptor interactions.[38,132,134] Studies show that the slow release of FGF-2, binding it to

immobilized heparin from the surface of a collagen matrix, promotes vascularization over time in a wound site.[129] In addition, binding FGF-2 to a fibrin thread showed an increase in cell proliferation and migration with increased levels of FGF-2 on the surface, but at high concentration, the growth factors influence decreased and eventually plateaued.[43]

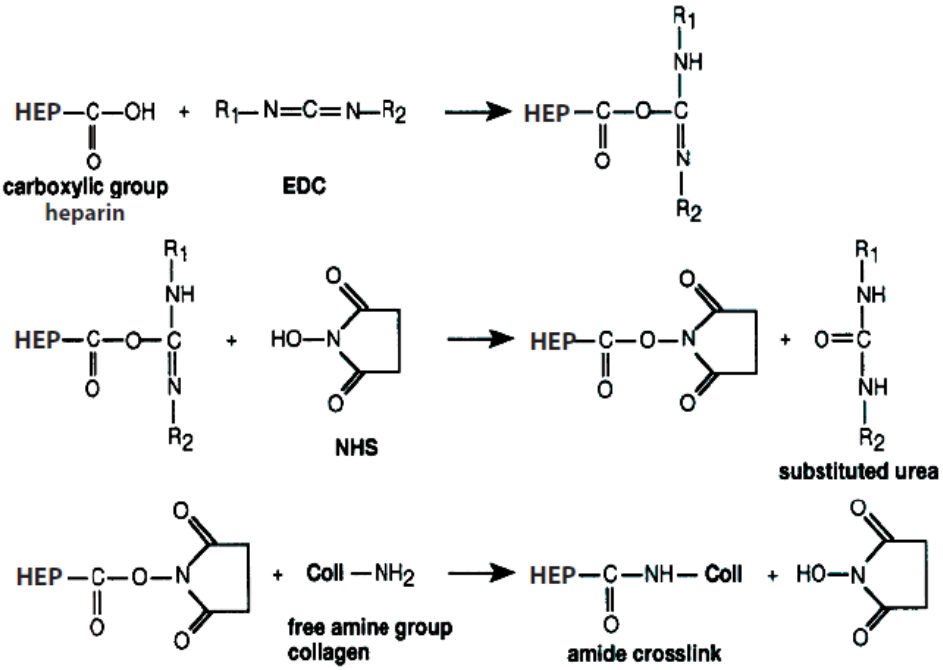

Figure 4: Conjugation of heparin to collagen using EDC/NHS

Mechanism of covalent attachment of heparin to collagen using and EDC/NHS solution (Figure adapted from[28]).

2.4. Muscle Derived Fibroblastic Cells for Muscle Regeneration

Currently, tissue engineered muscle constructs are created using myoblasts or satellite cells since they are extracted easily from muscle and can be expanded *in vitro*.[44,45] Studies using myoblasts to create three-dimensional engineered muscles show that they readily proliferate, respond well to environmental and chemical cues, and they fuse into myotubes *in vitro* by manipulating the culture conditions.[114] Although studies with myoblasts have been successful in creating functional muscles tissues *in vitro* and in animal models, in clinical human applications,

there are several limitations including the need to deliver a large quantity of cells, loss of myogenicity of implanted cells expanded *in vitro*, and a low percentage of cells that survive upon implantation into a muscle defect.[27] Other studies suggested that implanting the smallest quantity of satellite cells possible into a defect would led to minimal cell death and increased myofibers regeneration, but this approach would not be useful clinically.[11] Another limitation of using satellite cells for tissue-engineered muscle is that when culturing satellite cells in a culture dish, the cells do not maintain their stemness, becoming differentiation-committed satellite cells instead of self-renewing.[11] Continued research is still being explored into the method needed to efficiently regenerate muscle in a human muscle defect.

2.4.1. Dedifferentiation of Fibroblast Cells using FGF-2

One potential way to overcome the limitations of using myoblasts, muscle precursor cells, or satellite cells, undifferentiated skeletal muscle progenitor cells, for engineered muscle regeneration is by using induced pluripotent stem (iPS) cells, which can be differentiated into any cell type.[5,11] An iPS cell is a mammalian somatic cell, or any cell in the body in its differentiated state, that has been forced into a pluripotent state by the expression of embryonic transcription factors.[135] Studies have shown that introducing iPS cells to satellite cell differentiation cues *in vitro* before implantation can help differentiate them into functional myoblasts *in vivo*. Clinically, research into overcoming the limitations related to using iPS cells, such as tumor formation, is being studied.[11] Since there is still the limitation of having a low quantity of autologous cells available, researchers have looked into inducing FGF-2 to fibroblasts to express stem cell like characteristics.[46,136] By activating stem cell specific markers, such as OCT4 and SOX2, in fibroblast cells, it gives rise to the potential of using a large quantity of autologous cells for muscle regeneration.[46,136-138] In order to stimulate fibroblasts to exhibit

stem cell properties without differentiation, the cells need to be cultured continuously with FGF-2, on specific cell culture surfaces, and in a low oxygen environment.[46,139,140]

In this study, we propose to use braided collagen microthreads seeded with muscle-derived fibroblastic cells (MDFCs) as a scaffold to aid in muscle regeneration since it will provide a structure to create longitudinally aligned myotubes.[37,125,126] Although braided collagen microthreads are not parallel to one another like each myofiber in native skeletal muscle, by weaving the microthreads together, the scaffold structure can be maintained without thread spreading from one another during hydration. When a full thickness defect occurs, the entire depth of the muscle is damaged, resulting in the destruction of many myofibers.[17,18] Since the diameter of one microthread is smaller than that of a myofiber, which ranges from 20 to 100 μm, by braiding the threads together, the dimensions of the microthreads can be increased to fill a larger defect area.[7,17] Studies have shown using a biomaterial with stiffness close to that of native muscle, 12 kPa, for engineering skeletal muscle can affect the length, alignment, and contractibility of the formed myofibers.[47,141-143] Using EDC/NHS crosslinking, the mechanical properties of the braided collagen microthreads can be controlled to enhance myofiber formation. When a large muscle defect occurs, the native skeletal muscle cannot regenerate itself since the satellite cells within the basal lamina have been destroyed, so there is a need for a way to deliver satellite like cells to the defect area to enhance regeneration.[73] By attaching heparin and FGF-2 to the surface of the braided collagen scaffold may serve to help bind, modulate, and release FGF-2 to the seeded cells and the surrounding environment. In addition, the presence of FGF-2 on the surface of the scaffold will provide a method to release a controlled amount of the growth factor to the cells to maintain the undifferentiated state of the muscle derived fibroblast cells.

This will insure a population of dedifferentiated fibroblast cells will be delivered to the defect site to behave like satellite cells to induce muscle regeneration.

Chapter 3: Hypothesis and Specific Aims

We hypothesize that binding growth factors to the surface of crosslinked braided collagen scaffolds will promote muscle-derived fibroblastic cell (MDFC) attachment and growth, which could serve as a platform for delivering cells to large muscle defects for muscle regeneration. Specifically, characterization of the surface and mechanical strength of the braided collagen scaffold will verify that the scaffolds are suitable for integrating into native skeletal muscle. In addition, quantitative and qualitative analysis of cell attachment, growth, and alignment through immunocytochemistry and cell growth assays will confirm that surface modifications facilitate the growth of MDFCs on braided collagen scaffolds.

Specific Aim 1: Characterize the Structural Properties of Braided Collagen Scaffolds

Here we hypothesize that braided collagen scaffolds are suitable for integrating into a skeletal muscle defect and maintain mechanical stability. To test this we braided three braids of six individual self assembled collagen microthreads together in a three strand braid to form a final eighteen microthread braided collagen scaffold. Next, the scaffolds were crosslinked using EDC/NHS with or without heparin and FGF-2 in concentrations of 5 ng/mL, 10 ng/mL, or 50 ng/mL was passively adsorbed to the surface. The braided collagen scaffolds were characterized through immunocytochemistry and mechanical testing. Due to limitations involved with imaging a three-dimensional braided scaffold, single threads were passively adsorbed with different concentrations of FGF-2 and treated with the standard protocol for immunocytochemistry. This was used to show that different concentrations of FGF-2 were bound to the surface of the braided collagen scaffolds. Next, to test the mechanical stability of the braided collagen scaffolds, uncrosslinked and crosslinked scaffolds were loaded in uniaxial

tension to extrapolate the measured ultimate load at failure, strain at failure, and maximum tangent modulus (MTM).

Specific Aim 2: Develop a novel cell seeding method to achieve uniform and reproducible MDFC attachment on braided collagen scaffolds

Here we hypothesize that development of a novel seeding method will enhance uniformity, efficiency, and reproducibility of MDFC seeding on braided collagen scaffolds. The first step in developing this method was to provide the optimal environment to promote cell attachment onto braided collagen scaffolds. Polydimethylsiloxane (PDMS) molds were created with two posts in the center creating a seeding channel with a dimension of either 2.0 mm by 12 mm or 1.0 mm by 12 mm. Cells were seeded onto braided collagen scaffolds using both channel dimensions, cultured for 24 hours, and analyzed for uniformity to determine which PDMS mold provided the most reproducible results. Second, we determined the most advantageous way to visualize the MDFCs on the braided collagen scaffolds for qualitative analysis. The collagen microthreads exhibit significant autofluorescence when exposed to DNA binding dyes directly, so to address this issue, MDFCs were preloaded with either a MitoTracker Green or Hoechst dye before seeding the cells onto the braided collagen scaffolds. The seeded scaffolds were imaged to determine which dye provided more quantitative information to be used for analysis.

Specific Aim 3: Quantify cell attachment and growth on collagen braided scaffolds with different surface modifications

Finally, we hypothesize that FGF-2 modified surfaces will promote MDFC attachment and growth on braided collagen scaffolds. Braided collagen scaffolds that were uncrosslinked, EDC/NHS crosslinked, EDC/NHS crosslinked with heparin, and EDC/NHS crosslinked with heparin with 5 ng/mL, 10 ng/mL, or 50 ng/mL FGF-2 were seeded with MDFCs that were

preloaded with Hoechst dye. After culture for 1, 5, or 7 days, the scaffolds were removed and analyzed both quantitatively and qualitatively. Using image J software, the number of Hoechst stained nuclei per 10,000 μm^2 was counted to determine cell density and cell distribution. In addition, scaffolds were stained with phalloidin, a fluorescent stain that binds to the f-actin filaments, to characterize the cellular alignment of MDFCs on braided collagen scaffolds.

Chapter 4: Materials and Methods

In this chapter, the procedures used to achieve the specific aims will be described. The design of a novel engineered muscle construct from self-assembled collagen microthreads will be described, as well as the development of a method to seed MDFCs onto a three dimensional scaffold. In addition, this chapter describes the procedures used to characterization the braided collagen scaffold and the cell attachment and growth both quantitatively and qualitatively.

4.1. Type I Collagen Extraction from Rat Tendon

Acid-soluble type I collagen was extracted from rat tail tendons as previously described.[36,144] Briefly, tendons were removed from 13 Sprague-Dawley rat tails with a hemostat, rinsed in phosphate buffered saline (PBS, pH 7.4), and dissolved in 1600 mL of 3% (vol/ vol) acetic acid overnight at 4ºC. The collagen solution was filtered through layered cheesecloth and centrifuged for 2 hours at 8500 rpm at 4ºC. Discarding the pellet, a salt precipitation was performed where 320 mL of 30% NaCl (wt/ vol) solution was dripped into the supernatant. The solution was allowed to sit overnight at 4ºC. The entire solution was then centrifuged at 4ºC for 40 minutes at 4900 rpm, and the resulting pellet was resuspended on a stir plate in 400 mL of 0.6% (vol/ vol) acetic acid at 4ºC until the pellet had dissolved completely. The solution was placed in dialysis membranes (Spectrum Laboratories, Inc., Rancho Dominguez, CA) and dialyzed at room temperature in 1 mM HCl changing the dialysate every 4 hours until the solution was clear. The type I collagen solution was lyophilized and stored at 4ºC. Prior to use, the lyophilized collagen fleece is dissolved in 5 mM HCl at a concentration of 10 mg/mL.

4.2. Self Assembled Collagen Thread Extrusion

Self-assembled collagen threads were produced from acid soluble type I collagen using methods described previously.[35] Briefly, type I collagen (10 mg/mL in 5 mM HCl) was placed in a 5 mL syringe connected to a polyethylene tube with an inner diameter of 0.86 mm (Becton Dickinson, Franklin, NJ). Using a syringe pump, the solution was extruded through the tubing at a rate of 0.255 mm/min into a 37ºC bath of fiber formation buffer (pH 7.4, 135 mM NaCl, 30 mM Tris Base, 30 mM Tris HCl, and 5 mM $NaPO_4$ dibasic; Sigma, St. Louis, MO) and incubated for 24 hours (*Figure 5*). The formed threads were transferred to a 37ºC bath consisting of fiber incubation buffer (pH 7.4, 135 mM NaCl, 10 mM Tris Base, 10 mM Tris HCl, and 30 mM $NaPO_4$ dibasic; Sigma) for an additional 24 hours. The threads were then washed in a 37ºC bath of distilled water for 24 hours to remove the salt, air dried, and stored at room temperature in a dessicator until use.

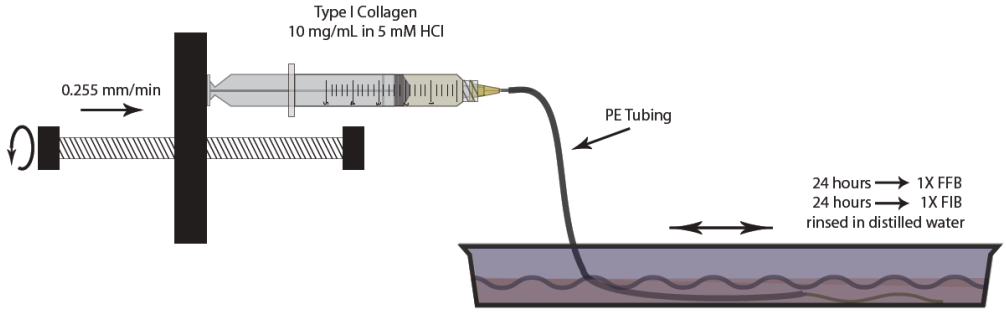

Figure 5: Self assembled collagen thread extrusion

Type I collagen (10 mg/mL in 5 mM HCl) was placed in a 5 mL syringe connected to a polyethylene tube with an inner diameter of 0.86 mm. Using a syringe pump, the solution was extruded through the tubing at a rate of 0.255 mm/min into a 37ºC bath of fiber formation buffer and incubated for 24 hours. The formed threads were transferred to a 37ºC bath consisting of fiber incubation buffer for an additional 24 hours. The threads were then washed in a 37ºC bath of distilled water for 24 hours and air dried.

4.3. Braided Scaffold Preparation

To create braided collagen scaffolds, first six type I collagen microthreads were attached to a single point and split into three groups of two threads each (*Figure 6A*). The grouped threads were braided together with 28 crossovers per centimeter. A crossover is defined as one group crossing over an adjacent group (*Figure 6B* and *C*). The final braided scaffold was produced by attaching three six-thread braids to a single point and braiding them together with 26 crossovers per centimeter (*Figure 6D*). The final braided scaffolds containing 18 self-assembled threads were attached to PDMS (Dow Corning, Midland, MI) rings with an inner diameter of 14 mm using Silastic Silicone Medical Adhesive Type A (Dow Corning, Midland, MI) in order to easy fit inside a 12 well tissue culture plate (*Figure 6E*).

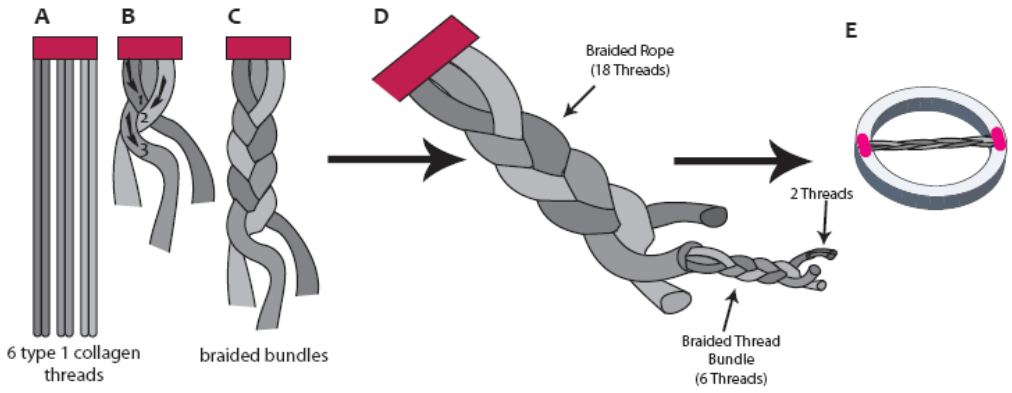

Figure 6: Braided collagen scaffold preparation

To create braided collagen scaffolds, first six type I collagen microthreads were attached to a single point and split into three groups of two threads each (A). The grouped threads were braided together with 28 crossovers per centimeter (B and C). The final braided scaffold was produced by attaching three six-thread braids to a single point and braiding them together with 26 crossovers per centimeter (D). The final braided scaffolds were attached to PDMS rings using Silastic Silicone Medical Adhesive Type (E).

The phase images and table below compare the size of single threads, 6 thread braids, and 18 thread braids both dry and hydrated in PBS (*Figure 7* and *Table 3*). Phase images were obtained using an Olympus IX81 motorized inverted microscope coupled to a 12-bit Hamamatzu CCD camera and processed using Slidebook®.

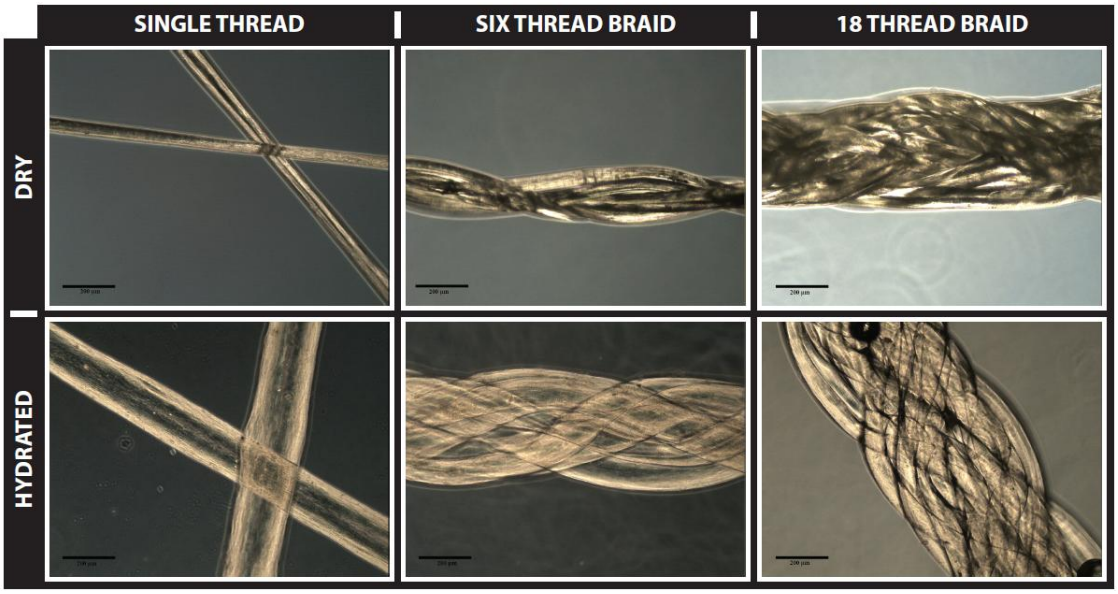

Figure 7: Phase images of single threads, six thread braids, and 18 thread braids

Phase images comparing the size of single threads, six thread braids, and 18 thread braids both dry (top row) and hydrated in PBS (bottom row). Scale bar = 200 µm.

Thread Configuration	Sample Size (n)	Dry Diameter (µm ± S.D.)	Hydrated Diameter (µm ± S.D.)
Single	6	50 ± 20	180 ± 20
6 Braid	6	250 ± 30	400 ± 50
18 Braid	6	450 ± 25	600 ± 50

Table 3: Width comparison of single threads, 6 thread braids, and 18 thread braids

4.4. Microthread Crosslinking with Heparin

Braided collagen scaffolds were crosslinked using the chemical crosslinker 1-ethyl-3-(3-dimethyl aminopropyl) carbodiimide (EDC; Sigma) and N-hydroxysuccinimide (NHS; Sigma) with and without heparin sodium salt (Calbiochem, Gibbstown, NJ) (*Figure 8*).[40,133,144] In a sterile field, braided collagen scaffolds were inverted and inserted into a 12 well plate with one scaffold per well, and they were washed with 70% (vol/ vol) ethanol 4 times for 30 minutes each and 40% (vol/ vol) ethanol 5 times for 15 minutes each to sterilize. Subsequently, the scaffolds were submerged in 3 mL of sterile filtered 40% (vol/ vol) ethanol including 50 mM 2-

morpholinoethane sulphonic acid (MES, pH 5.0; Sigma) for 30 minutes at room temperature. Next, the scaffolds were incubated in 2 mL of sterile filtered 40% (vol/ vol) ethanol including 50 mM MES, 14 mM EDC, 8 mM NHS, with and without 100 µg/mL heparin for 4 hours at room temperature. The scaffolds were washed in 70% (vol/ vol) ethanol 5 times for 10 minutes each with a final overnight wash at 4ºC.

4.5. FGF-2 Binding through Passive Adsorption

Fibroblast growth factor (FGF-2; Chemicon, Temecula, CA) in varying concentrations was passively adsorbed to the surface of braided collagen scaffolds crosslinked with EDC/NHS and heparin using methods previously described (*Figure 8*).[38] Due to material limitations, passively adsorbing FGF-2 to the surface of uncrosslinked and EDC/NHS crosslinked scaffolds without heparin was not tested, but in the future, it will be beneficial to study these interactions as well. Briefly, scaffolds were washed 5 times for 10 minutes with sterile Dulbecco's phosphate buffered saline (DPBS, pH 7.4) without calcium and magnesium at room temperature. Subsequently, the chamber walls, PDMS ring, silicone adhesive and nonspecific binding sites on the braided collagen scaffolds were blocked using a blocking solution of 3 mL of sterile filtered DPBS containing 0.25% (wt/ vol) bovine serum albumin (BSA; Sigma) for 1 hour at room temperature. Next the blocking solution was aspirated from each well, and replaced with 2 mL of sterile DPBS containing 0.25% (wt/ vol) BSA with FGF-2 at a concentration of either 5 ng/mL, 10 ng/mL, or 50 ng/mL. The scaffolds were incubated for 2 hours at room temperature. The braided collagen scaffolds were washed in DPBS 5 times for 10 minutes each and stored at 4ºC in DPBS until use.

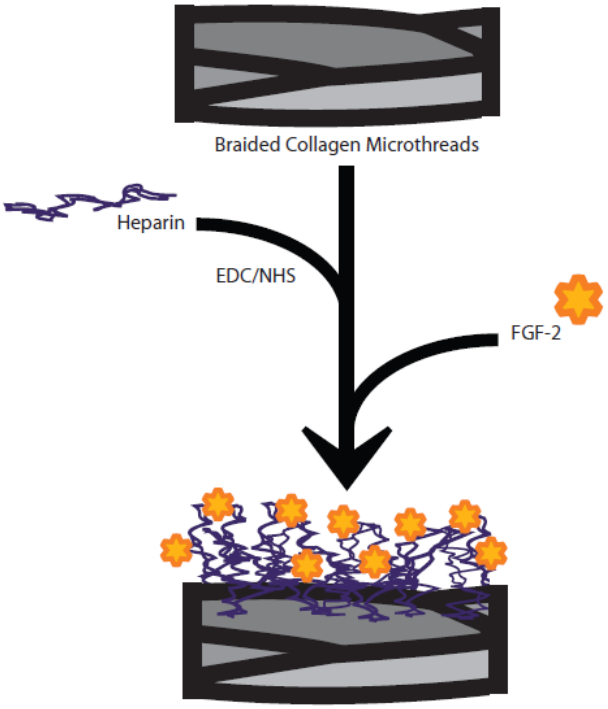

Figure 8: Passive adsorption of FGF-2 to braided collagen threads

Heparin is covalently bound to the surface of the collagen braided scaffold using EDC/NHS crosslinking. Next, FGF-2 is electrostatically bound to the heparin through passive adsorption.

4.6. Braided Collagen Scaffold Structural Characterization

4.6.1. Characterization of Bound FGF-2

To verify that FGF-2 has bound to the surface of the scaffolds immunocytochemistry was performed. Due to imaging limitations of the geometry of braided collagen scaffolds, single collagen threads were used to characterize the localization of FGF-2 on the surfaces. Single collagen threads were EDC/NHS crosslinked in the presence of heparin and then loaded with FGF-2 at the concentrations mentioned above. Single collagen threads that were EDC/NHS crosslinked in the presence of heparin were used as negative controls. DPBS was removed from the wells by aspiration, and the threads were incubated at room temperature in 300 µL of 1 µg/mL FGF-2 goat polyclonal IgG (Santa Cruz Biotechnology, Inc., Santa Cruz, CA) in PBS

with 0.05% Tween-20 (Promega Corporation, Madison, WI) for 30 minutes. The threads were washed with 500 µL of PBS with 0.05% Tween-20 for 5 minutes three times. The threads were then incubated in 300 µL of 5 µg/mL Alexa Fluor 647 donkey anti-goat IgG (Invitrogen, Carlsbad, CA) in PBS with 0.05% Tween-20 for 30 minutes. They were then washed in 500 µL of PBS with 0.05% Tween-20 for 5 minutes twice. Single collagen threads were imaged using fluorescence microscopy on an Olympus IX81 motorized inverted microscope coupled to a 12-bit Hamamatzu CCD camera and processed using Slidebook®.

4.6.2. Mechanical Testing of Braided Collagen Scaffolds

In order to determine the effect of surface modifications on mechanical strength, EDC/NHS crosslinked and uncrosslinked braided collagen threads were analyzed by mechanically loading the hydrated samples in uniaxial tension. Braided collagen scaffolds that were crosslinked with heparin and exposed to FGF-2 were not tested in this study. Braided collagen threads were cut to a sample length of 30 mm with the last 5 mm of each end bound and sealed using Silastic Silicone Medical Adhesive Type A (Dow Corning, Midland, MI). For tensile testing, the samples were secured horizontally with 2711 Series Lever Action Fiber Grips (Instron, Norwood, MA) on an E1000 ElectroPuls mechanical testing system (Instron, Norwood, MA) with a fixed 50 kN Dynacell dynamic load cell (Instron, Norwood, MA) (*Figure 9A*). The mechanical testing system and data acquisition were controlled using Bluehill 2 Materials Testing software (Instron, Norwood, MA). The samples were secured insuring that the silicone adhesive remained outside of the outer grip boundary (*Figure 9B*). An initial gauge length of 7.0 mm was defined as the distance between the inner grip boundaries, and the braids were loaded to failure at a 50% strain rate (3.5 mm/min).

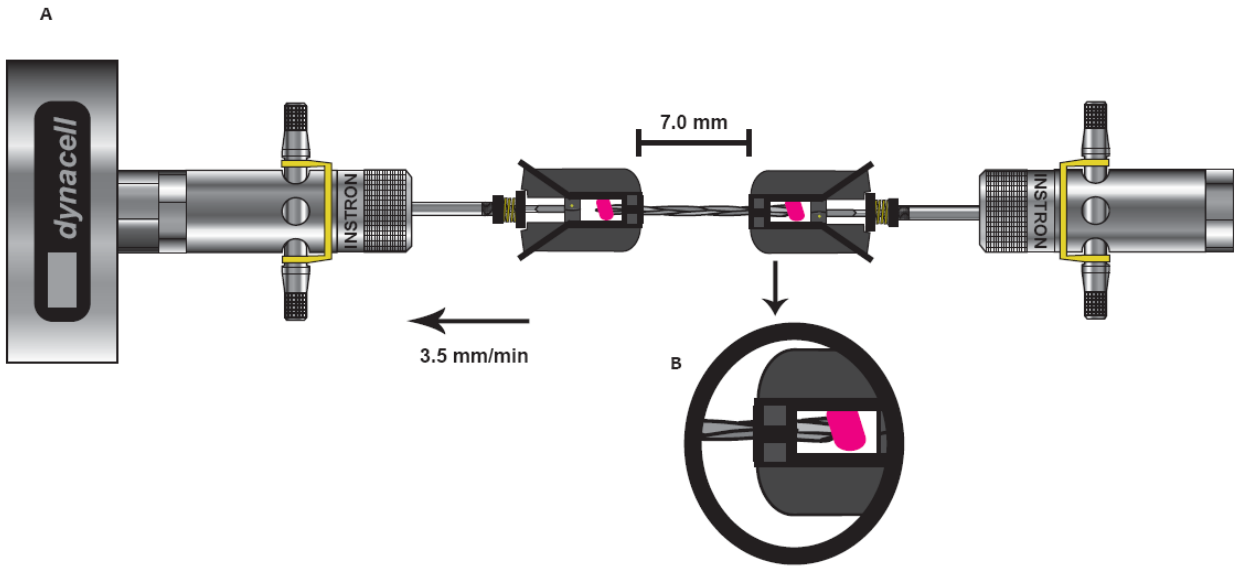

Figure 9: Schematic of mechanical testing of samples

Braided collagen threads were cut to a sample length of 30 mm with the last 5 mm of each end bound and sealed using Silastic Silicone Medical Adhesive Type A. The samples were secured horizontally with 2711 series grips on a mechanical testing system with a fixed 50 kN load cell (A). The samples were secured insuring that the silicone adhesive remained outside of the outer grip boundary (B). An initial gauge length of 7.0 mm was defined as the distance between the inner grip boundaries, and the braids were loaded to failure at a 50% strain rate (3.5 mm/min).

To calculate the ultimate tensile strength, the cross-sectional area of the samples was approximated using histological sections of hematoxylin and eosin stained unseeded braided collagen threads at five different locations. Although the scaffolds will shrink due to dehydration after processing, using the histological sections will give a better cross-sectional estimation since using a cylindrical model will not represent the shape accurately. Bright field images were obtained using an Olympus IX81 motorized inverted microscope coupled to a 12-bit Hamamatzu CCD camera and processed using Slidebook®, and analyzed using Image J software (U.S. National Institutes of Health, Bethesda, MD) (*Figure 10A*). The outer edge of the braided collagen threads was traced to measure the cross-sectional area (*Figure 10B* and *Figure 10C)*. The stress-strain curve, the load at failure, ultimate tensile strength (UTS), stain at failure

(SAF), and maximum tangent modulus or stiffness (MTM) were calculated from the data obtained during testing.

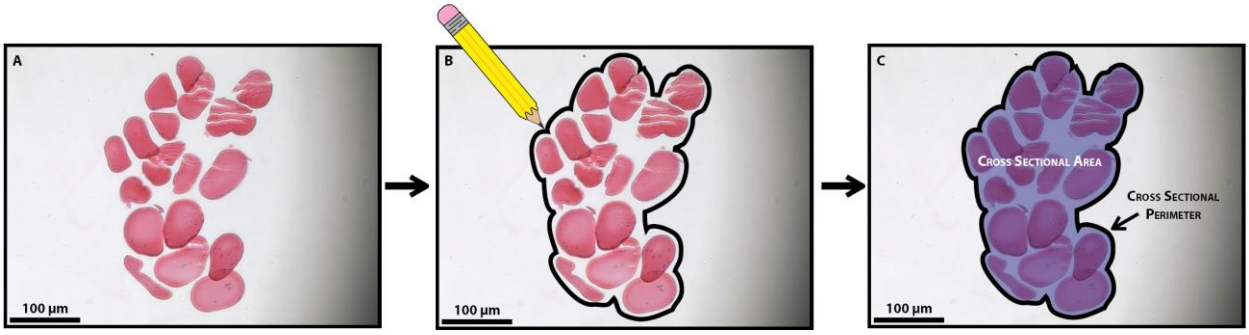

Figure 10: Braided collagen threads cross-sectional area

The cross-sectional area of five samples was approximated using histological sections of hematoxylin and eosin stained unseeded braided collagen threads, and analyzed using Image J software (A). The outer edge of the braided collagen threads was traced to measure the cross-sectional area (B and C).

In post processing of the data, a strain of zero was defined as the point where the braided collagen scaffolds were minimally loaded to a threshold of 0.01 grams, or less than 1% the ultimate load of the weakest uncrosslinked scaffold. In addition, load-elongation curves were truncated when the load fell by 20% of the ultimate load, or the point of the initial break (*Figure 11A*). After this point, as each individual thread within the braided collagen scaffold broke, they created peaks lower than the ultimate load until each thread in the scaffold failed. For the purpose of this analysis, only the ultimate load was considered (*Figure 11B*). The stiffness was defined as the maximum value for a tangent to the stress-strain curve over an incremental strain of 0.03.

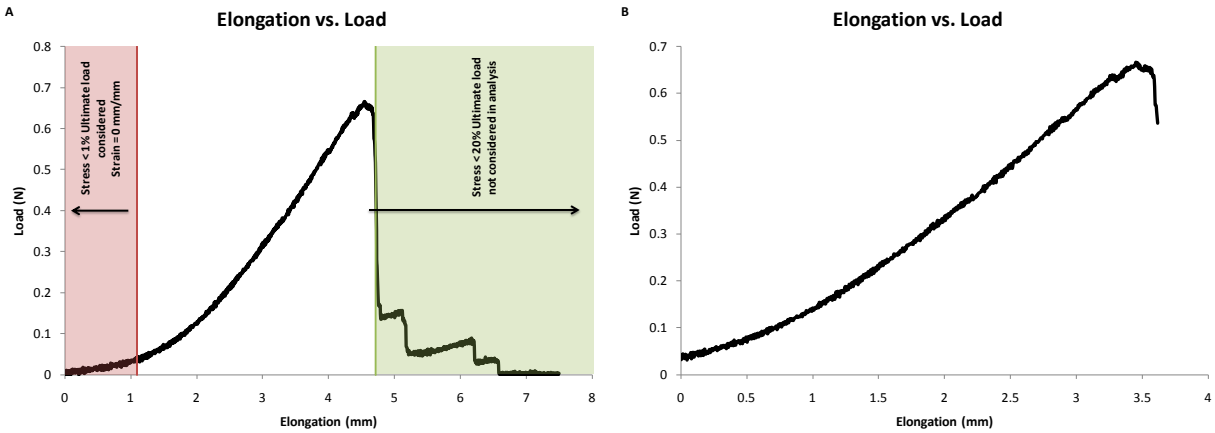

Figure 11: Post processing of mechanical data

Load-elongation curves were truncated when the load fell by 20% of the ultimate load, or the point of the initial break (A). Only the ultimate load of the load-elongation curve was considered (B).

4.7. MDFC Seeding to Braided Collagen Scaffolds

The procedures described in this section focus on the development on a novel method to seed MDFCs onto braided collagen scaffolds. Initially, MDFCs were preloaded with Mitotracker Green and seeded onto the scaffold using the PDMS mold with a 2.0 mm wide seeding channel in the middle. While this method allowed for qualitative analysis of cell attachment and growth, individual cells were not distinguishable because it was not clear how many mitochondria were in each MDFC. In addition, the channel width was much larger than the width of the braided collagen scaffolds, which led to the procedure having low reproducibility and seeding efficiency. Consequently, we developed a more reproducible seeding method and cell labeling procedure.

4.7.1. MDFC Culture and Braided Collagen Scaffold Sterilization

The MDFCs were extracted from the calf flexor muscle of a human adult male through methods described previously.[46] The MDFCs were grown in culture media (40% DMEM, 40% F-12, 20% FC III serum; Mediatech, Inc, Manassas, VA and Hyclone, Logan, UT) supplemented

with 10 ng/mL epidermal growth factor (EGF, Chemicon, Temecula, CA) at ambient conditions (20% O_2 and 5% CO_2) until culture flasks were confluent. Passages 7-8 were used for all cell-seeding experiments. Prior to MDFC seeding, the braided collagen scaffolds were incubated at room temperature with 3% penicillin/streptomycin (Pen/ Strep; Gibco BRL, Gaithersburg, MD) in DPBS (vol/ vol) for one week changing the antibiotic solution every 2 days to sterilize scaffolds.

4.7.2. Preliminary Cell Seeding Method

Prior to seeding MDFCs, the cells were preloaded with Mitotracker Green (Invitrogen, Eugene, OR), a mitochondrial dye. The MDFCs were incubated with 500 nM of Mitotracker Green in DMEM for 30 minutes at 37ºC on the day of initial seeding. The cells were washed twice with DPBS and placed back into 37ºC incubation with fresh medium until seeding. To seed MDFCs on braided collagen scaffolds, a PDMS mold was created with an outer circular well with a diameter of 24 mm with two posts in the center creating a channel with a dimension of 2.0 mm by 12 mm (*Figure 12A*). This channel was sealed at each end using a thin layer of medical grade silicone adhesive (*Figure 12B*). The PDMS mold was sterilized by autoclaving. Next, the silicone adhesive was notched in order to create a wedge to place the braided scaffold through (*Figure 12C*). The braided collagen scaffolds were inverted, inserted into the wedge, and sealed into place using sterile vacuum grease (*Figure 12D*). The MDFCs in a cell suspension of 200,000 cells in 90 μL of serum free medium (50% DMEM, 50% F-12) were seeded on the scaffolds and incubated for 4 hours at 37ºC (*Figure 12E*). Serum free medium was used for the MDFCs attachment to avoid masking the surface biochemical properties of the braided collagen scaffolds. The seeded braided collagen scaffolds were subsequently removed from the PDMS molds, inverted, and placed in a 12-well plate containing culture medium (45%

DMEM, 45% F-12, 10% FC III serum) (*Figure 12F*). During preliminary studies, uncrosslinked and EDC/NHS crosslinked braided collagen scaffolds were seeded, incubated for 24 hours, and then fixed in 4% paraformaldehyde solution in PBS (USB, Cleveland, OH) for 20 minutes at room temperature. The scaffolds were imaged using fluorescence microscopy on an Olympus IX81 motorized inverted microscope coupled to a 12-bit Hamamatzu CCD camera and processed using Slidebook®. The results showed (*Results in Sections 5.2.1. Preliminary Cell Seeding Method, Page 76*) that it was not possible to distinguish or quantify single cells since it is unknown how many mitochondria are inside a MDFC. As such, this labeling method did not allow for quantitative analysis. In addition, further development of the mold needed to be performed to eliminate the detachment of the braided collagen scaffolds from the PDMS ring during insertion into the channel wedge and to optimize the number of cells attaching to the scaffold.

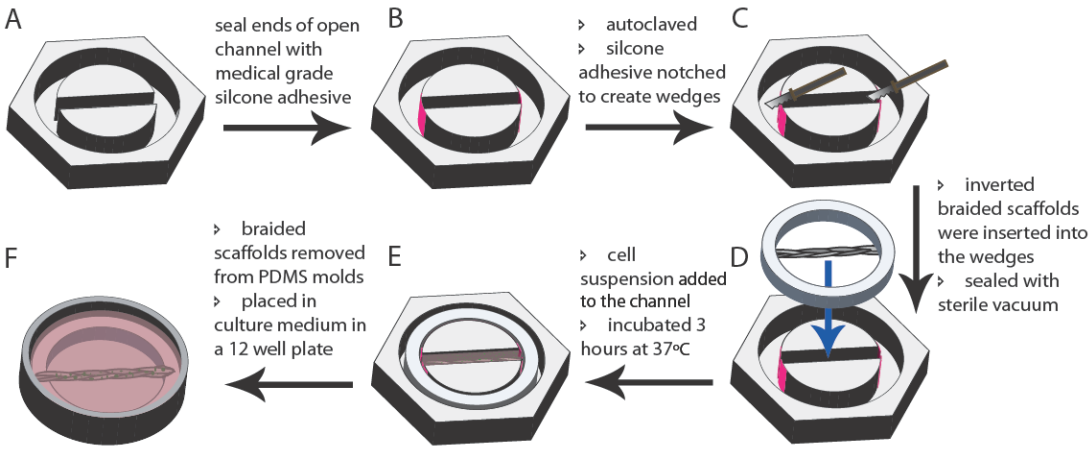

Figure 12: Preliminary seeding method

A PDMS mold was created with an outer circular well with a diameter of 24 mm with two posts in the center creating a channel with a dimension of 2.0 mm by 12 mm (A). This channel was sealed at each end using a thin layer of medical grade silicone adhesive (B). The PDMS mold was sterilized by autoclaving. Next, the silicone adhesive was notched in order to create a wedge to place the braided scaffold through (C). The braided collagen scaffolds were inverted, inserted into the wedge, and sealed into place using sterile vacuum grease (D). The MDFCs were seeded on the scaffolds and incubated for 4 hours at 37ºC (E). The seeded braided collagen scaffolds were subsequently removed from the PDMS molds, inverted, and placed in a 12-well plate containing culture (F).

4.7.3. Optimizing the Cell Seeding Method

To overcome the limitations associated with using Mitotracker Green prior to seeding on the braided collagen scaffold, MDFCs were incubated with 5 µg/mL Hoechst dye (Invitrogen, Carlsbad, CA) in culture medium for 15 minutes at 37ºC on the day of initial seeding. The cells were washed twice with DPBS and placed back into 37ºC incubation with fresh medium until seeding. To determine the optimal environment for uniform and reproducible seeding, the channel within the PDMS mold designed with dimensions of either 2.0 mm by 12 mm or 1.0 mm by 12 mm (*Figure 13A*). A smaller channel width was used to eliminate the void space around the scaffold when inserted into the channel. The molds were sterilized by autoclaving, and the channels were sealed at the ends using a thin layer of sterile vacuum grease (*Figure 13B*). The sterile braided collagen scaffolds were inverted and inserted into the vacuum grease such that the braid lies on the bottom of the channel (*Figure 13C*). The MDFCs were seeded on the scaffolds by adding a cell suspension in serum free medium (50% DMEM, 50% F-12) to the channel containing the braided scaffolds and incubated for 4 hours at 37ºC (*Figure 13D*). A cell suspension of 200,000 cells in 90 µL was used for the 2.0 mm by 12 mm channel, and a suspension of 150,000 cells in 30 µL was used for the 1.0 mm by 12 mm channel (*Table 4*). Different seeding volumes were used since 90 µL of solution exceeded the volume of the smaller channel. The seeded braided scaffolds were removed from the PDMS molds and placed in a 12-well plate containing culture medium (45% DMEM, 45% F-12, 10% FC III serum) supplemented with 1% pen/strep (*Figure 13E*). The seeded scaffolds were incubated at 37ºC. Uncrosslinked and EDC/NHS crosslinked braided collagen scaffolds were seeded, incubated for 24 hours, and then fixed in 4% paraformaldehyde solution in PBS (USB, Cleveland, OH) for 20 minutes at room temperature. The scaffolds were imaged using fluorescence microscopy with an

Olympus IX81 motorized inverted microscope coupled to a 12-bit Hamamatzu CCD camera and processed using Slidebook®. Due to better seeding uniformity and more reproducible data (*Results in Section 5.2.2. Optimizing the Cell Seeding Method, Page 77*), the PDMS mold with a channel dimension of 1.0 mm by 12 mm was used in all subsequent experiments.

Channel Dimension	# Cells Initially Seeded	Seeding Volume
2.0 mm X 12 mm	200,000	90 µL
1.0 mm X 12 mm	150,000	30 µL

Table 4: Preliminary Cell Seeding Method Development

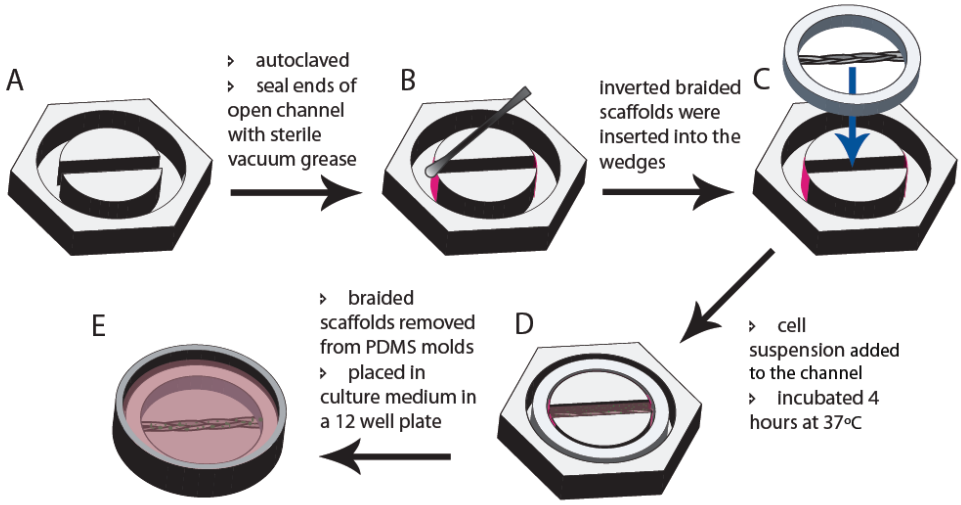

Figure 13: Seeding MDFCs onto a braided collagen scaffold

To determine the optimal environment for uniform and reproducible seeding, the channel within the PDMS mold designed with dimensions of either 2.0 mm by 12 mm or 1.0 mm by 12 mm (A). The molds were sterilized by autoclaving, and the channels were sealed at the ends using a thin layer of sterile vacuum grease (B). The sterile braided collagen scaffolds were inverted and inserted into the vacuum grease such that the braid lies on the bottom of the channel (C). The MDFCs were seeded on the scaffolds by adding a cell suspension in serum free medium to the channel containing the braided scaffolds and incubated for 4 hours at 37ºC (D). The seeded braided scaffolds were removed from the PDMS molds and placed in a 12-well plate containing culture medium (E).

4.8. Quantification of Cell Number on Braided Collagen Threads

The procedures described in this section focus on methods used to determine the effect of surface modifications, specifically FGF-2 adsorption, on cell attachment and growth. Braided collagen scaffolds with surfaces that were uncrosslinked, EDC/NHS crosslinked, EDC/NHS

crosslinked with heparin, and EDC/NHS crosslinked with heparin and different concentrations of FGF-2 bound were cultured with MDFCs for various times and analyzed using fluorescence microscopy.

4.8.1. Cell Attachment

To determine the effects of different surface modifications on attachment of MDFCs to braided collagen scaffolds, MDFCs were seeded as described above onto uncrosslinked scaffolds and scaffolds treated with EDC/NHS, EDC/NHS with heparin, or EDC/NHS with heparin coated with FGF-2 at concentrations of either 5 ng/mL, 10 ng/mL, or 50 ng/mL. Unseeded braided collagen scaffolds were used as controls. Seeded braided collagen scaffolds were cultured at 37ºC for 24 hours before fixing in 4% paraformaldehyde solution in PBS (USB, Cleveland, OH) for 20 minutes at room temperature. Scaffolds were washed twice for 5 minutes in PBS, and stored in PBS at 4ºC until imaging. In order to image the braided scaffolds, they were removed from the PDMS ring (*Figure 14A*) and placed on a glass slide covered with enough PBS to maintain hydration throughout the imaging process (*Figure 14B*). For each condition, 8 to 14 scaffolds were imaged from 4 separate experiments by fluorescence microscopy on an Olympus IX81 motorized inverted microscope coupled to a 12-bit Hamamatzu CCD camera and processed using Slidebook® (*Figure 14C*). Imaging locations were chosen for cell quantification at 10X magnification in nonoverlapping focal regions across the entire length of the scaffold by placing it on the slide parallel to the x-axis. This resulted in 5 to 18 images per scaffold depending on the number of focal regions in the z-direction.

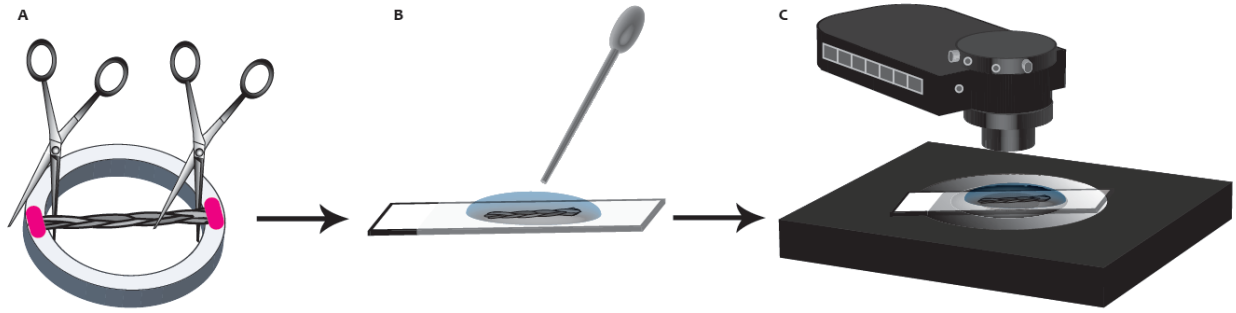

Figure 14: Fluorescence microscopy procedure

In order to image the seeded braided scaffolds, they were removed from the PDMS ring (A) and placed on a glass slide covered with enough PBS to maintain hydration throughout the imaging process (B). For each condition, 8 to 14 scaffolds were imaged from 4 separate experiments by fluorescence microscopy (C). Imaging locations were chosen for cell quantification at 10X magnification in nonoverlapping focal regions across the entire length of the scaffold by placing it on the slide parallel to the x-axis.

The images were analyzed using Image J software with the grid and cell counter plug-in for cell attachment and cell distribution across the length of the scaffold. A grid was placed on each image with an area of 10,000 μm^2 (1.55 pixels/μm) between each grid line (*Figure 15A*). Using the cell counter plug-in, raw data was collected from each image as the average number of Hoechst dye stained nuclei counted in four separate regions (*Figure 15B*). Not all of the cells are in the focal plane of the each image because of the limited focal depth when imaging three-dimensional scaffolds. As such, the data was normalized by reporting it as the number of cells within an area of 10,000 μm^2. To determine whether there was an equal cell distribution across length of the braided collagen scaffold, cells were counted using the procedure described above for images taken every 900 μm along the length of the scaffold (*Figure 16*). Although the majority of the scaffolds were seeded over the entire surface area, for the purposes of this cell attachment assay and cell distribution, only one side of the braided scaffold was analyzed. There was no difference in seeding throughout the surface area of the scaffold.

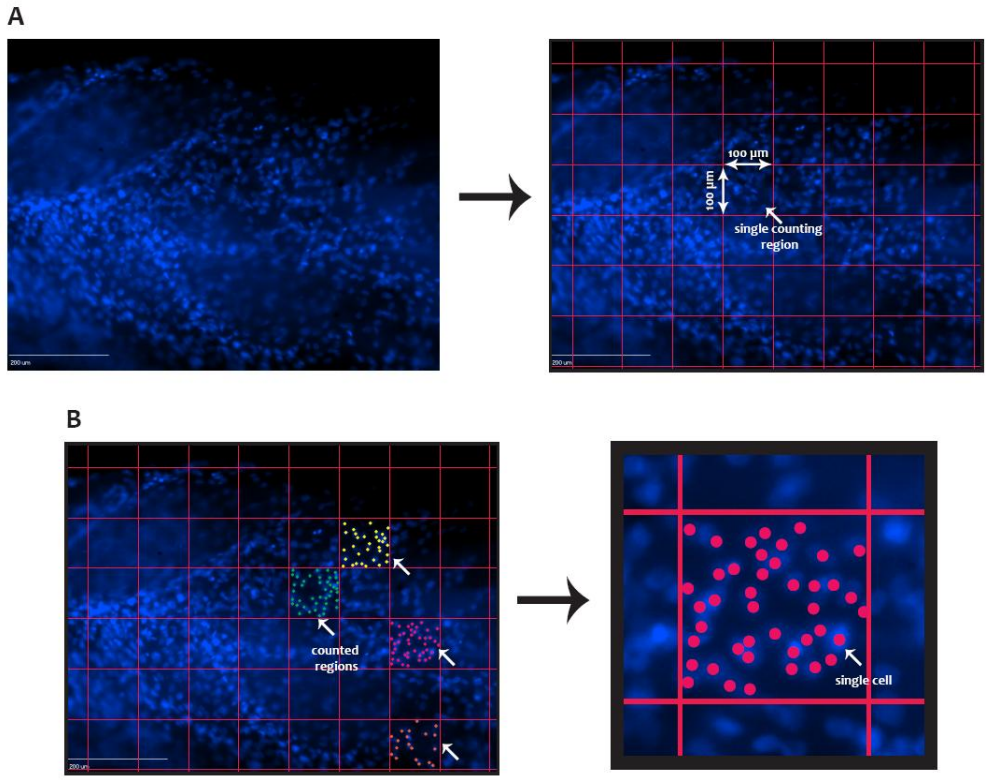

Figure 15: Image analysis procedure

The images were analyzed using Image J software with the grid and cell counter plug-in for cell attachment and cell distribution across the length of the scaffold. A grid was placed on each image with an area of 10,000 µm^2 (1.55 pixels/µm) between each grid line (A). Using the cell counter plug-in, raw data was collected from each image as the average number of Hoechst dye stained nuclei counted in four separate regions (B).

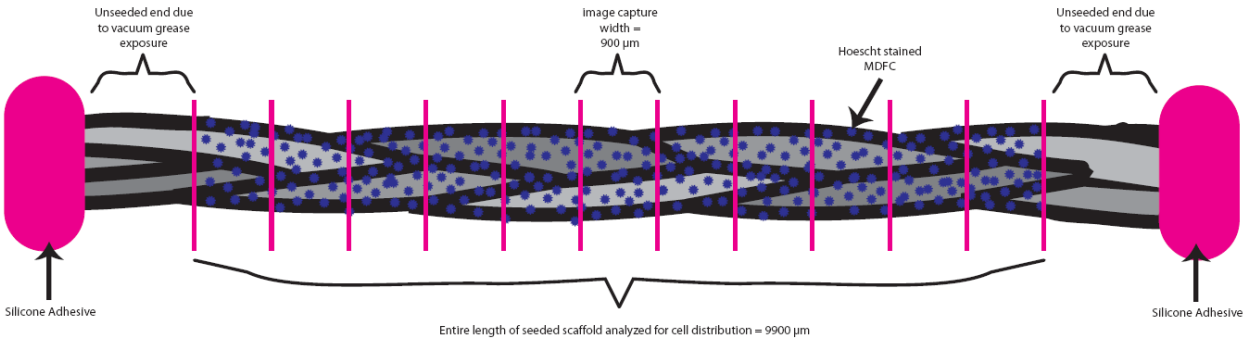

Figure 16: Diagram of MDFCs on braided collagen scaffold for cell distribution analysis

To determine whether there was an equal cell distribution across length of the braided collagen scaffold, cells were counted for images taken every 900 µm along the length of the scaffold.

4.8.2. Cell Growth

To determine the effects of different surface biochemistries on the growth of MDFCs on braided collagen scaffolds, MDFCs preloaded with Hoechst dye were seeded as described above onto uncrosslinked scaffolds and scaffolds treated with EDC/NHS, EDC/NHS with heparin, and EDC/NHS with heparin coated with FGF-2 at concentrations of either 5 ng/mL, 10 ng/mL, or 50 ng/mL. Unseeded scaffolds were used as controls. Seeded braided collagen scaffolds were cultured at 37ºC moving the scaffolds to a new sterile 12 well plate with fresh medium every other day to prevent contamination during extended culture periods. Scaffolds were cultured for 5 days and 7 days before fixing in 4% paraformaldehyde solution in PBS for 20 minutes at room temperature. Scaffolds were washed twice for 5 minutes in PBS, and stored in PBS at 4ºC until imaging. Seeded scaffolds cultured for 5 and 7 days were analyzed for cell growth in the same manner as described previously for cell attachment and cell distribution.

4.8.3. Estimation of Total Cell Attachment and Growth

To compare the cell attachment and growth to results found in literature, the total number of cells attached to the braided collagen at each time point needed to be approximated. The cross sectional perimeter was established using the histological sections of three hematoxylin and eosin stained unseeded braided collagen threads. The outer edge of the scaffolds was traced using Image J software in order to obtain an approximate surface perimeter. To account for the differences in surface topography on the scaffold, sections were measured at four different locations along the length of the scaffold and averaged together. When the braided collagen scaffold is placed inside the PDMS mold, the ends of the scaffold are exposed to sterile vacuum grease, which prevents MDFCs from attaching beyond this boundary. Using the cell distribution data, the length of the seeded area of the braided collagen scaffold can be determined. Using the

assumption that all sides have been seeded with MDFCs, the total surface area of the braided collagen scaffold can be determined by multiplying the cross sectional perimeter by the length of the seeded area of the braid. Using this information, the total number of MDFCs attached to the surface at each time point can be extrapolated by multiplying the number of cells counted per 10,000 μm^2 region by the total seeded surface area. In addition to total cell attachment and growth calculations, the percentage of the cells seeded that attached to the surface and the fold increases of the cells over time was calculated. The increase in cell number over the number of cells that attached, T_d, was calculated using the following equation, where q_1 is the average number of cells attached for each surface modification and q_2 is the number of cells at counted at 5 and 7 days.

$$T_d = \frac{q_2}{q_1}$$

4.9. Qualitative Analysis of Cell Density and Cellular Alignment

The procedures described in this section focus on the analysis of how the surface modifications affect cell density and cellular alignment. These assays were run to determine how the cells were interacting with the surfaces after specific durations.

4.9.1. Histological Analysis of Cell Density

To assess cell density and nuclei conformation on braided collagen thread scaffolds, cell outgrowth and alignment were evaluated after 1 or 7 days with each surface modification type as well as unseeded controls. Scaffolds were fixed in 4% paraformaldehyde solution in PBS for 40 minutes at room temperature, washed twice for 5 minutes in PBS. Prior to placement in tissue cassettes (Fisher Scientific, Pittsburg, PA), samples were embedded in 2% (wt/ vol) Lonza SeaKem LE Agarose (Fisher Scientific, Pittsburg, PA) in distilled water to maintain the structural characteristics of the braid, and then all samples in tissue cassettes were placed into

70% (vol/ vol) ethanol overnight. Next, scaffolds were processed for embedding by dehydrating in a series of increasing concentrations of ethanol, from 70% (vol/ vol) to 100% (vol/ vol), cleared with xylene, and embedded in paraffin wax at 60ºC. Samples were embedded to analyze the cross section of the braid by cutting the braid orthogonal to the long axis and mounting the cut pieces vertically in the paraffin. Sections were cut at 5 µm on a rotary microtome (Nikon), mounted on Superfrost Plus slides (VWR, West Chester, PA) with Permount (Fisher Scientific, Pittsburg, PA), and stained with Modified Harris Hematoxylin and Eosin (H&E; Richard-Allan Scientific, Kalamazoo, MI). Sections were imaged using an Olympus IX81 motorized inverted microscope coupled to a 12-bit Hamamatzu CCD camera and processed using Slidebook® to determine cell density.

4.9.2. Fluorescence Microscopic Analysis of Cell Density and Cellular Alignment

To determine MDFC alignment and orientation on braided collagen scaffolds, scaffolds were seeded with MDFCs, incubated and stained to illuminate the f-actin filaments. Braided collagen scaffolds of each type were assembled and seeded as described previously and incubated for 1, 5, or 7 days. After incubation for the designated period, scaffolds were rinsed twice in PBS and fixed with 4% paraformaldehyde solution in PBS for 20 minutes at room temperature. Scaffolds were then rinsed twice in PBS for 5 minutes and stained with 165 mM Alexafluor 488 phalloidin (Molecular Probes, Eugene, OR) for 45 minutes. To image the braided scaffolds, they were removed from PDMS rings and placed on a glass slide covered with enough PBS to maintain hydration throughout the imaging process. To analyze cell density, scaffolds were imaged by fluorescence microscopy on an Olympus IX81 motorized inverted microscope coupled to a 12-bit Hamamatzu CCD camera and processed using Slidebook® under 4X magnification to visualize the Hoechst stained nuclei. Cellular alignment was determined by

removing scaffolds incubated for 1 or 7 days from PDMS rings (*Figure 17A*) and placing them into 35 mm diameter glass bottom culture dishes with a 10 mm diameter cover slip in the middle with a thickness of 0.19 mm (MatTek Corporation, Ashland, MA). The braids were held flat against the cover glass surface using vacuum grease and covered with enough PBS to maintain hydration throughout the imaging process (*Figure 17B*). The scaffolds were imaged using fluorescence microscopy on a Leica TCS SP5 II point scanning confocal microscope (Leica Microsystems Inc., Bannockburn, IL) under an oil immersion 20X magnification lens to visualize the nuclei and f-actin filaments. Images were taken along the z-axis at a depth of 100 to 150 μm of the braided collagen scaffold. Cellular alignment was qualitatively analyzed by determining if the cells aligned with the curvature of the braids or parallel to the x-axis after 7 days in culture.

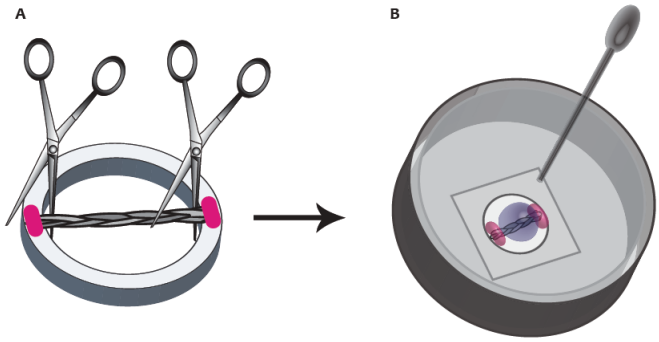

Figure 17: Confocal microscope procedure for imaging

Cellular alignment was determined by removing scaffolds incubated for 1 or 7 days from PDMS rings (A) and placing them into 35 mm diameter glass bottom culture dishes with cover slip in the middle. The braids were held flat against the cover glass surface using vacuum grease and covered with enough PBS to maintain hydration throughout the imaging process (B). The scaffolds were imaged using fluorescence microscopy on a confocal microscope.

4.10. Statistics

Statistical analyses were executed using SigmaPlot 11.0 (Systat Software, Inc, Point Richmond, CA). For the mechanical data analysis, statistical differences between the uncrosslinked and crosslinked samples were evaluated using a Student's T-test or the Mann

Whitney Rank Sum test for cases of unequal variance. For all cell-based assay experiements, statistical difference between scaffolds was analyzed using one-way analysis of variance (ANOVA) with Holm-Sidak post hoc testing. In cases where data failed the normality test an ANOVA on Ranks followed by a Dunn's post hoc test was used since the group sizes were unequal. Significance was established for $p < 0.05$.

Chapter 5: Results

5.1. Braided Collagen Scaffold Material Characterization

5.1.1. Characterization of Localized FGF-2

To verify and characterize the localization of FGF-2 on braided collagen scaffolds, different concentrations of FGF-2 were bound to single collagen threads that were crosslinked with EDC/NHS in the presence of heparin. The threads were immunostained and the results are shown in Figure 18. Threads crosslinked with EDC/NHS and heparin in the presence of FGF-2 showed FGF-2 on the surfaces of the threads when compared to the control braids that were crosslinked with EDC/NHS and heparin, but not exposed to FGF-2 (*Figure 18A*). Immunocytochemical analysis of threads exposed to 5 ng/mL FGF-2 showed FGF-2 having inconsistent coverage on the surface (*Figure 18B*). To determine further if this inconsistency was due to an imaging artifact, it would be beneficial to image the threads using a scanning confocal microscope. Although it is apparent that FGF-2 was present on the surface, it is not uniform along the length of the thread. Threads exposed to 10 ng/mL FGF-2 (*Figure 18C*) and 50 ng/mL FGF-2 (*Figure 18D*) showed similar localization and uniform coverage of FGF-2 along the length of the thread. Threads exposed to 50 ng/mL FGF-2 seem to have a more FGF-2 bound to the surface due to the higher fluorescence intensity across the whole surface. However, these differences were not evaluated quantitatively.

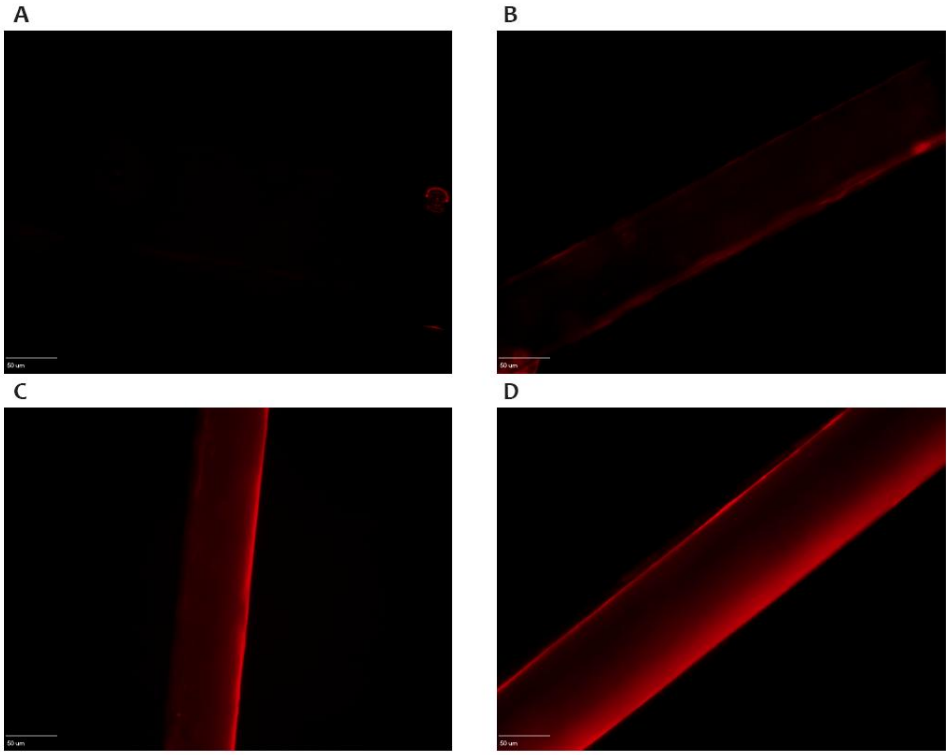

Figure 18: Immunocytochemistry verifying the presence of FGF-2 on collagen threads

EDC/NHS crosslinked collagen threads with heparin (A), and EDC/NHS crosslinked with heparin and passively adsorbed with 5 ng/mL (B), 10 ng/mL (C), or 50 ng/mL FGF-2 (D). Scale bar = 200 μm

5.1.2. Mechanical Testing of Braided Collagen Scaffolds

To characterize the mechanical properties of braided collagen scaffolds, uncrosslinked and EDC/NHS crosslinked braids were loaded under uniaxial tension until failure. The results of this analysis are summarized in Table 5. Raw data including individual measurements for each braid, cross-sectional area calculations, and statistics can be found in Appendix A: Mechanical Testing Data Analysis. Characteristic load-elongation curves for each of the individual uncrosslinked and crosslinked braided collagen scaffolds showed a generally linear shape with the scaffold failure occurring as the first of the three internal braids fails (*Figure 19*). After the point of ultimate failure, the load drops in an incremental manner until each of threads has broken. In addition, each individual braid shows similar curves demonstrating that the

production of the braided collagen scaffold from self-assembled type I collagen microthread extrusion to braid development is consistent and reproducible.

	Sample Size	Cross-sectional Area (mm^2 ± SD)	Ultimate Load (N ± SD)	UTS (MPa ± SD)	Strain at Failure (mm/mm ± SD)	Maximum Tangent Modulus (MPa ± SD)
Uncrosslinked	16	0.115 ± 0.025∗	0.591 ± 0.076∗	5.130 ± 0.662∗	0.420 ± 0.064∗	13.60 ± 2.668∗
Crosslinked	16	0.072 ± 0.013	1.979 ± 0.237	26.97 ± 2.835	0.516 ± 0.118	68.52 ± 8.242

Table 5: Mechanical properties summary table for braided collagen microthreads

∗ Indicates statistically significant differences between uncrosslinked and crosslinked braided collagen scaffolds with $p < 0.05$ using Mann-Whitney Rank Sum Test.

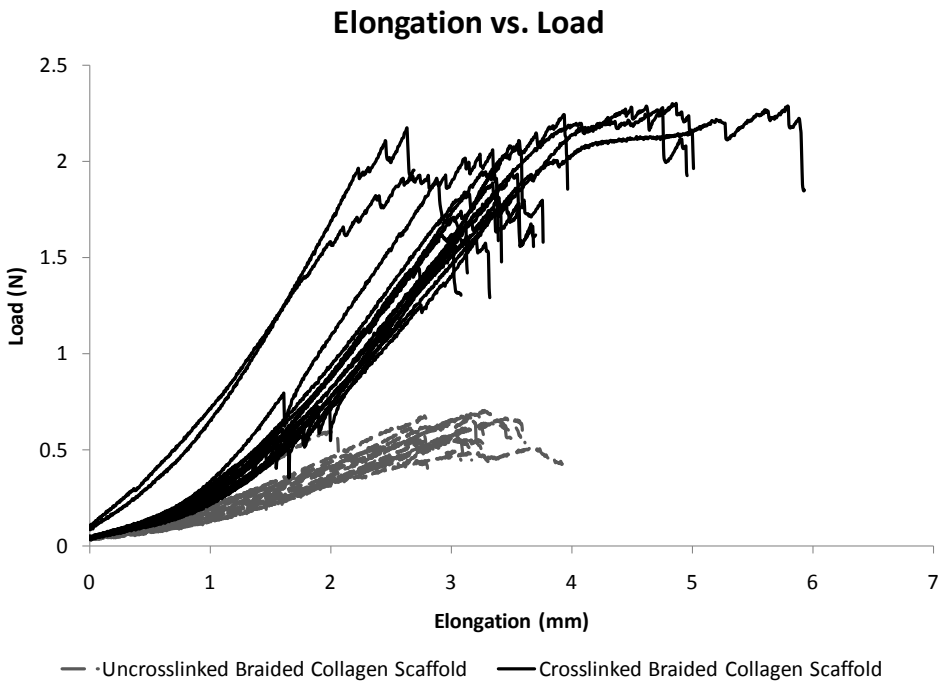

Figure 19: Characteristic load-elongation relationship for braided collagen microthreads

Characteristic load-elongation curves for each of the individual uncrosslinked and EDC/NHS crosslinked braided collagen scaffolds showed a generally linear shape with the scaffold failure occurring as the first of the three internal braids fails (n = 16)

In order to calculate the stress-strain curves of the braids, the cross-section areas were calculated using the histological cross-sections of hydrated braids. The average cross-sectional area of an uncrosslinked and crosslinked braided collagen scaffold was calculated to be 0.115 ±

0.025 mm^2 (*Figure 20A*) and 0.072 ± 0.013 mm^2 (*Figure 20B*) respectively. The representative stress-strain curves comparing uncrosslinked to crosslinked braids also shows they are roughly linear in shape with crosslinked threads withstanding a greater amount of stress per unit strain (*Figure 21*). The curve measurements allow for the measurement of the maximum tangent modulus (MTM) of each sample to be calculated as the maximum slope of the stress-strain curve. Relative to uncrosslinked braided collagens scaffolds, the ultimate load and ultimate tensile strength of crosslinked scaffolds were increased significantly by crosslinking using EDC/NHS (*Figure 22A* and *Figure 22B*). The crosslinked braids were able withstand an ultimate load almost three times that of uncrosslinked scaffolds. Similarly, the strain at failure and maximum tangent modulus of the crosslinked scaffolds were significantly higher relative to uncrosslinked collagen scaffolds (*Figure 23A* and *Figure 23B*). Even though the crosslinked braids are approximately five times stiffer than uncrosslinked scaffolds, the crosslinked braids have a significantly increased strain at failure.

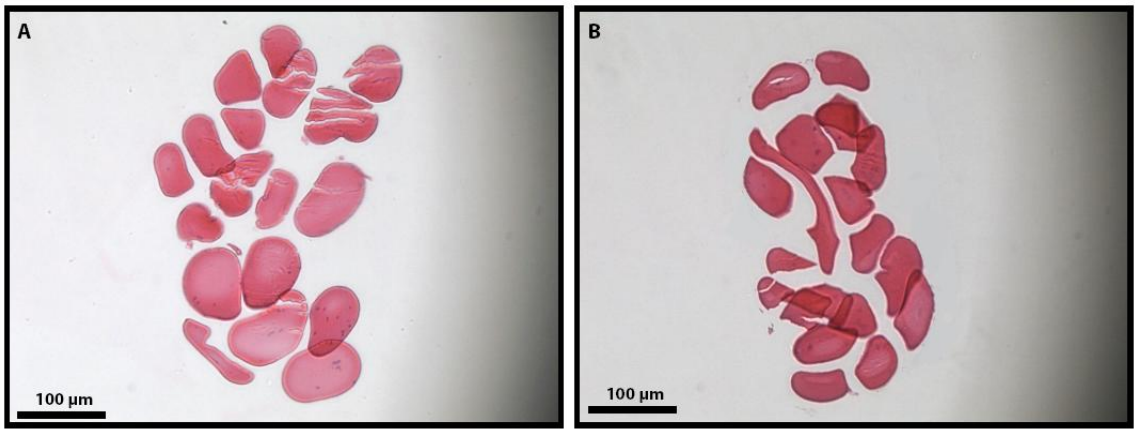

Figure 20: Cross-sections of braided collagen threads

H&E stained histological cross-sections of uncrosslinked (A) and EDC/NHS crosslinked (B) braided collagen threads. Scale bar = 100 µm.

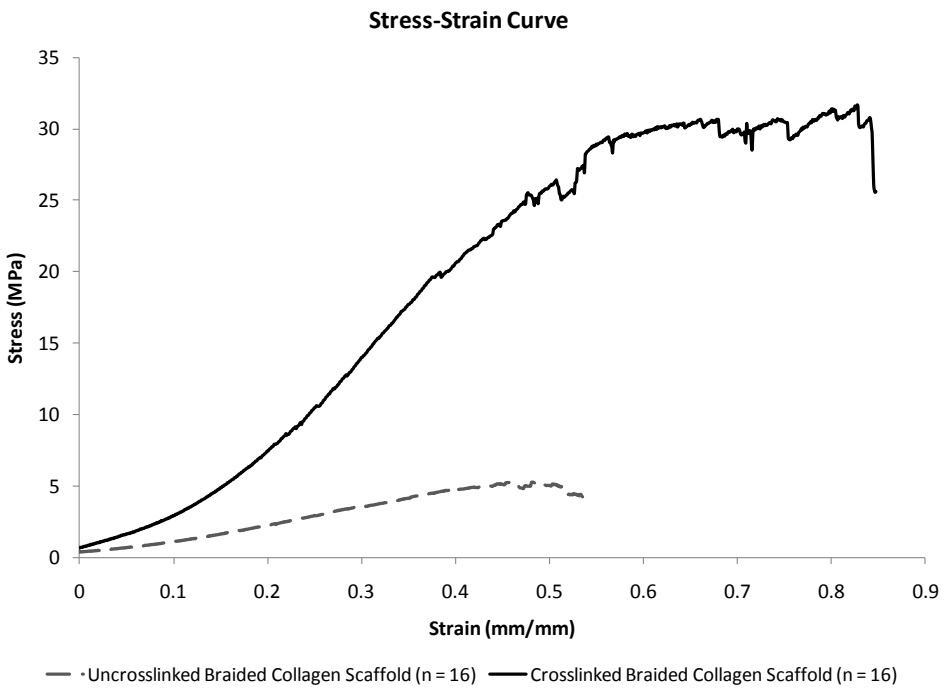

Figure 21: Characteristic stress-strain curve relationship for braided collagen microthreads

The representative stress-strain curves comparing uncrosslinked to crosslinked braids also show they are roughly linear in shape with crosslinked threads withstanding a greater amount of stress per unit strain (n = 16).

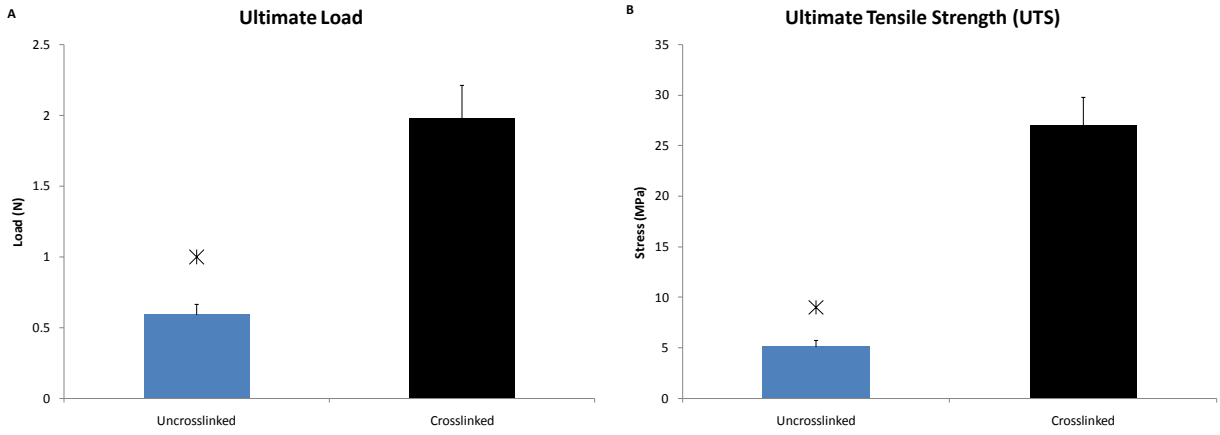

Figure 22: Ultimate Load and UTS at failure for braided collagen microthreads

Ultimate Load (A) and UTS (B). ✳ Indicates $p < 0.05$ using Mann-Whitney Rank Sum Test. Bars indicate mean ± SD (each representing the data in Table 5 having n = 16).

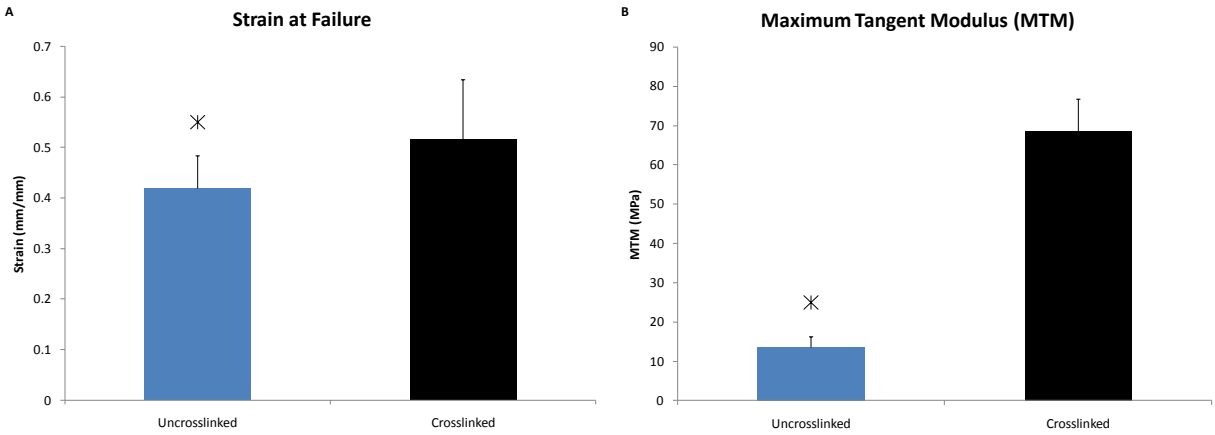

Figure 23: Strain at failure and maximum tangent modulus for braided collagen microthreads

Strain at failure (A) and MTM (B). ✳ Indicates $p < 0.05$ using Mann-Whitney Rank Sum Test. Bars indicate mean ± SD (each representing the data in Table 5 having n = 16).

5.2. MDFC Seeding to Braided Collagen Scaffold

5.2.1. Preliminary Cell Seeding Method

In the first stage of developing a reproducible cell seeding method that allowed for quantitative analysis of MDFCs on braided collagen scaffolds, MDFCs were preloaded with Mitotracker Green and seeded onto scaffolds using a mold with a seeding channel of 2.0 mm x 12.0 mm. Following the protocol, it was found that sealing the channel with the silicone adhesive caused a fraction of the braided collagen scaffolds to break from the PDMS ring while trying to insert the braid into the wedge opening. Although the majority of the scaffolds were not damaged when they were inserted into the mold, this iteration of the PDMS cell-seeding mold does not allow for sufficient reproducibility. Compared to the unseeded braided collagen scaffold (*Figure 24A*), it appears that using the PDMS mold to seed the braided collagen scaffolds is successful since a fluorescent signal appears on the seeded scaffolds. Fluorescence microscopy images of uncrosslinked (*Figure 24B*) and crosslinked (*Figure 24C*) seeded braided collagen scaffolds show that seeding with the cell suspension method ensures that the entire

braid is exposed to the MDFCs. The results show that MDFCs attached predominately in the grooves of the braids. By visual inspection, it appeared that the uncrosslinked and crosslinked braided collagen scaffolds had similar seeding efficiencies. Unfortunately, fluorescently tagging the mitochondria within the MDFCs only allowed for qualitative analysis because the mitochondria stain did not facilitate discrete cell counting, so cell attachment differences between uncrosslinked and crosslinked scaffolds could not be analyzed. In addition, the large amount of void space in the seeding channel may not facilitate a high seeding efficiency.

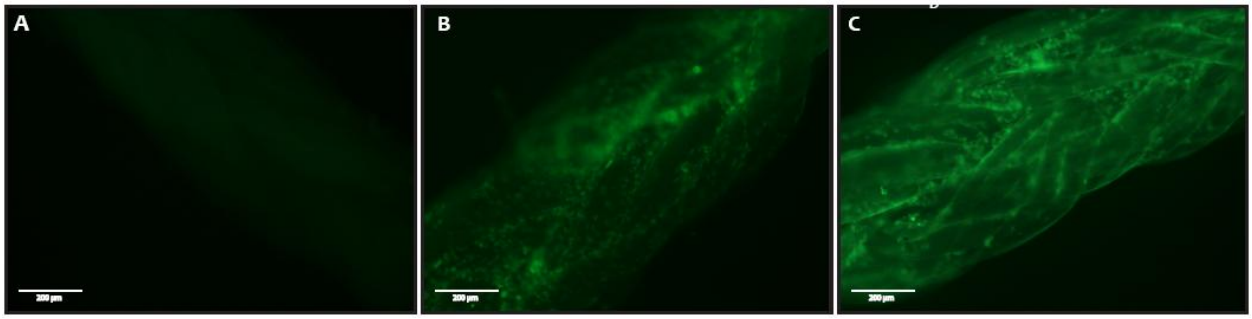

Figure 24: MDFCs labeled with Mitotracker Green on braided collagen scaffolds

Unseeded (A), uncrosslinked (B), and EDC/NHS crosslinked (C) braided collagen scaffolds. MDFCs were preloaded with Mitotracker Green prior to seeding. Scale bar = 200 µm.

5.2.2. Optimizing the Cell Seeding Method

In order to rectify the limitations discovered in the analysis of the preliminary cell seeding results, MDFCs were loaded with Hoechst dye prior to seeding onto braided collagen scaffolds instead of Mitotracker green. MDFCs were seeded onto uncrosslinked and crosslinked braided collagen scaffolds using PDMS molds with channel widths of either 2.0 mm or 1.0 mm, and the results are summarized in Table 6. Raw data including cell counts, total cell and percentage calculations, and statistics can be found in Appendix B: Optimizing Cell Seeding Method Data. Using a channel sealed with sterile vacuum grease resulted in elimination of scaffold breakage, but there was still a risk of the cell suspension leaking out of the ends of the

channel. Since more than fifty percent of the braided collagen scaffolds seeded in both PDMS mold channel types, this was not considered a significant problem. Hoechst stained images of uncrosslinked and crosslinked braided collagen scaffolds seeding using the two channel widths are shown in Figure 25. These images do not show large visual difference between the surface treatments due to limitations in imaging a three-dimension scaffold, but in contrast to scaffolds preloaded with Mitotracker green, individual cells can be distinguished from one another enabling quantitative analysis. It is apparent that the MDFCs attached onto the scaffolds seeded in the 1.0 mm wide channel more uniformly with a clear increase in cell number compared to the scaffolds seeded using the wider channel.

		Uncrosslinked	EDC/NHS
2.0 mm x 12.0 mm	**Sample Size**	3	3
	Total Scaffolds Successfully Seeded (%)	66.7	100
	MDFC Attachment (# of cells/10,000 μm^2 ± SEM)	23.4 ± 0.70	29.9 ± 1.2
	Total MDFC attachment (# cells ± SEM)	23,501 ± 704.6	30,087 ± 1,230
	Total MDFCs Successfully Seeded (% ± SEM)	11.8 ± 0.4∗	15.0 ± 0.6∗
1.0 mm x 12.0 mm	**Sample Size**	4	4
	Total Scaffolds Successfully Seeded (%)	100	75
	MDFC Attachment (# of cells/10,000 μm^2 ± SEM)	31.1 ±1.12	36.1 ± 0.91
	Total MDFC attachment (# cells ± SEM)	31,277 ± 1,038	36,356 ± 914.8
	Total MDFCs Successfully Seeded (% ± SEM)	20.9 ± 0.7	24.2 ± 0.6

Table 6: Cell seeding optimization summary table comparing different seeding channel dimensions

∗ Indicates statistically significant differences between 2.0 mm wide channels and 1.0 mm wide channels with $p < 0.05$ using Kruskal-Wallis One Way ANOVA on Ranks with Dunn's Method.

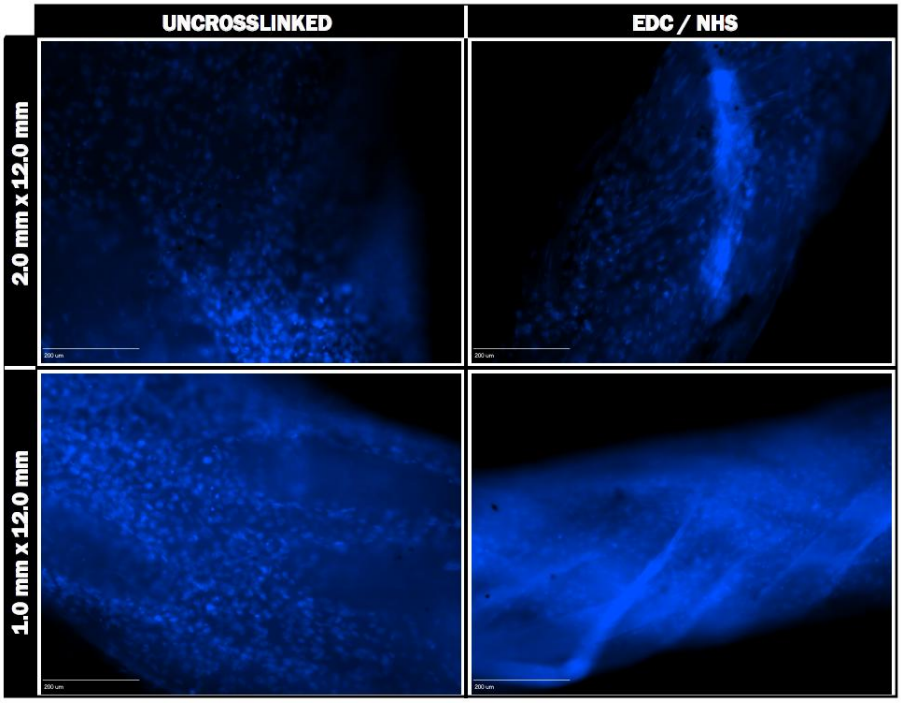

Figure 25: Hoechst stained MDFCs seeded onto braided collagen scaffolds using different methods

Fluorescence images comparing attachment of MDFCs on uncrosslinked and EDC/NHS crosslinked braided collagen scaffolds using 2.0 mm wide channels (top row) or 1.0 mm channels (bottom row) for seeding. MDFCs were preloaded with Hoechst dye. Scale bar = 200 µm.

The density of cells that attached to the braided collagen scaffolds in an area of 10,000 μm^2 were counted visually to compare the two different seeding methods. Seeding with either the 2.0 mm wide channel or the 1.0 mm wide channel showed a significant increase in cell density between uncrosslinked and crosslinked scaffolds (*Figure 26*). The results show seeding using the narrower channel significantly increased the seeding density on both uncrosslinked and crosslinked scaffolds compared to the wider channel.

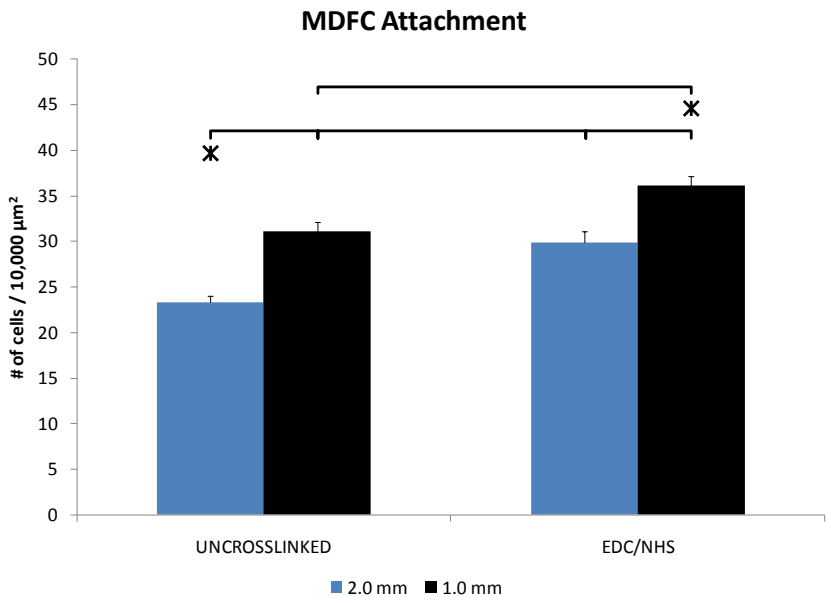

Figure 26: Comparison of MDFC attachment seeding with different channel dimensions

The density of cells that attached to the braided collagen scaffolds in an area of 10,000 μm^2 were counted visually to compare with seeding using either the 2.0 mm wide channel or the 1.0 mm wide channel showed a significant increase in cell density between uncrosslinked and crosslinked scaffolds. ∗ Indicates $p < 0.05$ using Kruskal-Wallis One Way ANOVA on Ranks with Dunn's Method. Bars indicate mean ± SEM (total n numbers indicated in Table 6).

The total number of MDFCs that attached to the braided collagen scaffold was approximated in order to determine which channel width resulted in the better seeding efficiency. As expected from the regional cell attachment counts, seeding with the narrower channel caused significantly more cells to attach to the surface compared to the wider channel with at least 6,000 more cells attached in both uncrosslinked and crosslinked scaffolds (*Figure 27*). Since the channels were seeded with different cell suspension concentrations to adjust for the different channel volumes, the total cell attachment was normalized by calculating the percentage of MDFCs used in the cell suspension that actually seeded (*Figure 28*). Using the narrower channel to seed MDFCs resulted in 20-25% of the cells in the suspension attaching to the braided collagen scaffold, which was significantly higher than the wider channel, which resulted in less than 15% attachment on each surface modification.

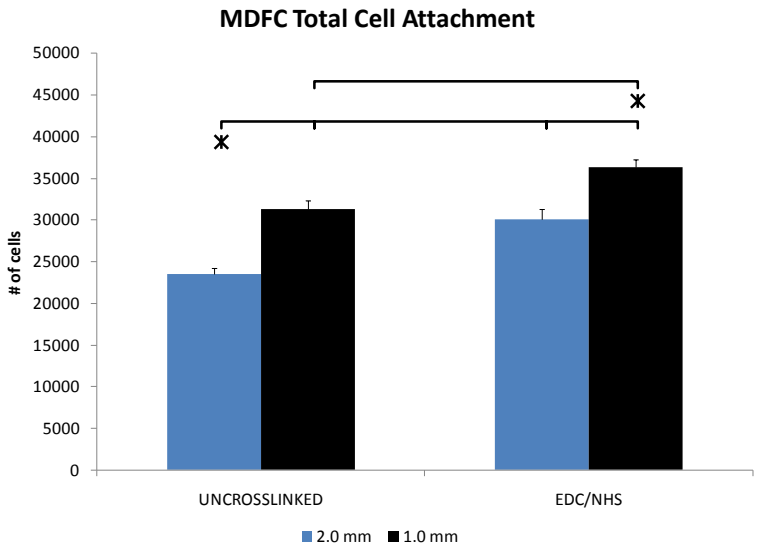

Figure 27: Comparison of total MDFC attachment seeing with different channel dimensions

The total number of MDFCs that attached to the braided collagen scaffold was approximated in order to determine which channel width resulted in the better seeding efficiency. Seeding with the narrower channel caused significantly more cells to attach to the surface compared to the wider channel with at least 6,000 more cells attached in both uncrosslinked and crosslinked scaffolds. ∗ Indicates $p < 0.05$ using Kruskal-Wallis One Way ANOVA on Ranks with Dunn's Method. Bars indicate mean ± SEM (total n numbers indicated in Table 6).

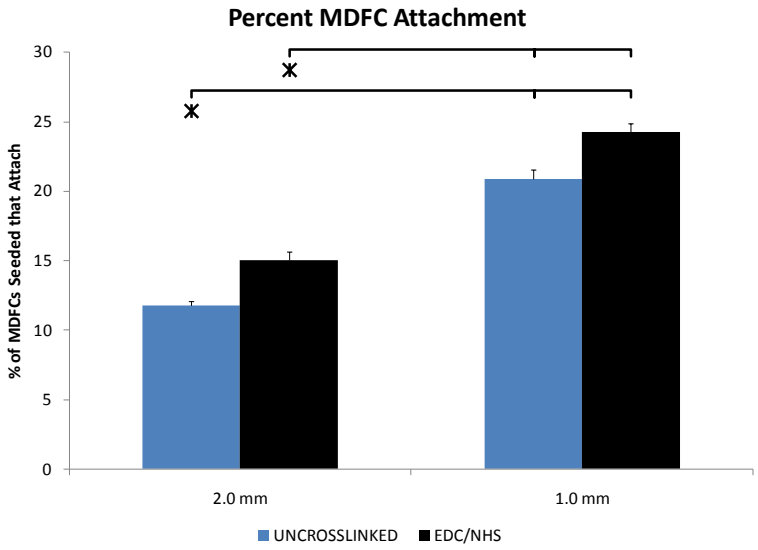

Figure 28: Percentage of MDFCs seeded that attached to the braided collagen scaffold

Since the channels were seeded with different cell suspension concentrations to adjust for the different channel volumes, the total cell attachment was normalized by calculating the percentage of MDFCs used in the cell suspension that actually seeded. ∗ Indicates $p < 0.05$ using Kruskal-Wallis One Way ANOVA on Ranks with Dunn's Method. Bars indicate mean ± SEM (total n numbers indicated in Table 6).

5.3. Quantification of Cell Number on Different Surface Modifications

Based on the results of the development of the cell seeding protocol, all further cell attachment and growth experiments, MDFCs were loaded with Hoechst dye prior to seeding to allow for quantitative analysis. In addition, due to the higher seeding efficiency, the narrower channels were used for all future attachment and growth experiments.

5.3.1. Cell Attachment

In order to determine the effects of surface modifications on MDFC attachment, braided collagen scaffolds with different surface modifications were seeded with MDFCs and incubated for 24 hours. The results of the cell attachment assay are summarized in Table 7, with the raw cell counts from each scaffold including statistics in Appendix C.1: Cell Attachment Data. Fluorescence images of the Hoechst dye stained braided collagen scaffolds are shown in Figure 29. The MDFCs seeded uniformly spread over the entire surface of the braided collagen scaffold. The images show a clear increase in cell attachment from the uncrosslinked scaffold surface (*Figure 29A*) to the crosslinked and FGF-2 bound scaffold surfaces. The EDC/NHS HEP (*Figure 29C*) braided collagen scaffold appears to have a higher density of cells compared to the EDC/NHS (*Figure 29B*), 5 ng/mL FGF-2 (*Figure 29D*), 10 ng/mL FGF-2 (*Figure 29E*), and 50 ng/mL FGF-2 (*Figure 29F*) braided collagen scaffolds.

	Sample Size	MDFC Attachment (# of cells / 10,000 μm^2 ± SEM)
UNCROSSLINKED	13	34.9 ± 0.69∗
EDC/NHS	13	41.6 ± 0.76
EDC/NHS HEP	11	46.5 ± 0.99†
5 ng/mL FGF2	12	40.3 ± 0.73
10 ng/mL FGF2	8	39.2 ± 0.70
50 ng/mL FGF2	8	40.7 ± 0.99

Table 7: Cell Attachment summary table comparing different surface modifications

∗ Indicates statistically significant differences between uncrosslinked and all other conditions with $p < 0.05$ using Kruskal-Wallis One Way ANOVA on Ranks with Dunn's Method. † Indicates statistically significant differences between uncrosslinked and all other conditions with $p < 0.05$ using Kruskal-Wallis One Way ANOVA on Ranks with Dunn's Method.

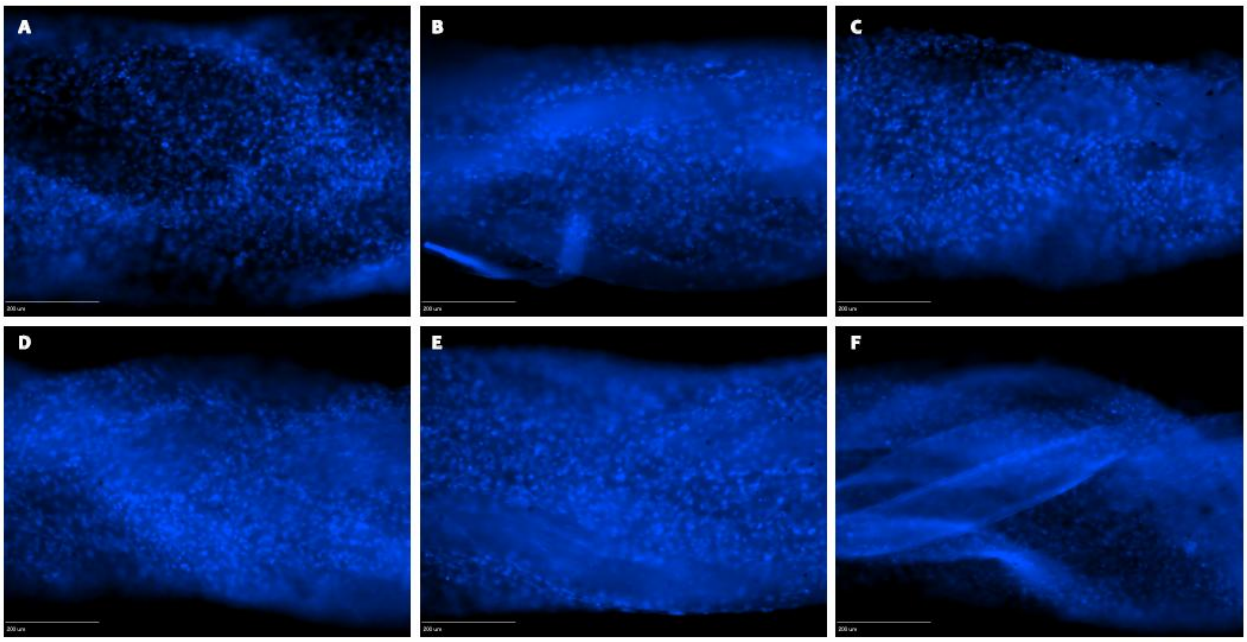

Figure 29: Hoechst stained MDFCs on braided collagen scaffolds on day 1

Uncrosslinked (A), EDC/NHS (B), EDC/NHS HEP (C), 5 ng/mL FGF-2 (D), 10 ng/mL FGF-2 (E), and 50 ng/mL FGF-2 (F); Scale bar = 200 μm.

The density of cells that attached to the braided collagen scaffolds in an area of 10,000 μm^2 were counted visually to compare how surface modifications affected cell attachment (*Figure 30*). There was a significant increase in cell attachment from uncrosslinked braided

collagen scaffolds to braids with surface modifications. Braided collagen scaffolds that were EDC/NHS crosslinked with heparin promoted a significantly higher cell attachment to its surface than all other scaffold surfaces. Increasing the amount of FGF-2 bound to the surface does not significantly affect cell attachment. There was not a significant difference in cell attachment between EDC/NHS crosslinked scaffolds and all scaffolds with FGF-2 bound to the surface.

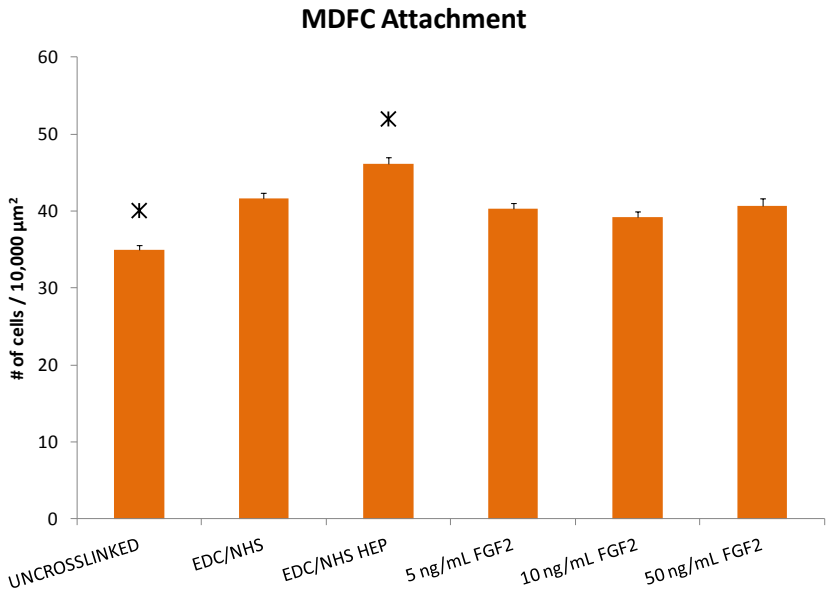

Figure 30: MDFC attachment for different surface modifications

The density of cells that attached to the braided collagen scaffolds in an area of 10,000 µm^2 were counted visually to compare how surface modifications affected cell attachment. ✳ Indicates $p < 0.05$ using Kruskal-Wallis One Way ANOVA on Ranks with Dunn's Method. Bars indicate mean ± SEM (total n numbers indicated in Table 7).

To determine if seeding using the PDMS mold distributes the MDFCs uniformly across the entire length of the scaffold, images were taken in adjacent regions across the entire length of the braids and cells were counted. The results are reported as the average number of cells per 10,000 µm^2 for every 900 µm across the scaffolds on the x-axis (*Figure 31*). The raw data for each scaffold can be found in Appendix C.2: Summary of Cell Distribution Data. These results show that using the PDMS mold to seed the braided collagen scaffolds resulted in uniform distribution across the length of the braid, with approximately 7,392 ± 1,669 µm of the scaffold

being exposed to cells on average. Although only one side of the scaffold was analyzed for cell distribution, it was apparent from visual analysis that the majority of the scaffolds seeded uniformly across the entire surface area.

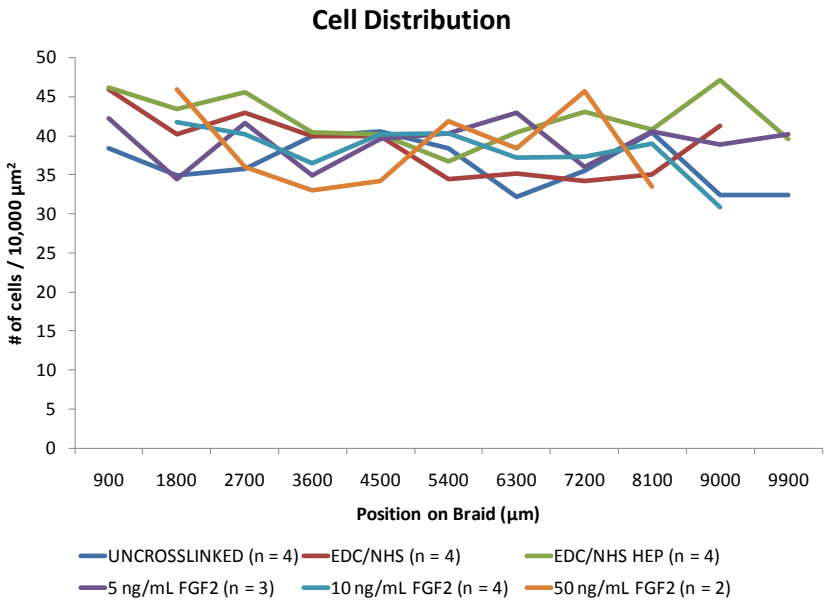

Figure 31: Cell distribution on braided collagen scaffolds after 1 day

Images were taken in adjacent regions across the entire length of the braids and cells were counted to determine cell distribution. The results are reported as the average number of cells per 10,000 µm^2 for every 900 µm across the scaffolds on the x-axis.

5.3.2. Cell Growth

The effect of binding FGF-2 on MDFC growth and proliferation was determined by seeding MDFCs and incubating them on the braided collagen scaffolds for 1 day, 5 days, or 7 days. The results of the cell growth assay are summarized in Table 8, with raw cell counts from each scaffold including statistics in Appendix D: Cell Growth Data. Fluorescence images of Hoechst dye stained braided collagen scaffolds are shown in Figure 32. During incubation, MDFCs seeded uniformly showing a minor increase in cell concentration in the grooves of the braid topography, and by the seventh day, cells have completely spread out to cover the surface of the braid. All braided scaffolds showed an increase in cell density from 1 day to 7 days

showing most of the growth happening between 5 and 7 days. The greatest overall cellular growth appears to occur within the scaffolds with FGF-2 bound to the surface.

	1 DAY		5 DAYS		7 DAYS	
	Sample Size	$\frac{\#\ of\ cells}{10{,}000\ \mu m^2} \pm SEM$	Sample Size	$\frac{\#\ of\ cells}{10{,}000\ \mu m^2} \pm SEM$	Sample Size	$\frac{\#\ of\ cells}{10{,}000\ \mu m^2} \pm SEM$
UNCROSSLINKED	13	34.9 ± 0.69	10	37.0 ± 0.91	10	47.7 ± 0.89†
EDC/NHS	13	41.6 ± 0.76	10	44.1 ± 0.79†	9	50.8 ± 1.07†
EDC/NHS HEP	11	46.5 ± 0.99	9	46.2 ± 0.75	9	53.3 ± 1.26∗
5 ng/mL FGF-2	12	40.3 ± 0.73	9	47.1 ± 0.77∗	9	55.6 ± 1.18∗
10 ng/mL FGF-2	8	39.2 ± 0.70	10	42.5 ± 0.71∗	10	63.5 ± 1.36††
50 ng/mL FGF-2	8	40.7 ± 0.99	8	44.8 ± 0.91	9	73.2 ± 1.63††

Table 8: Cell growth summary table comparing different surface modifications

∗ Indicates statistically significant differences between the growth of that surface modification at that day and the growth at all previous days with $p < 0.05$ using Kruskal-Wallis One Way ANOVA on Ranks with Dunn's Method. † Indicates statistically significant differences between the growth of that surface modification at that day and the growth at all previous days with $p < 0.05$ using One Way ANOVA with Holm-Sidak method. †† Indicates statistically significant differences between 10 ng/mL FGF-2 and 50 ng/mL FGF-2 and all other modifications at 7 days as well as statistically significant differences between the cell growth of these modifications at 7 days and the growth at 1 day and 5 days with $p < 0.05$ using Kruskal-Wallis One Way ANOVA on Ranks with Dunn's Method.

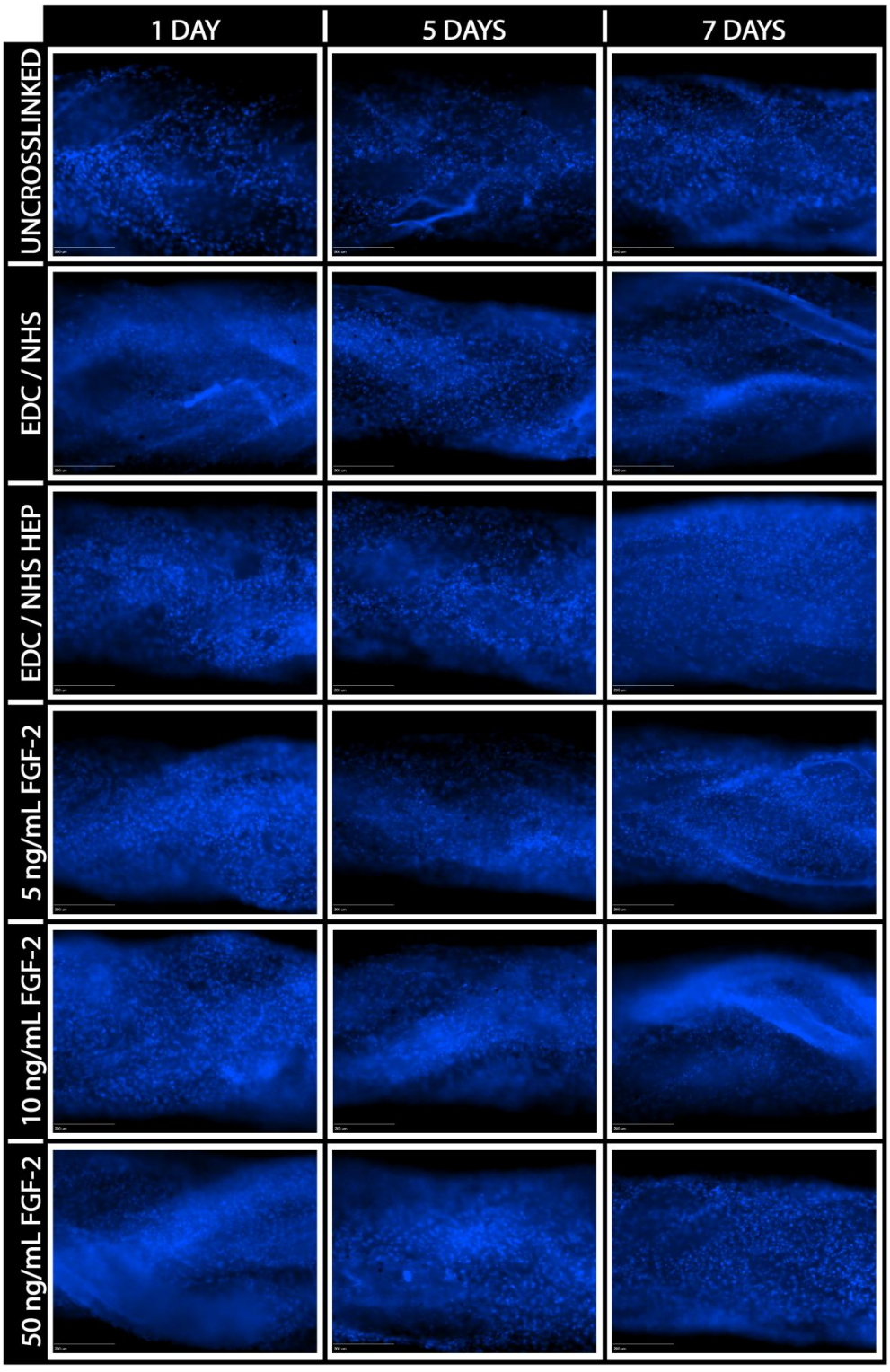

Figure 32: Hoechst stained images of MDFC Growth on braided collagen scaffolds

Hoechst stained images of MDFC growth at 1 day, 5 days, and 7 days (columns) on uncrosslinked, EDC/NHS crosslinked, EDC/NHS crosslinked with heparin, and EDC/NHS crosslinked with heparin and 5 ng/mL, 10 ng/mL, or 50 ng/mL FGF-2 braided collagen scaffolds (rows). Scale bar = 200 µm.

The density of cells that attached to the braided collagen scaffolds in an area of 10,000 μm^2 were counted visually to compare how surface modifications affected cell growth after 7 days in culture (*Figure 33*). The concentration of MDFCs on the surface of the braids increased on both control and modified braids between day 1 and day 7. After 5 days in culture, the number of cells on each of the braid types did not increase significantly except for cells attached to braids modified with EDC/NHS crosslinking and 5 ng/mL and 10 ng/mL of FGF2. Uncrosslinked scaffolds had significantly fewer cells on the surface than all other scaffold types, and scaffolds modified with 5 ng/mL FGF-2 had a significantly higher cell densities than all other braids except types modified with EDC/NHS and heparin and 50 ng/mL FGF-2. By day 7, all braided collagen scaffolds showed a significant increase in cell concentration compared to day 1. In addition, between day 5 and day 7, scaffolds modified with different concentrations of FGF-2 showed a significant increase in cell growth compared to the controls with increasing levels of FGF-2 (*Figure 34*).

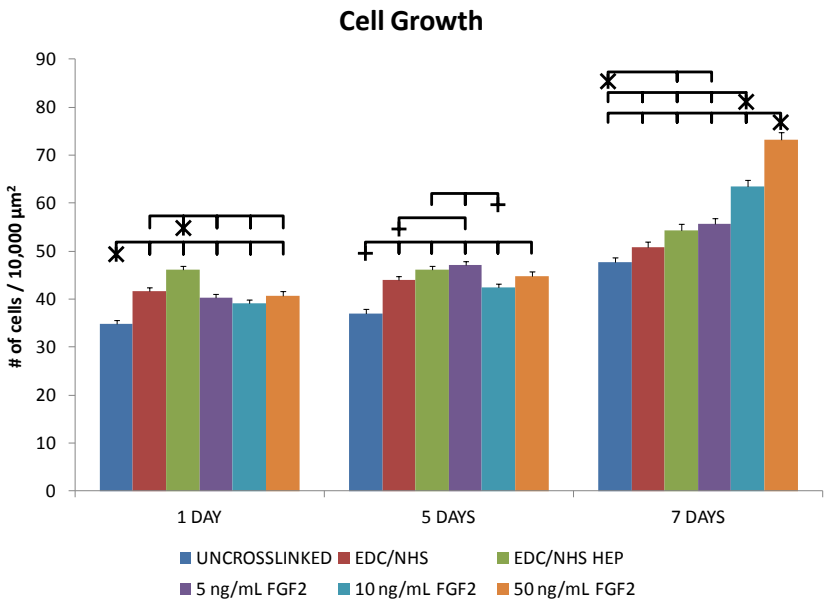

Figure 33: Cell growth comparison of different surface modifications

∗ Indicates $p < 0.05$ using Kruskal-Wallis One Way ANOVA on Ranks with Dunn's Method, and † indicates $p < 0.05$ using One Way ANOVA with Holm-Sidak method. Bars indicate mean ± SEM (total n numbers indicated in Table 8).

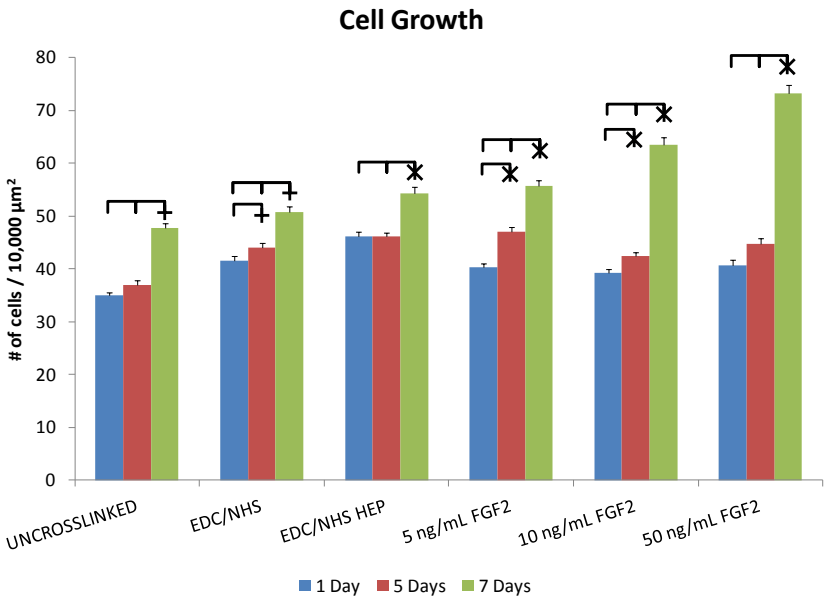

Figure 34: Cell growth comparison after 7 days in culture

∗ Indicates $p < 0.05$ using Kruskal-Wallis One Way ANOVA on Ranks with Dunn's Method, and † indicates $p < 0.05$ using One Way ANOVA with Holm-Sidak method. Bars indicate mean ± SEM (total n numbers indicated in Table 8).

The cell distribution data for the cell growth over 7 days on the different surface modifications shows the cells grow evenly along the length of the scaffold (*Figure 35*). The raw data for each scaffold can be found in Appendix C.2: Summary of Cell Distribution Data, Appendix D.4: Summary of Cell Distribution Data – 5 Days, and Appendix D.5: Summary of Cell Distribution Data – 7 Days. The trend of the distribution lines (solid) fluctuate around the average cell growth (dashed) for each braided scaffold with minimal changes between 1 and 5 days. Interestingly, scaffolds loaded with 10 ng/mL and 50 ng/mL FGF-2 shows a statistically significant difference in growth from 5 to 7 days.

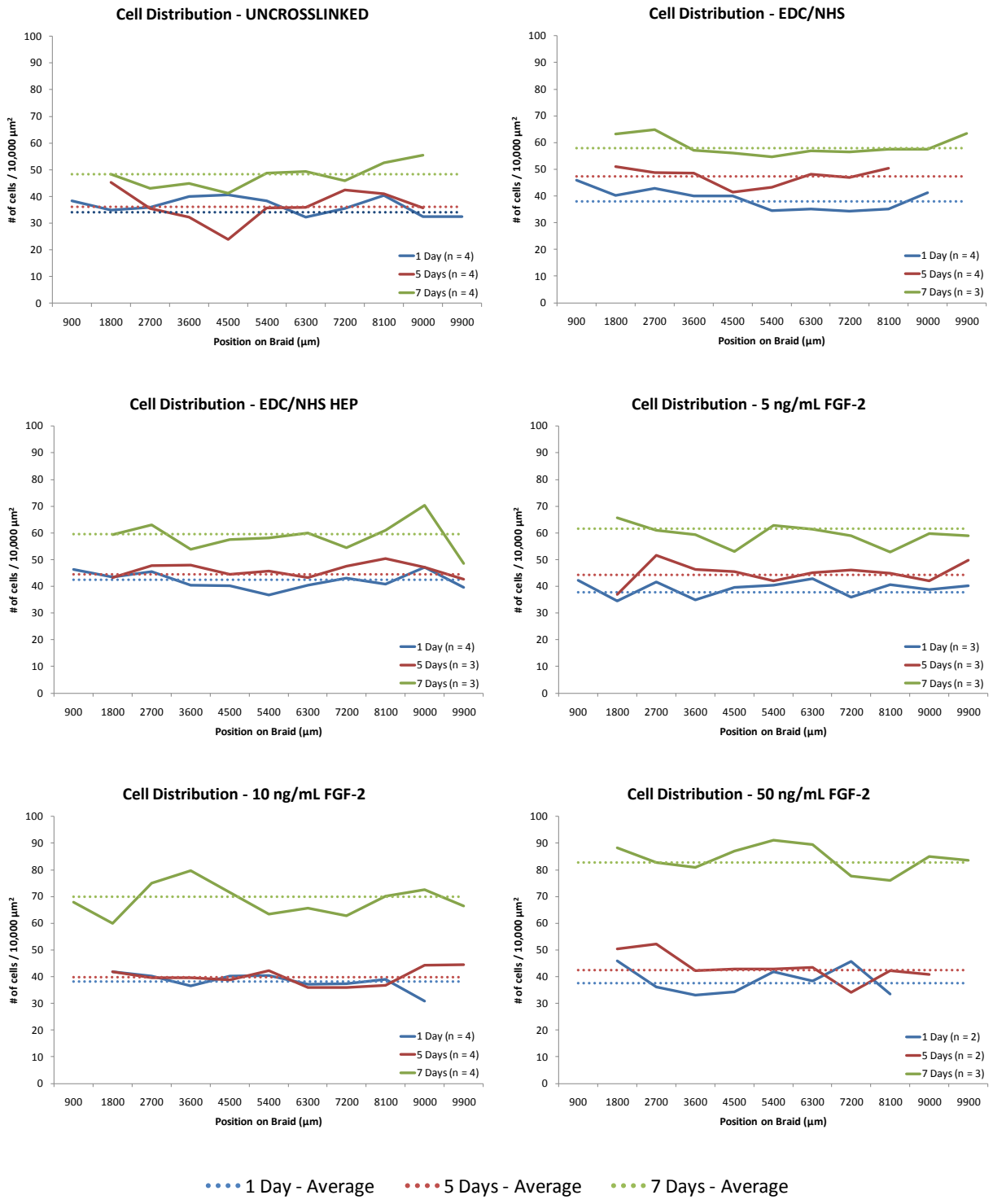

Figure 35: Cell Distribution for braided collagen scaffolds over 7 days

Solid lines indicate average cell distributions for representative scaffolds in each group at 1, 5, and 7 days (n numbers indicated within each legend). Dashed lines indicate the average attachment of all scaffolds analyzed for each group (total n numbers for 1 Day – Average, 5 Days – Average, and 7 Days – Average indicated in Table 8).

5.3.3. Estimation of Total Cell Attachment and Growth

The total number of cells that attach to the braided collagen scaffolds was determined by multiplying the results in Table 7 by the surface area of an unseeded braided collagen scaffold calculated from histological cross-sections. The cross-sectional perimeter of a braid containing 18 collagen microthreads, which was not significantly different between each surface modification, was found to be 1,361 ± 278 μm. The cross-sectional perimeter was then multiplied by the length of the seeded portion of the braid, which was determined using the cell distribution data, to get a total surface area of 10,059,532 ± 2,058,025 μm^2. In order to calculate the total attachment, the results in Table 7 were multiplied by 1,006 ± 205.8, which is the surface area divided by 10,000 μm^2. The results of the total cell attachment are summarized in Table 9, with the total cell calculations including surface area calculations, total attachment calculations, percentage calculations, and statistics for each scaffold detailed in Appendix E: Total Cell Attachment Data.

	Total MDFC Attachment (# of cells ± SEM)	Percentage of Attached Cells (% of 150,000 cells seeded ± SEM)
UNCROSSLINKED	35,139 ± 693∗	23.4 ± 0.5∗
EDC/NHS	41,893 ± 765	27.9 ± 0.5
EDC/NHS HEP	46,386 ± 913†	30.9 ± 0.6†
5 ng/mL FGF2	40,511 ± 736	27.0 ± 0.5
10 ng/mL FGF2	39,414 ± 700	26.3 ± 0.5
50 ng/mL FGF2	40,912 ± 1,000	27.3 ± 0.7

Table 9: Total cell attachment summary table on different surface modifications

∗ Indicates statistically significant differences between uncrosslinked and all other conditions with $p < 0.05$ using Kruskal-Wallis One Way ANOVA on Ranks with Dunn's Method. † Indicates statistically significant differences between uncrosslinked and all other conditions with $p < 0.05$ using Kruskal-Wallis One Way ANOVA on Ranks with Dunn's Method.

The total number of MDFCs that attached to the braided collagen scaffolds was approximated to determine which surface treatment promoted more cellular attachment. As

expected from the regional cell attachment counts, uncrosslinked braided collagen scaffolds promoted significantly less cell attachment than the other braided collagen scaffolds while EDC/NHS with heparin scaffolds promoted significantly more cells to attach (*Figure 36*). In order to determine which scaffold had the best seeding efficiency, the percentage of the total amount of cell in the suspension that actually attached to the scaffolds was calculated (*Figure 37*). Uncrosslinked braided collagen scaffolds resulted in a significantly lower seeding percentage compared to the other surface modifications with approximately 23% attachment. EDC/NHS with heparin scaffolds resulted in a significantly higher seeding percentage with approximately 31% attachment.

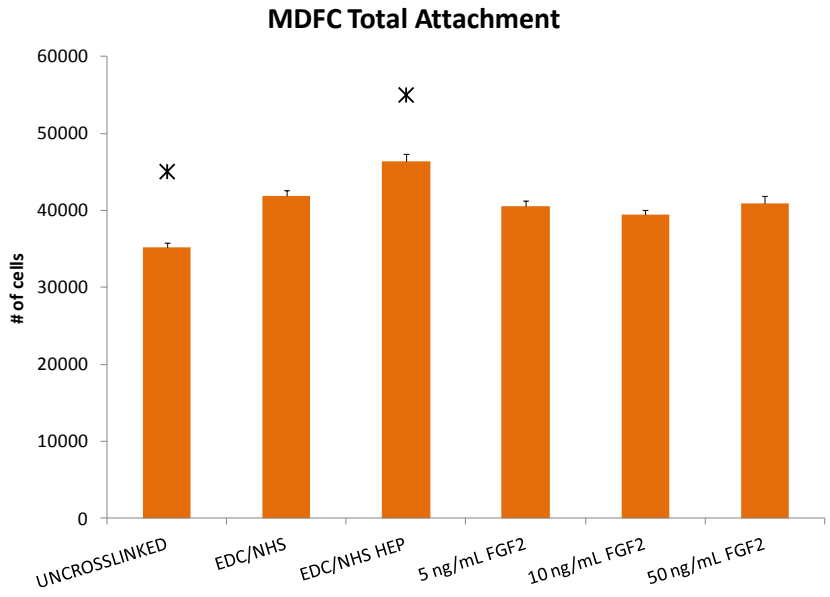

Figure 36: MDFC total attachment for different surface modifications

The total number of MDFCs that attached to the braided collagen scaffolds was approximated to determine which surface treatment promoted more cellular attachment. ∗ Indicates $p < 0.05$ using Kruskal-Wallis One Way ANOVA on Ranks with Dunn's Method. Bars indicate mean ± SEM (total n numbers indicated in Table 8).

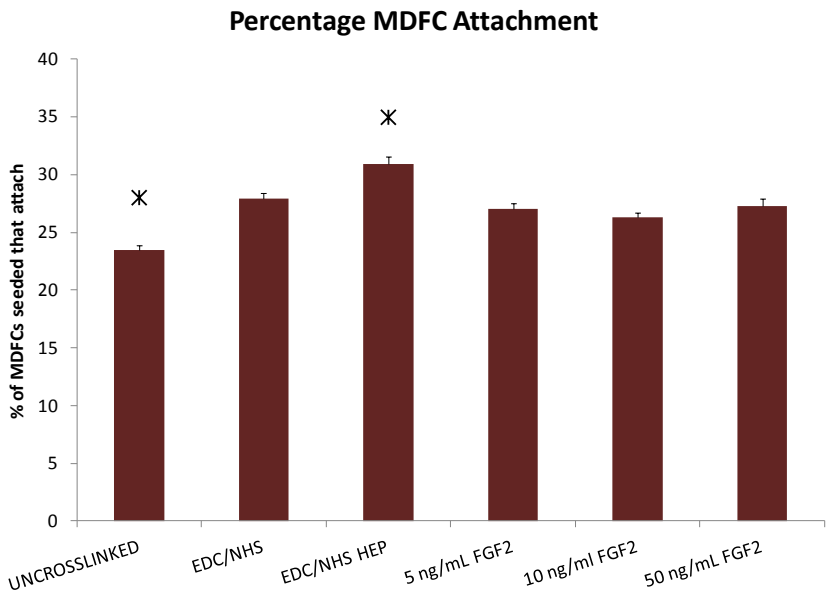

Figure 37: Percentage of MDFC seeded that attached to the braided collagen scaffolds

In order to determine which scaffold had the best seeding efficiency, the percentage of the total amount of cell in the suspension that actually attached to the scaffolds was calculated by dividing the number of cells attached by the initial number of cells seeded. ∗ Indicates $p < 0.05$ using Kruskal-Wallis One Way ANOVA on Ranks with Dunn's Method. Bars indicate mean ± SEM (total n numbers indicated in Table 8).

The effect the surface modifications have on the rate of MDFCs growth was determined by extrapolating the doubling time from the total MDFC growth after 5 and 7 days. The results of the total cell growth are summarized in Table 10. The total cell calculations including doubling time calculations and statistics for each scaffold are detailed in Appendix F: Total Cell Growth Data.

	5 DAYS		7 DAYS	
	Total MDFC Growth (# of cells ± SEM)	Fold Increase (increase ± SEM)	Total MDFC Growth (# of cells ± SEM)	Fold Increase (increase ± SEM)
UNCROSSLINKED	37,205 ± 918	1.06 ± 0.026	47,978 ± 893	1.37 ± 0.025
EDC/NHS	44,337 ± 794	1.06 ± 0.019	51,123 ± 1,080	1.22 ± 0.026
EDC/NHS HEP	46,670 ± 753	1.00 ± 0.017	54,670 ± 1,265	1.18 ± 0.027
5 ng/mL FGF-2	47,399 ± 770	1.17 ± 0.019	55,977 ± 1,187	1.38 ± 0.029
10 ng/mL FGF-2	42,742 ± 712	1.08 ± 0.018	63,907 ± 1,371∗	1.62 ± 0.035∗
50 ng/mL FGF-2	45,094 ± 916	1.10 ± 0.022	73,610 ± 1,639∗	1.80 ± 0.040∗

Table 10: Total cell growth summary table on different surface modifications

∗ Indicates statistically significant differences between the growth / increase over attachment of MDFCs at 7 days for 10 ng/mL and 50 ng/mL FGF-2 and all other surface modifications with $p < 0.05$ using Kruskal-Wallis One Way ANOVA on Ranks with Dunn's Method.

The total number of MDFCs present on the braided collagen scaffold after 5 and 7 days in culture was approximated to determine which surface modification promoted the highest growth rate. As expected from the regional cell growth counts, after 5 days in culture, none of the modified braid types promoted significant cell growth relative to the day 1 attachment data expect braids with 5 ng/mL FGF-2 bound to the surface. However, there was significant growth after 7 days, with surfaces modified with 50 ng/mL FGF-2 having approximately 74,000 cells present, which was significantly higher than all other conditions (*Figure 38*). To determine which scaffold promoted the highest growth rate, the fold increase in cell number normalized to the average cell attachment for each condition was calculated (*Figure 39*). After 5 days, all control surface modifications as well as scaffolds modified with 10 ng/mL FGF-2 had significantly less growth than surfaces modified with 5 ng/mL FGF-2. After 7 days, the growth rate on EDC/NHS crosslinked scaffolds and EDC/NHS crosslinked with heparin scaffolds was

significantly less than all other conditions, and scaffolds modified with 10 and 50 ng/mL FGF-2 had significantly higher growth rates than all other scaffold types.

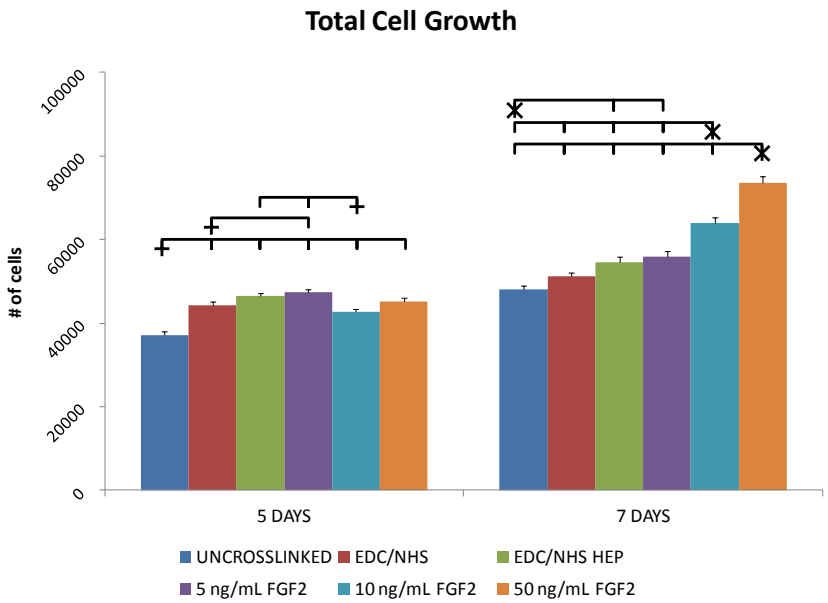

Figure 38: Total cell growth after 7 days in culture

∗ Indicates $p < 0.05$ using Kruskal-Wallis One Way ANOVA on Ranks with Dunn's Method, and † indicates $p < 0.05$ using One Way ANOVA with Holm-Sidak method. Bars indicate mean ± SEM (total n numbers indicated in Table 8).

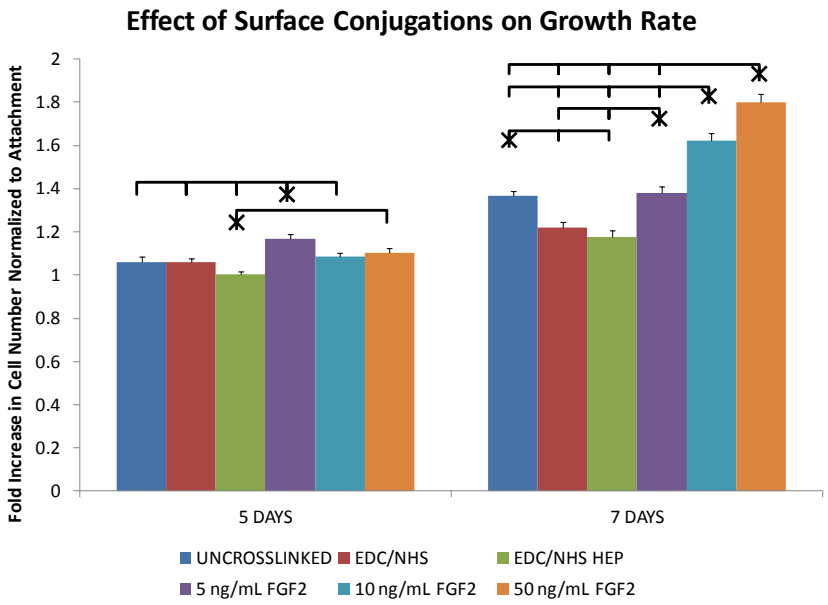

Figure 39: Effect of surface modifications on growth rate

∗ Indicates $p < 0.05$ using Kruskal-Wallis One Way ANOVA on Ranks with Dunn's Method, and † indicates $p < 0.05$ using One Way ANOVA with Holm-Sidak method. Bars indicate mean ± SEM (total n numbers indicated in Table 8).

5.4. Qualitative Analysis of Cell Density and Cellular Alignment

5.4.1. Histological Analysis of Cell Density

Differences in cell density on braided collagen scaffolds with different surface modifications was analyzed using histological sections of MDFCs on braids after 1 and 7 days in culture stained with H&E. The sections were imaged to determine qualitatively the cell thickness and homogeneity on the surface of the braid (*Figure 40*). After 1 day in culture, the MDFCs are located on the surface of the braided collagen scaffolds showing very little spreading. The cells are attached to the braids in clusters with heterogeneous cell density distributions. After 7 days, the amount of cells on the surface seems to have decreased, but the cells appear more uniformly spread throughout the surface of the braid creating a more homogenous thickness.

Figure 40: H&E stained braided collagen threads at 1 and 7 days

H&E stained histological sections of braided collagen scaffolds with different surface modifications (rows) at 1 day and 7 days using 20X and 40X magnification (columns). Scale bar = 100 µm.

5.4.2. Fluorescence Microscopic Analysis of Cell Density and Cellular Alignment

The effect of FGF-2 surface modifications on MDFC cell density and cellular alignment was determined by seeding MDFCs and incubating them on braided collagen scaffolds for 1, 5, and 7 days. The scaffolds were imaged either to determine cell density using Hoechst dye fluorescence microscopy, or to determine cellular alignment using phalloidin confocal fluorescence microscopy. The Hoechst stained cells at 1, 5, or 7 days shows uniform cell density over each surface modification (*Figure 41*). The uncrosslinked scaffolds show a higher concentration of cells in the grooves between threads, and all braided scaffolds with surface modification showed a more uniform density across the entirety of the braid. The uniform concentration of cells indicates that imaging a small subsection of the braid would be a satisfactory representation of the alignment over the seeded area. Since the working distance of the confocal microscope was not large enough to image through the entire scaffold, only a small fraction of the braid could be analyzed per image. Confocal images of phalloidin stained braids at 1 day and 7 days, showed a distinct difference in the f-actin configurations between the two time points (*Figure 42*). At 1 day, all scaffolds exhibit a lack of cellular alignment, with f-actin filaments spread out with no specific orientation. At 7 days, the cells began to orient themselves along the linear axis, meaning the direction of the threads not accounting for the curvature of the braids, on uncrosslinked braids and braids crosslinked with and without heparin. The f-actin filaments appear to be aligned parallel to each other over the braid structure with some following the curvature of the individual braided threads. Braided collagen scaffolds modified with different concentrations of FGF-2 showed limited alignment resembling the 1 day scaffolds as opposed to the 7 day uncrosslinked and crosslinked with and without heparin scaffolds.

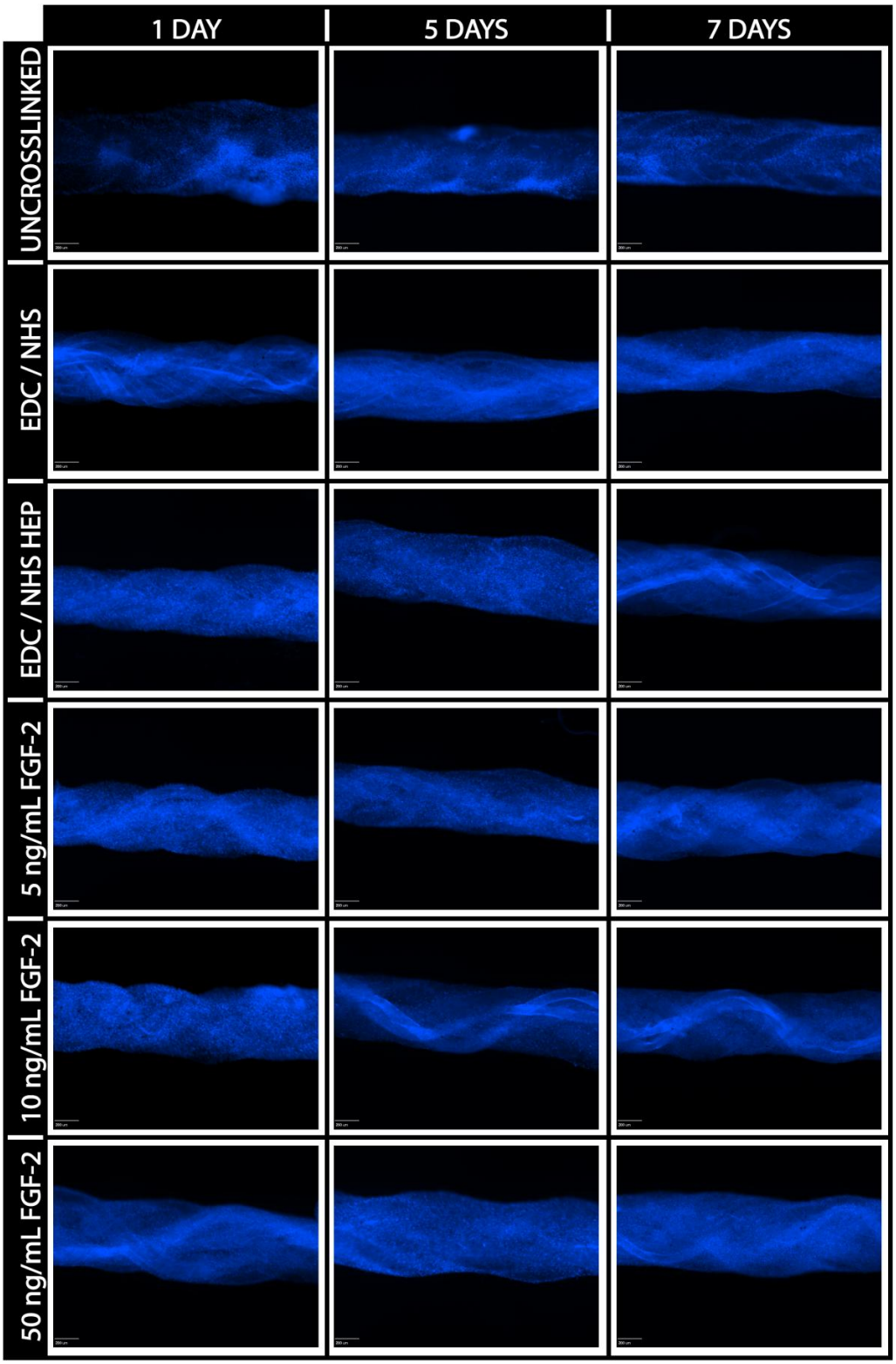

Figure 41: Qualitative analysis of cell density

Hoechst stained MDFCs on braided collagen scaffolds with different surface modifications (rows) at 1 day, 5 days, and 7 days (columns) under 4X magnification. Scale bar = 200 μm.

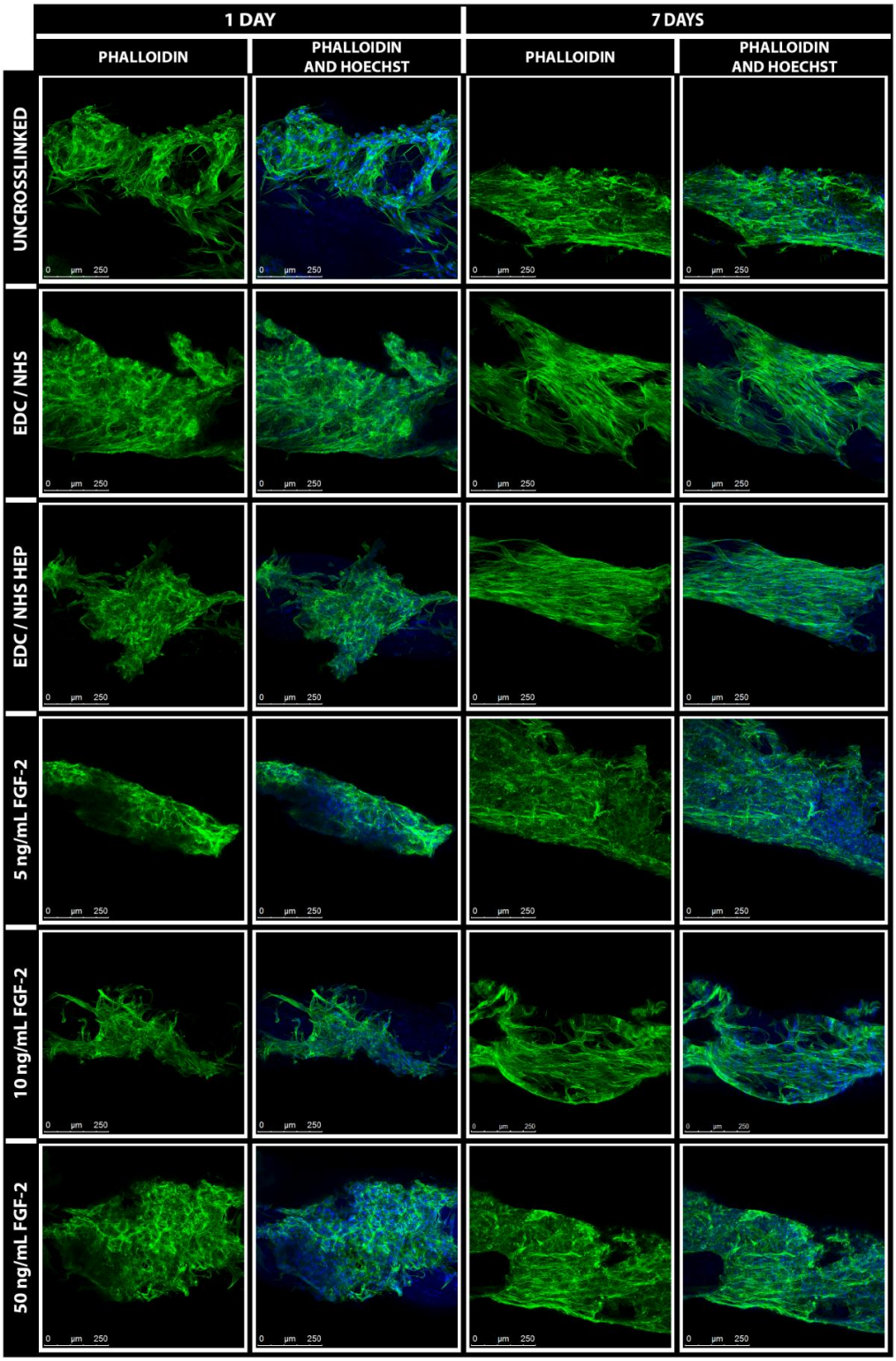

Figure 42: Analysis of alignment using phalloidin staining

Representative images for alignment analysis of braided collagen scaffolds with different surface modifications (rows) at 1 day and 7 days (columns) using phalloidin staining (green) and Hoechst stained nuclei (blue). Scale bar = 250 µm .

Chapter 6: Discussion

The goal of this project was to investigate a novel method to attach and growth muscle derived fibroblastic cells on collagen microthreads that could be used to regenerate skeletal muscle in large defects. This project has succeeded in characterizing the mechanical properties of the braids, developing a novel seeding method to attach MDFCs to braided collagen scaffolds, quantifying the number of cells that attached and grew on the braids in culture. This section illustrates the significance of these results in terms of the aim of this project.

6.1. Braided Collagen Scaffold Material Characterization

6.1.1. Characterization of Localized FGF-2

The immunocytochemistry of the single collagen threads verified that FGF-2 was bound to the surface, and the fluorescence expression increased depending on the concentration of FGF-2 in the solution. Initially, immunocytochemistry performed on braided collagen scaffolds to verify the localization of FGF-2 on the surface did not give conclusive results due to the limitations of imaging the entire braid in one plane of the z-axis (results not shown). Since the surface area of single collagen microthreads exposed to EDC/NHS with heparin and FGF-2 is much smaller than braided collagen threads (5.46 ± 2.55 mm^2 to 19.05 ± 3.90 mm^2 respectively), one can assume that binding heparin and FGF-2 to single thread using the same protocol will validate that braided threads have it on the surface.[36] Threads exposed to 5 ng/mL FGF-2 showed minimal surface binding with areas containing higher fluorescence intensity than others, which suggests that the heparin FGF-2 binding was not homogeneous throughout the surface. When threads were exposed to 10 ng/mL and 50 ng/mL of FGF-2, the difference between the fluorescence intensity along the thread was less apparent, however the 50 ng/mL FGF-2 threads showed a greater overall surface coverage.

Studies show that culturing fibroblasts in culture medium supplemented with 4 ng/mL FGF-2 in low oxygen conditions (5% O_2, 5% CO_2) for weeks allows for dedifferentiation into stem-like cells, and with continued exposure to FGF-2, the stem cell marker expression could be maintained.[46] Levenstein et al. showed that culturing human embryonic stem cells with media supplemented with 100 ng/mL FGF-2 maintained the pluripotency of the cells through multiple passages in the absence of fibroblasts, which is standard for growing stem cells.[139] Mizuno et al. was able to induce differentiation of iPS cells reprogrammed from fibroblasts into myoblasts and maintain the stemness for 24 weeks on Matrigel-coated plates.[145] By binding FGF-2 to the surface of the braided scaffolds, the cells will have prolonged exposure to the growth factor during *in vitro* culture and after *in vivo* implantation. Since FGF-2 has a short half-life, approximately 12 hours *in vitro*, when not electrostatically bound to a surface, binding heparin to the scaffold using EDC/NHS before passive adsorption of FGF-2, will help to maintain the stability of the growth factor to ensure extended cell exposure.[132,146] Relative to adding growth factor into the culture medium, when binding it to the surface, it is not known how much of the FGF-2 actually binds, and the quantity that is needed to maintain the stemness of the fibroblasts for an extended period. For the purpose of this study, it was not necessary to determine accurately the amount of FGF-2 that bound since the cells were not going to be cultured long enough to show detectable levels of stem cell markers, which previous studies prove to be expressed after 7 days.[46] Future studies should analyze the effects of FGF-2 surface concentrations on MDFC stem cell marker expression.

Previous studies indicate that immobilizing heparin onto the surface of insoluble collagen sponges and films doubles the amount of FGF-2 that adsorbs to the surface compared to sponges without heparin.[38,132] After reviewing these studies, it may be beneficial for future experiments

using braided collagen scaffolds to use larger quantities of heparin and FGF-2. Although it is clear that both are present on the surface of the scaffold, for long term studies, FGF-2 needs to be available during both *in vitro* culture and *in vivo* implantation studies. Wissink et al. crosslinked insoluble collagen films with different molar ratios of EDC/NHS to heparin.[132] The results showed that molar ratios between 0.4 and 0.6, which corresponds to 14 mM EDC, 8 mM NHS, with between 1.5 mM and 1.0 mM heparin respectively, yielded 20-30 mg of heparin per gram of collagen immobilized within the sponge.[132] It was found that a maximum of 22% of the FGF-2 added to solution will bind to the heparin on the surface, leading to the conclusion that one FGF-2 molecule will bind to heparin per 1000 heparin molecules. When detecting how much FGF-2 is released from the scaffold over time, the study showed that after 10 days approximately 60% of the growth factor was still present within the sponge.[41,132] Pieper et al. crosslinked collagen sponges with 960 µM heparin sulfate and 7 µg/mL FGF-2, and found that 36% of the loaded FGF-2 was bound to the scaffold, with 53% of the growth factor being released after 4 weeks.[38]

These results suggest that by crosslinking the braided collagen scaffolds with 1.9% (w/v) heparin and passively adsorbing concentrations of FGF-2 between 50 ng/mL and 100 ng/mL to the surface, the rate of release can be predicted to create the optimal environment for maintained stemness over long intervals. Based on the study by Wissink et al., by adsorbing 50 ng/mL FGF-2 in 1.0 mL of solution, one can predict approximately 11 ng will bind to the surface, which will correlate to releasing 4.5 ng to the cells in the first 10 days of culture. This would be consistent with the concentration of FGF-2 that cells are exposed to when it is incorporated into the culture medium *in vitro*. The aim of this preliminary study was to confirm that FGF-2 bound to the heparin and influenced the growth of MDFCs on braided collagen scaffolds, so it was not

imperative to achieve the maximal binding efficiency of FGF-2 using heparin. In future studies, it will be necessary to determine the quantity and the release rate of heparin and FGF-2 to determine the optimal level needed to maintain the stemness long enough to promote muscle regeneration.

Besides maintaining the cell phenotype, FGF-2 promotes vascularization of a wound site when implanted into a defect. Studies show FGF-2 upregulates vascular endothelial growth factor (VEGF), which stimulates angiogenesis, and prevents the degradation of the capillaries formed.[134,147] Nillesen et al. EDC/NHS crosslinked collagen sponges with heparin and FGF-2, resulting in 68 mg heparin and 1.6 µg FGF attaching per mg scaffold. After extracting the scaffolds from a rat model 21 days after implantation, the FGF-2 scaffolds stimulated proliferation and differentiation of granulocytes, endothelial cells, fibroblasts in the surrounding tissue, which are responsible for revascularization.[148] Pieper et al. found implanting a crosslinked collagen sponge with 60 mg heparin and 1260 µg FGF per gram of the matrix resulted in capillary formation after 4 weeks.[38] Another study found that EDC/NHS crosslinking collagen films with 18.6 mg per gram collagen and 3.4 ng per scaffold elicited a vascular response 3 weeks after implantation.[129] Vascularization is imperative for the formation of healthy skeletal muscle since it provides the oxygen needed to maintain the viability of the differentiating satellite cells, so these results suggested that by binding FGF-2 to the surface of the braided collagen scaffolds will help initiate vascularization in large muscle defects.

6.1.2. Mechanical Testing of Braided Collagen Scaffolds

Previous studies by Cornwell et al. on single collagen threads for tissue engineered ligament applications showed crosslinking with EDC increased the mechanical strength significantly compared to uncrosslinked threads.[36] These results suggest EDC crosslinked

microthreads have potential to be used for load bearing tissue regeneration. Similarly, tissue engineered skeletal muscle needs to be able to withstand the high tensile loads involved with muscle movement, specifically the muscle contraction involved with myofiber formation and function. A single EDC crosslinked microthread has a cross sectional area larger than a single myofiber when hydrated, approximately 12,100 μm^2 to 7900 μm^2, but this would not be sufficient to fill a large muscle defect, which involves severing of multiple myofibers.[36,94] By braiding 18 collagen threads together to form a scaffold, the cross sectional area is increased to 91,900 μm^2, which is approximately the size of 12 myofibers. When hydrated, bundles of unbraided threads attached to one another at each end tend to separate from one another, leaving large gaps, which will cause inconsistencies in myofiber formation and little interaction between cells on different threads. By braiding the threads together, the integrity of the structure can be controlled by altering the braiding angle between each thread. This also insures cells on each thread can interact with each other.

Fiber or thread-based scaffolds have been used extensively in ligament regeneration research using collagen, fibrin, silk, PGA, poly-L-lactic acid (PLLA), and polylactic-co-glycolic acid (PLAGA).[36,126,149-151] The mechanical properties of single collagen threads have been researched comparing crosslinked to uncrosslinked conditions, but the strength of braided self-assembled collagen threads has yet to be characterized. For mechanical testing, only uncrosslinked and EDC/NHS crosslinked braided collagen threads were used. Similar to single threads, uniaxial tensile tests of braided collagen scaffolds were conducted and showed a significant increase in strength and stiffness when the braids were crosslinked using EDC/NHS. Due to the large difference in cross sectional area, the results show that braided uncrosslinked threads increases the failure load from 0.389 ± 0.052 N to 0.591 ± 0.076 N. Crosslinking the

braids increased the strength of the scaffold at failure to 1.979 ± 0.237 N compared to single crosslinked threads, which has a failure load of 1.33 ± 0.484 N.[36] Interestingly, braiding the collagen threads increased the UTS of the uncrosslinked and crosslinked single threads. The UTS of single uncrosslinked threads was found to be 1.5 ± 0.2 MPa, while braiding the threads increased it to 5.11 ± 0.7 MPa. Crosslinking the single threads using EDC/NHS resulted in a UTS of 11 ± 4 MPa, and braiding these threads increased the UTS to 27 ± 3 MPa. This shows that by braiding the threads to one another, the mechanical strength of the threads can be increased because the woven design prevents catastrophic failure. Interestingly, the strain at failure is the same for uncrosslinked braids and threads, but crosslinking braids resulted in a 3-fold increase in failure strain over crosslinked threads. However, braiding crosslinked collagen threads did not affect the stiffness of the threads as both braids and single threads had an maximum tangent modulus of approximately 68 MPa. [36] Since the threads in braided collagen scaffolds are woven together, it gives the threads added support when pulled uniaxially. A limitation of using braided collagen threads for muscle regeneration pertains to the elasticity of the scaffold since it is significantly higher than that of human muscle, which is 12 kPa.[47,141,142] A study varying the stiffness of polyethylene glycol (PEG) hydrogels found that hydrogels with a stiffness of 12 kPa maintained the optimal environment for sustained satellite cell self-renewal and proliferation.[143] In future studies, it will be necessary to determine if using growth factors, such as FGF-2 or IGF-I, are able to mimic the environment created using the optimal elasticity to satellite cell self-renewal.

Braided synthetic polymer threads composed of PGA, PLLA, and PLAGA have been researched as possible tissue engineered solutions to repair ligament damage.[149,152] By keeping the braiding angle constant for each polymer composition, the uniaxial mechanical results

showed braided PGA fibers were the strongest with a maximum load of 502 N, and PLLA were the weakest mechanically with a maximum load of 298 N.[149] As expected, synthetic fibers have a much higher mechanical strength compared to collagen braids, which is beneficial for engineered ligaments since they must endure higher loads. For muscle regeneration, such high mechanical strength is not necessary since the loads are not as large. A limitation in the current study of braided collagen threads was the absence of braiding angle characterization. In the future, it would be beneficial to study how different braiding angles affects the mechanical strength of the collagen braids. Another important reason to classify the braiding angle would be to give insight into the pore size, or the space between the individual threads, which will verify that cells and nutrients have the ability to diffuse into the scaffold for the best tissue ingrowth.[37]

It is important to characterize the acellular braided collagen scaffolds in relation to their failure loads, but a limitation of this study is that it does not determine how the scaffolds will respond to native skeletal muscle cues when implanted into an animal model. Native skeletal muscle produces isometric forces due to twitch and tetanic contraction, which are impaired when an injury occurs. Iwata et al. characterized the isometric force production of rats with a contusion injury to the plantar flexor muscles, and found the isometric force dropped significantly, approximately 45% that of a healthy skeletal muscle, 2 days after injury onset and returned to normal after 21 days.[153] Another method created large muscle defects in the biceps femoris muscle of a rat model, which showed after 42 days the deficit isometric force remained constant and did not improve. This confirms that the truncated myofibers are unable to regenerate and bridge the gap caused by the defect without a scaffold present leaving the muscle permanently impaired.[154]

The method proposed in this study involves seeding and inducing pluripotency of fibroblasts on the scaffold to initiate muscle regeneration in the wound bed. In addition, the scaffold will have to maintain its structural integrity as the seeded iPS cells differentiate into myoblasts and fuse during tissue remodeling while restoring muscle function. One approach of mimicking this environment *in vitro* would be to induce differentiation of the iPS cells prior to implantation and measure the contractile forces as well as the force produced by the construct. This can be achieved by electrical and mechanical stimulation as well as measuring the forces produced by stretching and relaxing the construct.[94,106] Furthermore, since the scaffold will be introduced to native myoblasts and stem cells through endogenous cell migration, it may be beneficial to seed them to the scaffold as well, to evaluate whether it can handle the native tissue response *in vitro*.

6.2. MDFC Seeding to Braided Collagen Scaffolds

The next step in the development of a tissue engineered skeletal muscle is to determine a procedure to attach MDFCs to the surface of the braid in the most reproducible and uniform manner. Previous studies characterized the biocompatibility and migration rate of fibroblasts onto single collagen threads, but a method to attach cells onto threads has not been investigated.[35,36] Once attached to the scaffolds, a method to visualize the cells on the surface needed to be developed.

In this study, two channel widths, 1.0 mm and 2.0 mm, were examined to determine which resulted in the highest seeding efficiency. It was found that using a channel width of 1.0 mm resulted in 21% and 24% of the MDFCs attaching to the uncrosslinked and EDC/NHS crosslinked braids, respectively since it had less void space around the braid in the channel. A limitation of this novel MDFC seeding method is the braids are not exposed consistently to cells

throughout the entire surface area. When seeding within the channel, it is not easy to control how the braids lies on the bottom of the PDMS mold, so if the braid is touching the bottom, the cells in the suspension are unable to flow under the braid to attach. This resulted in an influx of cells on either side of the braided threads in the channel. If the braid is lifted slightly from the bottom of the PDMS mold, then cells are able to flow under the scaffold, exposing the underside of the braid to cells. There was no difference in seeding uniformity and concentration between scaffolds that seeded on the whole surface area and ones that only seeded on half.

There are several ways to overcome this limitation during the cell seeding process. Cornwell et al. seeded bundles of fibrin threads by exposing a cell suspension to the threads on a Thermanox® square, but since braided collagen threads are much larger and more structurally dense, using this method resulted in the braid drying out after 30 minutes.[43,151] Altman et al. used a Teflon seeding chamber similar to the PDMS mold used in this study to seed their silk fiber cords. Instead of exposing one area of the cords to the cell suspension, the cords were rotated 90 degrees while adding additional cells to the chamber until the entire cord was exposed to cells.[150,155-157] Using the Teflon seeding chamber, the seeding efficiency was approximately 10%, but since cells have a greater affinity for collagen and using longer cell suspension exposure times, the efficiency can be increased during the seeding period.[158] To create the effect of physically rotating the scaffold in the chamber, a bioreactor can be utilized that will rotate the chamber around the scaffold at a controlled rate.

A second limitation to overcome was how to visually characterize the MDFCs on the threads. It was observed that using a Mitrotracker dye was sufficient to visualize cells attached to the braids, but it was not possible to quantify discrete cells since it is difficult to correlate mitochondria with cell numbers. Fluorescently tagging MDFCs with Hoechst dye prior to

seeding onto braided collagen scaffolds allowed for quantification of MDFCs and was used for the remainder of the experiments in this study. Limitations of using Hoechst dye are that time lapse experiments using the same scaffold is not possible since exposing the Hoechst loaded cells to ultraviolet light activates the dye, which can cause mutations in the DNA, and autofluorescence of collagen between 320 nm and 461 nm can make seeing the cells difficult. Another limitation of using Hoechst dye is that it is unknown if cells expel the dye over a period of time, which could create inconsistencies in cell counts between experiments. One way to overcome these limitations on the braids would be to express green fluorescent protein (GFP) in the MDFCs because in this excitation range, the collagen is less autofluorescent. In addition, using GFP will allow cells to be visualized on braids for time-lapse experiments.[35,36,43]

6.3. Quantification of Cell Number on Different Surface Modifications

6.3.1. Attachment

Using FGF-2 to enhance the regenerative process in tissue engineering has been extensively researched due to its involvement in native tissue development and healing of tissues including bone, nerve, lung, and connective tissues.[159] Studies show that FGF-2, which is located in the basal lamina surrounding myofibers, is upregulated during skeletal muscle regeneration and is involved in the proliferation and fusion of developing myofibers.[49] Due to the angiogenic properties of the protein, FGF-2 also plays a role in revascularizing the defect during the inflammatory and degradation stages of muscle wound healing.[2] During *in vivo* studies, the injection of FGF-2 into injured muscle expedited the wound healing process, decreasing the formation of scar tissue and increasing function and movement of the muscle.[49] The goal of this study was to determine the effects of FGF-2 and heparin on MDFCs attachment, which was analyzed by seeding MDFCs to braided collagen scaffolds with different surface

modifications and observing the cellular attachment after 24 hours in culture. The results show a significant decrease in cellular affinity for uncrosslinked braided collagen scaffolds, and a significant increase in cellular affinity for EDC/NHS crosslinked with heparin braided collagen scaffolds. The difference in cell attachment between each of the FGF-2 bound scaffolds and the EDC/NHS crosslinked scaffolds were not significantly different.

In vitro studies comparing uncrosslinked controls with scaffolds with surface modifications, specifically heparin, show no difference in attachment on collagen scaffolds, which is inconsistent with our findings that heparin promotes higher MDFC attachment compared to all other surface treatments.[28,43,132,160] In this study, heparin promoted significantly higher attachment of MDFCs than all other braided collagen scaffold surfaces. One variation that could account for this difference is that braided collagen scaffolds were prepared for cell attachment without exposure to serum, which affects the interaction between the cell signals and the modifications on the surface. In addition, the cell seeding protocol was conducted without the addition of serum to the culture medium, in order to ensure the most accurate reflection on cell affinity for the different surface modifications. Another difference that could cause the inconsistencies between the previous observations and the current studies would be the seeding method. Wissink et al. loaded collagen sponges with different surface modifications by adding the cell suspension directly onto the surface, which eliminates attachment differences between the surface modifications.[132,160] Another study using fibrin threads exposed the bundles to fibroblast cells on a Thermanox® square directly below the microthreads, which allowed for the smallest possible volume of cell suspension for optimal cell attachment.[43] The current seeding method does not ensure all cells in the cell suspension will be exposed to the scaffold surface since the channel is higher and wider than the braided scaffold. This hypothesis is supported by

the observations that only 23-30% of the cells in the suspension attached to the braided collagen scaffolds.

Research by Cornwell et al. on the migration of fibroblast cells onto single uncrosslinked and EDC/NHS crosslinked microthreads showed a higher affinity for fibroblast migration onto uncrosslinked threads, but uncrosslinked braided collagen threads had significantly less attachment of MDFCs than all surface modifications.[36] This difference could be explained by protocol differences, in which the single threads were EDC/NHS crosslinked in the presence of distilled water whereas the braided scaffolds were crosslinked in ethanol. Pieper et al. showed fibroblasts and myoblasts were more viable when collagen sponges were crosslinked in the presence of ethanol.[28] In our study, heparin promoted significantly higher attachment of fibroblast cells, but other studies show the effect on attachment is not consistent with our findings.[39] Our attachment assay shows that varying the concentration of FGF-2 does not facilitate cell attachment, which was expected since studies do not show FGF-2 to affect the attachment of cells. Cornwell et al. loaded fibrin thread bundles with increasing concentrations of FGF-2, from 0 to 200 ng/mL, in the absence of heparin and observed that FGF-2 did not increase the attachment of fibroblast cells over the bundles without FGF-2.[43] Interestingly, with the addition of FGF-2 to EDC/NHS with heparin scaffolds, the attachment between EDC/NHS crosslinked scaffolds and FGF-2 bound scaffolds were not significantly different. By binding FGF-2 to the heparin, it appears to block the effects of the heparin on cell attachment leaving only the crosslinked surface to facilitate attachment.

6.3.2. Cell Growth

Since our studies and others showed that FGF-2 does not influence the attachment of cells to scaffolds, the next aspect needed to be evaluated was FGF-2 influence on the cell growth

of MDFCs when bound to heparin on braided collagen scaffolds. The results of our study showed that after five days, there was no significant increase in the number of MDFCs on the surface of the braid relative to day 1, except for scaffolds modified with EDC/NHS crosslinking and 5 ng/mL and 10 ng/mL FGF-2. After 7 days in culture, all braided collagen scaffolds with different modified surfaces, including uncrosslinked controls, promoted significant cell growth of MDFCs. A positive linear correlation was observed between the amount of FGF-2 on the surface of the scaffold and the rate of cell growth. The MDFCs grew uniformly across each surface type of the braids for the entirety of the culture period.

After 5 days in culture, the cell growth on each scaffold was insignificant showing no difference in scaffolds modified EDC/NHS with heparin and a 1.1 fold increase in scaffolds modified with EDC/NHS with heparin and 50 ng/mL FGF-2. The growth on modified surfaces was significantly higher than on uncrosslinked controls. Previous research supports the finding that the minimal growth of cells on scaffolds conjugated with heparin. It has been shown that heparin does not facilitate proliferation of endothelial cells on collagen films.[39] Contrary to our hypothesis, scaffolds modified with 5 ng/mL FGF-2 showed significant increases in growth over the 1 day data as well as a significant increases in growth over scaffolds exposed to 10 ng/mL FGF-2.

The observed similarity between the growth on controls and FGF-2 modified surfaces when normalized to attachment is expected because when FGF-2 is bound to heparin binding sites it is released at a controlled rate compared to binding it to the collagen scaffold directly.[132] Another reason for the limited growth after 5 days is that studies show that at low cell seeding densities, less than 10,000 cells/cm^2, FGF-2 does not begin to influence proliferation of endothelial cells until after 6 days in culture.[160] In the study performed by Wissink et al., they

used a collagen film that was over 2 cm^2 in surface area with a higher concentration of FGF-2 on the surface then on braided collagen scaffolds.[160] The significantly smaller surface area with less FGF-2 per square centimeter explains why the cells in contact with FGF-2 on the braids had the same growth reaction even though there were more cells per square centimeter. Another explanation for insignificant growth in cells at 5 days on the braided collagen scaffolds could be due to the decreased proliferation. Due to collagen autofluorescence, the cells could not be evaluated for viability after attachment, so it is not known if there was rapid cell death during the first few days in culture.

After 7 days in culture, the cells attached to the scaffolds have begun to proliferate showing significant growth on all surface modifications. The different concentrations of FGF-2 on the surface of the braids appear to influence the growth rate of the MDFCs. Scaffolds modified using EDC/NHS crosslinking with heparin and exposed to 50 ng/mL FGF-2 increased 1.8 fold over the amount of cells initially attached to the surface, which was a significant increase over the growth after 5 days in culture. The growth rate of cells on braided collagen scaffolds were significantly higher than all control conditions, except there was no significant difference at day 7 between uncrosslinked and 5 ng/mL FGF-2 scaffolds.

Other studies have also observed similar effects of FGF-2 on the proliferation of cells on biodegradable scaffolds. To assess for the effect of FGF-2 on the proliferation of fibroblasts attached to fibrin microthreads, Cornwell et al. loaded varying concentrations of FGF-2 to bundles of fibrin microthreads and found after 2 days fibroblasts had growth 3 to 4 times over the attached number of cells, with a FGF-2 response plateau at 50 ng/mL.[43] The difference in initial growth on fibrin microthreads compared to braided collagen scaffolds can be explained by the addition of heparin binding on the braids. When FGF-2 is bound to the scaffold directly by

nonspecific interactions, there is an initial burst of the protein in the first 6 hours, which explains why the fibrin threads show a FGF-2 response after 2 days in culture.[43,132] The high affinity of FGF-2 for heparin binding sites allows for the protein to be released much slower, with only 15% of the protein being released after 2 days compared to almost 60% when not bound to heparin.[132] After 7 days in culture, fibroblast seeded to fibrin microthreads showed a similar growth pattern as on braided collagen scaffolds seeded with MDFCs with growth increasing with increased FGF-2 up to fibrin threads loaded with 50 ng/mL.[43]

In other studies, collagen films and PLGA scaffolds crosslinked with EDC/NHS in the presence of heparin with increasing concentrations of FGF-2 showed a controlled release of FGF-2 from the scaffold when seeded with endothelial cells after 10 days. Scaffolds exposed to FGF-2 without heparin showed lower amounts of bound FGF-2 with unpredictable proliferation rates up to 10 days. Heparin scaffolds had increased amounts of FGF-2 on the surface with proliferation rate increasing in proportion to the concentration of FGF-2.[132,161] FGF-2 binds to heparin molecules by electrostatically binding through interactions between the 2-*O*-sulfate groups and *N*-sulfate groups of the heparin binding sites with lysine and arginine residues on FGF-2 proteins.[42,162] The effect FGF-2 has on the growth of the MDFCs on the braided collagen scaffolds suggests that the heparin has protected the protein from the enzymatic degradation mediated by MDFCs.[132]

Hill et al. transplanted myoblasts seeded on alginate gels containing FGF-2 and HGF into mouse models and showed that the addition of growth factors increased transplanted cell participation in native muscle regeneration by promoting cell migration of both native and transplanted myoblasts. The study showed that it is imperative to determine the optimal rate of FGF-2 release to control myoblast viability and migration without initiating a myogenesis

response in the surrounding tissue.[70,163] Although our data suggests that the FGF-2 is bound to the collagen scaffolds by means of the heparin binding sites, the amount of heparin and FGF-2 on the surface has yet to be analyzed. The surface characteristics of these scaffolds would need to be determined in order to decipher the optimal release rate of FGF-2. In addition, it will be important to research the amount of FGF-2 needed to reach saturation of heparin binding sites and growth effects.

6.4. Qualitative Analysis of Cell Density and Cellular Alignment

In order to determine how the MDFCs are growing and spreading on the braided collagen scaffolds, the scaffolds were fixed, sectioned, and stained using H&E after 1 or 7 days in culture. The results showed that after 1 day, the cells were clustered on the surface of the side exposed during the seeding process. After 7 days, the cells are more spread along the surface, but the density and thickness is less than that at 1 day, which could be attributed to the cell spreading or limitations associated with fixing and sectioning the braided collagen scaffolds. Since, we showed that the number of cells on the scaffolds increases with time on each surface, the apparent decrease in cell number at day 7 could be caused by cells shearing off the surface during processing or by sectioning artifacts. During sectioning, it appeared that some of the braids were not embedding vertically, which is supported by the observation that not all sections contained 18 individual thread cross sections. In addition, the braids did not maintain the tight structure in which they were cultured, so when sectioned, the threads spread, which detached the cells from the surface. This is observed by the cells seen in the cross sections that are not near any collagen threads, such as with the scaffolds modified with 50 ng/mL FGF-2 at 7 days in culture. The limitations of analyzing the braided collagen scaffolds thorough histology could be corrected by fixing the scaffolds more thoroughly or using a higher concentration of agarose to

form a stiffer encapsulation around the braids. Using a 2% agarose in distilled water to maintain the structure may not be stiff enough to immobilize the scaffold during cutting.

An important aspect of engineered skeletal muscle constructs that must be addressed is how the scaffold facilitates alignment of the myotubes during regeneration. Myotubes, which are responsible for movement of the body, consist of bundles of linearly aligned myofibrils composed of fused myoblasts.[2] The engineered skeletal muscle should stimulate the alignment and fusion of myoblasts to mimic the native environment, and allow for optimal integration and function upon implantation into a wound area. To analyze the alignment of MDFCs on braided collagen scaffolds with different surface modifications, scaffolds seeded with MDFCs were imaged using a confocal microscope after 1 or 7 days in culture. At one day, phalloidin staining of the f-actin filaments on all surface modifications showed no distinct orientation. After 7 days in culture, all control scaffolds have cellular alignment along the linear axis of the braided collagen microthreads, but scaffolds modified with FGF-2 show limited alignment with most f-actin filaments having no specific orientation.

It may important to have the MDFCs aligned in the dedifferentiated state because it will facilitate the fusion of myoblasts with themselves and with host cells when the iPS cells are programmed to differentiate for muscle regeneration. By using microthreads, the myofiber-like structure of the biomaterial scaffold will promote the MDFCs to spread and proliferate along the linear axis of the braids. This will produce an organized skeletal muscle structure that will easily integrate into a large muscle defect. Braided collagen scaffolds modified using EDC/NHS crosslinking with heparin and FGF-2 showed limited alignment after 7 days, which is not consistent with previous research. Cornwell et al. observed bundles of fibrin microthreads with FGF-2 stimulated fibroblast cells alignment along the linear axis of the threads.[43] One

explanation of the limited alignment of MDFCs on FGF-2 modified braids could be the increased proliferation between 5 and 7 days in culture compared to the control scaffolds. With increased proliferation, the MDFCs could begin to stack on top of one another, limiting the contact of the MDFCs have with the braided collagen scaffold, which could eliminate the influence of the braid structure has on the alignment of the cells. In the future, the MDFC orientation and alignment on the FGF-2 modified braided collagen scaffolds should be analyzed between 1 and 7 days in culture as well as in prolonged studies to determine when MDFCs begin to align. It will be important to study the viability of the cells on the braided muscle construct as the cells proliferate and migrate outward to determine if there is a perfusion of nutrients to the inner layers, which can be an issue in three-dimensional engineered tissues. One approach that researchers have found to create alignment is using magnetic, electrical, and mechanical stimulation.[96,112,164] Studies show that exposing myogenic cells to a continuous magnetic field helps initiate the alignment, differentiation, and fusion of myoblasts into myotubes.[164]

Studies have also shown that using aligned electrospun nanofibers seeded with myoblasts for muscle regeneration can promote the fusion of longer aligned myotubes after 7 days.[24,31,85,165] After 14 days, cell nuclei begin to elongate and fuse exhibiting fast myosin heavy chains, which indicates the production of mature myotubes.[165] This shows potential for braided collagen scaffolds, which supported the alignment of MDFCs along the longitudinal axis of the braids after 7 days, to create aligned engineered muscle once MDFCs are programmed to differentiate into terminal myoblasts.

Researchers have also utilized microfluidic patterning to create channels to promote myofiber alignment.[115,166,167] Lam et al. investigated the effect of using different channel widths on myofiber alignment showing a widths of 6 μm promoted optimal alignment.[167] By seeding

myoblasts into synthetic polymer molds, the myoblasts are able to align parallel to the microgrooves, which then can be transferred into a collagen gel to create a three-dimensional muscle construct.[115] Zhao et al. showed potential for creating multilayer muscle constructs using microfluidics, but when adding cell layers to the aligned myofibers in the channels, the newly formed myotubes do not exhibit the same highly oriented alignment.[166] Shimuzi et al. created micropatterns using an abrasive substrate, which is used for biomaterial implants, and microchannels created with rougher surfaces encouraged a higher degree of alignment in myotubes.[168] The importance of these studies is to show how easily the structure of developing myotubes can be manipulated, which is beneficial to creating functional skeletal muscle. A limitation of using microfluidics to pattern aligned myofibers is the fibers do not fuse with one another until transferred out of the polymer. This effect may be corrected by using microthreads to align the cells since all cells in the structure are in direct contact with one another.

Chapter 7: Future Work and Implications

This study succeeded in demonstrating a novel engineered muscle construct that could be used to promote cell attachment and growth, which may be used to deliver cells to a large muscle defect to stimulate muscle regeneration in the future. The braided collagen microthread scaffold provides an organized structure to facilitate the growth of MDFCs, and using heparin to bind FGF-2 to the surface could induce MDFCs to exhibit a stem cell phenotype. After 7 days in culture, the seeded MDFCs had begun to align on the braided collagen scaffold, but it is not completely clear if they are aligning with the curvature of the collagen threads or with the x-axis. Further studies will need to be conducted in order to determine how the MDFCs are aligning, and if this is important when implanting stem-like cells into a large muscle defect. Another aspect of the project that needs additional investigation is the mechanical properties of the collagen microthreads. Since the thread stiffness is significantly greater than native skeletal muscle, other processing strategies, should be examined to better mimic the native mechanical environment. In future *in vivo* studies, delivering stem-like cells to a large muscle defect will promote the migration of surrounding satellite cells to the wound area as well as differentiate into myoblasts. The braided collagen muscle construct will integrate into the native muscle and help restore function by mimicking cells and responses of native muscle regeneration. However, before the braided collagen scaffold can be used for *in vivo* experimentation, further studies need to be performed to characterize and modify the scaffold and cellular stimuli to optimize the muscle delivery system.

As stated in the discussion, the seeded scaffolds were not cultured for a long enough period to express a stem cell markers and phenotype in the MDFCs. In order to show the release of FGF-2 from the scaffold is sufficient to stimulate dedifferentiation of MDFCs into stem like

cells, seeded scaffolds will have to be cultured for longer than 7 days and express the stem cell markers, OCT4, SOX2, and NANOG.[46,137] Once the stem cell phenotype is verified, *in vitro* studies into the maintenance of the stemness of these cells will have to be explored to ensure that the cells do not spontaneously differentiate before implantation into a wound site. Once the stemness can be controlled for extended periods and programmed to differentiate into myoblasts at the desired point, the braided collagen scaffolds will be optimal for the promotion of skeletal muscle regeneration.

In this study, FGF-2 was adsorbed to the surface of the braided collagen scaffold for the application of delivering stem-like cells to a large muscle defects to induce native skeletal muscle regeneration as well as satellite cell migration, differentiation, and myofiber maturation. In future studies, it would be important to investigate the effects of binding other growth factors important to regeneration in combination with and without FGF-2 to attempt to mimic the native environment. *In vivo*, IGF-I has been found to stimulate proliferation and differentiation of myoblasts into functional myotubes faster than native muscle regeneration with decreased fibrosis.[49,114] Shansky et al. created a bioartificial muscle (BAM) construct which secreted IGF-I, which has been known to prevent atrophy in developing muscles, and when the IGF-I modified BAM was cultured in a perfusion chamber with traditional BAM constructs, it caused the growth of more myofibers with larger diameters in traditional BAM constructs.[107] By incorporating IGF-I into the braided collagen scaffold, there could be increased regulation of myofiber formation upon initiation of differentiation iPS cells to better resemble native skeletal muscle.

Other studies have incorporated HGF, which is responsible for the activation and differentiation of satellite cells during wound healing, into the scaffolds for muscle regeneration.[70,163] The advantage of using HGF in combination with FGF-2 in scaffold

fabrication is that they both are heparin-binding proteins, which will allow for controlled release of both growth factors from the surface for optimal muscle regeneration. Studies show that incorporating HGF into a scaffold alongside FGF-2 enhances the regenerative properties of FGF-2 in the presence of myoblast cells.[163] Hill et al. found that HGF incorporation into alginate gels seeded with myoblasts stimulated increased viability, myoblast migration, and myotube formation after implantation.[70] Adding HGF to the scaffold could promote the native satellite cells to migrate into the muscle defect to regenerate full thickness wounds.

Since vascularization is imperative to the survival of soft tissue, the engineered muscle should provide factors that stimulate capillary growth within the wound site. VEGF in combination with FGF-2 has shown to promote vascularization and prevent the degradation of developing capillaries.[147] Borselli et al. injected VEGF and IGF-I into an ischemic mouse muscle and observed that the combination of growth factors enhanced regeneration, revascularization, reinnervation, and function of the injured muscle. When injected alone, VEGF improved the mechanical properties of the ischemic muscle by increasing the diameters of the developing myofibers.[169] Since studies show FGF-2 upregulates the activation of VEGF at the wound site, a combination of FGF-2 with VEGF bound to the surface of the scaffold will promote the vascular response and enhance the viability of the engineered muscle.[147]

Along with surface modifications that could enhance muscle regeneration using braided collagen scaffolds, structural changes could be explored to optimize proliferation and alignment of MDFCs on the surface of the scaffold. Although the size of the braided collagen scaffold is sufficient for large muscle defects in small animal models, for clinical use in humans, a method of scaling up the scaffold would have to be developed. One proposed method would be to create sheets of braided collagen microthreads that will allow for interaction of cells between each

braid. Neumann et al. developed a method to tether polypropylene fibers within a frame, which would create a sheet of long, contractile myofibers when seeded with myoblasts.[170] By developing a method to create sheets of stem cells for muscle delivery, the scaffold could be manipulated easily to fit into any defect shape and size.

Another way to modify the braided collagen scaffold would be to incorporate fibrin threads into the structure. Type I collagen is responsible for the formation of scar tissue within the wound site, so by limiting the amount of collagen introduced to a defect, fibrosis can be decreased or avoided.[1] Fibrin threads have potential in muscle regeneration due to the biochemical properties, including integrin-signaling cues for wound healing, and the threads degrade within 3-4 weeks in the presence of ECM proteins.[43,94] Another beneficial feature of fibrin microthreads is that growth factors can be integrated into the structure of the threads and be released as the threads degrade.[43] This aspect will allow multiple growth factors to be secreted from the scaffold to better emulate the native wound healing environment. A limitation of fibrin is that it does not possess the mechanical properties of collagen microthreads, which would mean modifications would have to be made to the scaffold structure, as in incorporating a twisting pattern into the braid.[126,151]

The braided collagen scaffolds are meant to be used to repair large muscle defects, which are unable to repair naturally since the entire basal lamina of the myotube has been destroyed eliminating the satellite cells needed for regeneration.[17] By delivering stem-like cells to the muscle defect, the satellite cell population within the wound is replenished, which will allow for new muscle formation. This would be an improvement over current methods, since it would not only fill the defect, but would make it functional. Future research still needs to be explored into the *in vivo* response of native tissue to the braided collagen scaffold.

Chapter 8: Conclusions

In summary, this study has characterized the effects of EDC/NHS crosslinking with and without heparin and different concentrations of FGF-2, on the MDFC activity on braided collagen threads as the preliminary steps to developing a dedifferentiated cell delivery system for muscle regeneration. Immunofluorescent characterization of the braided collagen scaffold showed the presence of FGF-2 bound to the surface of the threads with increased intensity when exposed to higher concentrations of FGF-2. The mechanical strength achieved by braided collagen scaffolds was higher than single collagen threads, and crosslinking using EDC/NHS significantly increase the UTS, ultimate load, strain at failure, and modulus over uncrosslinked braids. When determining the effects of surface modifications on cell attachment, growth, and alignment, the results demonstrate that modifying the surface using crosslinking, heparin, and FGF-2 significantly increased attachment over uncrosslinked surfaces. After 1 day, none of the MDFCs on braided collagen scaffolds exhibited any alignment. Between 1 and 5 days in culture, the surface modifications did not stimulate any significant growth of MDFCs implying a delayed activation of the proliferation of the cells. After 7 days, FGF-2 promoted the growth of MDFCs, with scaffolds exposed to 50 ng/mL FGF-2 having the highest growth rate. MDFCs responded to FGF-2 with increased growth rates with increasing concentrations of the growth factor. Cellular alignment on all control scaffolds was oriented in the direction of the linear axis of the braided collagen scaffold. MDFCs seeded on FGF-2 scaffolds showed limited alignment. These results suggest that MDFCs attached to braided collagen scaffolds modified using EDC/NHS crosslinking with heparin and a controlled release of FGF-2 may serve as a cell delivery scaffold for large muscle defect regeneration.

References

1. Grefte S, Kuijpers-Jagtman A, Torensma R, Von den Hoff J. Skeletal muscle development and regeneration. Stem Cells Dev 2007;16(5):857-68.
2. Chargé S, Rudnicki M. Cellular and molecular regulation of muscle regeneration. Physiol Rev 2004;84(1):209-38.
3. Cassano M, Quattrocelli M, Crippa S, Perini I, Ronzoni F, Sampaolesi M. Cellular mechanisms and local progenitor activation to regulate skeletal muscle mass. J Muscle Res Cell Motil 2009;30(7-8):243-53.
4. Huard J, Li Y, Fu F. Muscle injuries and repair: current trends in research. J Bone Joint Surg Am 2002;84-A(5):822-32.
5. Boldrin L, Muntoni F, Morgan J. Are human and mouse satellite cells really the same? J Histochem Cytochem 2010;58(11):941-55.
6. Quintero A, Wright V, Fu F, Huard J. Stem cells for the treatment of skeletal muscle injury. Clin Sports Med 2009;28(1):1-11.
7. Järvinen T, Järvinen T, Kääriäinen M, Äärimaa V, Vaittinen S, Kalimo H, Järvinen M. Muscle injuries: optimising recovery. Best Pract Res Clin Rheumatol 2007;21(2):317-31.
8. Bian W, Bursac N. Tissue engineering of functional skeletal muscle: challenges and recent advances. IEEE Eng Med Biol Mag 2008;27(5):109-13.
9. Mase VJ, Hsu J, Wolf S, Wenke J, Baer D, Owens J, Badylak S, Walters T. Clinical application of an acellular biologic scaffold for surgical repair of a large, traumatic quadriceps femoris muscle defect. Orthopedics 2010;33(7).
10. Lynch G, Schertzer J, Ryall J. Anabolic agents for improving muscle regeneration and function after injury. Clin Exp Pharmacol Physiol 2008;35(7):852-8.
11. Tedesco F, Dellavalle A, Diaz-Manera J, Messina G, Cossu G. Repairing skeletal muscle: regenerative potential of skeletal muscle stem cells. J Clin Invest 2010;120(1):11-9.
12. Ten Broek R, Grefte S, Von den Hoff J. Regulatory factors and cell populations involved in skeletal muscle regeneration. J Cell Physiol 2010;224(1):7-16.
13. Ambrosio F, Kadi F, Lexell J, Fitzgerald G, Boninger M, Huard J. The effect of muscle loading on skeletal muscle regenerative potential: an update of current research findings relating to aging and neuromuscular pathology. Am J Phys Med Rehabil 2009;88(2):145-55.
14. Jejurikar S, Kuzon WJ. Satellite cell depletion in degenerative skeletal muscle. Apoptosis 2003;8(6):573-8.
15. Eisenberg I, Eran A, Nishino I, Moggio M, Lamperti C, Amato A, Lidov H, Kang P, North K, Mitrani-Rosenbaum S and others. Distinctive patterns of microRNA expression in primary muscular disorders. Proc Natl Acad Sci U S A 2007;104(43):17016-21.
16. Liao H, Zhou G. Development and progress of engineering of skeletal muscle tissue. Tissue Eng Part B Rev 2009;15(3):319-31.
17. Järvinen T, Järvinen T, Kääriäinen M, Kalimo H, Järvinen M. Muscle injuries: biology and treatment. Am J Sports Med 2005;33(5):745-64.
18. Järvinen T, Kääriäinen M, Järvinen M, Kalimo H. Muscle strain injuries. Curr Opin Rheumatol 2000;12(2):155-61.
19. Beier J, Stern-Straeter J, Foerster V, Kneser U, Stark G, Bach A. Tissue engineering of injectable muscle: three-dimensional myoblast-fibrin injection in the syngeneic rat animal model. Plast Reconstr Surg 2006;118(5):1113-21; discussion 1122-4.

20. Saxena A, Marler J, Benvenuto M, Willital G, Vacanti J. Skeletal muscle tissue engineering using isolated myoblasts on synthetic biodegradable polymers: preliminary studies. Tissue Eng 1999;5(6):525-32.
21. Kamelger F, Marksteiner R, Margreiter E, Klima G, Wechselberger G, Hering S, Piza H. A comparative study of three different biomaterials in the engineering of skeletal muscle using a rat animal model. Biomaterials 2004;25(9):1649-55.
22. Delo D, Eberli D, Williams J, Andersson K, Atala A, Soker S. Angiogenic gene modification of skeletal muscle cells to compensate for ageing-induced decline in bioengineered functional muscle tissue. BJU Int 2008;102(7):878-84.
23. Hutmacher D. Scaffold design and fabrication technologies for engineering tissues--state of the art and future perspectives. J Biomater Sci Polym Ed 2001;12(1):107-24.
24. Choi J, Lee S, Christ G, Atala A, Yoo J. The influence of electrospun aligned poly(epsilon-caprolactone)/collagen nanofiber meshes on the formation of self-aligned skeletal muscle myotubes. Biomaterials 2008;29(19):2899-906.
25. Chevallay B, Herbage D. Collagen-based biomaterials as 3D scaffold for cell cultures: applications for tissue engineering and gene therapy. Med Biol Eng Comput 2000;38(2):211-8.
26. Ma L, Gao C, Mao Z, Zhou J, Shen J. Biodegradability and cell-mediated contraction of porous collagen scaffolds: the effect of lysine as a novel crosslinking bridge. J Biomed Mater Res A 2004;71(2):334-42.
27. Carnio S, Serena E, Rossi C, De Coppi P, Elvassore N, Vitiello L. Three-dimensional porous scaffold allows long-term wild-type cell delivery in dystrophic muscle. J Tissue Eng Regen Med 2010.
28. Pieper J, Oosterhof A, Dijkstra P, Veerkamp J, van Kuppevelt T. Preparation and characterization of porous crosslinked collagenous matrices containing bioavailable chondroitin sulphate. Biomaterials 1999;20(9):847-58.
29. Barnes C, Pemble C, Brand D, Simpson D, Bowlin G. Cross-linking electrospun type II collagen tissue engineering scaffolds with carbodiimide in ethanol. Tissue Eng 2007;13(7):1593-605.
30. Vandenburgh H, Del Tatto M, Shansky J, Goldstein L, Russell K, Genes N, Chromiak J, Yamada S. Attenuation of skeletal muscle wasting with recombinant human growth hormone secreted from a tissue-engineered bioartificial muscle. Hum Gene Ther 1998;9(17):2555-64.
31. Beier J, Klumpp D, Rudisile M, Dersch R, Wendorff J, Bleiziffer O, Arkudas A, Polykandriotis E, Horch R, Kneser U. Collagen matrices from sponge to nano: new perspectives for tissue engineering of skeletal muscle. BMC Biotechnol 2009;9:34.
32. Weadock K, Olson R, Silver F. Evaluation of collagen crosslinking techniques. Biomater Med Devices Artif Organs;11(4):293-318.
33. Fujita H, Shimizu K, Nagamori E. Novel method for measuring active tension generation by C2C12 myotube using UV-crosslinked collagen film. Biotechnol Bioeng 2010;106(3):482-9.
34. Yan W, George S, Fotadar U, Tyhovych N, Kamer A, Yost M, Price R, Haggart C, Holmes J, Terracio L. Tissue engineering of skeletal muscle. Tissue Eng 2007;13(11):2781-90.
35. Cornwell K, Downing B, Pins G. Characterizing fibroblast migration on discrete collagen threads for applications in tissue regeneration. J Biomed Mater Res A 2004;71(1):55-62.

36. Cornwell K, Lei P, Andreadis S, Pins G. Crosslinking of discrete self-assembled collagen threads: Effects on mechanical strength and cell-matrix interactions. J Biomed Mater Res A 2007;80(2):362-71.
37. Laurencin C, Freeman J. Ligament tissue engineering: an evolutionary materials science approach. Biomaterials 2005;26(36):7530-6.
38. Pieper J, Hafmans T, van Wachem P, van Luyn M, Brouwer L, Veerkamp J, van Kuppevelt T. Loading of collagen-heparan sulfate matrices with bFGF promotes angiogenesis and tissue generation in rats. J Biomed Mater Res 2002;62(2):185-94.
39. Wissink M, Beernink R, Pieper J, Poot A, Engbers G, Beugeling T, van Aken W, Feijen J. Immobilization of heparin to EDC/NHS-crosslinked collagen. Characterization and in vitro evaluation. Biomaterials 2001;22(2):151-63.
40. Pieper J, Hafmans T, Veerkamp J, van Kuppevelt T. Development of tailor-made collagen-glycosaminoglycan matrices: EDC/NHS crosslinking, and ultrastructural aspects. Biomaterials 2000;21(6):581-93.
41. Wissink M, Beernink R, Pieper J, Poot A, Engbers G, Beugeling T, van Aken W, Feijen J. Binding and release of basic fibroblast growth factor from heparinized collagen matrices. Biomaterials 2001;22(16):2291-9.
42. Harmer N. Insights into the role of heparan sulphate in fibroblast growth factor signalling. Biochem Soc Trans 2006;34(Pt 3):442-5.
43. Cornwell K, Pins G. Enhanced Proliferation and Migration of Fibroblasts on the Surface of FGF-2 Loaded Fibrin Microthreads. Tissue Eng Part A 2010.
44. Vandenburgh H. Functional assessment and tissue design of skeletal muscle. Ann N Y Acad Sci 2002;961:201-2.
45. Serena E, Flaibani M, Carnio S, Boldrin L, Vitiello L, De Coppi P, Elvassore N. Electrophysiologic stimulation improves myogenic potential of muscle precursor cells grown in a 3D collagen scaffold. Neurol Res 2008;30(2):207-14.
46. Page R, Ambady S, Holmes W, Vilner L, Kole D, Kashpur O, Huntress V, Vojtic I, Whitton H, Dominko T. Induction of stem cell gene expression in adult human fibroblasts without transgenes. Cloning Stem Cells 2009;11(3):417-26.
47. Cosgrove BD, Sacco A, Gilbert PM, Blau HM. A home away from home: challenges and opportunities in engineering in vitro muscle satellite cell niches. Differentiation 2009;78(2-3):185-94.
48. Bassel-Duby R, Olson E. Signaling pathways in skeletal muscle remodeling. Annu Rev Biochem 2006;75:19-37.
49. Menetrey J, Kasemkijwattana C, Day C, Bosch P, Vogt M, Fu F, Moreland M, Huard J. Growth factors improve muscle healing in vivo. J Bone Joint Surg Br 2000;82(1):131-7.
50. Shi X, Garry D. Muscle stem cells in development, regeneration, and disease. Genes Dev 2006;20(13):1692-708.
51. Grounds M. Towards understanding skeletal muscle regeneration. Pathol Res Pract 1991;187(1):1-22.
52. Tidball J. Inflammatory processes in muscle injury and repair. Am J Physiol Regul Integr Comp Physiol 2005;288(2):R345-53.
53. Morgan J, Partridge T. Muscle satellite cells. Int J Biochem Cell Biol 2003;35(8):1151-6.
54. Anderson J. The satellite cell as a companion in skeletal muscle plasticity: currency, conveyance, clue, connector and colander. J Exp Biol 2006;209(Pt 12):2276-92.

55. Zammit P, Partridge T, Yablonka-Reuveni Z. The skeletal muscle satellite cell: the stem cell that came in from the cold. J Histochem Cytochem 2006;54(11):1177-91.
56. Li Y, Huard J. Differentiation of muscle-derived cells into myofibroblasts in injured skeletal muscle. Am J Pathol 2002;161(3):895-907.
57. Montarras D, Morgan J, Collins C, Relaix F, Zaffran S, Cumano A, Partridge T, Buckingham M. Direct isolation of satellite cells for skeletal muscle regeneration. Science 2005;309(5743):2064-7.
58. Seale P, Rudnicki M. A new look at the origin, function, and "stem-cell" status of muscle satellite cells. Dev Biol 2000;218(2):115-24.
59. Lehto M, Järvinen M, Nelimarkka O. Scar formation after skeletal muscle injury. A histological and autoradiographical study in rats. Arch Orthop Trauma Surg 1986;104(6):366-70.
60. Hawke T, Garry D. Myogenic satellite cells: physiology to molecular biology. J Appl Physiol 2001;91(2):534-51.
61. Kawiak J, Brzóska E, Grabowska I, Hoser G, Stremińska W, Wasilewska D, Machaj E, Pojda Z, Moraczewski J. Contribution of stem cells to skeletal muscle regeneration. Folia Histochem Cytobiol 2006;44(2):75-9.
62. Sheehan S, Allen R. Skeletal muscle satellite cell proliferation in response to members of the fibroblast growth factor family and hepatocyte growth factor. J Cell Physiol 1999;181(3):499-506.
63. Tidball J. Mechanical signal transduction in skeletal muscle growth and adaptation. J Appl Physiol 2005;98(5):1900-8.
64. Pelosi L, Giacinti C, Nardis C, Borsellino G, Rizzuto E, Nicoletti C, Wannenes F, Battistini L, Rosenthal N, Molinaro M and others. Local expression of IGF-1 accelerates muscle regeneration by rapidly modulating inflammatory cytokines and chemokines. FASEB J 2007;21(7):1393-402.
65. Saxena A, Willital G, Vacanti J. Vascularized three-dimensional skeletal muscle tissue-engineering. Biomed Mater Eng 2001;11(4):275-81.
66. Ghaly A, Marsh D. Ischaemia-reperfusion modulates inflammation and fibrosis of skeletal muscle after contusion injury. Int J Exp Pathol 2010;91(3):244-55.
67. Peng H, Huard J. Muscle-derived stem cells for musculoskeletal tissue regeneration and repair. Transpl Immunol 2004;12(3-4):311-9.
68. Masini B, Waterman S, Wenke J, Owens B, Hsu J, Ficke J. Resource utilization and disability outcome assessment of combat casualties from Operation Iraqi Freedom and Operation Enduring Freedom. J Orthop Trauma 2009;23(4):261-6.
69. Kimura E, Han J, Li S, Fall B, Ra J, Haraguchi M, Tapscott S, Chamberlain J. Cell-lineage regulated myogenesis for dystrophin replacement: a novel therapeutic approach for treatment of muscular dystrophy. Hum Mol Genet 2008;17(16):2507-17.
70. Hill E, Boontheekul T, Mooney D. Designing scaffolds to enhance transplanted myoblast survival and migration. Tissue Eng 2006;12(5):1295-304.
71. Global burden of musculoskeletal disease revealed in new WHO report. Bull World Health Organ 2003;81(11):853-4.
72. Kannus P, Parkkari J, Järvinen T, Järvinen T, Järvinen M. Basic science and clinical studies coincide: active treatment approach is needed after a sports injury. Scand J Med Sci Sports 2003;13(3):150-4.

73. De Coppi P, Bellini S, Conconi M, Sabatti M, Simonato E, Gamba P, Nussdorfer G, Parnigotto P. Myoblast-acellular skeletal muscle matrix constructs guarantee a long-term repair of experimental full-thickness abdominal wall defects. Tissue Eng 2006;12(7):1929-36.
74. Thorrez L, Shansky J, Wang L, Fast L, VandenDriessche T, Chuah M, Mooney D, Vandenburgh H. Growth, differentiation, transplantation and survival of human skeletal myofibers on biodegradable scaffolds. Biomaterials 2008;29(1):75-84.
75. Qu Z, Balkir L, van Deutekom J, Robbins P, Pruchnic R, Huard J. Development of approaches to improve cell survival in myoblast transfer therapy. J Cell Biol 1998;142(5):1257-67.
76. van Wachem P, Brouwer L, van Luyn M. Absence of muscle regeneration after implantation of a collagen matrix seeded with myoblasts. Biomaterials 1999;20(5):419-26.
77. Koning M, Harmsen M, van Luyn M, Werker P. Current opportunities and challenges in skeletal muscle tissue engineering. J Tissue Eng Regen Med 2009;3(6):407-15.
78. Saxena A. Tissue engineering and regenerative medicine research perspectives for pediatric surgery. Pediatr Surg Int 2010;26(6):557-73.
79. Caplan A, Goldberg V. Principles of tissue engineered regeneration of skeletal tissues. Clin Orthop Relat Res 1999(367 Suppl):S12-6.
80. Dhawan V, Lytle I, Dow D, Huang Y, Brown D. Neurotization improves contractile forces of tissue-engineered skeletal muscle. Tissue Eng 2007;13(11):2813-21.
81. Kosnik P, Faulkner J, Dennis R. Functional development of engineered skeletal muscle from adult and neonatal rats. Tissue Eng 2001;7(5):573-84.
82. Stern-Straeter J, Bran G, Riedel F, Sauter A, Hörmann K, Goessler U. Characterization of human myoblast cultures for tissue engineering. Int J Mol Med 2008;21(1):49-56.
83. Fuchs J, Pomerantseva I, Ochoa E, Vacanti J, Fauza D. Fetal tissue engineering: in vitro analysis of muscle constructs. J Pediatr Surg 2003;38(9):1348-53.
84. Kim M, Jun I, Shin Y, Jang W, Kim S, Shin H. The development of genipin-crosslinked poly(caprolactone) (PCL)/gelatin nanofibers for tissue engineering applications. Macromol Biosci 2010;10(1):91-100.
85. Huang N, Patel S, Thakar R, Wu J, Hsiao B, Chu B, Lee R, Li S. Myotube assembly on nanofibrous and micropatterned polymers. Nano Lett 2006;6(3):537-42.
86. Williamson M, Adams E, Coombes A. Gravity spun polycaprolactone fibres for soft tissue engineering: interaction with fibroblasts and myoblasts in cell culture. Biomaterials 2006;27(7):1019-26.
87. Ren K, Crouzier T, Roy C, Picart C. Polyelectrolyte multilayer films of controlled stiffness modulate myoblast cells differentiation. Adv Funct Mater 2008;18(9):1378-1389.
88. Richert L, Schneider A, Vautier D, Vodouhe C, Jessel N, Payan E, Schaaf P, Voegel J, Picart C. Imaging cell interactions with native and crosslinked polyelectrolyte multilayers. Cell Biochem Biophys 2006;44(2):273-85.
89. Ren K, Fourel L, Rouvière C, Albiges-Rizo C, Picart C. Manipulation of the adhesive behaviour of skeletal muscle cells on soft and stiff polyelectrolyte multilayers. Acta Biomater 2010.
90. Cohen D, Malone E, Lipson H, Bonassar L. Direct freeform fabrication of seeded hydrogels in arbitrary geometries. Tissue Eng 2006;12(5):1325-35.

91. Gleghorn J, Lee C, Cabodi M, Stroock A, Bonassar L. Adhesive properties of laminated alginate gels for tissue engineering of layered structures. J Biomed Mater Res A 2008;85(3):611-8.
92. Boontheekul T, Hill E, Kong H, Mooney D. Regulating myoblast phenotype through controlled gel stiffness and degradation. Tissue Eng 2007;13(7):1431-42.
93. Rowley J, Madlambayan G, Mooney D. Alginate hydrogels as synthetic extracellular matrix materials. Biomaterials 1999;20(1):45-53.
94. Huang Y, Dennis R, Larkin L, Baar K. Rapid formation of functional muscle in vitro using fibrin gels. J Appl Physiol 2005;98(2):706-13.
95. Beier J, Kneser U, Stern-Sträter J, Stark G, Bach A. Y chromosome detection of three-dimensional tissue-engineered skeletal muscle constructs in a syngeneic rat animal model. Cell Transplant 2004;13(1):45-53.
96. Matsumoto T, Sasaki J, Alsberg E, Egusa H, Yatani H, Sohmura T. Three-dimensional cell and tissue patterning in a strained fibrin gel system. PLoS One 2007;2(11):e1211.
97. Nagamine K, Kawashima T, Ishibashi T, Kaji H, Kanzaki M, Nishizawa M. Micropatterning contractile C2C12 myotubes embedded in a fibrin gel. Biotechnol Bioeng 2010;105(6):1161-7.
98. Huang Y, Dennis R, Baar K. Cultured slow vs. fast skeletal muscle cells differ in physiology and responsiveness to stimulation. Am J Physiol Cell Physiol 2006;291(1):C11-7.
99. Borschel G, Dow D, Dennis R, Brown D. Tissue-engineered axially vascularized contractile skeletal muscle. Plast Reconstr Surg 2006;117(7):2235-42.
100. Borschel G, Dennis R, Kuzon WJ. Contractile skeletal muscle tissue-engineered on an acellular scaffold. Plast Reconstr Surg 2004;113(2):595-602; discussion 603-4.
101. Conconi M, De Coppi P, Bellini S, Zara G, Sabatti M, Marzaro M, Zanon G, Gamba P, Parnigotto P, Nussdorfer G. Homologous muscle acellular matrix seeded with autologous myoblasts as a tissue-engineering approach to abdominal wall-defect repair. Biomaterials 2005;26(15):2567-74.
102. Dennis R, Kosnik Pn. Excitability and isometric contractile properties of mammalian skeletal muscle constructs engineered in vitro. In Vitro Cell Dev Biol Anim 2000;36(5):327-35.
103. Dennis R, Kosnik Pn, Gilbert M, Faulkner J. Excitability and contractility of skeletal muscle engineered from primary cultures and cell lines. Am J Physiol Cell Physiol 2001;280(2):C288-95.
104. Larkin L, Van der Meulen J, Dennis R, Kennedy J. Functional evaluation of nerve-skeletal muscle constructs engineered in vitro. In Vitro Cell Dev Biol Anim 2006;42(3-4):75-82.
105. Vandenburgh H, Shansky J, Benesch-Lee F, Barbata V, Reid J, Thorrez L, Valentini R, Crawford G. Drug-screening platform based on the contractility of tissue-engineered muscle. Muscle Nerve 2008;37(4):438-47.
106. Powell C, Smiley B, Mills J, Vandenburgh H. Mechanical stimulation improves tissue-engineered human skeletal muscle. Am J Physiol Cell Physiol 2002;283(5):C1557-65.
107. Shansky J, Creswick B, Lee P, Wang X, Vandenburgh H. Paracrine release of insulin-like growth factor 1 from a bioengineered tissue stimulates skeletal muscle growth in vitro. Tissue Eng 2006;12(7):1833-41.

108. Gefen A, van Nierop B, Bader D, Oomens C. Strain-time cell-death threshold for skeletal muscle in a tissue-engineered model system for deep tissue injury. J Biomech 2008;41(9):2003-12.
109. Vandenburgh H, Shansky J, Benesch-Lee F, Skelly K, Spinazzola J, Saponjian Y, Tseng B. Automated drug screening with contractile muscle tissue engineered from dystrophic myoblasts. FASEB J 2009;23(10):3325-34.
110. Vandenburgh H. High-content drug screening with engineered musculoskeletal tissues. Tissue Eng Part B Rev 2010;16(1):55-64.
111. Yang J, Yamato M, Kohno C, Nishimoto A, Sekine H, Fukai F, Okano T. Cell sheet engineering: recreating tissues without biodegradable scaffolds. Biomaterials 2005;26(33):6415-22.
112. Yamasaki K, Hayashi H, Nishiyama K, Kobayashi H, Uto S, Kondo H, Hashimoto S, Fujisato T. Control of myotube contraction using electrical pulse stimulation for bio-actuator. J Artif Organs 2009;12(2):131-7.
113. Cheema U, Yang S, Mudera V, Goldspink G, Brown R. 3-D in vitro model of early skeletal muscle development. Cell Motil Cytoskeleton 2003;54(3):226-36.
114. Gawlitta D, Boonen K, Oomens C, Baaijens F, Bouten C. The influence of serum-free culture conditions on skeletal muscle differentiation in a tissue-engineered model. Tissue Eng Part A 2008;14(1):161-71.
115. Huang N, Lee R, Li S. Engineering of aligned skeletal muscle by micropatterning. Am J Transl Res 2010;2(1):43-55.
116. Kroehne V, Heschel I, Schügner F, Lasrich D, Bartsch J, Jockusch H. Use of a novel collagen matrix with oriented pore structure for muscle cell differentiation in cell culture and in grafts. J Cell Mol Med 2008;12(5A):1640-8.
117. Cimetta E, Flaibani M, Mella M, Serena E, Boldrin L, De Coppi P, Elvassore N. Enhancement of viability of muscle precursor cells on 3D scaffold in a perfusion bioreactor. Int J Artif Organs 2007;30(5):415-28.
118. Grefte S, Kuijpers-Jagtman A, Torensma R, Von den Hoff J. A Model for Muscle Regeneration around Fibrotic Lesions in Recurrent Strain Injuries. Med Sci Sports Exerc 2009.
119. Kin S, Hagiwara A, Nakase Y, Kuriu Y, Nakashima S, Yoshikawa T, Sakakura C, Otsuji E, Nakamura T, Yamagishi H. Regeneration of skeletal muscle using in situ tissue engineering on an acellular collagen sponge scaffold in a rabbit model. ASAIO J 2007;53(4):506-13.
120. Pins G, Christiansen D, Patel R, Silver F. Self-assembly of collagen fibers. Influence of fibrillar alignment and decorin on mechanical properties. Biophys J 1997;73(4):2164-72.
121. Wang M, Pins G, Silver F. Collagen fibres with improved strength for the repair of soft tissue injuries. Biomaterials 1994;15(7):507-12.
122. Kato Y, Dunn M, Zawadsky J, Tria A, Silver F. Regeneration of Achilles tendon with a collagen tendon prosthesis. Results of a one-year implantation study. J Bone Joint Surg Am 1991;73(4):561-74.
123. Silver F, Freeman J, Seehra G. Collagen self-assembly and the development of tendon mechanical properties. J Biomech 2003;36(10):1529-53.
124. Rovensky YuA, Samoilov V. Morphogenetic response of cultured normal and transformed fibroblasts, and epitheliocytes, to a cylindrical substratum surface. Possible role for the actin filament bundle pattern. J Cell Sci 1994;107 (Pt 5):1255-63.

125. Freeman J, Woods M, Laurencin C. Tissue engineering of the anterior cruciate ligament using a braid-twist scaffold design. J Biomech 2007;40(9):2029-36.
126. Horan R, Collette A, Lee C, Antle K, Chen J, Altman G. Yarn design for functional tissue engineering. J Biomech 2006;39(12):2232-40.
127. Khor E. Methods for the treatment of collagenous tissues for bioprostheses. Biomaterials 1997;18(2):95-105.
128. Friess W. Collagen--biomaterial for drug delivery. Eur J Pharm Biopharm 1998;45(2):113-36.
129. van Wachem P, Plantinga J, Wissink M, Beernink R, Poot A, Engbers G, Beugeling T, van Aken W, Feijen J, van Luyn M. In vivo biocompatibility of carbodiimide-crosslinked collagen matrices: Effects of crosslink density, heparin immobilization, and bFGF loading. J Biomed Mater Res 2001;55(3):368-78.
130. Caruso A, Dunn M. Changes in mechanical properties and cellularity during long-term culture of collagen fiber ACL reconstruction scaffolds. J Biomed Mater Res A 2005;73(4):388-97.
131. Gratzer P, Lee J. Control of pH alters the type of cross-linking produced by 1-ethyl-3-(3-dimethylaminopropyl)-carbodiimide (EDC) treatment of acellular matrix vascular grafts. J Biomed Mater Res 2001;58(2):172-9.
132. Wissink M, Beernink R, Poot A, Engbers G, Beugeling T, van Aken W, Feijen J. Improved endothelialization of vascular grafts by local release of growth factor from heparinized collagen matrices. J Control Release 2000;64(1-3):103-14.
133. Pieper J, van Wachem P, van Luyn MJA, Brouwer L, Hafmans T, Veerkamp J, van Kuppevelt T. Attachment of glycosaminoglycans to collagenous matrices modulates the tissue response in rats. Biomaterials 2000;21(16):1689-99.
134. Ornitz D, Itoh N. Fibroblast growth factors. Genome Biol 2001;2(3):REVIEWS3005.
135. Stadtfeld M, Hochedlinger K. Induced pluripotency: history, mechanisms, and applications. Genes Dev 2010;24(20):2239-63.
136. Takahashi K, Tanabe K, Ohnuki M, Narita M, Ichisaka T, Tomoda K, Yamanaka S. Induction of pluripotent stem cells from adult human fibroblasts by defined factors. Cell 2007;131(5):861-72.
137. Zhao R, Daley G. From fibroblasts to iPS cells: induced pluripotency by defined factors. J Cell Biochem 2008;105(4):949-55.
138. Takahashi K, Okita K, Nakagawa M, Yamanaka S. Induction of pluripotent stem cells from fibroblast cultures. Nat Protoc 2007;2(12):3081-9.
139. Levenstein M, Ludwig T, Xu R, Llanas R, VanDenHeuvel-Kramer K, Manning D, Thomson J. Basic fibroblast growth factor support of human embryonic stem cell self-renewal. Stem Cells 2006;24(3):568-74.
140. Yu J, Vodyanik M, Smuga-Otto K, Antosiewicz-Bourget J, Frane J, Tian S, Nie J, Jonsdottir G, Ruotti V, Stewart R and others. Induced pluripotent stem cell lines derived from human somatic cells. Science 2007;318(5858):1917-20.
141. Engler A, Griffin M, Sen S, Bönnemann C, Sweeney H, Discher D. Myotubes differentiate optimally on substrates with tissue-like stiffness: pathological implications for soft or stiff microenvironments. J Cell Biol 2004;166(6):877-87.
142. Chaudhuri T, Rehfeldt F, Sweeney H, Discher D. Preparation of collagen-coated gels that maximize in vitro myogenesis of stem cells by matching the lateral elasticity of in vivo muscle. Methods Mol Biol 2010;621:185-202.

143. Gilbert P, Havenstrite K, Magnusson K, Sacco A, Leonardi N, Kraft P, Nguyen N, Thrun S, Lutolf M, Blau H. Substrate elasticity regulates skeletal muscle stem cell self-renewal in culture. Science 2010;329(5995):1078-81.
144. Bush K, Pins G. Carbodiimide conjugation of fibronectin on collagen basal lamina analogs enhances cellular binding domains and epithelialization. Tissue Eng Part A 2010;16(3):829-38.
145. Mizuno Y, Chang H, Umeda K, Niwa A, Iwasa T, Awaya T, Fukada S, Yamamoto H, Yamanaka S, Nakahata T and others. Generation of skeletal muscle stem/progenitor cells from murine induced pluripotent stem cells. FASEB J 2010;24(7):2245-53.
146. Cushing M, Liao J, Jaeggli M, Anseth K. Material-based regulation of the myofibroblast phenotype. Biomaterials 2007;28(23):3378-87.
147. Zieris A, Prokoph S, Levental K, Welzel P, Grimmer M, Freudenberg U, Werner C. FGF-2 and VEGF functionalization of starPEG-heparin hydrogels to modulate biomolecular and physical cues of angiogenesis. Biomaterials 2010.
148. Nillesen S, Geutjes P, Wismans R, Schalkwijk J, Daamen W, van Kuppevelt T. Increased angiogenesis and blood vessel maturation in acellular collagen-heparin scaffolds containing both FGF2 and VEGF. Biomaterials 2007;28(6):1123-31.
149. Lu H, Cooper JJ, Manuel S, Freeman J, Attawia M, Ko F, Laurencin C. Anterior cruciate ligament regeneration using braided biodegradable scaffolds: in vitro optimization studies. Biomaterials 2005;26(23):4805-16.
150. Altman G, Horan R, Lu H, Moreau J, Martin I, Richmond J, Kaplan D. Silk matrix for tissue engineered anterior cruciate ligaments. Biomaterials 2002;23(20):4131-41.
151. Cornwell K, Pins G. Discrete crosslinked fibrin microthread scaffolds for tissue regeneration. J Biomed Mater Res A 2007;82(1):104-12.
152. Cooper J, Lu H, Ko F, Freeman J, Laurencin C. Fiber-based tissue-engineered scaffold for ligament replacement: design considerations and in vitro evaluation. Biomaterials 2005;26(13):1523-32.
153. Iwata A, Fuchioka S, Hiraoka K, Masuhara M, Kami K. Characteristics of locomotion, muscle strength, and muscle tissue in regenerating rat skeletal muscles. Muscle Nerve 2010;41(5):694-701.
154. Merritt E, Hammers D, Tierney M, Suggs L, Walters T, Farrar R. Functional assessment of skeletal muscle regeneration utilizing homologous extracellular matrix as scaffolding. Tissue Eng Part A 2010;16(4):1395-405.
155. Moreau J, Bramono D, Horan R, Kaplan D, Altman G. Sequential biochemical and mechanical stimulation in the development of tissue-engineered ligaments. Tissue Eng Part A 2008;14(7):1161-72.
156. Moreau J, Chen J, Kaplan D, Altman G. Sequential growth factor stimulation of bone marrow stromal cells in extended culture. Tissue Eng 2006;12(10):2905-12.
157. Chen J, Horan R, Bramono D, Moreau J, Wang Y, Geuss L, Collette A, Volloch V, Altman G. Monitoring mesenchymal stromal cell developmental stage to apply on-time mechanical stimulation for ligament tissue engineering. Tissue Eng 2006;12(11):3085-95.
158. Chen J, Altman G, Karageorgiou V, Horan R, Collette A, Volloch V, Colabro T, Kaplan D. Human bone marrow stromal cell and ligament fibroblast responses on RGD-modified silk fibers. J Biomed Mater Res A 2003;67(2):559-70.
159. Bikfalvi A, Klein S, Pintucci G, Rifkin D. Biological roles of fibroblast growth factor-2. Endocr Rev 1997;18(1):26-45.

160. Wissink M, Beernink R, Scharenborg N, Poot A, Engbers G, Beugeling T, van Aken W, Feijen J. Endothelial cell seeding of (heparinized) collagen matrices: effects of bFGF pre-loading on proliferation (after low density seeding) and pro-coagulant factors. J Control Release 2000;67(2-3):141-55.
161. Yoon J, Chung H, Lee H, Park T. Heparin-immobilized biodegradable scaffolds for local and sustained release of angiogenic growth factor. J Biomed Mater Res A 2006;79(4):934-42.
162. Guerrini M, Hricovíni M, Torri G. Interaction of heparins with fibroblast growth factors: conformational aspects. Curr Pharm Des 2007;13(20):2045-56.
163. Hill E, Boontheekul T, Mooney D. Regulating activation of transplanted cells controls tissue regeneration. Proc Natl Acad Sci U S A 2006;103(8):2494-9.
164. Coletti D, Teodori L, Albertini M, Rocchi M, Pristerà A, Fini M, Molinaro M, Adamo S. Static magnetic fields enhance skeletal muscle differentiation in vitro by improving myoblast alignment. Cytometry A 2007;71(10):846-56.
165. Aviss K, Gough J, Downes S. Aligned electrospun polymer fibres for skeletal muscle regeneration. Eur Cell Mater 2010;19:193-204.
166. Zhao Y, Zeng H, Nam J, Agarwal S. Fabrication of skeletal muscle constructs by topographic activation of cell alignment. Biotechnol Bioeng 2009;102(2):624-31.
167. Lam M, Sim S, Zhu X, Takayama S. The effect of continuous wavy micropatterns on silicone substrates on the alignment of skeletal muscle myoblasts and myotubes. Biomaterials 2006;27(24):4340-7.
168. Shimizu K, Fujita H, Nagamori E. Alignment of skeletal muscle myoblasts and myotubes using linear micropatterned surfaces ground with abrasives. Biotechnol Bioeng 2009;103(3):631-8.
169. Borselli C, Storrie H, Benesch-Lee F, Shvartsman D, Cezar C, Lichtman J, Vandenburgh H, Mooney D. Functional muscle regeneration with combined delivery of angiogenesis and myogenesis factors. Proc Natl Acad Sci U S A 2010;107(8):3287-92.
170. Neumann T, Hauschka S, Sanders J. Tissue engineering of skeletal muscle using polymer fiber arrays. Tissue Eng 2003;9(5):995-1003.

Appendix A: Mechanical Testing Data Analysis

Appendix A.1: Histological Cross-Sectional Area Measurements

Below is the summary of measurements of the histology cross sectional area measurements and statistics comparing each surface modification area.

Braided Collagen Scaffold Histology Cross Section Measurements			
Image	cross sectional area (cm^2)	cross sectional area (mm^2)	cross sectional area (μm^2)
NONE	0.001	0.1	100000
NONE	0.001	0.1	100000
NONE	0.00153	0.153	153000
NONE	0.001076	0.1076	107600
EDC/NHS	8.48E-04	0.08479	84790
EDC/NHS	8.22E-04	0.08222	82220
EDC/NHS	6.27E-04	0.06266	62660
EDC/NHS	5.99E-04	0.05987	59870
HEP	0.002	0.2	200000
HEP	0.002	0.2	200000
HEP	6.86E-04	0.06859	68590
5FGF	0.001	0.1	100000
5FGF	9.48E-04	0.09477	94770
5FGF	6.81E-04	0.0681	68100
5FGF	6.81E-04	0.06811	68110
10FGF	6.34E-04	0.06337	63370
10FGF	5.47E-04	0.0547	54700
10FGF	6.20E-04	0.06195	61950
10FGF	6.71E-04	0.06708	67080
50FGF	7.74E-04	0.07735	77350
50FGF	8.18E-04	0.08182	81820
50FGF	9.54E-04	0.09538	95380
50FGF	6.24E-04	0.06237	62370
AVERAGE	0.000919013	0.091901304	91901.30435
S.D.	0.000405447	0.040544687	40544.68694

t-test Monday, November 01, 2010, 3:17:03 PM

Data source: Data 1 in cross section

Normality Test (Shapiro-Wilk) Failed (P < 0.050)

Test execution ended by user request, Rank Sum Test begun

Mann-Whitney Rank Sum Test Monday, November 01, 2010, 3:17:03 PM

Data source: Data 1 in cross section

Group	N	Missing	Median	25%	75%
none	4	0	0.104	0.1000	0.142
edc	4	0	0.0724	0.0606	0.0841

Mann-Whitney U Statistic= 0.000

T = 26.000 n(small)= 4 n(big)= 4 P(est.)= 0.029 P(exact)= 0.029

The difference in the median values between the two groups is greater than would be expected by chance; there is a statistically significant difference (P = 0.029)

Test execution ended by user request, ANOVA on Ranks begun

Kruskal-Wallis One Way Analysis of Variance on Ranks Thursday, August 26, 2010, 11:23:58 AM

Data source: Data 1 in Notebook1

Group	N	Missing	Median	25%	75%
none	4	0	0.104	0.1000	0.142
edc	4	0	0.0724	0.0606	0.0841
hep	3	0	0.200	0.0686	0.200
5fgf	4	0	0.0814	0.0681	0.0987
10fgf	4	0	0.0627	0.0565	0.0662
50fgf	4	0	0.0796	0.0661	0.0920

H = 13.666 with 5 degrees of freedom. (P = 0.018)

The differences in the median values among the treatment groups are greater than would be expected by chance; there is a statistically significant difference (P = 0.018)

To isolate the group or groups that differ from the others use a multiple comparison procedure.

All Pairwise Multiple Comparison Procedures (Dunn's Method) :

Comparison	Diff of Ranks	Q	P<0.05
none vs 10fgf	15.000	3.128	Yes
none vs edc	10.750	2.242	No
none vs 50fgf	8.500	1.772	Do Not Test
none vs 5fgf	6.750	1.407	Do Not Test
none vs hep	0.917	0.177	Do Not Test
hep vs 10fgf	14.083	2.719	No
hep vs edc	9.833	1.898	Do Not Test

hep vs 50fgf	7.583	1.464	Do Not Test
hep vs 5fgf	5.833	1.126	Do Not Test
5fgf vs 10fgf	8.250	1.720	Do Not Test
5fgf vs edc	4.000	0.834	Do Not Test
5fgf vs 50fgf	1.750	0.365	Do Not Test
50fgf vs 10fgf	6.500	1.355	Do Not Test
50fgf vs edc	2.250	0.469	Do Not Test
edc vs 10fgf	4.250	0.886	Do Not Test

Note: The multiple comparisons on ranks do not include an adjustment for ties.

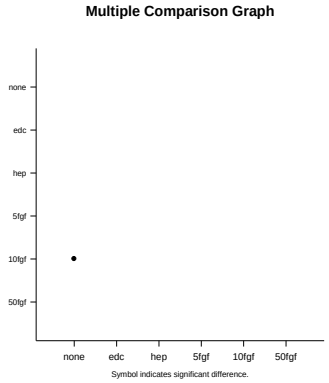

Appendix A.2: Mechanical Testing Raw Data

Uncrosslinked					Crosslinked				
Ultimate Load (N)	UTS (MPa)	Strain at Failure (mm/mm)	Modulus (MPa)		Ultimate Load (N)	UTS (MPa)	Strain at Failure (mm/mm)	Modulus (MPa)	
0.5914	5.135909683	0.287057143	21.04371744		1.9291	26.65054915	0.391442857	72.29195653	
0.5958	5.174120712	0.389185714	13.88588568		1.7382	24.01326242	0.440942857	66.98016339	
0.4777	4.148501954	0.309171429	14.38210251		1.6197	22.37618291	0.429042857	64.38177575	
0.6871	5.966999566	0.452528571	14.0351264		1.8201	25.1447123	0.479214286	65.50773343	
0.7032	6.106817195	0.467257143	15.23370774		1.6106	22.25046626	0.4474	61.5634467	
0.5533	4.805036908	0.392342857	12.5193199		2.0836	28.78496926	0.507457143	72.4761713	
0.5636	4.894485454	0.430014286	11.20497332		2.1739	30.03246529	0.375757143	93.5146282	
0.5511	4.785931394	0.437428571	12.56756695		1.81	25.00518063	0.484857143	63.11365812	
0.6745	5.857577073	0.396814286	15.78415017		1.7838	24.64322719	0.509657143	61.58192564	
0.4561	3.960920538	0.358371429	12.15064336		1.9407	26.81080334	0.501342857	69.56211856	
0.6608	5.738601824	0.450942857	14.71193488		1.9598	27.07467017	0.477385714	70.78923646	
0.5087	4.417716023	0.525814286	8.131810775		2.0624	28.4920909	0.477457143	76.94276024	
0.6666	5.788970908	0.493228571	13.33442771		2.3027	30.39580023	0.690742857	68.46694894	
0.5584	4.849326965	0.419814286	12.51850616		2.2426	30.98155695	0.5626	68.31268531	
0.6509	5.652627008	0.481514286	13.148952		2.2921	28.8167438	0.827685714	59.92088089	
0.552	4.793747286	0.426628571	12.97327299		2.2869	30.05180631	0.660714286	60.84914502	
Average	0.5907	5.129830656	0.419882143	13.60163113		1.9785125	26.97028044	0.51648125	68.51595216
S.D.	0.076223129	0.661946406	0.063794756	2.668028059		0.236927285	2.835373196	0.118181915	8.24196541

t-test – Ultimate Load Thursday, August 26, 2010, 12:43:03 PM

Data source: Data 1 in ultimate load

Normality Test (Shapiro-Wilk) Passed (P = 0.396)

Equal Variance Test: Failed (P < 0.050)

Test execution ended by user request, Rank Sum Test begun

Mann-Whitney Rank Sum Test Thursday, August 26, 2010, 12:43:03 PM

Data source: Data 1 in ultimate load

Group	N	Missing	Median	25%	75%
UNX	16	0	0.578	0.551	0.665
Crosslinked	16	0	1.950	1.790	2.225

Mann-Whitney U Statistic= 0.000

T = 136.000 n(small)= 16 n(big)= 16 (P = <0.001)

The difference in the median values between the two groups is greater than would be expected by chance; there is a statistically significant difference (P = <0.001)

---

t-test - UTS Monday, November 01, 2010, 4:13:44 PM

Data source: Data 1 in uts

Normality Test (Shapiro-Wilk) Passed (P = 0.287)

Equal Variance Test: Failed (P < 0.050)

Test execution ended by user request, Rank Sum Test begun

Mann-Whitney Rank Sum Test Monday, November 01, 2010, 4:13:44 PM

Data source: Data 1 in uts

Group	N	Missing	Median	25%	75%
UNX	16	0	5.015	4.788	5.776
Crosslinked	16	0	26.943	24.734	29.729

Mann-Whitney U Statistic= 0.000

T = 136.000 n(small)= 16 n(big)= 16 (P = <0.001)

The difference in the median values between the two groups is greater than would be expected by chance; there is a statistically significant difference (P = <0.001)

---

t-test – Strain at Failure Thursday, August 26, 2010, 12:46:20 PM

Data source: Data 1 in strain at failure

Normality Test (Shapiro-Wilk) Failed (P < 0.050)

Test execution ended by user request, Rank Sum Test begun

Mann-Whitney Rank Sum Test Thursday, August 26, 2010, 12:46:20 PM

Data source: Data 1 in strain at failure

Group	N	Missing	Median	25%	75%
Unx	16	0	0.428	0.390	0.464
crosslink	16	0	0.482	0.443	0.549

Mann-Whitney U Statistic= 59.000

T = 195.000 n(small)= 16 n(big)= 16 (P = 0.010)

The difference in the median values between the two groups is greater than would be expected by chance; there is a statistically significant difference (P = 0.010)

---

t-test - MTM Monday, November 01, 2010, 4:15:10 PM

Data source: Data 1 in modulus

Normality Test (Shapiro-Wilk) Failed (P < 0.050)

Test execution ended by user request, Rank Sum Test begun

Mann-Whitney Rank Sum Test Monday, November 01, 2010, 4:15:10 PM

Data source: Data 1 in modulus

Group	N	Missing	Median	25%	75%
unx	16	0	13.242	12.519	14.629
crosslink	16	0	67.646	61.965	71.916

Mann-Whitney U Statistic= 0.000

T = 136.000 n(small)= 16 n(big)= 16 (P = <0.001)

The difference in the median values between the two groups is greater than would be expected by chance; there is a statistically significant difference (P = <0.001)

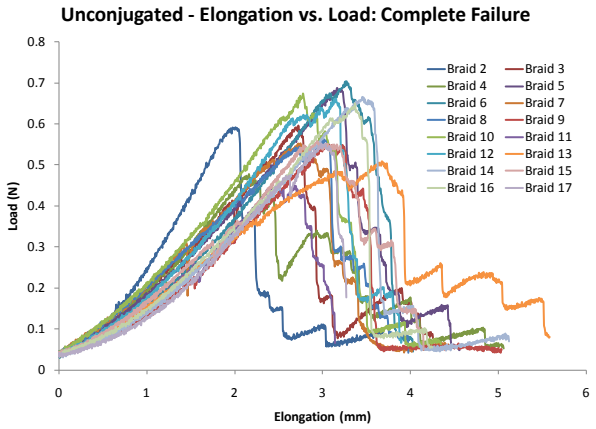

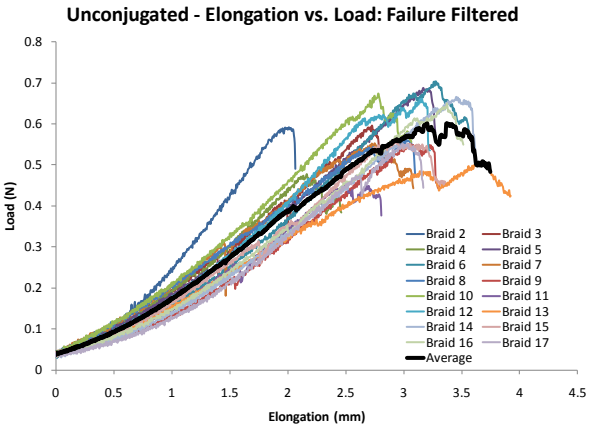

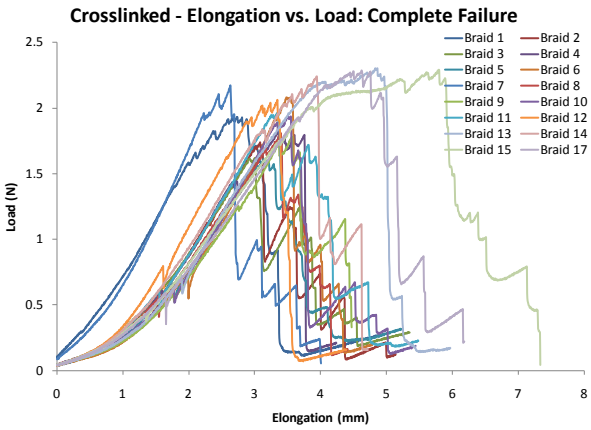

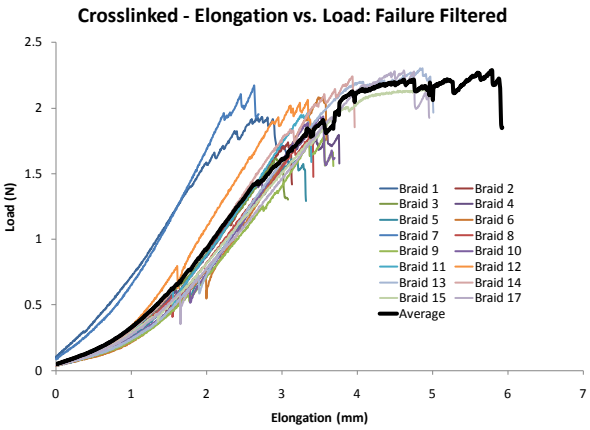

Appendix B: Optimizing Cell Seeding Method Data

	Large Channels: 7.8-7.9				Small Channels: 9.17-9.18		
	NONE				NONE		
	Average	S.D.	S.E.		Average	S.D.	S.E.
Section	23.36111111	4.202654112	0.700442352	Section	31.09042553	7.688823328	1.121530149
Total	23501.27778	4227.870037	704.6450062	Total	31276.96809	7115.457088	1037.896088
%	11.75063889	2.113935018	0.352322503	%	20.85131206	4.75943078	0.69423433
	EDC/NHS				EDC/NHS		
	Average	S.D.	S.E.		Average	S.D.	S.E.M.
Section	29.90909091	5.736031405	1.222926005	Section	36.13888889	3.857977051	0.909333912
Total	30088.54545	5770.447593	1230.263561	Total	36355.72222	3881.124914	914.789915
%	15.04427273	2.885223797	0.61513178	%	24.23714815	2.587416609	0.609859943

2.0 mm x 12 mm - NONE										
			Cell Number/ Region							
	N#	Image #	1	2	3	4		Average	Total Number of Cells	Precentage of cells seeded
7.8-7.9	1	A	20	30	25	24		24.75	24898.5	12.44925
		A (02)	28	21	19	25		23.25	23389.5	11.69475
		A (03)	14	8	26	21		17.25	17353.5	8.67675
		A (04)	33	24	12	26		23.75	23892.5	11.94625
		A (05)	27	30	25	19		25.25	25401.5	12.70075
		A (06)	21	19	22	29		22.75	22886.5	11.44325
		A (07)	17	12	21	21		17.75	17856.5	8.92825
		A (09)	35	33	11	18		24.25	24395.5	12.19775
		A (15)	16	27	13	30		21.5	21629	10.8145
		A (17)	9	13	11	29		15.5	15593	7.7965
		A (18)	35	32	26	15		27	27162	13.581
		A (19)	21	21	22	13		19.25	19365.5	9.68275
		A (2)	20	16	27	19		20.5	20623	10.3115
		A (21)	14	19	23	30		21.5	21629	10.8145
		a (22)	35	31	33	24		30.75	30934.5	15.46725
		A (23)	15	27	21	29		23	23138	11.569
		A (4)	18	19	19	25		20.25	20371.5	10.18575
		A (7)	21	19	15	23		19.5	19617	9.8085
		A (8)	26	12	19	25		20.5	20623	10.3115
		A (9)	33	33	28	31		31.25	31437.5	15.71875
	2	Cphal (02)	25	21	22	14		20.5	20623	10.3115
		Cphal (03)	17	22	10	17		16.5	16599	8.2995
		Cphal (04)	21	22	21	18		20.5	20623	10.3115
		Cphal (09)	21	36	44	26		31.75	31940.5	15.97025
		Cphal (10)	28	34	23	21		26.5	26659	13.3295
		Cphal (12)	32	29	34	21		29	29174	14.587
		Cphal (14)	20	26	39	21		26.5	26659	13.3295
		Cphal (16)	21	25	25	21		23	23138	11.569
		Cphal (19)	33	27	26	30		29	29174	14.587
		Cphal (20)	33	24	25	25		26.75	26910.5	13.45525
		Cphal (22)	20	14	27	31		23	23138	11.569
		Cphal (24)	36	25	18	32		27.75	27916.5	13.95825
		Cphal (25)	27	16	37	27		26.75	26910.5	13.45525
		Cphal (27)	23	17	26	30		24	24144	12.072
		Cphal (29)	14	17	22	32		21.25	21377.5	10.68875
		Cphal (31)	17	19	19	20		18.75	18862.5	9.43125

2.0 mm x 12.0 mm - EDC/NHS										
			Cell Number/ Region							
	N#	Image #	1	2	3	4		Average	Total Number of Cells	Precentage of cells seeded
7.8-7.9	1	A	36	30	28	21		28.75	28922.5	14.46125
		A (02)	22	12	20	17		17.75	17856.5	8.92825
		A (05)	26	26	20	12		21	21126	10.563
		A (06)	26	29	18	15		22	22132	11.066
		A (07)	24	23	36	27		27.5	27665	13.8325
		A (08)	50	32	27	28		34.25	34455.5	17.22775
		A (09)	30	29	23	27		27.25	27413.5	13.70675
	2	B	62	41	29	37		42.25	42503.5	21.25175
		B (02)	31	23	26	25		26.25	26407.5	13.20375
		B (03)	31	29	30	33		30.75	30934.5	15.46725
		B (04)	30	39	27	24		30	30180	15.09
		B (05)	30	27	33	25		28.75	28922.5	14.46125
		B (09)	38	37	33	37		36.25	36467.5	18.23375
	2	Cphal (03)	40	28	46	42		39	39234	19.617
		Cphal (04)	36	32	27	31		31.5	31689	15.8445
		Cphal (05)	31	32	29	20		28	28168	14.084
		Cphal (06)	39	38	33	32		35.5	35713	17.8565
		Cphal (07)	31	35	29	35		32.5	32695	16.3475
		Cphal (09)	27	23	35	34		29.75	29928.5	14.96425
		Cphal (11)	29	27	21	23		25	25150	12.575
		Cphal (12)	37	23	37	33		32.5	32695	16.3475
		Cphal (17)	30	34	28	34		31.5	31689	15.8445

1.0 mm x 12.0 mm - NONE										
			Cell Number/ Region							
	N#	Image #	1	2	3	4		Average	Total Number of Cells	Precentage of cells seeded
9.17-9.18	1	A (04)	52	32	27	43		38.5	38731	25.82066667
		A (05)	43	51	42	41		44.25	44515.5	29.677
		A (06)	34	39	17	32		30.5	30683	20.45533333
		A (07)	29	36	43	46		38.5	38731	25.82066667
		A (09)	25	37	40	41		35.75	35964.5	23.97633333
		A (10)	20	23	17	18		19.5	19617	13.078
		A (12)	27	23	12	25		21.75	21880.5	14.587
		A (13)	22	12	22	20		19	19114	12.74266667
		A (15)	30	14	31	26		25.25	25401.5	16.93433333
		A (17)	28	34	19	26		26.75	26910.5	17.94033333
		A (19)	19	27	36	17		24.75	24898.5	16.599
		A (23)	41	31	35	41		37	37222	24.81466667
		A (24)	29	44	36	28		34.25	34455.5	22.97033333
		A (26)	32	24	41	30		31.75	31940.5	21.29366667
	2	B	35	32	32	27		31.5	31689	21.126
		B (02)	19	35	29	27		27.5	27665	18.44333333
		B (05)	29	35	16	18		24.5	24647	16.43133333
		B (06)	27	19	24	29		24.75	24898.5	16.599
		B (07)	22	26	24	21		23.25	23389.5	15.593
		B (08)	32	26	21	28		26.75	26910.5	17.94033333
		B (09)	33	32	23	24		28	28168	18.77866667
		B (10)	20	16	15	20		17.75	17856.5	11.90433333
		B (11)	30	20	32	18		25	25150	16.76666667
		B (13)	30	23	25	24		25.5	25653	17.102
		B (14)	44	46	31	40		40.25	40491.5	26.99433333
		B (15)	41	41	55	38		43.75	44012.5	29.34166667
	3	C (03)	53	39	30	19		35.25	35461.5	23.641
		C (04)	37	30	46	21		33.5	33701	22.46733333
		C (06)	39	23	28	22		28	28168	18.77866667
		C (09)	37	49	38	40		41	41246	27.49733333
		C (10)	27	36	50	45		39.5	39737	26.49133333
		C (11)	34	36	32	40		35.5	35713	23.80866667
		C (13)	39	24	37	41		35.25	35461.5	23.641
		C (15)	32	45	28	38		35.75	35964.5	23.97633333
		C (17)	28	21	31	35		28.75	28922.5	19.28166667
		C (25)	34	36	27	40		34.25	34455.5	22.97033333
	4	D (03)	24	39	42	30		33.75	33952.5	22.635
		D (07)	47	31	32	28		34.5	34707	23.138
		D (11)	5	6	14	15		10	10060	6.706666667
		D (16)	33	21	21	16		22.75	22886.5	15.25766667
		D (17)	24	22	22	25		23.25	23389.5	15.593
		D (18)	37	27	38	30		33	33198	22.132
		D (26)	52	35	32	26		36.25	36467.5	24.31166667
		D (27)	39	45	46	42		43	43258	28.83866667
		D (31)	48	42	40	37		41.75	42000.5	28.00033333
		D (32)	52	37	40	30		39.75	39988.5	26.659
		D (33)	30	46	18	28		30.5	30683	20.45533333

1.0 mm x 12.0 mm - EDC/NHS										
			Cell Number/ Region							
	N#	Image #	1	2	3	4		Average	Total Number of Cells	Precentage of cells seeded
9.17-9.18	1	B (03)	51	38	40	39		42	42252	28.168
		B (02)	41	32	49	39		40.25	40491.5	26.99433333
		B (06)	41	36	36	21		33.5	33701	22.46733333
		B (09)	47	28	28	34		34.25	34455.5	22.97033333
		B (10)	38	40	35	27		35	35210	23.47333333
		B (11)	34	33	30	29		31.5	31689	21.126
		B (12)	44	40	40	39		40.75	40994.5	27.32966667
		B (13)	40	28	30	30		32	32192	21.46133333
	2	C (04)	50	40	38	39		41.75	42000.5	28.00033333
		C (05)	48	44	38	42		43	43258	28.83866667
		C (10)	39	34	31	31		33.75	33952.5	22.635
		C (12)	47	32	30	32		35.25	35461.5	23.641
	3	D (05)	33	29	32	29		30.75	30934.5	20.623
		D (08)	40	24	32	35		32.75	32946.5	21.96433333
		D (09)	46	34	33	38		37.75	37976.5	25.31766667
		D (11)	41	36	35	28		35	35210	23.47333333
		D (12)	38	38	39	28		35.75	35964.5	23.97633333
		D (13)	35	38	34	35		35.5	35713	23.80866667

One Way Analysis of Variance - Attachment Wednesday, August 25, 2010, 12:22:07 AM

Data source: Data 1 in attachment - optimizing

Normality Test (Shapiro-Wilk) Passed (P = 0.459)

Equal Variance Test: Failed (P < 0.050)

Test execution ended by user request, ANOVA on Ranks begun

Kruskal-Wallis One Way Analysis of Variance on Ranks Wednesday, August 25, 2010, 12:22:07 AM

Data source: Data 1 in attachment - optimizing

Group	N	Missing	Median	25%	75%
L-none	36	0	23.000	20.500	26.688
L-edc/nhs	22	0	29.875	27.000	32.938
s-none	47	0	31.750	25.000	36.250
s-edc/nhs	18	0	35.125	33.313	40.375

H = 46.073 with 3 degrees of freedom. (P = <0.001)

The differences in the median values among the treatment groups are greater than would be expected by chance; there is a statistically significant difference (P = <0.001)

To isolate the group or groups that differ from the others use a multiple comparison procedure.

All Pairwise Multiple Comparison Procedures (Dunn's Method) :

Comparison	Diff of Ranks	Q	P<0.05
s-edc/nhs vs L-none	64.528	6.270	Yes
s-edc/nhs vs L-edc/nhs	30.634	2.704	Yes
s-edc/nhs vs s-none	24.850	2.515	No
s-none vs L-none	39.677	5.025	Yes

s-none vs L-edc/nhs	5.783	0.628	No
L-edc/nhs vs L-none	33.894	3.513	Yes

Note: The multiple comparisons on ranks do not include an adjustment for ties.

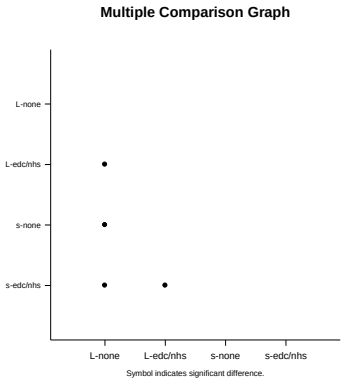

One Way Analysis of Variance – Total Cells Wednesday, August 25, 2010, 12:19:03 AM

Data source: Data 1 in total cells - optimizing

Normality Test (Shapiro-Wilk) Passed (P = 0.459)

Equal Variance Test: Failed (P < 0.050)

Test execution ended by user request, ANOVA on Ranks begun

Kruskal-Wallis One Way Analysis of Variance on Ranks Wednesday, August 25, 2010, 12:19:03 AM

Data source: Data 1 in total cells - optimizing

Group	N	Missing	Median	25%	75%
L-none	36	0	23138.000	20623.000	26847.625
L-edc/nhs	22	0	30054.250	27162.000	33135.125
s-none	47	0	31940.500	25150.000	36467.500
s-edc/nhs	18	0	35335.750	33512.375	40617.250

H = 46.073 with 3 degrees of freedom. (P = <0.001)

The differences in the median values among the treatment groups are greater than would be expected by chance; there is a statistically significant difference (P = <0.001)

To isolate the group or groups that differ from the others use a multiple comparison procedure.

All Pairwise Multiple Comparison Procedures (Dunn's Method) :

Comparison	Diff of Ranks	Q	P<0.05
s-edc/nhs vs L-none	64.528	6.270	Yes

s-edc/nhs vs L-edc/nhs	30.634	2.704	Yes
s-edc/nhs vs s-none	24.850	2.515	No
s-none vs L-none	39.677	5.025	Yes
s-none vs L-edc/nhs	5.783	0.628	No
L-edc/nhs vs L-none	33.894	3.513	Yes

Note: The multiple comparisons on ranks do not include an adjustment for ties.

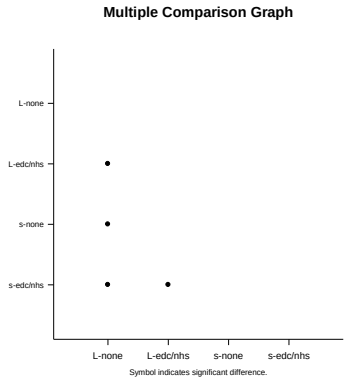

One Way Analysis of Variance - Precentage Wednesday, August 25, 2010, 12:24:21 AM

Data source: Data 1 in precentage - optimizing

Normality Test (Shapiro-Wilk) Passed (P = 0.184)

Equal Variance Test: Failed (P < 0.050)

Test execution ended by user request, ANOVA on Ranks begun

Kruskal-Wallis One Way Analysis of Variance on Ranks Wednesday, August 25, 2010, 12:24:21 AM

Data source: Data 1 in precentage - optimizing

Group	N	Missing	Median	25%	75%
L-none	36	0	11.569	10.312	13.424
L-edc/nhs	22	0	15.027	13.581	16.568
s-none	47	0	21.294	16.767	24.312
s-edc/nhs	18	0	23.557	22.342	27.078

H = 77.894 with 3 degrees of freedom. (P = <0.001)

The differences in the median values among the treatment groups are greater than would be expected by chance; there is a statistically significant difference (P = <0.001)

To isolate the group or groups that differ from the others use a multiple comparison procedure.

All Pairwise Multiple Comparison Procedures (Dunn's Method) :

Comparison	Diff of Ranks	Q	P<0.05
s-edc/nhs vs L-none	75.056	7.293	Yes
s-edc/nhs vs L-edc/nhs	50.977	4.499	Yes
s-edc/nhs vs s-none	17.441	1.765	No
s-none vs L-none	57.614	7.297	Yes
s-none vs L-edc/nhs	33.536	3.641	Yes
L-edc/nhs vs L-none	24.078	2.496	No

Note: The multiple comparisons on ranks do not include an adjustment for ties.

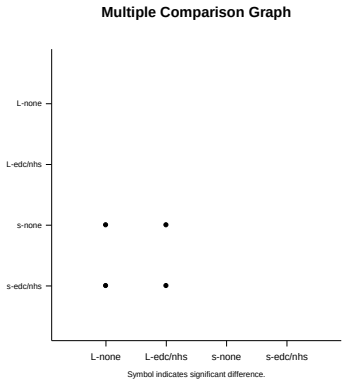

Appendix C: Cell Attachment

Appendix C.1: Cell Attachment Data

Summary of cell attachment calculations, including individual counts for each image, and statistics.

NONE					EDC/NHS					EDC/NHS HEP				
Total N #		13			Total N #		13			Total N #		11		
		Average	S.D.	S.E.			Average	S.D.	S.E.			Average	S.D.	S.E.
9.17-9.18	Section	31.09042553	7.688823328	1.12153	9.17-9.18	Section	36.13888889	3.857977051	0.909334	9.17-9.18	Section	44.2625	4.48130253	1.00205
			Section					Section					Section	
		Q1	25.125				Q1	33.5625				Q1	42.6875	
		Q3	36				Q3	39.625				Q3	48.3125	
		IQR	10.875				IQR	6.0625				IQR	5.625	
		LAV	8.8125				LAV	24.46875				LAV	34.25	
		UAV	52.3125				UAV	48.71875				UAV	56.75	
		Average	S.D.	S.E.			Average	S.D.	S.E.			Average	S.D.	S.E.
10.5-10.6	Section	36.56355932	7.964711126	1.036917	10.5-10.6	Section	38.6402439	5.398509279	0.843106	10.5-10.6	Section	41.80102041	5.943523171	0.849075
			Section					Section					Section	
		Q1	31.25				Q1	35.5				Q1	37.75	
		Q3	41.25				Q3	42				Q3	46.25	
		IQR	10				IQR	6.5				IQR	8.5	
		LAV	16.25				LAV	25.75				LAV	25	
		UAV	56.25				UAV	51.75				UAV	59	
		Average	S.D.	S.E.			Average	S.D.	S.E.			Average	S.D.	S.E.
11.18-11.19	Section	38.2	5.577537859	1.440114	11.18-11.19	Section	49.15	4.859453232	1.254705	11.18-11.19	Section	59.175	2.986195089	0.944318
			Section					Section					Section	
		Q1	34.625				Q1	45.25				Q1	57	
		Q3	42				Q3	52.75				Q3	61.875	
		IQR	7.375				IQR	7.5				IQR	4.875	
		LAV	23.5625				LAV	34				LAV	49.6875	
		UAV	53.0625				UAV	64				UAV	69.1875	
		Average	S.D.	S.E.			Average	S.D.	S.E.			Average	S.D.	S.E.
11.19-11.20	Section	38.425	3.576641037	1.131033	11.19-11.20	Section	48.95	3.909923273	1.009538	11.19-11.20	Section	57.85	5.119678809	1.618985
			Section					Section					Section	
		Q1	36.8125				Q1	47.25				Q1	58	
		Q3	39.25				Q3	51.5				Q3	60.5	
		IQR	2.4375				IQR	4.25				IQR	2.5	
		LAV	33.15625				LAV	40.875				LAV	54.25	
		UAV	42.90625				UAV	57.875				UAV	64.25	
		Average	S.D.	S.E.			Average	S.D.	S.E.			Average	S.D.	S.E.
All data	Section	34.92938931	7.88488542	0.688906	All data	Section	41.64325843	7.170497443	0.760071	All data	Section	46.10955056	8.56566838	0.907959
			Section					Section					Section	
		Q1	30.375				Q1	35.75				Q1	39.5	
		Q3	39.375				Q3	47.5				Q3	50.75	
		IQR	9				IQR	11.75				IQR	11.25	
		LAV	16.875				LAV	18.125				LAV	22.625	
		UAV	52.875				UAV	65.125				UAV	67.625	

5 ng/mL FGF2					10 ng/mL FGF2				50 ng/mL FGF2				
Total N #		12			Total N #		8		Total N #		8		
		Average	S.D.	S.E.			Average	S.D.	S.E.			Average	S.D.	S.E.
9.17-9.18	Section	36.30625	6.131174936	0.969424	9.17-9.18	Section	36.91666667	7.073666991	1.667279	9.17-9.18	Section	36.94444444	5.640293299	1.32943
			Section					Section					Section	
		Q1	32				Q1	31.75				Q1	34.4375	
		Q3	39.875				Q3	38.375				Q3	40.375	
		IQR	7.875				IQR	6.625				IQR	5.9375	
		LAV	20.1875				LAV	21.8125				LAV	25.53125	
		UAV	51.6875				UAV	48.3125				UAV	49.28125	
		Average	S.D.	S.E.			Average	S.D.	S.E.			Average	S.D.	S.E.
10.5-10.6	Section	39.12209302	5.007248345	0.763598	10.5-10.6	Section	38.61111111	3.946776409	0.537088	10.5-10.6	Section	38.02272727	5.67990877	1.210961
			Section					Section					Section	
		Q1	38				Q1	36.0625				Q1	33.6875	
		Q3	44.25				Q3	40.4375				Q3	40.25	
		IQR	6.25				IQR	4.375				IQR	6.5625	
		LAV	28.625				LAV	29.5				LAV	23.84375	
		UAV	53.625				UAV	47				UAV	50.09375	
		Average	S.D.	S.E.			Average	S.D.	S.E.			Average	S.D.	S.E.
11.18-11.19	Section	51.15	3.604010112	1.139688	11.18-11.19	Section	53.45	2.830635971	1.265899	11.18-11.19	Section	#DIV/0!	#DIV/0!	#DIV/0!
			Section					Section					Section	
		Q1	49.0625				Q1	54				Q1	#NUM!	
		Q3	53.75				Q3	55				Q3	#NUM!	
		IQR	4.6875				IQR	1				IQR	#NUM!	
		LAV	42.03125				LAV	52.5				LAV	#NUM!	
		UAV	60.78125				UAV	56.5				UAV	#NUM!	
		Average	S.D.	S.E.			Average	S.D.	S.E.			Average	S.D.	S.E.
11.19-11.20	Section	50.175	3.883816136	1.228171	11.19-11.20	Section	#DIV/0!	#DIV/0!	#DIV/0!	11.19-11.20	Section	49.01666667	4.360400812	1.125851
			Section					Section					Section	
		Q1	47.6875				Q1	#NUM!				Q1	45.625	
		Q3	52.25				Q3	#NUM!				Q3	51.25	
		IQR	4.5625				IQR	#NUM!				IQR	5.625	
		LAV	40.84375				LAV	#NUM!				LAV	37.1875	
		UAV	59.09375				UAV	#NUM!				UAV	59.6875	
		Average	S.D.	S.E.			Average	S.D.	S.E.			Average	S.D.	S.E.
All data	Section	40.26941748	7.4239353	0.731502	All data	Section	39.17857143	6.108780504	0.69616	All data	Section	40.66818182	7.370495257	0.993837
			Section					Section					Section	
		Q1	34.25				Q1	35.5				Q1	35.875	
		Q3	45.5				Q3	42				Q3	45.875	
		IQR	11.25				IQR	6.5				IQR	10	
		LAV	17.375				LAV	25.75				LAV	20.875	
		UAV	62.375				UAV	51.75				UAV	60.875	

1 DAY - NONE								
			Cell Number/ Region					
	N #	Image #	1	2	3	4		Average
9.17-9.18	1	A (04)	52	32	27	43		38.5
		A (05)	43	51	42	41		44.25
		A (06)	34	39	17	32		30.5
		A (07)	29	36	43	46		38.5
		A (09)	25	37	40	41		35.75
		A (10)	20	23	17	18		19.5
		A (12)	27	23	12	25		21.75
		A (13)	22	12	22	20		19
		A (15)	30	14	31	26		25.25
		A (17)	28	34	19	26		26.75
		A (19)	19	27	36	17		24.75
		A (23)	41	31	35	41		37
		A (24)	29	44	36	28		34.25
		A (26)	32	24	41	30		31.75
	2	B	35	32	32	27		31.5
		B (02)	19	35	29	27		27.5
		B (05)	29	35	16	18		24.5
		B (06)	27	19	24	29		24.75
		B (07)	22	26	24	21		23.25
		B (08)	32	26	21	28		26.75
		B (09)	33	32	23	24		28
		B (10)	20	16	15	20		17.75
		B (11)	30	20	32	18		25
		B (13)	30	23	25	24		25.5
		B (14)	44	46	31	40		40.25
		B (15)	41	41	55	38		43.75
	3	C (03)	53	39	30	19		35.25
		C (04)	37	30	46	21		33.5
		C (06)	39	23	28	22		28
		C (09)	37	49	38	40		41
		C (10)	27	36	50	45		39.5
		C (11)	34	36	32	40		35.5
		C (13)	39	24	37	41		35.25
		C (15)	32	45	28	38		35.75
		C (17)	28	21	31	35		28.75
		C (25)	34	36	27	40		34.25
	4	D (03)	24	39	42	30		33.75
		D (07)	47	31	32	28		34.5
		D (11)	5	6	14	15		10
		D (16)	33	21	21	16		22.75
		D (17)	24	22	22	25		23.25
		D (18)	37	27	38	30		33
		D (26)	52	35	32	26		36.25
		D (27)	39	45	46	42		43
		D (31)	48	42	40	37		41.75
		D (32)	52	37	40	30		39.75
		D (33)	30	46	18	28		30.5
		A	46	43	43	35		41.75
		A (02)	37	37	40	39		38.25
		A (03)	38	36	44	54		43
		A (05)	46	43	60	58		51.75
		A (06)	39	35	40	42		39
		A (07)	23	31	31	34		29.75
		A (08)	48	46	45	48		46.75
		A (09)	33	40	30	38		35.25

10.5-10.6	5	A (10)	35	46	49	41		42.75
		A (11)	23	29	48	39		34.75
		A (13)	30	31	30	31		30.5
		A (14)	39	41	35	43		39.5
		A (15)	35	43	30	42		37.5
		A (16)	56	51	40	53		50
		A (17)	27	32	30	20		27.25
		A (18)	41	44	25	33		35.75
		A (19)	34	39	37	49		39.75
	6	B	65	57	46	58		56.5
		B (02)	16	27	45	16		26
		B (03)	35	18	28	27		27
		B (04)	21	17	37	40		28.75
		B (05)	21	6	3	16		11.5
		B (06)	40	29	14	38		30.25
		B (07)	37	35	37	46		38.75
		B (08)	50	47	52	46		48.75
		B (09)	25	21	49	46		35.25
		B (10)	49	42	18	26		33.75
		B 2	40	23	31	38		33
		B 2 (02)	65	48	27	38		44.5
		B 2 (03)	39	32	28	42		35.25
		B 2 (04)	34	39	39	36		37
		B 2 (05)	31	42	42	19		33.5
		B 2 (06)	33	35	25	15		27
		B 2 (07)	44	19	24	43		32.5
		B 2 (08)	44	33	40	50		41.75
	7	C	21	30	35	35		30.25
		C (02)	38	33	30	36		34.25
		C (03)	37	21	34	31		30.75
		C (04)	38	38	42	39		39.25
		C (05)	30	42	43	39		38.5
		C (06)	46	38	27	30		35.25
		C (07)	32	22	32	36		30.5
		C (08)	36	47	26	37		36.5
		C (09)	46	40	57	36		44.75
		C (10)	44	52	70	34		50
	8	D	33	26	42	39		35
		D (02)	55	32	39	37		40.75
		D (03)	37	32	30	28		31.75
		D (04)	45	22	47	18		33
		D (06)	29	48	41	39		39.25
		D (07)	42	53	46	39		45
		D (08)	53	52	46	59		52.5
		D (09)	32	40	39	66		44.25
		D (10)	31	41	31	36		34.75
		D (11)	52	27	37	13		32.25
		D (12)	12	49	30	29		30
		D (13)	13	17	47	28		26.25
		D (14)	44	33	18	38		33.25
		D (15)	31	26	29	14		25
11.19	9	A	56	24	21	44		36.25
		A (02)	32	46	52	45		43.75
		A (03)	36	33	39	37		36.25
		A (04)	30	23	37	41		32.75
		A (05)	34	20	30	33		29.25
		B	28	34	41	37		35
		B (02)	42	34	27	46		37.25

11.18-[illegible]	10	**B (03)**	35	45	30	32		35.5
		B (04)	44	62	40	29		43.75
		B (05)	35	38	40	44		39.25
	11	**C**	23	30	37	47		34.25
		C (02)	32	16	46	43		34.25
		C (03)	43	33	52	40		42
		C (04)	31	48	50	39		42
		C (05)	53	50	38	65		51.5
11.19-11.20	12	**B**	43	40	41	58		45.5
		B (02)	22	44	45	40		37.75
		B (03)	38	45	26	48		39.25
		B (04)	48	35	39	33		38.75
		B (05)	40	23	32	34		32.25
	13	**C**	52	34	44	22		38
		C (02)	44	47	31	35		39.25
		C (03)	25	47	37	37		36.5
		C (04)	41	46	37	43		41.75
		C (05)	38	33	31	39		35.25

1 DAY - EDC/NHS								
			Cell Number/ Region					
	N #	Image #	1	2	3	4		Average
9.17-9.18	1	B (03)	51	38	40	39		42
		B (02)	41	32	49	39		40.25
		B (06)	41	36	36	21		33.5
		B (09)	47	28	28	34		34.25
		B (10)	38	40	35	27		35
		B (11)	34	33	30	29		31.5
		B (12)	44	40	40	39		40.75
		B (13)	40	28	30	30		32
	2	C (04)	50	40	38	39		41.75
		C (05)	48	44	38	42		43
		C (10)	39	34	31	31		33.75
		C (12)	47	32	30	32		35.25
	3	D (05)	33	29	32	29		30.75
		D (08)	40	24	32	35		32.75
		D (09)	46	34	33	38		37.75
		D (11)	41	36	35	28		35
		D (12)	38	38	39	28		35.75
		D (13)	35	38	34	35		35.5
10.5-10.6	4	A	62	40	36	35		43.25
		A (02)	49	67	50	36		50.5
		A (03)	53	51	45	49		49.5
		A (04)	43	35	46	42		41.5
		A (05)	47	37	48	46		44.5
		A (06)	39	40	37	26		35.5
		A (07)	36	33	24	27		30
		A (08)	21	20	27	26		23.5
		A (09)	45	41	31	31		37
		A (10)	59	53	35	42		47.25
	5	B	34	38	32	42		36.5
		B (02)	48	41	41	34		41
		B (03)	37	34	30	40		35.25
		B (04)	51	36	27	36		37.5
		B (05)	43	35	29	39		36.5
		B (06)	37	37	36	35		36.25
		B (07)	35	43	49	42		42.25
		B (08)	50	3	46	29		32
		B (09)	50	36	31	38		38.75
	6	C	44	50	42	29		41.25
		C (02)	51	43	42	38		43.5
		C (03)	47	34	45	39		41.25
		C (04)	35	43	46	46		42.5
		C (05)	35	30	33	30		32
		C (06)	47	36	34	40		39.25
		C (07)	31	33	33	39		34
		C (08)	39	39	32	27		34.25
		C (09)	35	23	32	32		30.5
		C (10)	32	37	38	34		35.25
		C (11)	42	37	37	31		36.75
		D	64	53	31	36		46
		D (02)	40	45	41	37		40.75

	7	D (03)	41	46	31	36		38.5
		D (04)	46	34	42	29		37.75
		D (05)	49	43	45	31		42
		D (06)	31	31	43	50		38.75
		D (07)	33	23	30	42		32
		D (08)	47	43	34	37		40.25
		D (09)	44	34	44	41		40.75
		D (10)	32	34	37	41		36
		D (11)	37	44	51	38		42.5
11.18-11.19	8	A	39	51	34	37		40.25
		A (02)	63	49	43	44		49.75
		A (03)	51	47	55	59		53
		A (04)	58	66	35	55		53.5
		A (05)	59	59	55	34		51.75
	9	B	53	56	56	56		55.25
		B (02)	49	45	52	36		45.5
		B (03)	47	49	53	46		48.75
		B (04)	59	57	53	56		56.25
		B (05)	53	41	39	40		43.25
	10	C	39	53	48	40		45
		C (02)	49	48	49	56		50.5
		C (03)	51	48	49	50		49.5
		C (04)	54	47	53	56		52.5
		C (05)	43	43	41	43		42.5
11.19-11.20	11	A	64	47	45	43		49.75
		A (02)	52	51	47	67		54.25
		A (03)	47	42	52	49		47.5
		A (04)	69	50	43	39		50.25
		A (05)	57	42	43	46		47
	12	B	44	42	49	41		44
		B (02)	55	47	53	48		50.75
		B (03)	38	43	39	41		40.25
		B (04)	66	65	44	44		54.75
		B (05)	60	61	36	50		51.75
	13	C	43	41	64	57		51.25
		C (02)	63	53	53	39		52
		C (03)	61	37	42	40		45
		C (04)	61	57	35	37		47.5
		C (05)	57	38	50	48		48.25

1 DAY - HEP								
			Cell Number/ Region					
	N #	Image #	1	2	3	4		Average
9.17-9.18	1	A (03)	38	41	48	43		42.5
		A (04)	62	48	47	46		50.75
		A (05)	59	33	55	46		48.25
		A (06)	34	56	31	35		39
		A (07)	40	52	57	54		50.75
		A (10)	41	28	39	33		35.25
		A (12)	41	27	45	40		38.25
		A (13)	50	38	39	45		43
		A (17)	53	42	39	38		43
		A (18)	42	48	28	32		37.5
		A (24)	59	60	43	34		49
		A (25)	46	40	43	45		43.5
	2	B (04)	44	49	41	37		42.75
	3	C (13)	42	44	43	42		42.75
		C (14)	61	52	44	38		48.75
		C (15)	50	47	50	46		48.25
		C (17)	51	48	39	36		43.5
		C (18)	44	40	57	42		45.75
		C (21)	44	49	48	36		44.25
		C (22)	58	59	36	41		48.5
10.5-10.6	4	A (02)	53	49	47	36		46.25
		A (03)	63	56	53	37		52.25
		A (04)	62	53	48	45		52
		A (05)	49	53	43	44		47.25
		A (06)	51	54	41	42		47
		A (07)	39	55	48	41		45.75
		A (08)	36	32	32	29		32.25
		A (09)	46	27	32	46		37.75
		A (10)	49	46	32	43		42.5
		A (11)	45	36	38	34		38.25
		A 2 (02)	29	49	50	41		42.25
		A 2 (03)	54	47	47	44		48
	5	B	56	49	38	50		48.25
		B (02)	55	46	44	48		48.25
		B (03)	32	25	37	33		31.75
		B (04)	38	35	41	34		37
		B (05)	34	31	30	29		31
		B (07)	34	43	54	37		42
		B (08)	51	45	39	27		40.5
	6	C (04)	27	31	41	20		29.75
		C (05)	61	41	41	43		46.5
		C (06)	39	45	41	43		42
		C (07)	53	55	33	38		44.75
		C (08)	41	52	46	47		46.5
		C (09)	36	41	41	34		38
		C (10)	64	49	32	38		45.75
		C (11)	38	35	36	32		35.25
		C (12)	39	35	40	36		37.5
		C (13)	35	27	49	41		38
		C (14)	39	37	37	61		43.5
		C (15)	39	40	39	53		42.75

		C (16)	46	48	42	48		46
		C (17)	34	35	44	55		42
		C (18)	52	54	46	56		52
		C (19)	37	31	26	31		31.25
	7	D (02)	34	38	37	47		39
		D (03)	41	48	35	34		39.5
		D (04)	28	35	26	37		31.5
		D 2 (02)	45	32	46	28		37.75
		D 2 (03)	31	42	37	40		37.5
		D 2 (04)	38	30	36	40		36
		D 2 (05)	52	58	43	49		50.5
		D 2 (06)	39	40	48	50		44.25
		D 2 (07)	49	35	43	58		46.25
		D 2 (08)	55	37	42	45		44.75
		D 2 (09)	38	46	51	54		47.25
		D 2 (10)	43	48	38	38		41.75
		D 2 (11)	36	40	64	37		44.25
		D 2 (12)	32	39	32	42		36.25
11.18-11.19	8	A	65	69	69	46		62.25
		A (02)	60	64	64	68		64
		A (03)	58	51	67	52		57
		A (04)	68	60	59	41		57
		A (05)	65	65	54	59		60.75
	9	B	74	60	63	52		62.25
		B (02)	67	55	50	63		58.75
		B (03)	53	53	61	57		56
		B (04)	67	55	58	41		55.25
		B (05)	60	65	53	56		58.5
11.19-11.20	10	A	62	51	49	61		55.75
		A (02)	61	68	49	54		58
		A (03)	56	62	58	56		58
		A (04)	61	65	51	62		59.75
		A (05)	45	47	40	46		44.5
	11	C	61	61	57	68		61.75
		C (02)	64	56	58	59		59.25
		C (04)	60	59	69	63		62.75
		C (05)	59	68	57	59		60.75
		C (06)	63	64	50	55		58

1 DAY - 5 NG/ML FGF2								
			Cell Number/ Region					
	N #	Image #	1	2	3	4		Average
9.17-9.18	1	A	41	29	29	32		32.75
		A (07)	37	25	38	33		33.25
		A (10)	29	29	34	33		31.25
		A (15)	32	51	38	20		35.25
		A (16)	35	30	42	35		35.5
		A (17)	49	38	59	60		51.5
		A (18)	47	42	45	44		44.5
		A (19)	35	33	29	40		34.25
		A (20)	44	51	33	26		38.5
		A (23)	48	39	41	31		39.75
	2	B (5)	40	42	36	43		40.25
		B (06)	30	40	30	27		31.75
		B (6)	58	48	47	26		44.75
		B (07)	39	34	29	32		33.5
		B (08)	38	36	31	32		34.25
		B (8)	59	60	46	50		53.75
		B (09)	30	40	38	35		35.75
	3	C (03)	48	38	34	60		45
		C (11)	38	46	43	53		45
		C (12)	29	24	35	42		32.5
		C (13)	47	35	38	48		42
		C (14)	39	32	37	32		35
		C (15)	41	45	45	44		43.75
		C (29)	39	30	29	30		32
		C (32)	40	41	29	24		33.5
		C (33)	23	25	43	33		31
		C (35)	49	45	32	42		42
	4	D (02)	40	34	34	42		37.5
		D (04)	23	35	35	28		30.25
		D (4)	38	31	36	32		34.25
		D (08)	22	21	40	28		27.75
		D (09)	27	33	30	28		29.5
		D (9)	30	32	38	30		32.5
		D (12)	37	26	27	22		28
		D (14)	37	33	31	27		32
		D (15)	28	33	33	32		31.5
		D (20)	35	28	15	42		30
		D (24)	29	36	40	43		37
		D (25)	29	39	39	32		34.75
		D (27)	40	37	40	23		35
	5	A (02)	26	25	23	32		26.5
		A (03)	51	47	48	31		44.25
		A (05)	46	31	29	29		33.75
	6	B (02)	37	47	43	44		42.75
		B (03)	39	36	37	29		35.25
		B (04)	46	43	41	35		41.25
		B (05)	44	49	47	38		44.5
		B (06)	28	39	33	25		31.25
		B (07)	34	43	49	33		39.75
		B (08)	41	37	42	40		40

10.5-10.6		B (09)	50	40	47	49		46.5
		B (10)	24	38	44	45		37.75
		B (11)	41	41	34	40		39
		B (12)	40	39	50	58		46.75
	7	C (02)	39	29	41	40		37.25
		C (03)	53	40	37	34		41
		C (04)	46	40	47	43		44
		C (05)	42	44	25	30		35.25
		C (06)	36	40	36	44		39
		C (07)	40	43	38	39		40
		C (08)	32	54	39	29		38.5
		C (09)	52	45	37	41		43.75
		C (10)	43	40	37	36		39
		C (11)	40	38	36	40		38.5
		C (12)	50	43	38	53		46
		C (13)	41	43	42	34		40
		C (14)	38	35	46	44		40.75
		C (15)	45	45	49	56		48.75
		C (16)	29	28	35	32		31
	8	D (02)	48	41	46	52		46.75
		D (03)	28	26	24	31		27.25
		D (04)	44	42	23	43		38
		D (05)	25	39	36	34		33.5
		D (06)	40	37	43	37		39.25
		D (07)	42	37	36	38		38.25
		D (08)	33	46	42	45		41.5
		D (09)	40	33	46	40		39.75
		D (10)	39	40	41	40		40
		D (11)	24	36	27	34		30.25
		D (12)	40	36	46	30		38
		D (13)	46	42	28	39		38.75
		D (14)	43	43	39	30		38.75
		D (15)	34	39	49	39		40.25
11.18-11.19	9	B	54	53	70	49		56.5
		B (02)	62	48	45	45		50
		B (03)	46	40	59	64		52.25
		B (04)	53	58	51	54		54
		B (05)	43	48	58	47		49
	10	C	55	50	40	45		47.5
		C (02)	65	64	41	42		53
		C (03)	63	62	45	50		55
		C (04)	52	57	42	46		49.25
		C (05)	46	50	38	46		45
11.19-11.20	11	A	46	43	57	41		46.75
		A (02)	64	43	46	40		48.25
		A (03)	45	38	58	53		48.5
		A (04)	65	54	45	48		53
		A (05)	40	46	44	55		46.25
	12	C	60	55	58	53		56.5
		C (02)	60	58	56	53		56.75
		C (03)	47	49	47	47		47.5
		C (04)	42	42	55	61		50
		C (05)	57	44	47	45		48.25

1 DAY - 10 NG/ML FGF2								
			Cell Number/ Region					
	N #	Image #	1	2	3	4		Average
9.17-9.18	1	A (06)	49	44	45	51		47.25
	2	B (04)	43	40	23	30		34
		B (09)	28	31	30	33		30.5
		B (10)	43	28	29	26		31.5
		B (11)	49	38	34	29		37.5
		B (13)	46	45	55	28		43.5
		B (20)	43	45	31	26		36.25
		B (21)	36	43	33	35		36.75
		B (25)	65	44	51	26		46.5
	3	C (06)	61	62	45	51		54.75
		C (07)	44	34	23	26		31.75
		C (08)	47	37	28	40		38
		C (09)	29	32	25	22		27
		C (10)	33	37	38	46		38.5
		C (12)	37	46	18	36		34.25
		C (18)	37	32	31	22		30.5
		C (19)	23	34	35	35		31.75
		C (23)	49	32	27	29		34.25
10.5-10.6	4	A (03)	34	39	38	34		36.25
		A (06)	36	37	29	37		34.75
		A 2	41	43	53	51		47
		A 2 (02)	37	30	40	53		40
		A 2 (03)	51	42	37	45		43.75
		A 2 (04)	34	42	36	46		39.5
		A 2 (05)	46	40	47	35		42
		A 2 (06)	49	40	46	35		42.5
		A 2 (07)	39	28	23	47		34.25
		A 2 (08)	35	38	46	28		36.75
		A 2 (09)	43	37	34	38		38
	5	B	43	41	52	51		46.75
		B (02)	42	43	39	47		42.75
		B (03)	46	38	28	40		38
		B (04)	43	39	27	34		35.75
		B (05)	33	31	38	42		36
		B (06)	45	41	48	40		43.5
		B (07)	36	36	41	35		37
		B (08)	36	39	29	52		39
		B (09)	41	38	40	39		39.5
		B (10)	38	46	47	44		43.75
		B (11)	36	45	40	34		38.75
		B (12)	24	33	35	43		33.75
		B (13)	40	36	42	48		41.5
		B (14)	52	29	38	42		40.25
		B (15)	50	50	30	24		38.5
		B (16)	57	45	48	39		47.25
		B (17)	34	31	37	38		35
		B (18)	31	35	24	28		29.5
		C	36	33	35	41		36.25
		C (02)	42	47	40	39		42
		C (03)	38	31	31	39		34.75

	6	C (04)	67	51	42	31		47.75
		C (05)	37	39	36	42		38.5
		C (06)	40	28	48	33		37.25
		C (07)	39	31	51	45		41.5
		C (08)	33	29	40	30		33
		C (09)	33	33	38	32		34
		C (10)	37	37	32	37		35.75
	7	D	35	38	40	42		38.75
		D (02)	42	36	36	41		38.75
		D (03)	40	40	39	27		36.5
		D (04)	35	32	35	27		32.25
		D (05)	30	37	43	32		35.5
		D (06)	32	50	42	32		39
		D (07)	35	43	46	31		38.75
		D (08)	39	43	40	35		39.25
		D (09)	37	34	44	44		39.75
		D (10)	44	41	34	41		40
		D (11)	37	38	39	31		36.25
		D (12)	43	44	38	37		40.5
		D (13)	48	48	34	25		38.75
		D (14)	41	31	36	39		36.75
		D (15)	26	31	33	39		32.25
11.18-11.19	8	A	65	54	52	49		55
		A (02)	70	60	43	49		55.5
		A (03)	53	55	42	44		48.5
		A (04)	66	64	53	33		54
		A (05)	45	65	53	54		54.25

1 DAY - 50 NG/ML FGF2								
			Cell Number/ Region					
	N #	Image #	1	2	3	4		Average
9.17-9.18	1	B	23	23	23	24		23.25
		B (03)	40	38	42	37		39.25
		B (06)	37	36	33	45		37.75
		B (07)	43	32	37	37		37.25
		B (09)	41	43	44	46		43.5
	2	C (06)	36	35	30	33		33.5
		C (08)	39	37	38	39		38.25
		C (09)	34	29	34	34		32.75
	3	D	47	53	42	42		46
		D (02)	52	44	32	35		40.75
		D (03)	34	44	38	40		39
		D (15)	40	43	28	43		38.5
		D (16)	22	27	29	32		27.5
		D (17)	36	26	26	32		30
		D (20)	34	46	39	36		38.75
		D (21)	55	42	39	27		40.75
		D (22)	50	36	43	34		40.75
		D (24)	40	40	47	23		37.5
10.5-10.6	4	A	44	47	49	44		46
		A (02)	36	40	42	44		40.5
		A (03)	43	39	37	36		38.75
		A (04)	28	30	33	41		33
		A (05)	36	39	35	27		34.25
		A (06)	41	52	55	65		53.25
		A (07)	38	36	36	43		38.25
		A (08)	40	50	33	40		40.75
		A (09)	42	57	53	37		47.25
		A (10)	35	35	31	33		33.5
		A 2	42	30	28	33		33.25
		A 2 (02)	24	23	37	33		29.25
		A 2 (03)	39	39	41	39		39.5
		A 2 (04)	43	37	39	27		36.5
		A 2 (05)	43	37	37	38		38.75
		A 2 (06)	36	34	39	34		35.75
	5	B	30	33	41	26		32.5
		B (02)	29	36	34	33		33
		B (03)	34	33	35	35		34.25
		B (04)	44	40	38	30		38
		B (05)	32	39	40	33		36
		B (06)	48	48	42	39		44.25
11.19-11.20	6	A	68	45	51	41		51.25
		A (02)	50	52	53	52		51.75
		A (03)	41	44	42	43		42.5
		A (04)	50	49	51	48		49.5
		A (05)	51	42	40	49		45.5
	7	B	70	61	56	46		58.25
		B (02)	52	50	59	38		49.75
		B (03)	48	42	41	43		43.5
		B (04)	54	46	39	60		49.75
		B (05)	59	59	53	48		54.75
		C	45	47	43	48		45.75
		C (02)	46	45	42	40		43.25

	8	C (03)	48	49	49	51		49.25
		C (04)	60	49	44	52		51.25
		C (05)	50	44	51	52		49.25

One Way Analysis of Variance - Attachment Thursday, April 22, 2010, 11:04:04 PM

Data source: Data 1 in 1 day thesis

Normality Test (Shapiro-Wilk) Failed (P < 0.050)

Test execution ended by user request, ANOVA on Ranks begun

Kruskal-Wallis One Way Analysis of Variance on Ranks Thursday, April 22, 2010, 11:04:04 PM

Data source: Data 1 in 1 day thesis

Group	N	Missing	Median	25%	75%
none	131	0	35.250	30.250	39.500
edc	89	0	41.250	35.625	47.500
hep	89	0	45.750	39.250	51.375
5fgf	103	0	39.750	34.250	46.000
10fgf	77	0	38.500	35.250	42.000
50fgf	55	0	39.250	35.750	46.000

H = 90.121 with 5 degrees of freedom. (P = <0.001)

The differences in the median values among the treatment groups are greater than would be expected by chance; there is a statistically significant difference (P = <0.001)

To isolate the group or groups that differ from the others use a multiple comparison procedure.

All Pairwise Multiple Comparison Procedures (Dunn's Method) :

Comparison	Diff of Ranks	Q	P<0.05
hep vs none	196.912	9.120	Yes
hep vs 10fgf	124.262	5.079	Yes
hep vs 5fgf	101.712	4.471	Yes
hep vs 50fgf	91.327	3.388	Yes
hep vs edc	71.747	3.045	Yes
edc vs none	125.164	5.797	Yes
edc vs 10fgf	52.515	2.147	No
edc vs 5fgf	29.964	1.317	Do Not Test
edc vs 50fgf	19.580	0.726	Do Not Test
50fgf vs none	105.585	4.181	Yes
50fgf vs 10fgf	32.935	1.187	Do Not Test
50fgf vs 5fgf	10.385	0.396	Do Not Test
5fgf vs none	95.200	4.599	Yes
5fgf vs 10fgf	22.550	0.952	Do Not Test
10fgf vs none	72.650	3.219	Yes

Note: The multiple comparisons on ranks do not include an adjustment for ties.

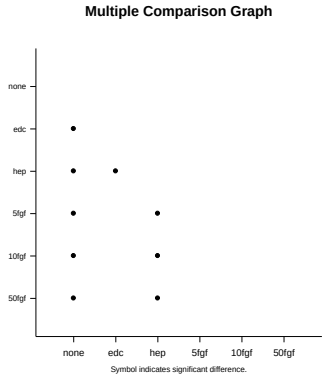

Appendix C.2: Summary of Cell Distribution Data

		NONE										
		Section / Distance										
		1	2	3	4	5	6	7	8	9	10	11
Scaffold		900	1800	2700	3600	4500	5400	6300	7200	8100	9000	9900
A		41.75	38.25	43	51.75	29.75	35.25	34.75	30.5	37.5	27.25	39.75
					39	46.75	42.75		39.5	50	35.75	
	Average	41.75	38.25	43	45.375	38.25	39	34.75	35	43.75	31.5	39.75
B 2				33	44.5	35.25	33.5	27	32.5	41.75		
						37						
	Average			33	44.5	36.125	33.5	27	32.5	41.75		
C			30.25	34.25	30.75	39.25	38.5	30.5	44.75	50		
							35.25	36.5				
	Average		30.25	34.25	30.75	39.25	36.875	33.5	44.75	50		
D		35	40.75	33	39.25	45	44.25	34.75	30	26.25	33.25	25
			31.75			52.5		32.25				
	Average	35	36.25	33	39.25	48.75	44.25	33.5	30	26.25	33.25	25
Total Average		38.375	34.91667	35.8125	39.96875	40.59375	38.40625	32.1875	35.5625	40.4375	32.375	32.375
Standard Deviation		4.772971	4.163332	4.827763	6.714703	5.591451	4.506217	3.508175	6.456182	10.08996	1.237437	10.42983

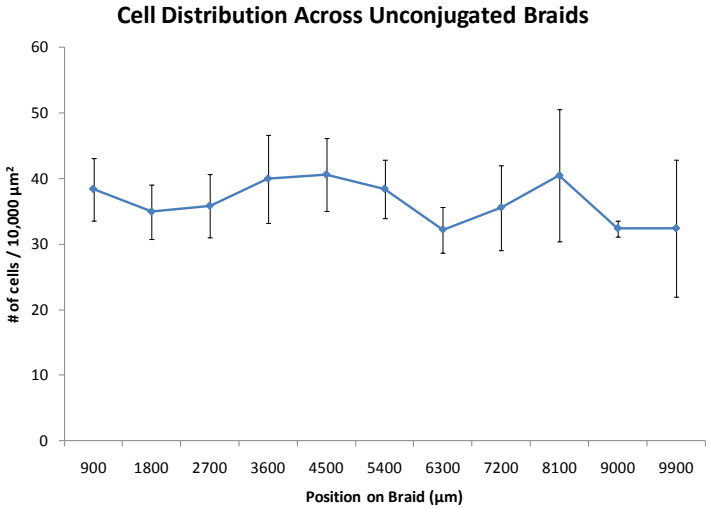

EDC/NHS												
		Section / Distance										
		1	2	3	4	5	6	7	8	9	10	11
Scaffold		900	1800	2700	3600	4500	5400	6300	7200	8100	9000	9900
A			43.25	50.5	49.5	44.5	35.5	30	23.5	37	47.25	
					41.5							
	Average		43.25	50.5	45.5	44.5	35.5	30	23.5	37	47.25	
B			36.5	41	35.25	37.5	36.5	36.25	42.25	32	38.75	
	Average		36.5	41	35.25	37.5	36.5	36.25	42.25	32	38.75	
C			41.25	43.5	42.5	39.25	34	34.25	30.5	35.25	36.75	
				41.25	32							
	Average		41.25	42.375	37.25	39.25	34	34.25	30.5	35.25	36.75	
D		46	40.75	37.75	42	38.75	32	40.25	40.75	36	42.5	
			38.5									
	Average	46	39.625	37.75	42	38.75	32	40.25	40.75	36	42.5	
Total Average		46	40.15625	42.90625	40	40	34.5	35.1875	34.25	35.0625	41.3125	
Standard Deviation			2.85295	5.421192	4.632314	3.088959	1.95789	4.26407	8.867074	2.16386	4.620493	

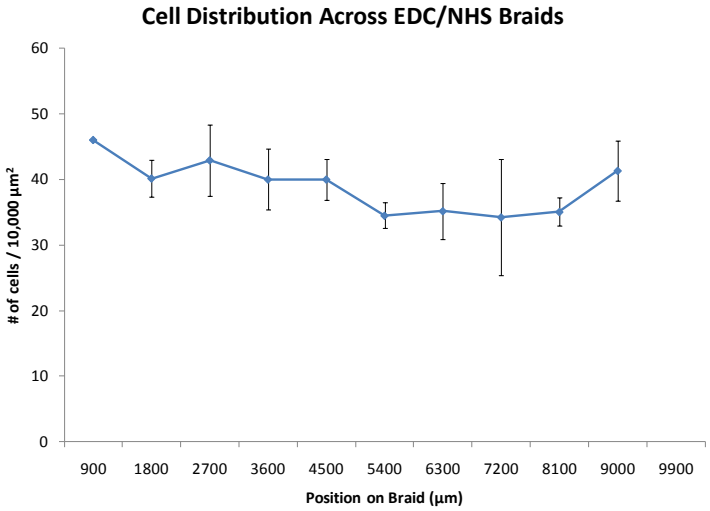

HEP												
		Section / Distance										
		1	2	3	4	5	6	7	8	9	10	11
Scaffold		900	1800	2700	3600	4500	5400	6300	7200	8100	9000	9900
A		46.25	52.25	52	47.25	45.75	32.25	37.75	42.5	38.25	42.25	48
					47							
	Average	46.25	52.25	52	47.125	45.75	32.25	37.75	42.5	38.25	42.25	48
B			48.25	48.25	31.75	37	31		42	40.5		
	Average		48.25	48.25	31.75	37	31		42	40.5		
C			29.75	46.5	44.75	38	35.25	38	43.5	46	52	31.25
				42	46.5	45.75	37.5		42.75	42		
	Average		29.75	44.25	45.625	41.875	36.375	38	43.125	44	52	31.25
D				37.75	37.5	36	50.5	46.25	47.25	44.25		
							44.25	44.75	41.75	36.25		
	Average			37.75	37.5	36	47.375	45.5	44.5	40.25		
Total Average		46.25	43.41667	45.5625	40.5	40.15625	36.75	40.41667	43.03125	40.75	47.125	39.625
Standard Deviation			12.00347	6.094311	7.204599	4.526974	7.446336	4.40407	1.08193	2.389212	6.894291	11.84404

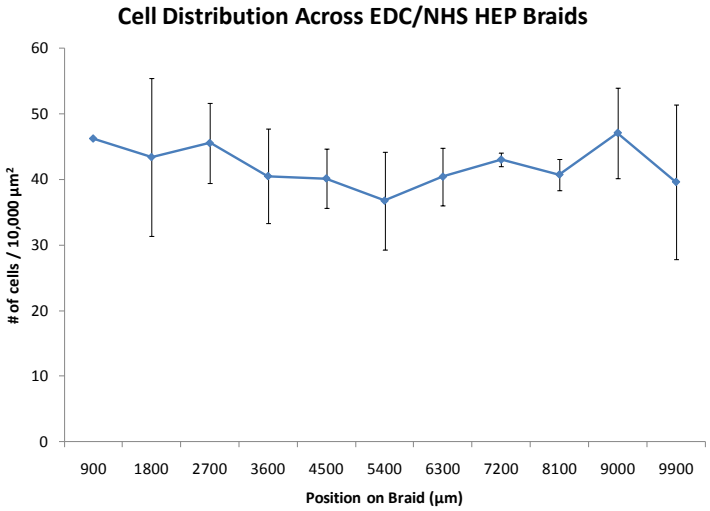

5 ng/mL FGF-2												
		Section / Distance										
		1	2	3	4	5	6	7	8	9	10	11
Scaffold		900	1800	2700	3600	4500	5400	6300	7200	8100	9000	9900
B		42.75	35.25	41.25	31.25	39.75	40	46.5	37.75	39	46.75	
				44.5								
	Average	42.75	35.25	42.875	31.25	39.75	40	46.5	37.75	39	46.75	
C		37.25	41	44	35.25	40	43.75	38.5	40	40.75	31	
					39	38.5	39	46		48.75		
	Average	37.25	41	44	37.125	39.25	41.375	42.25	40	44.75	31	
D		46.75	27.25	38	33.5	38.25	39.75	40	30.25	38	38.75	40.25
					39.25	41.5					38.75	
	Average	46.75	27.25	38	36.375	39.875	39.75	40	30.25	38	38.75	40.25
Total Average		42.25	34.5	41.625	34.91667	39.625	40.375	42.91667	36	40.58333	38.83333	40.25
Standard Deviation		4.769696	6.905614	3.189338	3.197493	0.330719	0.875	3.300884	5.105144	3.642915	7.875331	

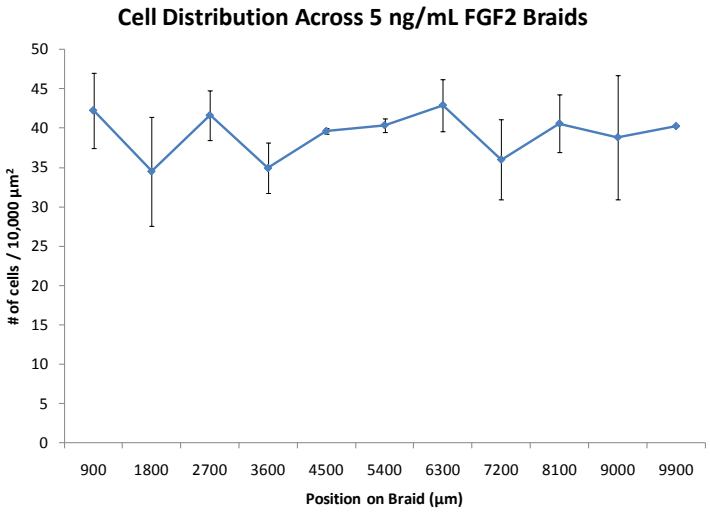

10 ng/mL FGF-2												
		Section / Distance										
		1	2	3	4	5	6	7	8	9	10	11
Scaffold		900	1800	2700	3600	4500	5400	6300	7200	8100	9000	9900
A				47	40	43.75	42	42.5	36.75	38		
						39.5		34.25				
	Average			47	40	41.625	42	38.375	36.75	38		
B			46.75	38	36	42.375	43.75	33.75	40.25	47.25	29.5	
			42.75	35.75	43.5	39.25	38.75	41.5	38.5	35		
					37							
	Average		44.75	36.875	38.83333	40.8125	41.25	37.625	39.375	41.125	29.5	
C				36.25	34.75	47.75	37.25	33	34			
				42		38.5	41.5		35.75			
	Average			39.125	34.75	43.125	39.375	33	34.875			
D			38.75	38.75	32.25	35.5	39	39.25	36.25	38.75	32.25	
				36.5			38.75	39.75	40.5	36.75		
								40				
	Average		38.75	37.625	32.25	35.5	38.875	39.66667	38.375	37.75	32.25	
Total Average			41.75	40.15625	36.45833	40.26563	40.375	37.16667	37.34375	38.95833	30.875	
Standard Deviation			4.242641	4.657403	3.596874	3.318342	1.489547	2.902944	1.969494	1.880547	1.944544	

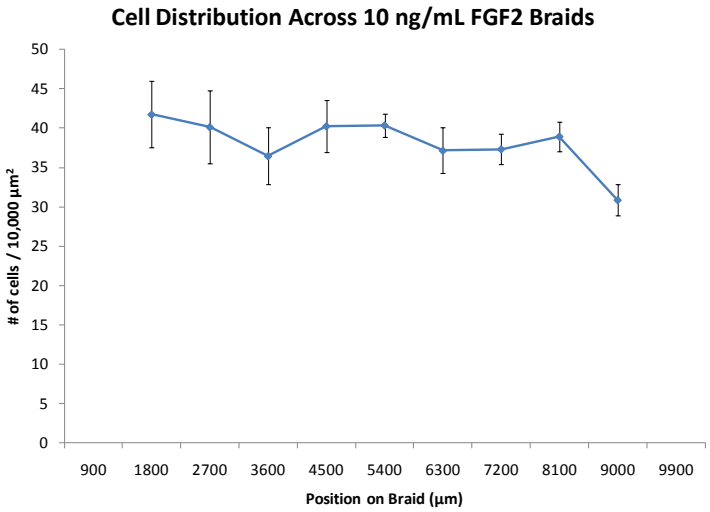

50 ng/mL FGF-2												
		Section / Distance										
		1	2	3	4	5	6	7	8	9	10	11
Scaffold		900	1800	2700	3600	4500	5400	6300	7200	8100	9000	9900
A			46	40.5	33	34.25	53.25	40.75	47.25	33.5		
				38.75			38.25					
	Average		46	39.625	33	34.25	45.75	40.75	47.25	33.5		
B				32.5	33	34.25	38	36	44.25			
	Average			32.5	33	34.25	38	36	44.25			
Total Average			46	36.0625	33	34.25	41.875	38.375	45.75	33.5		
Standard Deviation				5.038136	0	0	5.480078	3.358757	2.12132			

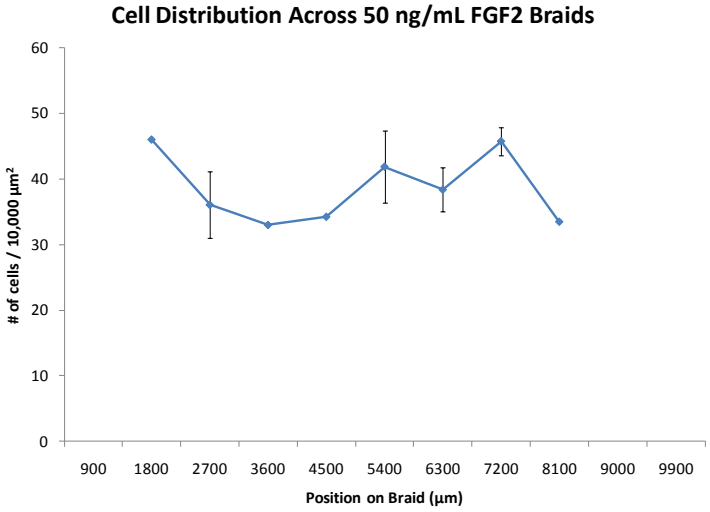

Appendix D: Cell Growth Data

Unseeded Control Scaffolds cultured for 7 days:

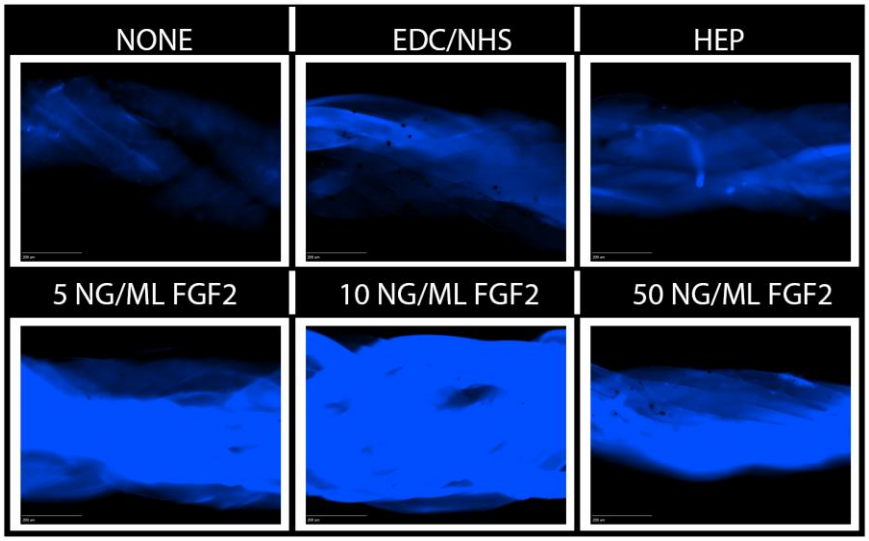

Summary of cell growth calculations for 5 and 7 days, including individual counts for each image, statistics, and cell distribution data.

Appendix D.1: Cell Growth Data – 5 Days

NONE					EDC/NHS					EDC/NHS HEP				
Total N #		10			Total N #		10			Total N #		9		
		Average	S.D.	S.E.			Average	S.D.	S.E.			Average	S.D.	S.E.
10.5-10.10	Section	36.06863	8.906329	1.247136	10.5-10.10	Section	47.34043	7.277763	1.061571	10.5-10.10	Section	44.42	6.891921	0.974665
			Section					Section					Section	
		Q1	32.375				Q1	42.5				Q1	41.0625	
		Q3	40.875				Q3	51.75				Q3	48.125	
		IQR	8.5				IQR	9.25				IQR	7.0625	
		LAV	19.625				LAV	28.625				LAV	30.46875	
		UAV	53.625				UAV	65.625				UAV	58.71875	
11.18-11.23		Average	S.D.	S.E.	11.18-11.23		Average	S.D.	S.E.	11.18-11.23		Average	S.D.	S.E.
	Section	39.48684	6.799445	1.5599		Section	41.94737	4.230822	0.970617		Section	49.42857	8.243233	1.798821
			Section					Section					Section	
		Q1	35				Q1	37.75				Q1	44.75	
		Q3	44.125				Q3	44.625				Q3	52.75	
		IQR	9.125				IQR	6.875				IQR	8	
		LAV	21.3125				LAV	27.4375				LAV	32.75	
		UAV	57.8125				UAV	54.9375				UAV	64.75	
11.19-11.24		Average	S.D.	S.E.	11.19-11.24		Average	S.D.	S.E.	11.19-11.24		Average	S.D.	S.E.
	Section	36.92647	8.926245	2.164932		Section	38.4125	5.462356	1.22142		Section	47.41176	3.57393	0.866805
			Section					Section					Section	
		Q1	27.75				Q1	34.9375				Q1	45	
		Q3	43.75				Q3	42.125				Q3	49.25	
		IQR	16				IQR	7.1875				IQR	4.25	
		LAV	3.75				LAV	24.15625				LAV	38.625	
		UAV	67.75				UAV	52.90625				UAV	55.625	
Alldata		Average	S.D.	S.E.	Alldata		Average	S.D.	S.E.	Alldata		Average	S.D.	S.E.
	Section	36.98276	7.894918	0.846424		Section	44.07267	7.319582	0.789291		Section	46.19318	7.024662	0.748831
			Section					Section					Section	
		Q1	31.875				Q1	39.625				Q1	42.6875	
		Q3	42.5				Q3	47.5				Q3	50.5625	
		IQR	10.625				IQR	7.875				IQR	7.875	
		LAV	15.9375				LAV	27.8125				LAV	30.875	
		UAV	58.4375				UAV	59.3125				UAV	62.375	

5 ng/mL FGF2					10 ng/mL FGF2					50 ng/mL FGF2				
Total N #		9			Total N #		10			Total N #		8		
		Average	S.D.	S.E.			Average	S.D.	S.E.			Average	S.D.	S.E.
10.5-10.10	Section	44.3125	7.166801	1.034439	10.5-10.10	Section	39.83523	4.904597	0.739396	10.5-10.10	Section	42.55	5.199221	0.949243
			Section					Section					Section	
		Q1	38.75				Q1	36.25				Q1	39.3125	
		Q3	49.375				Q3	44.0625				Q3	45.9375	
		IQR	10.625				IQR	7.8125				IQR	6.625	
		LAV	22.8125				LAV	24.53125				LAV	29.375	
		UAV	65.3125				UAV	55.78125				UAV	55.875	
		Average	S.D.	S.E.			Average	S.D.	S.E.			Average	S.D.	S.E.
11.18-11.23	Section	51.89474	5.927406	1.35984	11.18-11.23	Section	47.54412	6.500742	1.576662	11.18-11.23	Section	49.48438	8.12274	2.030685
			Section					Section					Section	
		Q1	48.875				Q1	41.5				Q1	43	
		Q3	54.625				Q3	52.25				Q3	56.5	
		IQR	5.75				IQR	10.75				IQR	13.5	
		LAV	40.25				LAV	25.375				LAV	22.75	
		UAV	63.25				UAV	68.375				UAV	76.75	
		Average	S.D.	S.E.			Average	S.D.	S.E.			Average	S.D.	S.E.
11.19-11.24	Section	49.42105	4.246774	0.974277	11.19-11.24	Section	44.40625	5.283524	1.320881	11.19-11.24	Section	44.45588	7.740032	1.877233
			Section					Section					Section	
		Q1	47				Q1	40.3125				Q1	40.75	
		Q3	51.875				Q3	47.125				Q3	50.5	
		IQR	4.875				IQR	6.8125				IQR	9.75	
		LAV	39.6875				LAV	30.09375				LAV	26.125	
		UAV	59.1875				UAV	57.34375				UAV	65.125	
		Average	S.D.	S.E.			Average	S.D.	S.E.			Average	S.D.	S.E.
All data	Section	47.11628	7.098643	0.765466	All data	Section	42.48701	6.211579	0.707875	All data	Section	44.8254	7.225715	0.910355
			Section					Section					Section	
		Q1	42.25				Q1	38				Q1	40	
		Q3	51.625				Q3	46.25				Q3	49.875	
		IQR	9.375				IQR	8.25				IQR	9.875	
		LAV	28.1875				LAV	25.625				LAV	25.1875	
		UAV	65.6875				UAV	58.625				UAV	64.6875	

5 DAYS - NONE								
			Cell Number/ Region					
	N #	Image #	1	2	3	4		Average
10.5-10.10	1	A	34	34	32	37		34.25
		A (02)	22	23	21	25		22.75
		A (03)	21	15	16	17		17.25
		A (04)	33	45	33	29		35
		A (05)	38	41	50	31		40
		A (07)	34	49	85	80		62
		A (08)	39	40	53	34		41.5
		A (09)	44	45	33	58		45
		A 2	45	47	55	43		47.5
		A 2 (02)	60	40	41	39		45
		A 2 (03)	12	24	34	54		31
		A 2 (05)	43	24	32	43		35.5
	2	B	42	35	38	49		41
		B (02)	30	21	21	23		23.75
		B (03)	19	34	28	25		26.5
		B (04)	28	23	16	19		21.5
	3	C (02)	42	35	38	46		40.25
		C (03)	27	36	40	38		35.25
		C (04)	35	30	27	51		35.75
		C (05)	33	40	45	27		36.25
		C (06)	52	34	33	40		39.75
		C (07)	46	47	47	23		40.75
		C (08)	54	27	53	41		43.75
		C (09)	38	47	38	38		40.25
		C (10)	28	39	28	28		30.75
		C (11)	42	37	24	41		36
		C (12)	49	46	45	36		44
		C (13)	31	37	53	39		40
		C (15)	46	41	17	39		35.75
		C 2	23	40	40	41		36
		C 2 (02)	15	21	43	19		24.5
		C 2 (04)	18	17	27	18		20
		C 2 (05)	39	35	26	34		33.5
		C 2 (06)	35	33	28	37		33.25
	4	D (02)	40	39	71	51		50.25
		D (04)	35	26	49	32		35.5
		D (05)	41	32	30	52		38.75
		D (06)	39	38	22	27		31.5
		D (07)	23	39	15	29		26.5
		D (08)	29	22	23	17		22.75
		D (09)	13	11	12	19		13.75
		D (10)	43	47	30	40		40
		D (11)	31	38	45	57		42.75
		D (12)	45	30	42	39		39
		D (13)	51	44	37	33		41.25
		D (15)	51	30	36	36		38.25
		D (17)	40	42	43	23		37
		D (18)	37	42	39	38		39
		D 2	45	38	41	34		39.5
		D 2 (02)	66	53	27	18		41
		D 2 (03)	62	56	34	38		47.5

11.18-11.23	5	**A**	71	65	33	14		45.75
		A (02)	23	33	32	36		31
		A(03)	51	50	47	48		49
		A(04)	47	33	46	35		40.25
		A (05)	40	33	37	28		34.5
		A 2	30	26	28	45		32.25
		A 2 (02)	31	39	42	30		35.5
		A 2 (03)	39	34	55	48		44
		A 2 (05)	36	38	35	41		37.5
	6	**B**	36	42	46	40		41
		B (02)	43	29	53	52		44.25
		B (03)	21	22	28	37		27
		B (04)	26	45	41	49		40.25
		B (05)	36	35	41	43		38.75
	7	**C**	38	58	53	55		51
		C (02)	44	43	45	42		43.5
		C (03)	48	42	48	31		42.25
		C (04)	25	31	25	29		27.5
		C (05)	37	47	45	51		45
11.19-11.24	8	**A**	43	37	65	50		48.75
		A (02)	22	20	22	30		23.5
		A(03)	34	29	29	29		30.25
		A(04)	37	43	41	40		40.25
		A (05)	47	48	35	44		43.5
		A (06)	36	50	56	42		46
	9	**B**	36	55	50	55		49
		B (02)	33	42	29	43		36.75
		B (03)	50	47	38	29		41
		B (04)	46	54	41	34		43.75
		B (05)	22	39	48	56		41.25
		B (06)	40	40	38	63		45.25
	10	**C**	30	29	32	20		27.75
		C (02)	33	24	25	25		26.75
		C (03)	29	22	25	23		24.75
		C (04)	21	31	20	30		25.5
		C (05)	31	32	39	33		33.75

5 DAYS - EDC/NHS								
			Cell Number/ Region					
	N #	Image #	1	2	3	4		Average
10.5-10.10	1	A (02)	68	77	71	42		64.5
		A (03)	56	61	56	58		57.75
		A (04)	54	50	60	51		53.75
		A (05)	68	70	41	65		61
		A (06)	54	44	62	45		51.25
		A (07)	53	52	37	32		43.5
		A (08)	42	43	48	38		42.75
		A (09)	45	36	42	38		40.25
		A (10)	54	54	49	40		49.25
	2	B	59	53	52	51		53.75
		B (02)	58	52	49	50		52.25
		B (03)	43	38	51	48		45
		B (04)	43	46	31	32		38
		B (05)	46	44	30	40		40
		B (06)	40	34	44	3		30.25
		B (07)	47	40	37	41		41.25
		B (08)	45	46	47	51		47.25
		B (10)	50	46	77	38		52.75
	3	C	42	32	38	31		35.75
		C (02)	38	51	45	46		45
		C (03)	54	44	41	37		44
		C (04)	47	47	50	46		47.5
		C (05)	42	51	50	53		49
		C (06)	39	48	43	39		42.25
		C (07)	46	43	46	38		43.25
		C (08)	52	45	36	56		47.25
		C (09)	41	44	41	37		40.75
		C (10)	58	43	61	52		53.5
		C (11)	55	44	48	48		48.75
		C (12)	59	36	54	38		46.75
		C (13)	55	68	52	48		55.75
		C (14)	75	71	65	43		63.5
		C (15)	45	43	39	31		39.5
		C (16)	45	43	43	40		42.75
	4	D	41	43	57	57		49.5
		D (02)	57	46	47	43		48.25
		D (03)	49	51	38	40		44.5
		D (04)	40	42	35	36		38.25
		D (05)	44	41	47	44		44
		D (06)	47	43	46	50		46.5
		D (07)	45	38	37	46		41.5
		D (08)	58	55	73	60		61.5
		D (09)	35	40	35	55		41.25
		D (10)	50	61	40	39		47.5
		D (11)	50	46	59	50		51.25
		D (12)	58	57	46	54		53.75
		D (13)	54	50	49	37		47.5
	5	A	23	27	61	36		36.75
		A (02)	50	49	36	52		46.75
		A(03)	39	36	34	45		38.5
		A(04)	51	45	55	39		47.5

11.18-11.23		A (05)	54	50	39	51		48.5
		A (06)	40	41	45	46		43
	6	B	50	53	42	41		46.5
		B (02)	41	41	40	48		42.5
		B (03)	44	34	39	31		37
		B (04)	39	43	48	36		41.5
		B (05)	45	39	37	52		43.25
		B (06)	46	48	50	33		44.25
	7	C	46	47	45	33		42.75
		C (02)	36	41	59	33		42.25
		C (03)	36	24	50	33		35.75
		C (04)	40	36	33	33		35.5
		C (05)	32	28	38	45		35.75
		C (06)	40	41	44	51		44
		C (07)	46	38	43	53		45
11.19-11.24	8	A	51	46	57	47		50.25
		A (02)	37	38	31	41		36.75
		A(03)	40	38	46	37		40.25
		A(04)	37	39	37	40		38.25
		A (05)	42	44	44	43		43.25
		A 2	39	36	30	31		34
		A 2 (02)	40	36	43	44		40.75
	9	B	41	43	40	31		38.75
		B (02)	35	35	27	38		33.75
		B (03)	38	29	33	31		32.75
		B (04)	25	25	26	29		26.25
		B (05)	33	25	37	24		29.75
		B (06)	37	32	37	35		35.25
		B (07)	42	38	32	39		37.75
	10	C	36	45	51	41		43.25
		C (02)	40	35	39	54		42
		C (03)	40	35	51	49		43.75
		C (04)	43	46	40	26		38.75
		C (05)	43	39	41	38		40.25
		C (06)	52	41	36	41		42.5

5 DAYS - HEP								
			Cell Number/ Region					
	N #	Image #	1	2	3	4		Average
10.5-10.10	1	A	53	33	35	55		44
		A (02)	23	38	37	44		35.5
		A (03)	52	41	48	49		47.5
		A (04)	40	44	38	34		39
		A (05)	45	44	43	39		42.75
	2	C	34	34	47	39		38.5
		C (02)	44	37	47	50		44.5
		C (03)	35	41	50	42		42
		C (04)	43	39	48	46		44
		C (05)	48	44	45	36		43.25
		C (06)	48	57	49	44		49.5
		C (07)	48	46	45	41		45
		C (08)	49	46	45	40		45
		C (09)	56	46	38	35		43.75
		C (10)	33	49	30	23		33.75
		C (11)	45	41	38	40		41
		C (12)	48	44	48	53		48.25
		C (13)	43	54	54	55		51.5
		C (14)	38	41	34	58		42.75
		C (15)	43	42	50	40		43.75
		C (16)	50	53	41	40		46
		C 2 (03)	50	45	52	39		46.5
		C 2 (04)	43	37	47	38		41.25
		C 2 (05)	37	33	44	30		36
		C 2 (06)	35	33	30	39		34.25
		C 2 (07)	45	56	43	47		47.75
		C 2 (08)	48	40	40	37		41.25
		C 2 (10)	39	36	24	35		33.5
		C 2 (11)	42	33	31	36		35.5
		C 2 (12)	42	39	50	39		42.5
		C 2 (13)	43	62	55	31		47.75
		C 2 (14)	24	39	36	38		34.25
	3	D	26	29	16	35		26.5
		D (02)	46	42	41	58		46.75
		D (03)	50	73	43	30		49
		D (04)	50	58	47	49		51
		D (05)	48	66	61	52		56.75
		D (06)	65	41	36	69		52.75
		D (07)	54	70	60	53		59.25
		D (08)	50	28	45	39		40.5
		D (09)	62	41	45	40		47
		D (10)	35	44	45	50		43.5
		D (11)	45	76	75	55		62.75
		D (12)	38	59	49	43		47.25
		D (13)	42	44	61	52		49.75
		D (14)	55	36	33	46		42.5
		D (15)	48	42	50	74		53.5
		D (16)	60	45	57	44		51.5
		D (17)	59	47	28	64		49.5
		D (18)	46	36	32	44		39.5

11.18-11.23	4	**A**	36	30	29	40		33.75
		A (02)	30	35	35	35		33.75
		A(03)	39	54	34	48		43.75
		A(04)	47	51	37	46		45.25
		A (05)	51	48	38	42		44.75
	5	**B**	57	44	55	45		50.25
		B (02)	45	44	47	47		45.75
		B (03)	56	48	45	57		51.5
		B (04)	47	47	38	46		44.5
		B (05)	46	37	56	64		50.75
		B (06)	49	54	48	68		54.75
		B (07)	51	57	46	57		52.75
		B (08)	58	71	64	52		61.25
	6	**C**	64	55	61	51		57.75
		C (02)	38	42	39	39		39.5
		C (03)	50	56	42	60		52
		C (04)	56	50	46	50		50.5
		C (05)	64	55	40	44		50.75
		C (06)	53	50	47	57		51.75
		C (07)	66	54	47	51		54.5
		C (08)	77	69	74	54		68.5
11.19-11.24	7	**A**	59	45	65	44		53.25
		A (02)	47	42	47	52		47
		A(03)	33	46	39	46		41
		A(04)	49	44	48	49		47.5
		A (05)	51	48	53	45		49.25
	8	**B**	54	45	55	52		51.5
		B (02)	53	42	40	57		48
		B (03)	47	41	45	41		43.5
		B (04)	59	52	45	40		49
		B (05)	39	47	56	44		46.5
	9	**C**	38	42	45	46		42.75
		C (02)	44	40	47	49		45
		C (03)	53	44	43	42		45.5
		C (04)	42	38	50	48		44.5
		C (05)	40	50	50	51		47.75
		C (06)	52	68	48	48		54
		C (07)	50	47	55	48		50

5 NG/ML FGF2								
			Cell Number/ Region					
	N #	Image #	1	2	3	4		Average
10.5-10.10	1	A	49	37	27	27		35
		A (02)	39	38	52	33		40.5
		A (03)	44	29	35	41		37.25
		A (04)	33	39	47	39		39.5
		A (05)	45	53	47	49		48.5
		A (06)	45	35	34	32		36.5
		A (07)	53	41	52	45		47.75
		A (08)	48	58	54	41		50.25
		A (09)	51	39	33	49		43
		A (10)	47	39	40	53		44.75
		A (11)	54	46	38	45		45.75
		A (12)	33	64	39	37		43.25
		A (13)	44	53	40	57		48.5
		A (14)	62	47	37	53		49.75
		A 2	38	49	40	41		42
		A 2 (02)	57	36	38	45		44
		A 2 (03)	39	30	38	39		36.5
		A 2 (04)	33	39	38	36		36.5
		A 2 (06)	46	44	42	36		42
		A 2 (07)	52	44	34	60		47.5
		A 2 (08)	35	40	28	56		39.75
		A 2 (09)	38	43	28	36		36.25
		A 2 (10)	29	26	32	44		32.75
	2	B (02)	40	28	35	41		36
		B (03)	44	56	54	53		51.75
		B (04)	66	58	74	64		65.5
		B (05)	54	50	49	56		52.25
		B (06)	64	49	50	42		51.25
		B (07)	40	41	39	36		39
		B (08)	56	49	44	37		46.5
		B (09)	32	36	31	31		32.5
		B (11)	53	59	40	45		49.25
		B (12)	46	50	48	32		44
		B (13)	51	42	42	48		45.75
		B (14)	49	52	52	48		50.25
		B (15)	48	35	36	36		38.75
		B (16)	50	35	29	28		35.5
	3	D (04)	44	43	40	35		40.5
		D (05)	40	45	42	59		46.5
		D (06)	34	30	33	33		32.5
		D (07)	57	54	57	60		57
		D (08)	50	53	71	46		55
		D (09)	50	49	52	49		50
		D (12)	54	61	49	54		54.5
		D (13)	59	55	47	44		51.25
		D (14)	46	44	31	34		38.75
		D (15)	52	51	44	46		48.25
		D (18)	49	52	50	37		47
		A	60	56	78	60		63.5
		A (02)	43	57	56	54		52.5
		A(03)	60	71	52	46		57.25

11.18-11.23	4	**A (04)**	52	51	54	53		52.5
		A (05)	41	41	56	40		44.5
		A (06)	67	62	59	61		62.25
		A (07)	39	32	42	46		39.75
		A (08)	41	44	52	56		48.25
	5	**B**	58	54	57	55		56
		B (02)	62	54	45	36		49.25
		B (03)	51	43	37	41		43
		B (04)	58	41	47	48		48.5
		B (05)	47	44	63	57		52.75
		B (06)	61	54	59	52		56.5
	6	**C**	48	51	58	52		52.25
		C (02)	48	47	51	53		49.75
		C (03)	56	56	54	47		53.25
		C (04)	55	48	49	52		51
		C (05)	53	49	50	61		53.25
11.19-11.24	7	**A**	47	45	50	46		47
		A (02)	48	48	41	68		51.25
		A(03)	49	44	52	41		46.5
		A (04)	50	54	46	45		48.75
		A (05)	56	56	55	43		52.5
		A (06)	46	44	65	48		50.75
	8	**B**	70	52	42	49		53.25
		B (02)	52	49	53	48		50.5
		B (03)	51	47	52	42		48
		B (04)	64	51	54	44		53.25
		B (05)	50	47	49	54		50
		B (06)	64	58	62	49		58.25
		B (07)	48	59	41	67		53.75
	9	**C**	40	39	37	35		37.75
		C (02)	50	38	53	59		50
		C (03)	40	45	51	52		47
		C (04)	50	49	44	45		47
		C (05)	47	50	49	46		48
		C (06)	42	46	44	50		45.5

10 NG/ML FGF2								
			Cell Number/ Region					
	N #	Image #	1	2	3	4		Average
10.5-10.10	1	A	41	51	42	63		49.25
		A (02)	42	38	32	37		37.25
		A (04)	52	40	33	36		40.25
		A (06)	35	33	24	27		29.75
		A (07)	49	48	43	38		44.5
		A (08)	41	42	46	53		45.5
		A (10)	42	21	34	37		33.5
		A (11)	34	34	25	26		29.75
		A (13)	31	36	38	25		32.5
		A (14)	35	39	42	33		37.25
		A (16)	41	42	41	53		44.25
		A (17)	44	38	44	42		42
		A (18)	54	51	41	42		47
	2	B	39	54	35	50		44.5
		B (03)	38	31	44	43		39
		B 2 (02)	41	40	52	47		45
		B 2 (03)	39	34	39	39		37.75
		B 2 (04)	41	33	50	56		45
		B 2 (05)	45	36	30	42		38.25
		B 2 (06)	33	33	56	39		40.25
		B 2 (07)	34	33	32	44		35.75
		B 2 (08)	34	36	42	33		36.25
		B 2 (09)	34	35	46	30		36.25
	3	C	35	38	33	31		34.25
		C (02)	53	41	41	34		42.25
		C (03)	37	33	35	33		34.5
		C (04)	40	35	35	30		35
		C (05)	23	39	30	46		34.5
		C (06)	57	44	41	34		44
		C (07)	40	30	37	39		36.5
		C (09)	37	35	41	44		39.25
		C (10)	55	43	41	44		45.75
		C (11)	49	39	39	28		38.75
		C 2 (02)	62	50	46	42		50
		C 2 (05)	43	34	52	41		42.5
		C 2 (06)	48	38	42	44		43
		C 2 (07)	44	51	32	40		41.75
		C 2 (08)	54	50	45	36		46.25
	4	D	33	34	38	53		39.5
		D (02)	43	35	37	40		38.75
		D (03)	40	44	39	46		42.25
		D (04)	46	47	37	31		40.25
		D (05)	32	43	40	36		37.75
		D (06)	34	32	42	33		35.25
23	5	A	67	54	57	41		54.75
		A (02)	31	38	43	40		38
		A (03)	43	51	50	51		48.75
		A (04)	45	39	38	45		41.75
		A (05)	49	51	64	47		52.75
		B	74	70	42	36		55.5
		B (02)	46	57	50	40		48.25

11.18-11.2	6	B (03)	35	45	40	46		41.5
		B (04)	40	42	32	43		39.25
		B (05)	40	40	39	34		38.25
	7	C	81	52	50	50		58.25
		C (02)	60	48	41	53		50.5
		C (03)	57	60	42	49		52
		C (04)	51	55	43	48		49.25
		C (05)	40	34	46	43		40.75
		C (06)	45	42	44	55		46.5
		C (07)	56	50	52	51		52.25
11.19-11.24	8	A	47	39	41	47		43.5
		A (02)	45	43	36	35		39.75
		A (03)	48	40	27	31		36.5
		A (04)	47	40	47	36		42.5
		A (05)	53	45	34	40		43
	9	B	58	41	51	30		45
		B (02)	39	26	41	43		37.25
		B (03)	43	36	44	39		40.5
		B (04)	54	41	52	41		47
		B (05)	40	43	57	45		46.25
	10	C	48	48	42	52		47.5
		C (02)	54	53	60	55		55.5
		C (03)	57	49	51	56		53.25
		C (04)	55	47	42	40		46
		C (05)	49	45	50	47		47.75
		C (06)	44	37	43	33		39.25

50 NG/ML FGF2								
			Cell Number/ Region					
	N #	Image #	1	2	3	4		Average
10.5-10.10	1	B (02)	61	56	54	43		53.5
		B (03)	36	43	61	53		48.25
		B (06)	35	34	43	32		36
		B (08)	39	38	42	44		40.75
		B (09)	44	44	39	41		42
		B (10)	52	38	43	33		41.5
		B (12)	40	42	43	34		39.75
		B (13)	26	36	34	37		33.25
		B (14)	38	40	41	38		39.25
		B (15)	49	53	34	48		46
		B (16)	34	38	43	41		39
		B (17)	38	54	43	33		42
		B 2	38	39	36	41		38.5
		B 2 (02)	36	50	38	36		40
		B 2 (03)	35	35	39	50		39.75
		B 2 (04)	35	36	33	50		38.5
		B 2 (05)	44	60	29	40		43.25
		B 2 (07)	37	36	37	35		36.25
	2	D	44	56	55	44		49.75
		D (02)	57	53	51	48		52.25
		D (03)	50	39	57	48		48.5
		D (05)	52	51	42	38		45.75
		D (06)	42	43	43	43		42.75
		D (07)	42	43	41	39		41.25
		D (08)	51	50	43	45		47.25
		D (09)	52	55	50	50		51.75
		D (10)	38	45	45	41		42.25
		D (11)	42	31	37	30		35
		D (12)	35	47	46	44		43
		D (13)	24	55	52	27		39.5
11.18-11.23	3	A	40	43	39	38		40
		A (02)	42	37	45	48		43
		A (03)	40	52	43	37		43
		A (04)	47	42	34	37		40
		A (05)	38	35	45	42		40
	4	B	58	56	47	44		51.25
		B (02)	48	44	48	47		46.75
		B (03)	65	65	54	41		56.25
		B (04)	51	45	65	42		50.75
		B (05)	61	66	57	55		59.75
		B (06)	52	53	62	62		57.25
		B (07)	63	65	51	53		58
		B (08)	70	62	64	70		66.5
	5	C	49	56	47	48		50
		C (02)	52	46	42	43		45.75
		C (03)	37	45	46	46		43.5
	6	A	40	34	55	34		40.75
		A (02)	37	43	42	43		41.25
		A (03)	49	42	41	38		42.5
		A (04)	45	49	33	37		41
		A (05)	60	55	58	60		58.25

11.19-11.24		A (06)	47	52	42	48		47.25
	7	B	50	60	57	43		52.5
		B (02)	48	56	51	51		51.5
		B (03)	52	52	43	45		48
		B (04)	47	47	53	48		48.75
		B (05)	58	58	49	53		54.5
		B (06)	45	58	50	49		50.5
	8	C	34	49	35	31		37.25
		C (02)	34	32	36	41		35.75
		C (03)	29	29	33	28		29.75
		C (04)	40	33	39	30		35.5
		C (05)	38	44	42	39		40.75

One Way Analysis of Variance – 5 DAYS Tuesday, August 03, 2010, 8:21:34 AM

Data source: Data 1 in Notebook1

Normality Test (Shapiro-Wilk) Passed (P = 0.303)

Equal Variance Test: Passed (P = 0.360)

Group Name	N	Missing	Mean	Std Dev	SEM
5 NONE	87	0	36.983	8.515	0.913
5 EDC	86	0	44.073	7.320	0.789
5 HEP	88	0	46.193	7.025	0.749
5 5FGF	86	0	47.116	7.099	0.765
5 10FGF	77	0	42.487	6.212	0.708
5 50FGF	63	0	44.825	7.226	0.910

Source of Variation	DF	SS	MS	F	P
Between Groups	5	5673.486	1134.697	21.374	<0.001
Residual	481	25534.702	53.087		
Total	486	31208.188			

The differences in the mean values among the treatment groups are greater than would be expected by chance; there is a statistically significant difference (P = <0.001).

All Pairwise Multiple Comparison Procedures (Holm-Sidak method):
Overall significance level = 0.05

Comparisons for factor:

Comparison	Diff of Means	t	Unadjusted P	Critical Level	Significant?
5 5FGF vs. 5 NONE	10.134	9.146	<0.001	0.003	Yes
5 HEP vs. 5 NONE	9.210	8.361	<0.001	0.004	Yes
5 50FGF vs. 5 NONE	7.843	6.507	<0.001	0.004	Yes
5 EDC vs. 5 NONE	7.090	6.399	<0.001	0.004	Yes
5 10FGF vs. 5 NONE	5.504	4.828	<0.001	0.005	Yes
5 5FGF vs. 5 10FGF	4.629	4.050	<0.001	0.005	Yes
5 HEP vs. 5 10FGF	3.706	3.260	0.001	0.006	Yes
5 5FGF vs. 5 EDC	3.044	2.739	0.006	0.006	Yes
5 HEP vs. 5 EDC	2.121	1.919	0.056	0.007	No
5 5FGF vs. 5 50FGF	2.291	1.896	0.059	0.009	No
5 50FGF vs. 5 10FGF	2.338	1.889	0.059	0.010	No

5 EDC vs. 5 10FGF	1.586	1.387	0.166	0.013	No
5 HEP vs. 5 50FGF	1.368	1.137	0.256	0.017	No
5 5FGF vs. 5 HEP	0.923	0.836	0.404	0.025	No
5 50FGF vs. 5 EDC	0.753	0.623	0.534	0.050	No

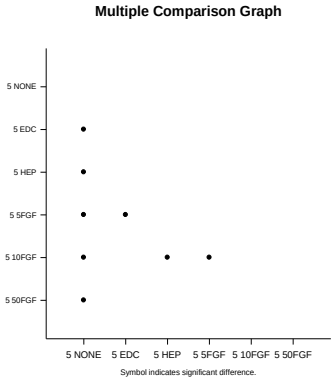

Appendix D.2: Cell Growth Data – 7 Days

NONE					EDC/NHS					EDC/NHS HEP				
Total N #		10			Total N #		9			Total N #		9		
		Average	S.D.	S.E.			Average	S.D.	S.E.			Average	S.D.	S.E.
10.5-10.12	Section	48.22093	7.885379	1.202509	10.5-10.12	Section	58.00862	6.653907	1.235599	10.5-10.12	Section	59.63393	11.98986	2.265871
			Section					Section					Section	
		Q1	43.375				Q1	52.5				Q1	53.625	
		Q3	53				Q3	62.5				Q3	67.4375	
		IQR	9.625				IQR	10				IQR	13.8125	
		LAV	28.9375				LAV	37.5				LAV	32.90625	
		UAV	67.4375				UAV	77.5				UAV	88.15625	
		Average	S.D.	S.E.			Average	S.D.	S.E.			Average	S.D.	S.E.
11.18-11.25	Section	49.7875	7.017963	1.569264	11.18-11.25	Section	44.0375	5.37861	1.202694	11.18-11.25	Section	54	7.010139	1.461715
			Section					Section					Section	
		Q1	45.9375				Q1	39.4375				Q1	48	
		Q3	51.125				Q3	46.8125				Q3	59.875	
		IQR	5.1875				IQR	7.375				IQR	11.875	
		LAV	38.15625				LAV	28.375				LAV	30.1875	
		UAV	58.90625				UAV	57.875				UAV	77.6875	
		Average	S.D.	S.E.			Average	S.D.	S.E.			Average	S.D.	S.E.
11.19-11.26	Section	44.09722	8.479274	1.998584	11.19-11.26	Section	46.52941	5.14469	1.247771	11.19-11.26	Section	46.55556	5.831302	1.374451
			Section					Section					Section	
		Q1	38.5625				Q1	52.5				Q1	42.9375	
		Q3	47.9375				Q3	62.5				Q3	48.4375	
		IQR	9.375				IQR	10				IQR	5.5	
		LAV	24.5				LAV	37.5				LAV	34.6875	
		UAV	62				UAV	77.5				UAV	56.6875	
		Average	S.D.	S.E.			Average	S.D.	S.E.			Average	S.D.	S.E.
All data	Section	47.69136	7.985952	0.887328	All data	Section	50.81818	8.721718	1.073569	All data	Section	54.3442	10.44507	1.257438
			Section					Section					Section	
		Q1	43.5				Q1	45.0625				Q1	46.75	
		Q3	52.5				Q3	57.25				Q3	61.5	
		IQR	9				IQR	12.1875				IQR	14.75	
		LAV	30				LAV	26.78125				LAV	24.625	
		UAV	66				UAV	75.53125				UAV	83.625	

5 ng/mL FGF2					10 ng/mL FGF2					50 ng/mL FGF2				
Total N #		9			Total N #		10			Total N #		9		
		Average	S.D.	S.E.			Average	S.D.	S.E.			Average	S.D.	S.E.
10.5-10.12	Section	61.625	10.47578	1.851874	10.5-10.12	Section	69.88793	11.71343	1.538048	10.5-10.12	Section	82.77273	10.90602	1.644145
			Section					Section					Section	
		Q1	54.625				Q1	61				Q1	75.75	
		Q3	69.1875				Q3	75.5				Q3	88.8125	
		IQR	14.5625				IQR	14.5				IQR	13.0625	
		LAV	32.78125				LAV	39.25				LAV	56.15625	
		UAV	91.03125				UAV	97.25				UAV	108.4063	
		Average	S.D.	S.E.			Average	S.D.	S.E.			Average	S.D.	S.E.
11.18-11.25	Section	53.1125	4.828285	1.079637	11.18-11.25	Section	52.82895	4.66745	1.070786	11.18-11.25	Section	69.8125	5.471743	1.223519
			Section					Section					Section	
		Q1	49.5625				Q1	50.125				Q1	66.3125	
		Q3	57.25				Q3	56.625				Q3	74.25	
		IQR	7.6875				IQR	6.5				IQR	7.9375	
		LAV	38.03125				LAV	40.375				LAV	54.40625	
		UAV	68.78125				UAV	66.375				UAV	86.15625	
		Average	S.D.	S.E.			Average	S.D.	S.E.			Average	S.D.	S.E.
11.19-11.26	Section	47.81944	5.419061	1.277285	11.19-11.26	Section	54.31944	11.67287	2.751322	11.19-11.26	Section	53.43056	6.155345	1.450829
			Section					Section					Section	
		Q1	45.125				Q1	44.4375				Q1	50.8125	
		Q3	49.6875				Q3	57.375				Q3	55.6875	
		IQR	4.5625				IQR	12.9375				IQR	4.875	
		LAV	38.28125				LAV	25.03125				LAV	43.5	
		UAV	56.53125				UAV	76.78125				UAV	63	
		Average	S.D.	S.E.			Average	S.D.	S.E.			Average	S.D.	S.E.
All data	Section	55.64286	9.868021	1.179454	All data	Section	63.52632	13.2795	1.362448	All data	Section	73.17073	14.75054	1.628925
			Section					Section					Section	
		Q1	48.5625				Q1	53.5				Q1	64.8125	
		Q3	60.6875				Q3	72.375				Q3	81.875	
		IQR	12.125				IQR	18.875				IQR	17.0625	
		LAV	30.375				LAV	25.1875				LAV	39.21875	
		UAV	78.875				UAV	100.6875				UAV	107.4688	

7 DAYS - NONE								
			Cell Number/ Region					
	N #	Image #	1	2	3	4		Average
10.5-10.12	1	A	58	48	44	43		48.25
		A (02)	50	60	63	41		53.5
		A (03)	57	46	45	62		52.5
		A (04)	61	57	50	62		57.5
		A (05)	43	47	45	40		43.75
		A (06)	50	57	35	45		46.75
		A (07)	49	49	38	45		45.25
		A (08)	59	54	52	48		53.25
		A (09)	43	60	56	45		51
		A (10)	63	52	54	58		56.75
		A (11)	39	43	46	43		42.75
		A (12)	64	59	47	32		50.5
		A (13)	44	47	47	73		52.75
		A (14)	60	48	56	69		58.25
	2	B	27	35	40	29		32.75
		B (02)	41	36	41	32		37.5
		B (03)	58	52	49	42		50.25
		B (04)	51	44	51	51		49.25
		B (05)	53	41	36	54		46
		B (06)	60	44	56	44		51
		B (07)	44	50	57	40		47.75
		B (08)	32	27	45	40		36
	3	C	50	48	44	28		42.5
		C (02)	45	49	33	52		44.75
		C (03)	75	60	52	50		59.25
		C (04)	43	49	46	42		45
		C (05)	52	41	66	55		53.5
		C (06)	93	66	45	44		62
		C (07)	77	72	55	48		63
		C (08)	48	59	40	56		50.75
		C (10)	66	55	66	34		55.25
		C 2	60	48	45	38		47.75
		C 2 (02)	68	47	52	38		51.25
		C 2 (03)	54	46	62	49		52.75
		C 2 (04)	81	60	49	48		59.5
		C 2 (05)	56	46	48	51		50.25
		C 2 (06)	38	27	56	51		43
		C 2 (07)	42	34	49	37		40.5
	4	D	42	40	31	28		35.25
		D (02)	31	27	29	19		26.5
		D (03)	56	38	35	37		41.5
		D (04)	42	47	36	39		41
		D (05)	44	33	45	58		45
	5	A	78	65	42	73		64.5
		A (02)	54	47	57	44		50.5
		A (03)	54	53	50	45		50.5
		A (04)	51	34	51	56		48
		A (05)	77	57	65	56		63.75
		A (06)	36	43	49	53		45.25
		A (07)	28	37	54	65		46
		B	44	33	27	33		34.25

11.18-11.25	6	B (02)	49	50	70	29		49.5
		B (03)	45	37	54	47		45.75
		B (04)	34	54	40	46		43.5
		B (05)	48	55	49	35		46.75
		B (06)	51	48	43	38		45
	7	C	56	56	64	66		60.5
		C (02)	30	54	61	51		49
		C (03)	62	59	47	49		54.25
		C (04)	57	52	32	48		47.25
		C (05)	59	53	44	56		53
		C (06)	48	49	55	50		50.5
		C (07)	56	45	46	45		48
11.19-11.26	8	A	31	35	27	30		30.75
		A (02)	54	50	46	41		47.75
		A (03)	36	45	45	57		45.75
		A (04)	35	31	32	31		32.25
		A (05)	35	34	34	31		33.5
		A (06)	49	35	39	41		41
	9	B	69	55	47	68		59.75
		B (02)	55	47	62	31		48.75
		B (03)	61	33	43	55		48
		B (04)	68	59	62	56		61.25
		B (05)	28	40	34	39		35.25
	10	C	47	59	29	43		44.5
		C (02)	51	52	47	26		44
		C (03)	48	45	48	48		47.25
		C (04)	71	48	35	52		51.5
		C (05)	32	38	39	42		37.75
		C (06)	47	44	38	39		42
		C (07)	44	47	41	39		42.75

7 DAYS - EDC/NHS								
			Cell Number/ Region					
	N #	Image #	1	2	3	4		Average
10.5-10.12	1	B	72	66	57	53		62
		B (02)	107	52	60	78		74.25
		B (03)	70	81	64	50		66.25
		B (04)	80	49	52	75		64
		B (05)	58	52	53	52		53.75
		B (06)	43	59	52	81		58.75
		B (07)	46	48	47	45		46.5
		B (08)	54	40	49	53		49
		B (09)	61	61	53	55		57.5
		B (10)	75	71	55	53		63.5
	2	C	70	54	43	63		57.5
		C (02)	56	48	54	49		51.75
		C (03)	43	58	50	54		51.25
		C (04)	74	51	45	47		54.25
		C (05)	60	50	44	48		50.5
		C (06)	66	54	65	70		63.75
		C (07)	63	65	73	49		62.5
	3	D	60	78	52	67		64.25
		D (02)	85	73	63	53		68.5
		D (03)	48	54	62	62		56.5
		D (04)	71	57	39	43		52.5
		D (05)	61	54	54	46		53.75
		D (06)	58	58	66	49		57.75
		D (07)	44	46	49	55		48.5
		D (08)	53	51	49	48		50.25
		D (09)	62	61	62	62		61.75
		D (10)	60	51	60	74		61.25
		D (11)	55	50	48	85		59.5
		D (12)	51	53	48	91		60.75
11.18-11.25	4	A	56	46	49	55		51.5
		A (02)	48	52	50	44		48.5
		A (03)	49	44	40	69		50.5
		A (04)	34	43	40	41		39.5
		A (05)	55	47	42	40		46
		A (06)	57	50	41	43		47.75
		A (07)	49	43	41	43		44
	5	B	47	40	46	47		45
		B (02)	38	33	42	44		39.25
		B (03)	37	39	39	36		37.75
		B (04)	42	38	32	40		38
		B (05)	50	47	44	40		45.25
		B (06)	43	45	45	44		44.25
		B (07)	40	39	35	44		39.5
	6	C	47	56	59	59		55.25
		C (02)	52	42	37	55		46.5
		C (03)	43	33	56	46		44.5
		C (04)	54	40	44	45		45.75
		C (05)	46	35	37	34		38
		C (06)	36	33	33	34		34

11.19-11.26	7	**A**	52	49	49	47		49.25
		A (02)	52	49	45	45		47.75
		A (03)	50	43	42	51		46.5
		A (04)	49	49	43	65		51.5
		A (05)	52	47	51	63		53.25
	8	**B**	60	48	44	45		49.25
		B (02)	60	47	50	49		51.5
		B (03)	52	45	46	61		51
		B (04)	44	44	36	37		40.25
		B (05)	44	33	44	41		40.5
		B (06)	42	41	32	42		39.25
	9	**C**	58	50	46	46		50
		C (02)	56	47	58	51		53
		C (03)	41	40	39	43		40.75
		C (04)	40	31	43	45		39.75
		C (05)	58	49	39	40		46.5
		C (06)	39	44	46	35		41

7 DAYS - HEP								
			Cell Number/ Region					
	N #	Image #	1	2	3	4		Average
10.5-10.12	1	A	79	87	47	75		72
		A (02)	67	89	56	64		69
		A (03)	50	49	39	45		45.75
		A (04)	38	32	32	29		32.75
		A (07)	50	35	39	44		42
		A (08)	43	67	72	40		55.5
		A (09)	83	68	49	58		64.5
		A (10)	74	74	65	118		82.75
		A (11)	76	80	72	80		77
		A (12)	76	77	72	78		75.75
		A 2 (02)	61	57	48	44		52.5
		A 2 (03)	43	41	42	43		42.25
	2	B	91	63	76	90		80
		B (02)	70	48	59	57		58.5
		B (03)	59	62	68	57		61.5
	3	C	48	49	45	45		46.75
		C (02)	55	52	77	57		60.25
		C (03)	59	49	46	62		54
		C (04)	93	72	51	59		68.75
		C (05)	65	58	51	47		55.25
		C (06)	41	59	60	78		59.5
		C (07)	45	54	78	63		60
		C (08)	49	37	82	55		55.75
		C (09)	55	59	62	58		58.5
		C (10)	69	66	70	63		67
		C (11)	61	70	56	60		61.75
		C (12)	75	59	57	57		62
		C (13)	55	50	47	42		48.5
11.18-11.25	4	A	72	74	72	46		66
		A (02)	49	56	55	92		63
		A (03)	61	55	49	54		54.75
		A (04)	54	48	66	70		59.5
		A (05)	50	45	45	56		49
		A (06)	43	56	46	47		48
		A (07)	64	54	52	53		55.75
		A (08)	59	51	49	47		51.5
	5	B	45	48	52	47		48
		B (02)	42	41	48	41		43
		B (03)	43	48	37	46		43.5
		B (04)	46	41	43	57		46.75
		B (05)	45	48	46	50		47.25
		B (06)	51	46	55	56		52
		B (07)	51	53	55	52		52.75
		B (08)	49	53	46	39		46.75
	6	C	64	59	52	47		55.5
		C (02)	65	58	57	71		62.75
		C (03)	44	54	69	66		58.25
		C (04)	63	70	64	51		62
		C (05)	61	59	58	63		60.25
		C (06)	55	48	50	50		50.75
		C (07)	67	58	59	76		65

11.19-11.26	7	**A**	41	41	42	47		42.75
		A (02)	36	42	47	42		41.75
		A (03)	46	37	37	38		39.5
		A (04)	42	44	51	29		41.5
		A (05)	44	43	51	45		45.75
		A (06)	48	46	36	44		43.5
	8	**B**	52	44	46	51		48.25
		B (02)	49	51	56	53		52.25
		B (03)	60	48	48	55		52.75
		B (04)	42	42	49	48		45.25
		B (05)	55	45	41	46		46.75
		B (06)	51	48	52	50		50.25
		B (07)	46	43	46	43		44.5
	9	**C**	47	51	47	49		48.5
		C (02)	69	66	60	57		63
		C (03)	51	44	47	48		47.5
		C (04)	54	40	48	46		47
		C (05)	35	28	44	42		37.25

7 DAYS - 5 NG/ML FGF2								
			Cell Number/ Region					
	N #	Image #	1	2	3	4		Average
10.5-10.12	1	A	84	79	48	72		70.75
		A (02)	70	67	67	56		65
		A (03)	60	65	62	57		61
		A (04)	60	59	59	52		57.5
		A (05)	52	52	58	48		52.5
		A (06)	54	44	38	32		42
		A (07)	43	53	58	54		52
		A (08)	87	33	48	53		55.25
		A (09)	50	50	54	52		51.5
		A (10)	48	42	51	42		45.75
	2	B	72	78	67	65		70.5
		B (02)	74	82	69	57		70.5
		B (03)	75	57	51	63		61.5
		B (04)	69	56	77	73		68.75
		B (05)	68	76	81	102		81.75
		B (06)	88	64	63	74		72.25
		B (07)	67	61	60	65		63.25
		B (08)	68	76	54	59		64.25
		B 2 (02)	72	61	103	58		73.5
		B 2 (03)	85	115	89	52		85.25
		B 2 (04)	74	85	105	61		81.25
	3	D	54	60	52	59		56.25
		D (02)	57	66	64	73		65
		D (03)	52	41	53	51		49.25
		D (04)	52	50	41	68		52.75
		D (05)	56	58	61	48		55.75
		D (06)	48	71	76	49		61
		D (07)	72	49	55	51		56.75
		D (08)	71	49	60	68		62
		D (09)	44	41	57	52		48.5
		D (10)	81	51	61	46		59.75
		D (11)	54	74	59	49		59
11.18-11.25	4	A	62	51	47	59		54.75
		A (02)	49	58	60	46		53.25
		A (03)	66	60	52	54		58
		A (04)	56	48	54	50		52
		A (05)	52	56	49	48		51.25
		A (06)	55	50	54	45		51
		A (07)	54	45	46	47		48
		A (08)	42	33	42	57		43.5
	5	B	40	46	52	51		47.25
		B (02)	53	42	52	46		48.25
		B (03)	44	45	54	48		47.75
		B (04)	54	54	53	39		50
		B (05)	64	58	58	49		57.25
	6	C	58	60	60	51		57.25
		C (02)	64	75	60	50		62.25
		C (03)	61	62	58	52		58.25
		C (04)	55	53	62	52		55.5
		C (05)	52	56	62	64		58.5
		C (06)	54	55	60	57		56.5

		C (07)	51	50	55	51		51.75
11.19-11.26	7	A	44	44	40	52		45
		A (02)	52	48	41	35		44
		A (03)	51	50	54	43		49.5
		A (04)	47	40	48	65		50
		A (05)	55	50	44	43		48
	8	B	56	55	46	50		51.75
		B (02)	39	49	47	53		47
		B (03)	51	47	46	54		49.5
		B (04)	65	63	58	45		57.75
		B (05)	66	69	52	51		59.5
		B (06)	52	47	47	42		47
	9	C	49	47	44	42		45.5
		C (02)	45	44	42	35		41.5
		C (03)	51	45	50	53		49.75
		C (04)	48	40	48	43		44.75
		C (05)	50	45	47	53		48.75
		C (06)	45	47	44	6		35.5
		C (07)	45	46	47	46		46

7 DAYS - 10 NG/ML FGF2

			Cell Number/ Region					
	N #	Image #	1	2	3	4		Average
10.5-10.12	1	A	48	43	36	40		41.75
		A (02)	65	76	69	58		67
		A (03)	107	88	91	68		88.5
		A (04)	100	96	100	77		93.25
		A (05)	69	65	47	59		60
		A (06)	63	52	52	61		57
		A (07)	45	40	56	52		48.25
		A (08)	60	47	56	52		53.75
		A (09)	49	55	64	48		54
		A (10)	42	41	43	53		44.75
		A (11)	80	68	62	62		68
		A (12)	56	45	60	79		60
	2	B	63	62	50	57		58
		B (02)	74	71	56	73		68.5
		B (03)	77	55	57	77		66.5
		B (04)	69	63	68	75		68.75
		B (05)	84	58	76	76		73.5
		B (06)	71	65	105	54		73.75
		B (07)	62	100	65	63		72.5
		B (08)	80	52	46	99		69.25
		B (09)	63	76	67	67		68.25
		B (10)	68	105	104	79		89
		B (11)	97	59	49	59		66
		B (12)	93	65	68	62		72
		B (13)	117	81	59	58		78.75
		B (14)	72	64	75	104		78.75
		B (15)	88	120	59	81		87
		B (16)	75	86	73	111		86.25
		B (17)	54	84	57	79		68.5
	3	C	74	75	62	63		68.5
		C (02)	65	73	73	70		70.25
		C (03)	89	81	120	56		86.5
		C (04)	68	79	70	75		73
		C (05)	110	112	100	82		101
		C (06)	65	84	91	97		84.25
		C (07)	85	63	67	65		70
		C (08)	77	72	85	70		76
		C (09)	66	75	70	62		68.25
		C (10)	67	61	58	57		60.75
		C (11)	78	70	89	66		75.75
		C (12)	49	70	80	48		61.75
	4	D	76	75	80	88		79.75
		D (02)	79	70	87	66		75.5
		D (03)	61	65	62	68		64
		D (04)	77	71	81	73		75.5
		D (05)	94	83	86	83		86.5
		D (06)	70	70	69	80		72.25
		D (07)	76	75	77	72		75
		D (08)	55	59	81	86		70.25
		D (09)	68	49	63	60		60

		D (10)	65	53	74	51		60.75
		D (11)	71	45	69	47		58
		D (12)	66	75	58	53		63
		D (13)	70	74	79	78		75.25
		D (14)	67	62	58	54		60.25
		D (15)	65	72	77	71		71.25
		D (16)	57	53	63	55		57
		D (17)	64	70	80	73		71.75
11.18-11.25	5	A	56	59	57	57		57.25
		A (02)	40	58	60	48		51.5
		A (03)	59	45	54	47		51.25
		A (04)	53	51	54	48		51.5
		A (05)	63	45	43	53		51
		A (06)	58	55	51	44		52
	6	B	49	58	52	54		53.25
		B (02)	60	54	59	70		60.75
		B (03)	57	58	54	55		56
		B (04)	54	48	54	84		60
		B (05)	60	42	48	47		49.25
		B (06)	50	56	52	38		49
		B (07)	49	52	58	63		55.5
	7	C	45	62	54	69		57.5
		C (02)	61	56	62	51		57.5
		C (03)	45	46	53	50		48.5
		C (04)	35	48	49	35		41.75
		C (05)	50	46	47	52		48.75
		C (06)	51	50	50	55		51.5
11.19-11.26	8	A	71	74	67	58		67.5
		A (02)	62	59	47	63		57.75
		A (03)	41	42	47	44		43.5
		A (04)	52	53	70	50		56.25
		A (05)	53	52	53	61		54.75
		A (06)	60	64	42	49		53.75
	9	B	40	50	39	40		42.25
		B (02)	49	46	45	53		48.25
		B (03)	47	45	38	33		40.75
		B (04)	49	47	44	49		47.25
		B (05)	43	44	41	43		42.75
		B (06)	47	48	32	44		42.75
	10	C	75	78	67	66		71.5
		C (02)	47	59	63	52		55.25
		C (03)	73	71	78	93		78.75
		C (04)	75	71	60	91		74.25
		C (05)	45	43	55	62		51.25
		C (06)	49	54	45	49		49.25

7 DAYS - 50 NG/ML FGF-2								
			Cell Number/ Region					
	N #	Image #	1	2	3	4		Average
10.5-10.12	1	A	90	84	98	111		95.75
		A (02)	76	83	85	92		84
		A (03)	84	85	84	73		81.5
		A (04)	87	81	82	72		80.5
		A (05)	94	84	78	83		84.75
		A (06)	83	74	67	73		74.25
		A (07)	93	80	85	101		89.75
		A (08)	86	76	71	79		78
		A (09)	86	89	83	107		91.25
		A (10)	70	75	68	87		75
		A (11)	82	73	77	73		76.25
		A (12)	94	81	78	79		83
		A (13)	84	80	127	84		93.75
		A (14)	92	90	82	76		85
		A (15)	77	84	96	77		83.5
	2	B	85	83	82	87		84.25
		B (02)	83	71	73	82		77.25
		B (03)	93	90	61	91		83.75
		B (04)	94	93	82	85		88.5
		B (05)	85	84	101	94		91
		B (06)	142	139	95	116		123
		B (07)	91	95	83	92		90.25
		B (08)	89	125	87	91		98
		B (09)	88	84	91	85		87
		B (10)	139	90	82	138		112.25
		B (11)	77	81	82	81		80.25
		B (12)	52	89	78	75		73.5
		B (13)	77	87	63	77		76
		B (14)	80	73	79	68		75
	3	D	73	73	61	68		68.75
		D (02)	70	70	82	64		71.5
		D (03)	67	71	96	70		76
		D (04)	80	79	77	79		78.75
		D (05)	75	65	82	63		71.25
		D (06)	79	68	72	70		72.25
		D (07)	92	83	60	71		76.5
		D (08)	68	87	84	65		76
		D 2	83	73	73	93		80.5
		D 2 (02)	73	64	66	84		71.75
		D 2 (03)	77	81	71	70		74.75
		D 2 (04)	100	102	72	89		90.75
		D 2 (05)	78	93	102	89		90.5
		D 2 (06)	67	99	87	75		82
		D 2 (07)	89	56	56	57		64.5
	4	A	74	74	70	72		72.5
		A (02)	65	70	68	94		74.25
		A (03)	67	74	67	70		69.5
		A (04)	72	70	65	72		69.75
		A (05)	61	60	78	64		65.75
		A (06)	72	76	65	71		71
		A (07)	92	81	76	69		79.5

11.18-11.25		A (08)	82	66	68	81		74.25
	5	B	75	90	56	48		67.25
		B (02)	73	66	67	60		66.5
		B (03)	70	71	68	54		65.75
		B (04)	65	52	65	57		59.75
	6	C	74	83	72	73		75.5
		C (02)	66	74	70	61		67.75
		C (03)	75	66	64	93		74.5
		C (04)	71	73	56	52		63
		C (05)	87	82	70	71		77.5
		C (06)	60	57	68	55		60
		C (07)	61	65	84	65		68.75
		C (08)	61	75	82	76		73.5
11.19-11.26	7	A	46	47	44	53		47.5
		A (02)	55	54	53	41		50.75
		A (03)	58	51	48	55		53
		A (04)	48	43	42	44		44.25
		A (05)	51	38	40	42		42.75
	8	B	70	69	79	66		71
		B (02)	65	52	48	58		55.75
		B (03)	54	70	60	50		58.5
		B (04)	44	48	47	65		51
		B (05)	49	50	56	49		51
		B (06)	50	53	52	67		55.5
		B (07)	50	51	52	48		50.25
	9	C	64	48	44	64		55
		C (02)	58	55	61	58		58
		C (03)	56	53	58	61		57
		C (04)	60	52	53	52		54.25
		C (05)	53	50	55	53		52.75
		C (06)	55	56	50	53		53.5

One Way Analysis of Variance – 7 DAYS Friday, August 27, 2010, 1:50:38 AM

Data source: Data 1 in all complete comparison

Normality Test (Shapiro-Wilk) Failed (P < 0.050)

Test execution ended by user request, ANOVA on Ranks begun

Kruskal-Wallis One Way Analysis of Variance on Ranks Friday, August 27, 2010, 1:50:38 AM

Data source: Data 1 in all complete comparison

Group	N	Missing	Median	25%	75%
7 NONE	81	0	47.750	43.250	52.625
7 EDC	66	0	50.375	44.875	57.500
7 HEP	69	0	52.750	46.750	61.625
7 5FGF	70	0	54.000	48.438	61.000
7 10FGF	95	0	60.750	53.250	72.500
7 50FGF	82	0	74.250	64.125	82.250

H = 160.922 with 5 degrees of freedom. (P = <0.001)

The differences in the median values among the treatment groups are greater than would be expected by chance; there is a statistically significant difference (P = <0.001)

To isolate the group or groups that differ from the others use a multiple comparison procedure.

All Pairwise Multiple Comparison Procedures (Dunn's Method) :

Comparison	Diff of Ranks	Q	P<0.05
7 50FGF vs 7 NONE	230.303	10.987	Yes
7 50FGF vs 7 EDC	195.916	8.854	Yes
7 50FGF vs 7 HEP	158.301	7.242	Yes
7 50FGF vs 7 5FGF	142.425	6.541	Yes
7 50FGF vs 7 10FGF	71.139	3.527	Yes
7 10FGF vs 7 NONE	159.164	7.866	Yes
7 10FGF vs 7 EDC	124.777	5.820	Yes
7 10FGF vs 7 HEP	87.162	4.118	Yes
7 10FGF vs 7 5FGF	71.286	3.382	Yes
7 5FGF vs 7 NONE	87.878	4.025	Yes
7 5FGF vs 7 EDC	53.492	2.330	No
7 5FGF vs 7 HEP	15.877	0.699	Do Not Test
7 HEP vs 7 NONE	72.002	3.285	Yes
7 HEP vs 7 EDC	37.615	1.633	Do Not Test
7 EDC vs 7 NONE	34.387	1.550	No

Note: The multiple comparisons on ranks do not include an adjustment for ties.

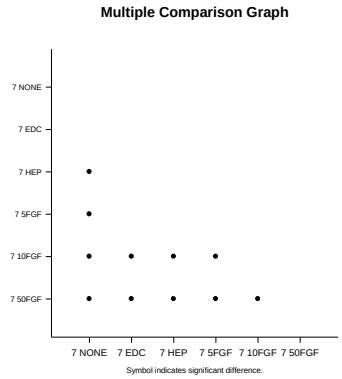

Appendix D.3: Cell Growth Comparison for Each Treatment

One Way Analysis of Variance - NONE Friday, August 27, 2010, 1:25:18 AM

Data source: Data 1 in all complete comparison

Normality Test (Shapiro-Wilk) Passed (P = 0.086)

Equal Variance Test: Passed (P = 0.666)

Group Name	N	Missing	Mean	Std Dev	SEM
1 NONE	131	0	34.929	7.885	0.689
5 NONE	87	0	36.983	8.515	0.913

7 NONE	81	0	47.691	7.986	0.887

Source of Variation	DF	SS	MS	F	P
Between Groups	2	8643.320	4321.660	65.873	<0.001
Residual	296	19419.292	65.606		
Total	298	28062.612			

The differences in the mean values among the treatment groups are greater than would be expected by chance; there is a statistically significant difference (P = <0.001).

All Pairwise Multiple Comparison Procedures (Holm-Sidak method):
Overall significance level = 0.05

Comparisons for factor:

Comparison	Diff of Means	t	Unadjusted P	Critical Level	Significant?
7 NONE vs. 1 NONE	12.762	11.147	<0.001	0.017	Yes
7 NONE vs. 5 NONE	10.709	8.563	<0.001	0.025	Yes
5 NONE vs. 1 NONE	2.053	1.833	0.068	0.050	No

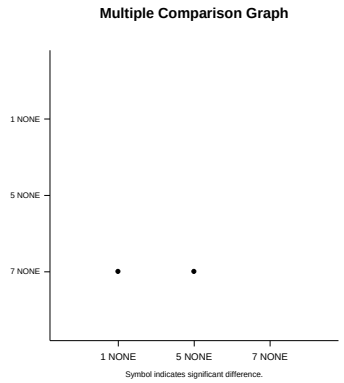

One Way Analysis of Variance – EDC/NHS Friday, August 27, 2010, 1:27:32 AM

Data source: Data 1 in all complete comparison

Normality Test (Shapiro-Wilk) Passed (P = 0.073)

Equal Variance Test: Passed (P = 0.161)

Group Name	N	Missing	Mean	Std Dev	SEM
1 EDC	89	0	41.643	7.170	0.760
5 EDC	86	0	44.073	7.320	0.789
7 EDC	66	0	50.818	8.722	1.074

Source of Variation	DF	SS	MS	F	P
Between Groups	2	3310.837	1655.419	28.096	<0.001
Residual	238	14023.037	58.920		
Total	240	17333.874			

The differences in the mean values among the treatment groups are greater than would be expected by chance; there is a statistically significant difference (P = <0.001).

All Pairwise Multiple Comparison Procedures (Holm-Sidak method):
Overall significance level = 0.05

Comparisons for factor:

Comparison	Diff of Means	t	Unadjusted P	Critical Level	Significant?
7 EDC vs. 1 EDC	9.175	7.358	<0.001	0.017	Yes
7 EDC vs. 5 EDC	6.746	5.370	<0.001	0.025	Yes
5 EDC vs. 1 EDC	2.429	2.093	0.037	0.050	Yes

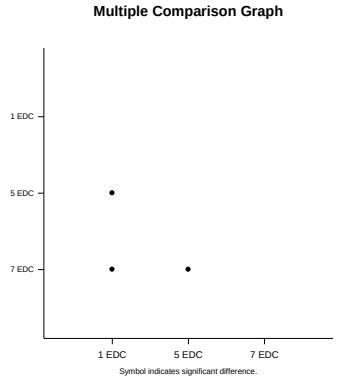

One Way Analysis of Variance - HEP Friday, August 27, 2010, 1:39:17 AM

Data source: Data 1 in all complete comparison

Normality Test (Shapiro-Wilk) Failed (P < 0.050)

Test execution ended by user request, ANOVA on Ranks begun

Kruskal-Wallis One Way Analysis of Variance on Ranks Friday, August 27, 2010, 1:39:17 AM

Data source: Data 1 in all complete comparison

Group	N	Missing	Median	25%	75%
1 HEP	89	0	44.750	39.250	51.375
5 HEP	88	0	46.250	42.563	50.688
7 HEP	69	0	52.750	46.750	61.625

H = 31.182 with 2 degrees of freedom. (P = <0.001)

The differences in the median values among the treatment groups are greater than would be expected by chance; there is a statistically significant difference (P = <0.001)

To isolate the group or groups that differ from the others use a multiple comparison procedure.

All Pairwise Multiple Comparison Procedures (Dunn's Method) :

Comparison	Diff of Ranks	Q	P<0.05
7 HEP vs 1 HEP	58.408	5.117	Yes
7 HEP vs 5 HEP	54.043	4.723	Yes
5 HEP vs 1 HEP	4.364	0.408	No

Note: The multiple comparisons on ranks do not include an adjustment for ties.

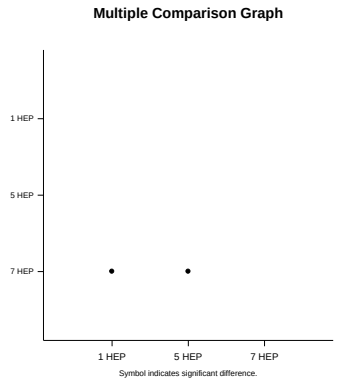

One Way Analysis of Variance – 5 NG/ML FGF2 Friday, August 27, 2010, 1:41:04 AM

Data source: Data 1 in all complete comparison

Normality Test (Shapiro-Wilk) Failed (P < 0.050)

Test execution ended by user request, ANOVA on Ranks begun

Kruskal-Wallis One Way Analysis of Variance on Ranks Friday, August 27, 2010, 1:41:04 AM

Data source: Data 1 in all complete comparison

Group	N	Missing	Median	25%	75%
1 5FGF	103	0	39.750	34.250	46.000
5 5FGF	86	0	48.125	42.000	51.875
7 5FGF	70	0	54.000	48.438	61.000

H = 95.291 with 2 degrees of freedom. (P = <0.001)

The differences in the median values among the treatment groups are greater than would be expected by chance; there is a statistically significant difference (P = <0.001)

To isolate the group or groups that differ from the others use a multiple comparison procedure.

All Pairwise Multiple Comparison Procedures (Dunn's Method) :

Comparison	Diff of Ranks	Q	P<0.05
7 5FGF vs 1 5FGF	112.371	9.684	Yes
7 5FGF vs 5 5FGF	54.804	4.545	Yes
5 5FGF vs 1 5FGF	57.567	5.261	Yes

Note: The multiple comparisons on ranks do not include an adjustment for ties.

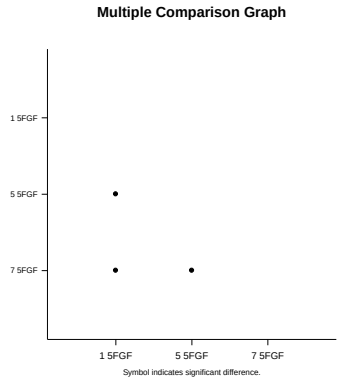

One Way Analysis of Variance – 10 NG/ML FGF2 Friday, August 27, 2010, 1:42:57 AM

Data source: Data 1 in all complete comparison

Normality Test (Shapiro-Wilk) Failed (P < 0.050)

Test execution ended by user request, ANOVA on Ranks begun

Kruskal-Wallis One Way Analysis of Variance on Ranks Friday, August 27, 2010, 1:42:57 AM

Data source: Data 1 in all complete comparison

Group	N	Missing	Median	25%	75%
1 10FGF	77	0	38.500	35.250	42.000
5 10FGF	77	0	42.000	37.875	46.375
7 10FGF	95	0	60.750	53.250	72.500

H = 148.620 with 2 degrees of freedom. (P = <0.001)

The differences in the median values among the treatment groups are greater than would be expected by chance; there is a statistically significant difference (P = <0.001)

To isolate the group or groups that differ from the others use a multiple comparison procedure.

All Pairwise Multiple Comparison Procedures (Dunn's Method) :

Comparison	Diff of Ranks	Q	P<0.05
7 10FGF vs 1 10FGF	126.448	11.449	Yes
7 10FGF vs 5 10FGF	97.941	8.868	Yes
5 10FGF vs 1 10FGF	28.506	2.456	Yes

Note: The multiple comparisons on ranks do not include an adjustment for ties.

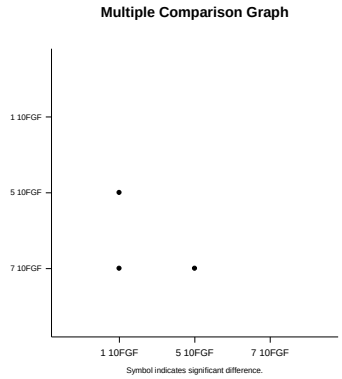

One Way Analysis of Variance – 50 NG/ML FGF2 Friday, August 27, 2010, 1:53:47 AM

Data source: Data 1 in all complete comparison

Normality Test (Shapiro-Wilk) Failed (P < 0.050)

Test execution ended by user request, ANOVA on Ranks begun

Kruskal-Wallis One Way Analysis of Variance on Ranks Friday, August 27, 2010, 1:53:47 AM

Data source: Data 1 in all complete comparison

Group	N	Missing	Median	25%	75%
1 50FGF	55	0	39.250	35.750	46.000
5 50FGF	63	0	43.000	40.000	50.000
7 50FGF	82	0	74.250	64.125	82.250

H = 131.530 with 2 degrees of freedom. (P = <0.001)

The differences in the median values among the treatment groups are greater than would be expected by chance; there is a statistically significant difference (P = <0.001)

To isolate the group or groups that differ from the others use a multiple comparison procedure.

All Pairwise Multiple Comparison Procedures (Dunn's Method) :

Comparison	Diff of Ranks	Q	P<0.05
7 50FGF vs 1 50FGF	105.103	10.419	Yes
7 50FGF vs 5 50FGF	84.415	8.705	Yes
5 50FGF vs 1 50FGF	20.688	1.937	No

Note: The multiple comparisons on ranks do not include an adjustment for ties.

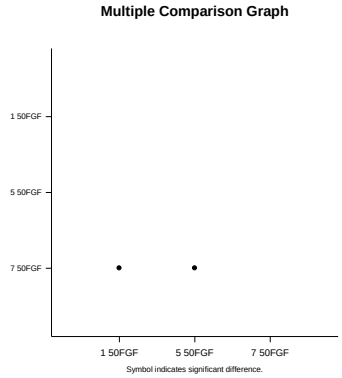

Appendix D.4: Summary of Cell Distribution Data – 5 Days

NONE											
[redacted]		Section / Distance									
		1	2	3	4	5	6	7	8	9	10	11
Scaffold		900	1800	2700	3600	4500	5400	6300	7200	8100	9000	9900
A				34.25	22.75	17.25	35	40	62	45		
									41.5			
	Average			34.25	22.75	17.25	35	40	51.75	45		
B					41	23.75	26.5	21.5				
	Average				41	23.75	26.5	21.5				
C			40.25	35.25	35.75	36.25	39.75	43.75	30.75	40	35.75	
							40.75	40.25	36			
									44			
	Average		40.25	35.25	35.75	36.25	40.25	42	36.91667	40	35.75	
D			50.25	35.5	31.5	22.75	40	39	38.25	37		
				38.75	26.5	13.75	42.75	41.25		39		
	Average		50.25	37.125	29	18.25	41.375	40.125	38.25	38		
Total Average			45.25	35.54167	32.125	23.875	35.78125	35.90625	42.30556	41	35.75	
Standard Deviation			7.071068	1.459523	7.949057	8.730932	6.782618	9.647633	8.206253	3.605551		

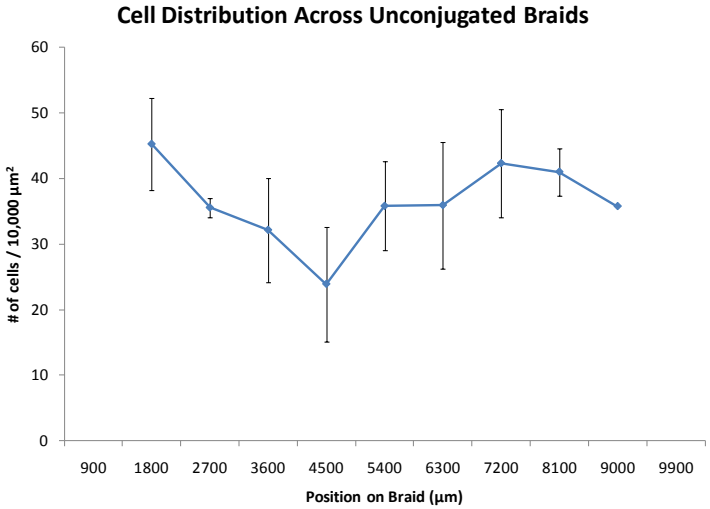

EDC/NHS												
		Section / Distance										
		1	2	3	4	5	6	7	8	9	10	11
Scaffold		900	1800	2700	3600	4500	5400	6300	7200	8100	9000	9900
A			64.5	57.75	61	51.25	43.5	42.75	40.25	49.25		
				53.75								
	Average		64.5	55.75	61	51.25	43.5	42.75	40.25	49.25		
B			53.75	45	38	30.25	41.25	47.25		52.75		
			52.25		40							
	Average		53	45	39	30.25	41.25	47.25		52.75		
C			35.75	45	47.5	42.25	47.25	53.5	46.75	63.5		
				44	49	43.25	40.75	48.75	55.75	39.5		
										42.75		
	Average		35.75	44.5	48.25	42.75	44	51.125	51.25	48.58333		
D				49.5	48.25	38.25	46.5	61.5	47.5	53.75		
					44.5	44	41.5	41.25	51.25	47.5		
	Average			49.5	46.375	41.125	44	51.375	49.375	50.625		
Total Average			51.08333	48.6875	48.65625	41.34375	43.1875	48.125	46.95833	50.30208		
Standard Deviation			14.47052	5.217658	9.146593	8.626132	1.312996	4.050463	5.884744	1.840068		

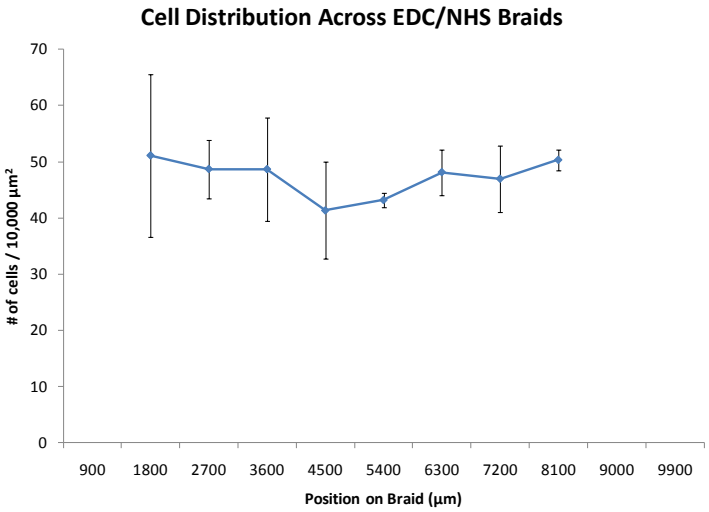

HEP												
		Section / Distance										
		1	2	3	4	5	6	7	8	9	10	11
Scaffold		900	1800	2700	3600	4500	5400	6300	7200	8100	9000	9900
A					44	35.5	47.5	39	42.75			
	Average				44	35.5	47.5	39	42.75			
C			38.5	44.5	42	49.5	45	33.75	48.25	51.5	43.75	46
					44	45	43.75	41		42.75		
					43.25							
	Average		38.5	44.5	43.08333	47.25	44.375	37.375	48.25	47.125	43.75	46
D			46.75	51	56.75	52.75	47	62.75	51.875	53.5	51.5	39.5
			49			59.25	43.5	47.25			49.5	
						40.5		49.75				
	Average		47.875	51	56.75	50.83333	45.25	53.25	51.875	53.5	50.5	39.5
Total Average			43.1875	47.75	47.94444	44.52778	45.70833	43.20833	47.625	50.3125	47.125	42.75
Standard Deviation			6.629126	4.596194	7.639596	8.020951	1.612129	8.734212	4.594494	4.507806	4.772971	4.596194

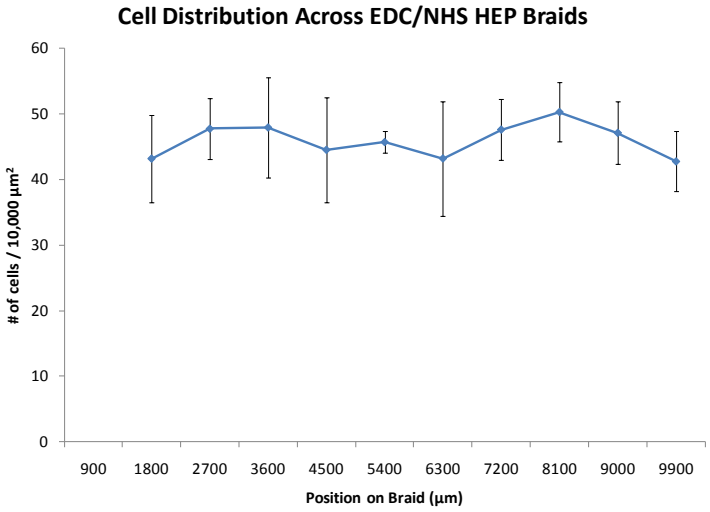

5 NG/ML FGF2												
		Section / Distance										
		1	2	3	4	5	6	7	8	9	10	11
Scaffold		900	1800	2700	3600	4500	5400	6300	7200	8100	9000	9900
A			35	40.5	37.25	39.5	48.5	47.75	44.75	43.25	48.5	49.75
							36.5	50.25	45.75			
								43				
	Average		35	40.5	37.25	39.5	42.5	47	45.25	43.25	48.5	49.75
B			36	51.75	52.25	39	32.5	49.25	44	50.25	35.5	
				65.5	51.25	46.5			45.75	38.75		
	Average		36	58.625	51.75	42.75	32.5	49.25	44.875	44.5	35.5	
D			40.5	57	50	54.5	51.25	38.75	48.25	47		
			46.5	55								
			32.5									
	Average		39.83333	56	50	54.5	51.25	38.75	48.25	47		
Total Average			36.94444	51.70833	46.33333	45.58333	42.08333	45	46.125	44.91667	42	49.75
Standard Deviation			2.551325	9.795035	7.914912	7.891187	9.381942	5.528336	1.849831	1.909407	9.192388	

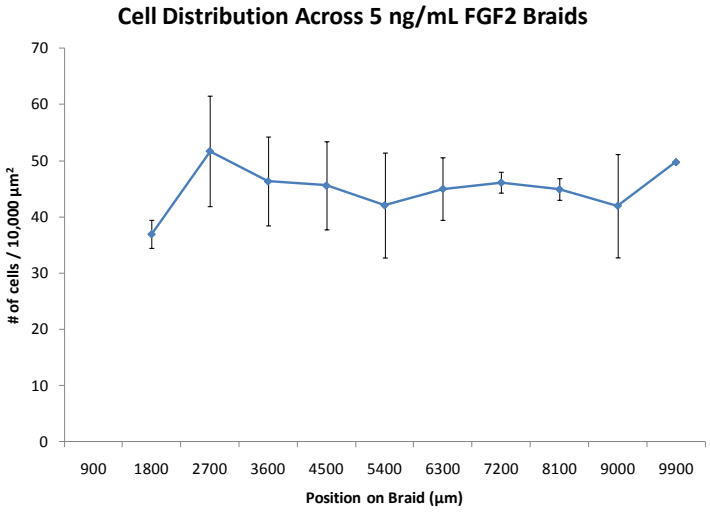

10 NG/ML FGF2												
		Section / Distance										
		1	2	3	4	5	6	7	8	9	10	11
Scaffold		900	1800	2700	3600	4500	5400	6300	7200	8100	9000	9900
A			49.25	37.25	40.25	29.75	45.5	33.5	29.75	32.5	44.25	42
						44.5				37.25		47
	Average		49.25	37.25	40.25	37.125	45.5	33.5	29.75	34.875	44.25	44.5
B					45	37.75	38.25	35.75	36.25			
						45	40.25		36.25			
	Average				45	41.375	39.25	35.75	36.25			
C			34.25	42.25	34.5	35	44	36.5	39.25	38.75		
						34.5			45.75			
	Average		34.25	42.25	34.5	34.75	44	36.5	42.5	38.75		
D				39.5	38.75	42.25	40.25	37.75	35.25			
	Average			39.5	38.75	42.25	40.25	37.75	35.25			
Total Average			41.75	39.66667	39.625	38.875	42.25	35.875	35.9375	36.8125	44.25	44.5
Standard Deviation			10.6066	2.504163	4.332532	3.545831	2.979094	1.785357	5.225638	2.740039		

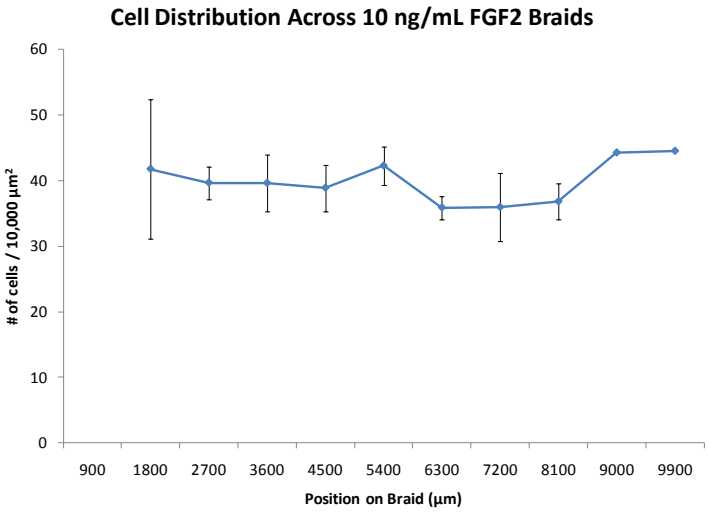

50 NG/ML FGF2												
		Section / Distance										
		1	2	3	4	5	6	7	8	9	10	11
Scaffold		900	1800	2700	3600	4500	5400	6300	7200	8100	9000	9900
B			53.5		36	40.75	41.5	39.75	33.25	39.25	42	
			48.25			42				46		
										39		
	Average		50.875		36	41.375	41.5	39.75	33.25	41.41667	42	
D			49.75	52.25	48.5	45.75	41.25	51.75	35	43	39.5	
						42.75	47.25	42.25				
	Average		49.75	52.25	48.5	44.25	44.25	47	35	43	39.5	
Total Average			50.3125	52.25	42.25	42.8125	42.875	43.375	34.125	42.20833	40.75	
Standard Deviation			0.795495		8.838835	2.032932	1.944544	5.126524	1.237437	1.119586	1.767767	

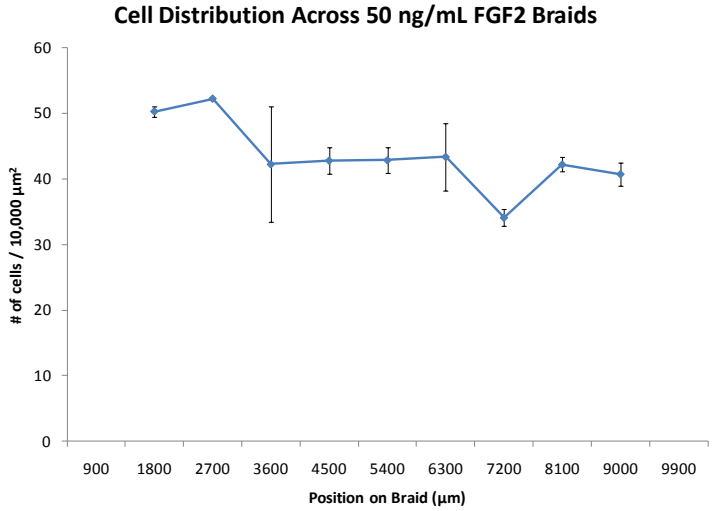

Appendix D.5: Summary of Cell Distribution Data – 7 Days

		NONE										
		Section / Distance										
		1	2	3	4	5	6	7	8	9	10	11
Scaffold		900	1800	2700	3600	4500	5400	6300	7200	8100	9000	9900
A			48.25	53.5	52.5	43.75	46.75	45.25	53.25	56.75	52.75	
					57.5				51	42.75	58.25	
										50.5		
	Average		48.25	53.5	55	43.75	46.75	45.25	52.125	50	55.5	
B				32.75	37.5	50.25	46	47.75	36			
						49.25	51					
	Average			32.75	37.5	49.75	48.5	47.75	36			
C				42.5	44.75	45	53.5	63	50.75	55.25		
					59.25		62					
	Average			42.5	52	45	57.75	63	50.75	55.25		
D					35.25	26.5	41.5	41	45			
	Average				35.25	26.5	41.5	41	45			
Total Average			48.25	42.91667	44.9375	41.25	48.625	49.25	45.96875	52.625	55.5	
Standard Deviation				10.38127	10.00495	10.16735	6.77157	9.580797	7.327442	3.712311		

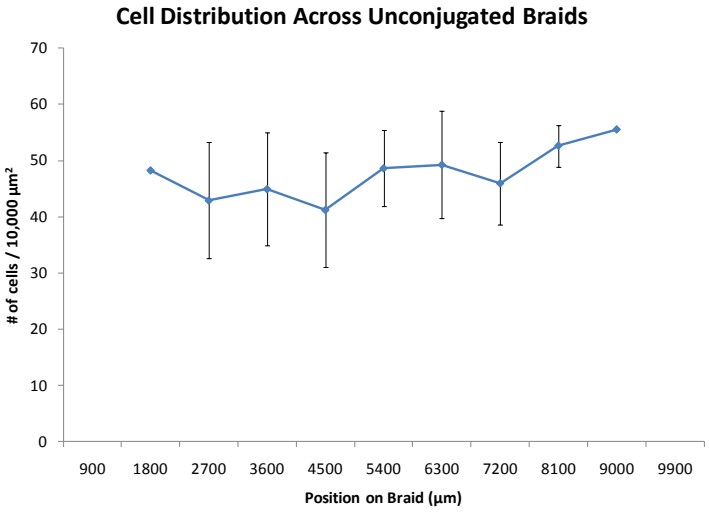

EDC/NHS											
		Section / Distance									
		1	2	3	4	5	6	7	8	9	10	11
Scaffold		900	1800	2700	3600	4500	5400	6300	7200	8100	9000	9900
B			62	74.25	66.25	64	53.75	58.75	46.5	49	57.5	63.5
	Average		62	74.25	66.25	64	53.75	58.75	46.5	49	57.5	63.5
C				57.5	51.75	51.25	54.25	50.5	63.75	62.5		
	Average			57.5	51.75	51.25	54.25	50.5	63.75	62.5		
D			64.25	68.5	52.5	57.75	50.25	61.25	59.5	60.75		
				56.5	53.75	48.5	61.75					
	Average		64.25	62.5	53.125	53.125	56	61.25	59.5	60.75		
Total Average			63.125	64.75	57.04167	56.125	54.66667	56.83333	56.58333	57.41667	57.5	63.5
Standard Deviation			1.59099	8.598692	8.004231	6.884085	1.181454	5.625463	8.98726	7.341378		

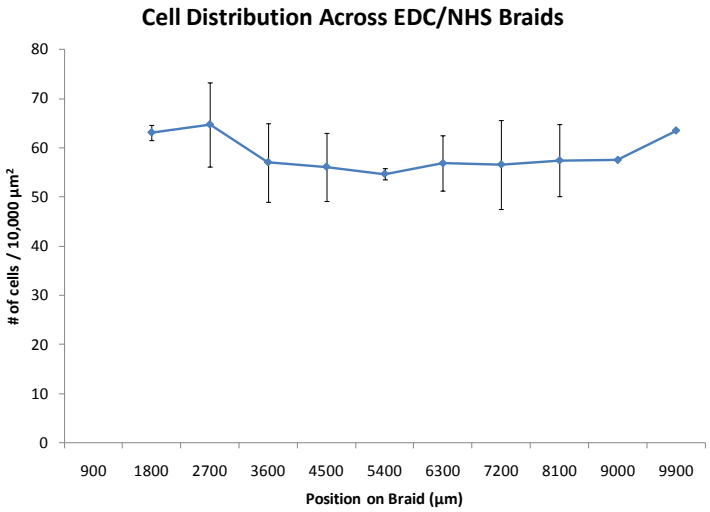

HEP											
		Section / Distance									
		1	2	3	4	5	6	7	8	9	10	11
Scaffold		900	1800	2700	3600	4500	5400	6300	7200	8100	9000	9900
A			72	69	45.75	32.75			42	55.5	82.75	
										64.5	77	
											75.75	
	Average		72	69	45.75	32.75			42	60	78.5	
B						80	58.5	61.5				
	Average					80	58.5	61.5				
C			46.75	60.25	68.75	59.5	60	58.5	67	61.75	62	48.5
				54	55.25		55.75					
	Average		46.75	57.125	62	59.5	57.875	58.5	67	61.75	62	48.5
Total Average			59.375	63.0625	53.875	57.41667	58.1875	60	54.5	60.875	70.25	48.5
Standard Deviation			17.85445	8.396893	11.49049	23.69379	0.441942	2.12132	17.67767	1.237437	11.66726	

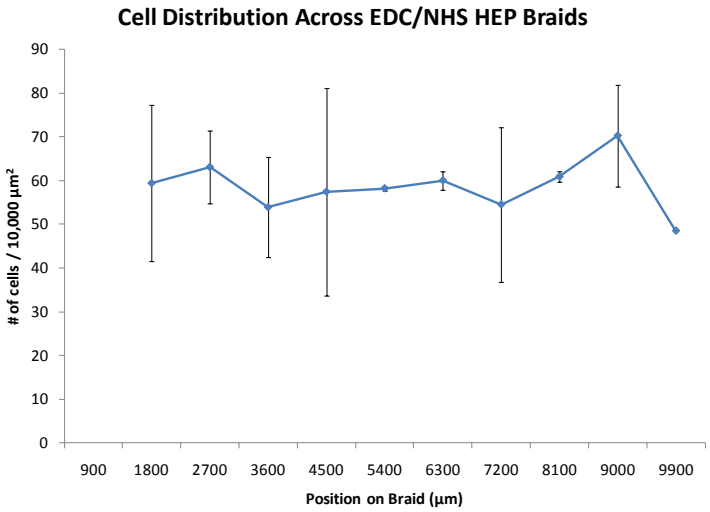

5 NG/ML FGF-2												
			Section / Distance									
		1	2	3	4	5	6	7	8	9	10	11
Scaffold		900	1800	2700	3600	4500	5400	6300	7200	8100	9000	9900
A			70.75	65	57.5	42	52	55.25	51.5	45.75		
				61	52.5							
	Average		70.75	63	55	42	52	55.25	51.5	45.75		
B				70.5	70.5	61.5	68.75	72.25	63.25	64.25		
							81.75					
	Average			70.5	70.5	61.5	75.25	72.25	63.25	64.25		
D			56.25	49.25	52.75	55.75	61	56.75	62	48.5	59.75	59
			65									
	Average		60.625	49.25	52.75	55.75	61	56.75	62	48.5	59.75	59
Total Average			65.6875	60.91667	59.41667	53.08333	62.75	61.41667	58.91667	52.83333	59.75	59
Standard Deviation			7.159456	10.7771	9.664152	10.01977	11.72337	9.411872	6.453358	9.982276		

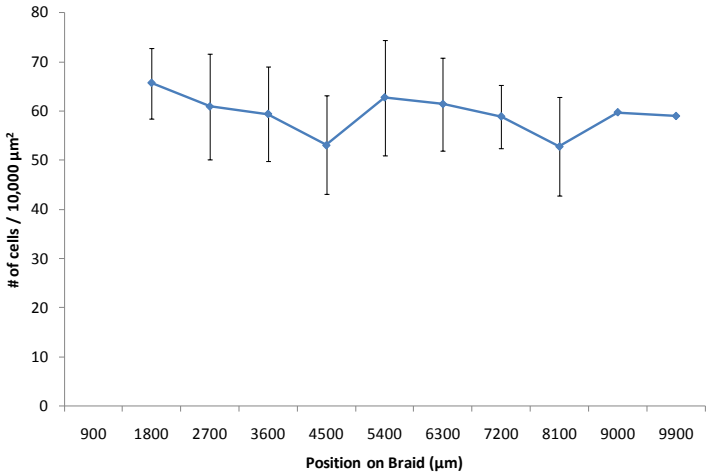

10 NG/ML FGF-2												
		Section / Distance										
		1	2	3	4	5	6	7	8	9	10	11
Scaffold		900	1800	2700	3600	4500	5400	6300	7200	8100	9000	9900
A			41.75	67	93.25	60	48.25	53.75	44.75	68	60	
				88.5		57		54				
	Average		41.75	77.75	93.25	58.5	48.25	53.875	44.75	68	60	
B		58	68.5	66.5	73.5	72.5	68.25	89	72	78.75	86.25	68.5
				68.75	73.75	69.25		66	78.75	87		
	Average	58	68.5	67.625	73.625	70.875	68.25	77.5	75.375	82.875	86.25	68.5
C				68.5	70.25	73	84.25	76	60.75	61.75		
					86.5	101	70	68.25	75.75			
	Average			68.5	78.375	87	77.125	72.125	68.25	61.75		
D		79.75	64	86.5	72.25	70.25	60	60.75	63	75.25	71.25	57
		75.5	75.5		75			58		60.25		71.75
	Average	77.625	69.75	86.5	73.625	70.25	60	59.375	63	67.75	71.25	64.375
Total Average		67.8125	60	75.09375	79.71875	71.65625	63.40625	65.71875	62.84375	70.09375	72.5	66.4375
Standard Deviation		13.87697	15.81732	8.877274	9.294586	11.7062	12.28794	10.95986	13.08521	8.997323	13.16957	2.916815

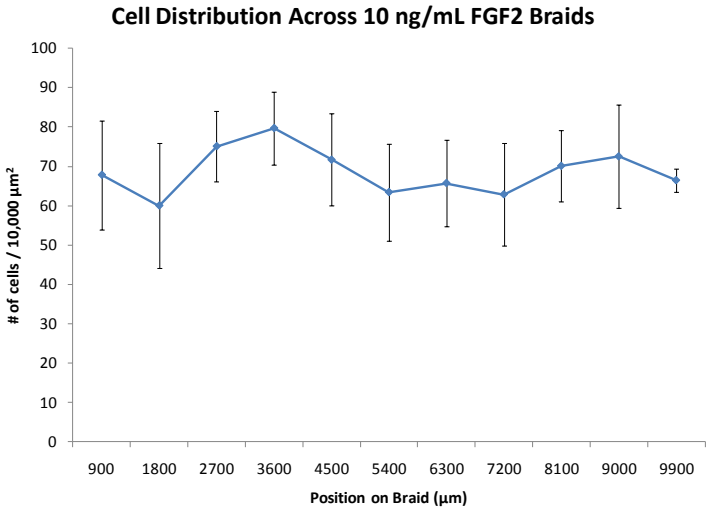

50 NG/ML FGF-2												
		Section / Distance										
		1	2	3	4	5	6	7	8	9	10	11
Scaffold		900	1800	2700	3600	4500	5400	6300	7200	8100	9000	9900
A			95.75	84	81.5	84.75	89.75	78	76.25	83	85	83.5
					80.5	74.25		91.25		93.75		
								75				
	Average		95.75	84	81	79.5	89.75	81.41667	76.25	88.375	85	83.5
B			84.25	83.75	88.5	123	98	112.25	73.5	75		
			77.25		91	90.25	87	80.25	76			
	Average		80.75	83.75	89.75	106.625	92.5	96.25	74.75	75		
D				80.5	71.75	74.75	90.75	90.5	82	64.5		
	Average			80.5	71.75	74.75	90.75	90.5	82	64.5		
Total Average			88.25	82.75	80.83333	86.95833	91	89.38889	77.66667	75.95833	85	83.5
Standard Deviation			10.6066	1.952562	9.001157	17.19663	1.391941	7.478828	3.826988	11.96632		

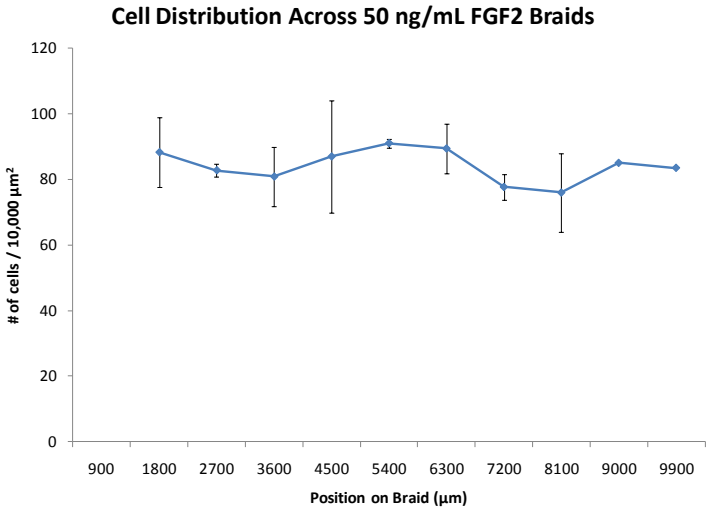

Appendix E: Total Cell Attachment Data

Appendix E.1: Surface Area Calculations

Braided Collagen Scaffold Histology Surface Area Measurements					
Image	Perimeter (cm)	Perimeter (μm)	Surface Area (7392 μm in seeded length) (μm^2)	Surface Area (mm^2)	amount of times 10,000 μm^2 fits in total area
NONE	0.154	1540	11383680	11.38368	1138.368
NONE	0.149	1490	11014080	11.01408	1101.408
NONE	0.224649	2246.49	16606054.08	16.60605408	1660.605408
NONE	0.138346	1383.46	10226536.32	10.22653632	1022.653632
EDC/NHS	0.177	1770	13083840	13.08384	1308.384
EDC/NHS	0.148	1480	10940160	10.94016	1094.016
EDC/NHS	0.111	1110	8205120	8.20512	820.512
EDC/NHS	0.108	1080	7983360	7.98336	798.336
HEP	0.158	1580	11679360	11.67936	1167.936
HEP	0.158	1580	11679360	11.67936	1167.936
HEP	0.119	1190	8796480	8.79648	879.648
5FGF	0.145	1450	10718400	10.7184	1071.84
5FGF	0.152	1520	11235840	11.23584	1123.584
5FGF	0.115	1150	8500800	8.5008	850.08
5FGF	0.114	1140	8426880	8.42688	842.688
10FGF	0.116	1160	8574720	8.57472	857.472
10FGF	0.108	1080	7983360	7.98336	798.336
10FGF	0.107	1070	7909440	7.90944	790.944
10FGF	0.112	1120	8279040	8.27904	827.904
50FGF	0.129	1290	9535680	9.53568	953.568
50FGF	0.13	1300	9609600	9.6096	960.96
50FGF	0.137	1370	10127040	10.12704	1012.704
50FGF	0.12	1200	8870400	8.8704	887.04
Average	0.136086739	1360.867391	10059531.76	10.05953176	1005.953176
S.D.	0.027841251	278.4125117	2058025.287	2.058025287	205.8025287

One Way Analysis of Variance – surface area Friday, August 27, 2010, 2:18:22 PM

Data source: Data 1 in perimeter

Normality Test (Shapiro-Wilk) Passed (P = 0.097)

Equal Variance Test: Passed (P = 0.130)

Group Name	N	Missing	Mean	Std Dev	SEM
none	4	0	1230.759	290.599	145.300
edc	4	0	1005.312	242.701	121.350
hep	3	0	1071.840	166.443	96.096
5fgf	4	0	972.048	146.665	73.332
10fgf	4	0	818.664	30.403	15.202
50fgf	4	0	953.568	51.568	25.784

Source of Variation	DF	SS	MS	F	P
Between Groups	5	371059.080	74211.816	2.250	0.096
Residual	17	560743.898	32984.935		
Total	22	931802.978			

The differences in the mean values among the treatment groups are not great enough to exclude the possibility that the difference is due to random sampling variability; there is not a statistically significant difference (P = 0.096).

Appendix E.2: Total Cell Attachment

NONE					EDC/NHS					EDC/NHS HEP				
Total N #		13			Total N #		13			Total N #		11		
		Average	S.D.	S.E.			Average	S.D.	S.E.			Average	S.D.	S.E.
9.17-9.18	total	31276.96809	7734.956268	1128.259	9.17-9.18	total	36355.72222	3881.124914	914.7899	9.17-9.18	total	44528.075	4508.190346	1008.062
			Section					Section					Section	
		Q1	25275.75				Q1	33763.875				Q1	42943.625	
		Q3	36216				Q3	39862.75				Q3	48602.375	
		IQR	10940.25				IQR	6098.875				IQR	5658.75	
		LAV	8865.375				LAV	24615.5625				LAV	34455.5	
		UAV	52626.375				UAV	49011.0625				UAV	57090.5	
		Average	S.D.	S.E.			Average	S.D.	S.E.			Average	S.D.	S.E.
10.5-10.6	total	36782.94068	8012.499393	1043.139	10.5-10.6	total	38872.08537	5430.900335	848.1641	10.5-10.6	total	42051.82653	5979.18431	854.1692
			Section					Section					Section	
		Q1	31437.5				Q1	35713				Q1	37976.5	
		Q3	41497.5				Q3	42252				Q3	46527.5	
		IQR	10060				IQR	6539				IQR	8551	
		LAV	16347.5				LAV	25904.5				LAV	25150	
		UAV	56587.5				UAV	52060.5				UAV	59354	
		Average	S.D.	S.E.			Average	S.D.	S.E.			Average	S.D.	S.E.
11.18-11.19	total	38429.2	5611.003086	1448.755	11.18-11.19	total	49444.9	4888.609951	1262.234	11.18-11.19	total	59530.05	3004.11226	949.9837
			Section					Section					Section	
		Q1	34832.75				Q1	45521.5				Q1	57342	
		Q3	42252				Q3	53066.5				Q3	62246.25	
		IQR	7419.25				IQR	7545				IQR	4904.25	
		LAV	23703.875				LAV	34204				LAV	49985.625	
		UAV	53380.875				UAV	64384				UAV	69602.625	
		Average	S.D.	S.E.			Average	S.D.	S.E.			Average	S.D.	S.E.
11.19-11.20	total	38655.55	3598.100884	1137.819	11.19-11.20	total	49243.7	3933.382813	1015.595	11.19-11.20	total	58197.1	5150.396882	1628.699
			Section					Section					Section	
		Q1	37033.375				Q1	47533.5				Q1	58348	
		Q3	39485.5				Q3	51809				Q3	60863	
		IQR	2452.125				IQR	4275.5				IQR	2515	
		LAV	33355.1875				LAV	41120.25				LAV	54575.5	
		UAV	43163.6875				UAV	58222.25				UAV	64635.5	
		Average	S.D.	S.E.			Average	S.D.	S.E.			Average	S.D.	S.E.
All data	total	35138.96565	7932.194732	693.0391	All data	total	41893.11798	7213.520428	764.6316	All data	total	46386.20787	8617.06239	913.4068
			Section					Section					Section	
		Q1	30557.25				Q1	35964.5				Q1	39737	
		Q3	39611.25				Q3	47785				Q3	51054.5	
		IQR	9054				IQR	11820.5				IQR	11317.5	
		LAV	16976.25				LAV	18233.75				LAV	22760.75	
		UAV	53192.25				UAV	65515.75				UAV	68030.75	

5 ng/mL FGF2					10 ng/mL FGF2				50 ng/mL FGF2			
Total N #		12			Total N #		8		Total N #		8	
		Average	S.D.	S.E.			Average	S.D.	S.E.		Average	S.D.	S.E.
9.17-9.18	total	36524.0875	6167.961985	975.2404	9.17-9.18	total	37138.16667	7116.108993	1677.283	total	37166.11111	5674.135059	1337.406
			Section					Section				Section	
		Q1	32192				Q1	31940.5			Q1	34644.125	
		Q3	40114.25				Q3	38605.25			Q3	40617.25	
		IQR	7922.25				IQR	6664.75			IQR	5973.125	
		LAV	20308.625				LAV	21943.375			LAV	25684.4375	
		UAV	51997.625				UAV	48602.375			UAV	49576.9375	
		Average	S.D.	S.E.			Average	S.D.	S.E.		Average	S.D.	S.E.
10.5-10.6	total	39356.82558	5037.291835	768.1798	10.5-10.6	total	38842.77778	3970.457068	540.3108	total	38250.86364	5713.988223	1218.226
			Section					Section				Section	
		Q1	38228				Q1	36278.875			Q1	33889.625	
		Q3	44515.5				Q3	40680.125			Q3	40491.5	
		IQR	6287.5				IQR	4401.25			IQR	6601.875	
		LAV	28796.75				LAV	29677			LAV	23986.8125	
		UAV	53946.75				UAV	47282			UAV	50394.3125	
		Average	S.D.	S.E.			Average	S.D.	S.E.		Average	S.D.	S.E.
11.18-11.19	total	51456.9	3625.634173	1146.526	11.18-11.19	total	53770.7	2847.619787	1273.494	total	#DIV/0!	#DIV/0!	#DIV/0!
			Section					Section				Section	
		Q1	49356.875				Q1	54324			Q1	#NUM!	
		Q3	54072.5				Q3	55330			Q3	#NUM!	
		IQR	4715.625				IQR	1006			IQR	#NUM!	
		LAV	42283.4375				LAV	52815			LAV	#NUM!	
		UAV	61145.9375				UAV	56839			UAV	#NUM!	
		Average	S.D.	S.E.			Average	S.D.	S.E.		Average	S.D.	S.E.
11.19-11.20	total	50476.05	3907.119033	1235.54	11.19-11.20	total	#DIV/0!	#DIV/0!	#DIV/0!	total	49310.76667	4386.563217	1132.606
			Section					Section				Section	
		Q1	47973.625				Q1	#NUM!			Q1	45898.75	
		Q3	52563.5				Q3	#NUM!			Q3	51557.5	
		IQR	4589.875				IQR	#NUM!			IQR	5658.75	
		LAV	41088.8125				LAV	#NUM!			LAV	37410.625	
		UAV	59448.3125				UAV	#NUM!			UAV	60045.625	
		Average	S.D.	S.E.			Average	S.D.	S.E.		Average	S.D.	S.E.
All data	total	40511.03398	7468.478912	735.8911	All data	total	39413.64286	6145.433187	700.3371	total	40912.19091	7414.718229	999.8004
			Section					Section				Section	
		Q1	34455.5				Q1	35713			Q1	36090.25	
		Q3	45773				Q3	42252			Q3	46150.25	
		IQR	11317.5				IQR	6539			IQR	10060	
		LAV	17479.25				LAV	25904.5			LAV	21000.25	
		UAV	62749.25				UAV	52060.5			UAV	61240.25	

One Way Analysis of Variance – total attachment Wednesday, August 25, 2010, 12:54:55 AM

Data source: Data 1 in 1 day total thesis

Normality Test (Shapiro-Wilk) Failed (P < 0.050)

Test execution ended by user request, ANOVA on Ranks begun

Kruskal-Wallis One Way Analysis of Variance on Ranks Wednesday, August 25, 2010, 12:54:55 AM

Data source: Data 1 in 1 day total thesis

Group	N	Missing	Median	25%	75%
none	131	0	35461.500	30431.500	39737.000
edc	89	0	41497.500	35838.750	47785.000
hep	89	0	45018.500	39485.500	51683.250
5fgf	103	0	39988.500	34455.500	46276.000
10fgf	77	0	38731.000	35461.500	42252.000
50fgf	55	0	39485.500	35964.500	46276.000

H = 89.874 with 5 degrees of freedom. (P = <0.001)

The differences in the median values among the treatment groups are greater than would be expected by chance; there is a statistically significant difference (P = <0.001)

To isolate the group or groups that differ from the others use a multiple comparison procedure.

All Pairwise Multiple Comparison Procedures (Dunn's Method) :

Comparison	Diff of Ranks	Q	P<0.05
hep vs none	196.566	9.104	Yes
hep vs 10fgf	123.959	5.067	Yes
hep vs 5fgf	101.302	4.453	Yes
hep vs 50fgf	90.933	3.373	Yes
hep vs edc	71.382	3.029	Yes
edc vs none	125.184	5.798	Yes
edc vs 10fgf	52.577	2.149	No
edc vs 5fgf	29.919	1.315	Do Not Test
edc vs 50fgf	19.551	0.725	Do Not Test
50fgf vs none	105.634	4.183	Yes
50fgf vs 10fgf	33.026	1.190	Do Not Test
50fgf vs 5fgf	10.369	0.395	Do Not Test
5fgf vs none	95.265	4.602	Yes
5fgf vs 10fgf	22.657	0.957	Do Not Test
10fgf vs none	72.608	3.217	Yes

Note: The multiple comparisons on ranks do not include an adjustment for ties.

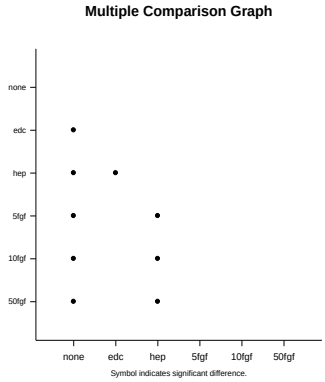

Appendix E.3: Attachment Percentage Data

NONE					EDC/NHS					EDC/NHS HEP				
Total N #		13			Total N #		13			Total N #		11		
		Average	S.D.	S.E.			Average	S.D.	S.E.			Average	S.D.	S.E.
9.17-9.18	Precent	20.85131206	5.156637512	0.752173	9.17-9.18	Percent	24.23714815	2.587416609	0.60986	9.17-9.18	Percent	29.68538333	3.00546023	0.672041
			Section					Section					Section	
		Q1	16.8505				Q1	22.50925				Q1	28.62908333	
		Q3	24.144				Q3	26.57516667				Q3	32.40158333	
		IQR	7.2935				IQR	4.065916667				IQR	3.7725	
		LAV	5.91025				LAV	16.410375				LAV	22.97033333	
		UAV	35.08425				UAV	32.67404167				UAV	38.06033333	
		Average	S.D.	S.E.			Average	S.D.	S.E.			Average	S.D.	S.E.
10.5-10.6	Precent	24.52196045	5.341666262	0.695426	10.5-10.6	Percent	25.91472358	3.620600223	0.565443	10.5-10.6	Percent	28.03455102	3.986122874	0.569446
			Section					Section					Section	
		Q1	20.95833333				Q1	23.80866667				Q1	25.31766667	
		Q3	27.665				Q3	28.168				Q3	31.01833333	
		IQR	6.706666667				IQR	4.359333333				IQR	5.700666667	
		LAV	10.89833333				LAV	17.26966667				LAV	16.76666667	
		UAV	37.725				UAV	34.707				UAV	39.56933333	
		Average	S.D.	S.E.			Average	S.D.	S.E.			Average	S.D.	S.E.
11.18-11.19	Precent	25.61946667	3.740668724	0.965837	11.18-11.19	Percent	32.96326667	3.259073301	0.841489	11.18-11.19	Percent	39.6867	2.002741507	0.633322
			Section					Section					Section	
		Q1	23.22183333				Q1	30.34766667				Q1	38.228	
		Q3	28.168				Q3	35.37766667				Q3	41.4975	
		IQR	4.946166667				IQR	5.03				IQR	3.2695	
		LAV	15.80258333				LAV	22.80266667				LAV	33.32375	
		UAV	35.58725				UAV	42.92266667				UAV	46.40175	
		Average	S.D.	S.E.			Average	S.D.	S.E.			Average	S.D.	S.E.
11.19-11.20	Precent	25.77036667	2.398733922	0.758546	11.19-11.20	Percent	32.82913333	2.622255208	0.677063	11.19-11.20	Percent	38.79806667	3.433597921	1.085799
			Section					Section					Section	
		Q1	24.68891667				Q1	31.689				Q1	38.89866667	
		Q3	26.32366667				Q3	34.53933333				Q3	40.57533333	
		IQR	1.63475				IQR	2.850333333				IQR	1.676666667	
		LAV	22.23679167				LAV	27.4135				LAV	36.38366667	
		UAV	28.77579167				UAV	38.81483333				UAV	43.09033333	
		Average	S.D.	S.E.			Average	S.D.	S.E.			Average	S.D.	S.E.
All data	Precent	23.4259771	5.288129822	0.462026	All data	Percent	27.92874532	4.809013618	0.509754	All data	Percent	30.92413858	5.74470826	0.608938
			Section					Section					Section	
		Q1	20.3715				Q1	23.97633333				Q1	26.49133333	
		Q3	26.4075				Q3	31.85666667				Q3	34.03633333	
		IQR	6.036				IQR	7.880333333				IQR	7.545	
		LAV	11.3175				LAV	12.15583333				LAV	15.17383333	
		UAV	35.4615				UAV	43.67716667				UAV	45.35383333	

5 ng/mL FGF2					10 ng/mL FGF2				50 ng/mL FGF2			
Total N #		12			Total N #	8			Total N #	8		
		Average	S.D.	S.E.		Average	S.D.	S.E.		Average	S.D.	S.E.
9.17-9.18	Percent	24.34939167	4.111974657	0.65016	9.17-9.18 Percent	24.75877778	4.744072662	1.118189	9.17-9.18 Percent	24.77740741	3.782756706	0.891604
			Section				Section				Section	
		Q1	21.46133333			Q1	21.29366667			Q1	23.09608333	
		Q3	26.74283333			Q3	25.73683333			Q3	27.07816667	
		IQR	5.2815			IQR	4.443166667			IQR	3.982083333	
		LAV	13.53908333			LAV	14.62891667			LAV	17.12295833	
		UAV	34.66508333			UAV	32.40158333			UAV	33.05129167	
		Average	S.D.	S.E.		Average	S.D.	S.E.		Average	S.D.	S.E.
10.5-10.6	Percent	26.23788372	3.358194557	0.51212	10.5-10.6 Percent	25.89518519	2.646971379	0.360207	10.5-10.6 Percent	25.50057576	3.809325482	0.812151
			Section				Section				Section	
		Q1	25.48533333			Q1	24.18591667			Q1	22.59308333	
		Q3	29.677			Q3	27.12008333			Q3	26.99433333	
		IQR	4.191666667			IQR	2.934166667			IQR	4.40125	
		LAV	19.19783333			LAV	19.78466667			LAV	15.99120833	
		UAV	35.9645			UAV	31.52133333			UAV	33.59620833	
		Average	S.D.	S.E.		Average	S.D.	S.E.		Average	S.D.	S.E.
11.18-11.19	Percent	34.3046	2.417089449	0.764351	11.18-11.19 Percent	35.84713333	1.898413191	0.848996	11.18-11.19 Percent	#DIV/0!	#DIV/0!	#DIV/0!
			Section				Section				Section	
		Q1	32.90458333			Q1	36.216			Q1	#NUM!	
		Q3	36.04833333			Q3	36.88666667			Q3	#NUM!	
		IQR	3.14375			IQR	0.670666667			IQR	#NUM!	
		LAV	28.18895833			LAV	35.21			LAV	#NUM!	
		UAV	40.76395833			UAV	37.89266667			UAV	#NUM!	
		Average	S.D.	S.E.		Average	S.D.	S.E.		Average	S.D.	S.E.
11.19-11.20	Percent	33.6507	2.604746022	0.823693	11.19-11.20 Percent	#DIV/0!	#DIV/0!	#DIV/0!	11.19-11.20 Percent	32.87384444	2.924375478	0.755071
			Section				Section				Section	
		Q1	31.98241667			Q1	#NUM!			Q1	30.59916667	
		Q3	35.04233333			Q3	#NUM!			Q3	34.37166667	
		IQR	3.059916667			IQR	#NUM!			IQR	3.7725	
		LAV	27.39254167			LAV	#NUM!			LAV	24.94041667	
		UAV	39.63220833			UAV	#NUM!			UAV	40.03041667	
		Average	S.D.	S.E.		Average	S.D.	S.E.		Average	S.D.	S.E.
All data	Percent	27.00735599	4.978985941	0.490594	All data Percent	26.2757619	4.096955458	0.466891	All data Percent	27.27479394	4.943145486	0.666534
			Section				Section				Section	
		Q1	22.97033333			Q1	23.80866667			Q1	24.06016667	
		Q3	30.51533333			Q3	28.168			Q3	30.76683333	
		IQR	7.545			IQR	4.359333333			IQR	6.706666667	
		LAV	11.65283333			LAV	17.26966667			LAV	14.00016667	
		UAV	41.83283333			UAV	34.707			UAV	40.82683333	

One Way Analysis of Variance - Percentage Wednesday, August 25, 2010, 12:59:23 AM

Data source: Data 1 in 1 day percent thesis

Normality Test (Shapiro-Wilk) Failed (P < 0.050)

Test execution ended by user request, ANOVA on Ranks begun

Kruskal-Wallis One Way Analysis of Variance on Ranks Wednesday, August 25, 2010, 12:59:23 AM

Data source: Data 1 in 1 day percent thesis

Group	N	Missing	Median	25%	75%
none	131	0	23.641	20.288	26.491
edc	89	0	27.665	23.892	31.857
hep	89	0	30.012	26.324	34.456
5fgf	103	0	26.659	22.970	30.851
10fgf	77	0	25.821	23.641	28.168
50fgf	55	0	26.324	23.976	30.851

H = 89.874 with 5 degrees of freedom. (P = <0.001)

The differences in the median values among the treatment groups are greater than would be expected by chance; there is a statistically significant difference (P = <0.001)

To isolate the group or groups that differ from the others use a multiple comparison procedure.

All Pairwise Multiple Comparison Procedures (Dunn's Method) :

Comparison	Diff of Ranks	Q	P<0.05
hep vs none	196.566	9.104	Yes
hep vs 10fgf	123.959	5.067	Yes
hep vs 5fgf	101.302	4.453	Yes
hep vs 50fgf	90.933	3.373	Yes
hep vs edc	71.382	3.029	Yes
edc vs none	125.184	5.798	Yes
edc vs 10fgf	52.577	2.149	No
edc vs 5fgf	29.919	1.315	Do Not Test
edc vs 50fgf	19.551	0.725	Do Not Test
50fgf vs none	105.634	4.183	Yes
50fgf vs 10fgf	33.026	1.190	Do Not Test
50fgf vs 5fgf	10.369	0.395	Do Not Test
5fgf vs none	95.265	4.602	Yes
5fgf vs 10fgf	22.657	0.957	Do Not Test
10fgf vs none	72.608	3.217	Yes

Note: The multiple comparisons on ranks do not include an adjustment for ties.

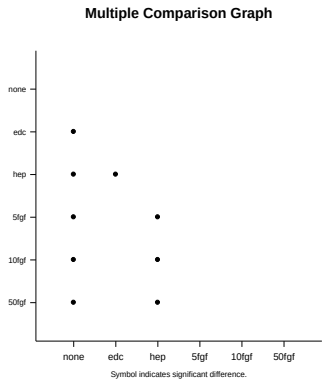

Appendix F: Total Cell Growth Data

Appendix F.1: Total Cell Growth – 5 Days

NONE					EDC/NHS					EDC/NHS HEP				
Total N #		10			Total N #		10			Total N #		9		
		Average	S.D.	S.E.			Average	S.D.	S.E.			Average	S.D.	S.E.
10.5-10.10	Section	36285.04	8959.767	1254.618	10.5-10.10	Section	47624.47	7321.429	1067.94	10.5-10.10	Section	44686.52	6933.272	980.5128
			Section					Section					Section	
		Q1	32569.25				Q1	42755				Q1	41308.88	
		Q3	41120.25				Q3	52060.5				Q3	48413.75	
		IQR	8551				IQR	9305.5				IQR	7104.875	
		LAV	19742.75				LAV	28796.75				LAV	30651.56	
		UAV	53946.75				UAV	66018.75				UAV	59071.06	
		Average	S.D.	S.E.			Average	S.D.	S.E.			Average	S.D.	S.E.
11.18-11.23	Section	39723.76	6840.242	1569.259	11.18-11.23	Section	42199.05	4256.207	976.4408	11.18-11.23	Section	49725.14	8292.693	1809.614
			Section					Section					Section	
		Q1	35210				Q1	37976.5				Q1	45018.5	
		Q3	44389.75				Q3	44892.75				Q3	53066.5	
		IQR	9179.75				IQR	6916.25				IQR	8048	
		LAV	21440.38				LAV	27602.13				LAV	32946.5	
		UAV	58159.38				UAV	55267.13				UAV	65138.5	
		Average	S.D.	S.E.			Average	S.D.	S.E.			Average	S.D.	S.E.
11.19-11.24	Section	37148.03	8979.802	2177.922	11.19-11.24	Section	38642.98	5495.13	1228.749	11.19-11.24	Section	47696.24	3595.374	872.0063
			Section					Section					Section	
		Q1	27916.5				Q1	35147.13				Q1	45270	
		Q3	44012.5				Q3	42377.75				Q3	49545.5	
		IQR	16096				IQR	7230.625				IQR	4275.5	
		LAV	3772.5				LAV	24301.19				LAV	38856.75	
		UAV	68156.5				UAV	53223.69				UAV	55958.75	
		Average	S.D.	S.E.			Average	S.D.	S.E.			Average	S.D.	S.E.
All data	Section	37204.66	8565.764	918.3463	All data	Section	44337.11	7363.499	794.0265	All data	Section	46470.34	7066.81	753.3244
			Section					Section					Section	
		Q1	32066.25				Q1	39862.75				Q1	42943.63	
		Q3	42755				Q3	47785				Q3	50865.88	
		IQR	10688.75				IQR	7922.25				IQR	7922.25	
		LAV	16033.13				LAV	27979.38				LAV	31060.25	
		UAV	58788.13				UAV	59668.38				UAV	62749.25	

5 ng/mL FGF2					10 ng/mL FGF2					50 ng/mL FGF2				
Total N #		9			Total N #		10			Total N #		8		
		Average	S.D.	S.E.			Average	S.D.	S.E.			Average	S.D.	S.E.
10.5-10.10	Section	44578.38	7209.801	1040.645	10.5-10.10	Section	40074.24	4934.024	743.8321	10.5-10.10	Section	42805.3	5230.416	954.939
			Section					Section					Section	
		Q1	38982.5				Q1	36467.5				Q1	39548.38	
		Q3	49671.25				Q3	44326.88				Q3	46213.13	
		IQR	10688.75				IQR	7859.375				IQR	6664.75	
		LAV	22949.38				LAV	24678.44				LAV	29551.25	
		UAV	65704.38				UAV	56115.94				UAV	56210.25	
11.18-11.23		Average	S.D.	S.E.	11.18-11.23		Average	S.D.	S.E.	11.18-11.23		Average	S.D.	S.E.
	Section	52206.11	5962.97	1367.999		Section	47829.38	6539.747	1586.122		Section	49781.28	8171.477	2042.869
			Section					Section					Section	
		Q1	49168.25				Q1	41749				Q1	43258	
		Q3	54952.75				Q3	52563.5				Q3	56839	
		IQR	5784.5				IQR	10814.5				IQR	13581	
		LAV	40491.5				LAV	25527.25				LAV	22886.5	
		UAV	63629.5				UAV	68785.25				UAV	77210.5	
11.19-11.24		Average	S.D.	S.E.	11.19-11.24		Average	S.D.	S.E.	11.19-11.24		Average	S.D.	S.E.
	Section	49717.58	4272.254	980.1224		Section	44672.69	5315.225	1328.806		Section	44722.62	7786.472	1888.497
			Section					Section					Section	
		Q1	47282				Q1	40554.38				Q1	40994.5	
		Q3	52186.25				Q3	47407.75				Q3	50803	
		IQR	4904.25				IQR	6853.375				IQR	9808.5	
		LAV	39925.63				LAV	30274.31				LAV	26281.75	
		UAV	59542.63				UAV	57687.81				UAV	65515.75	
All data		Average	S.D.	S.E.	All data		Average	S.D.	S.E.	All data		Average	S.D.	S.E.
	Section	47398.98	7141.235	770.0592		Section	42741.94	6248.848	712.1223		Section	45094.35	7269.069	915.8166
			Section					Section					Section	
		Q1	42503.5				Q1	38228				Q1	40240	
		Q3	51934.75				Q3	46527.5				Q3	50174.25	
		IQR	9431.25				IQR	8299.5				IQR	9934.25	
		LAV	28356.63				LAV	25778.75				LAV	25338.63	
		UAV	66081.63				UAV	58976.75				UAV	65075.63	

One Way Analysis of Variance – Total cells: 5 days Friday, August 27, 2010, 3:19:51 PM

Data source: Data 1 in Notebook2

Normality Test (Shapiro-Wilk) Passed (P = 0.303)

Equal Variance Test: Passed (P = 0.360)

Group Name	N	Missing	Mean	Std Dev	SEM
none 5	87	0	37204.655	8565.764	918.346
edc 5	86	0	44337.110	7363.499	794.027
hep 5	88	0	46470.341	7066.810	753.324
5 ng 5	86	0	47398.977	7141.235	770.059
10 ng 5	77	0	42741.935	6248.848	712.122
50 ng 5	63	0	45094.349	7269.069	915.817

Source of Variation	DF	SS	MS	F	P
Between Groups	5	5741772302.582	1148354460.516	21.374	<0.001
Residual	481	25842037591.575	53725649.879		
Total	486	31583809894.157			

The differences in the mean values among the treatment groups are greater than would be expected by chance; there is a statistically significant difference (P = <0.001).

All Pairwise Multiple Comparison Procedures (Holm-Sidak method):
Overall significance level = 0.05

Comparisons for factor:

Comparison	Diff of Means	t	Unadjusted P	Critical Level	Significant?
5 ng 5 vs. none 5	10194.322	9.146	<0.001	0.003	Yes
hep 5 vs. none 5	9265.686	8.361	<0.001	0.004	Yes
50 ng 5 vs. none 5	7889.694	6.507	<0.001	0.004	Yes
edc 5 vs. none 5	7132.455	6.399	<0.001	0.004	Yes
10 ng 5 vs. none 5	5537.280	4.828	<0.001	0.005	Yes
5 ng 5 vs. 10 ng 5	4657.042	4.050	<0.001	0.005	Yes
hep 5 vs. 10 ng 5	3728.406	3.260	0.001	0.006	Yes
5 ng 5 vs. edc 5	3061.866	2.739	0.006	0.006	Yes
hep 5 vs. edc 5	2133.230	1.919	0.056	0.007	No
5 ng 5 vs. 50 ng 5	2304.628	1.896	0.059	0.009	No
50 ng 5 vs. 10 ng 5	2352.414	1.889	0.059	0.010	No
edc 5 vs. 10 ng 5	1595.175	1.387	0.166	0.013	No
hep 5 vs. 50 ng 5	1375.992	1.137	0.256	0.017	No
5 ng 5 vs. hep 5	928.636	0.836	0.404	0.025	No
50 ng 5 vs. edc 5	757.239	0.623	0.534	0.050	No

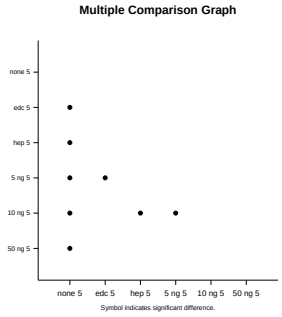

Appendix F.2: Increase over Attachment Data – 5 Days

NONE					EDC/NHS					EDC/NHS HEP				
Total N #		10			Total N #		10			Total N #		9		
		Average	S.D.	S.E.			Average	S.D.	S.E.			Average	S.D.	S.E.
10.5-10.10	Section	1.032615	0.254981	0.035704	10.5-10.10	Section	1.136809	0.174764	0.025492	10.5-10.10	Section	0.963358	0.149468	0.021138
			Section					Section					Section	
		Q1	0.92687				Q1	1.020573				Q1	0.890542	
		Q3	1.170218				Q3	1.242698				Q3	1.04371	
		IQR	0.243348				IQR	0.222125				IQR	0.153168	
		LAV	0.561848				LAV	0.687386				LAV	0.66079	
		UAV	1.53524				UAV	1.575885				UAV	1.273462	
		Average	S.D.	S.E.			Average	S.D.	S.E.			Average	S.D.	S.E.
11.18-11.23	Section	1.130476	0.194663	0.044659	11.18-11.23	Section	1.007303	0.101597	0.023308	11.18-11.23	Section	1.071981	0.178775	0.039012
			Section					Section					Section	
		Q1	1.002022				Q1	0.906509				Q1	0.970515	
		Q3	1.263263				Q3	1.071602				Q3	1.144015	
		IQR	0.261241				IQR	0.165093				IQR	0.1735	
		LAV	0.61016				LAV	0.65887				LAV	0.710265	
		UAV	1.655125				UAV	1.319241				UAV	1.404264	
		Average	S.D.	S.E.			Average	S.D.	S.E.			Average	S.D.	S.E.
11.19-11.24	Section	1.057175	0.255551	0.06198	11.19-11.24	Section	0.922418	0.13117	0.029331	11.19-11.24	Section	1.028242	0.07751	0.018799
			Section					Section					Section	
		Q1	0.79446				Q1	0.838971				Q1	0.975937	
		Q3	1.252527				Q3	1.011568				Q3	1.068108	
		IQR	0.458067				IQR	0.172597				IQR	0.092172	
		LAV	0.107359				LAV	0.580076				LAV	0.837679	
		UAV	1.939627				UAV	1.270464				UAV	1.206366	
		Average	S.D.	S.E.			Average	S.D.	S.E.			Average	S.D.	S.E.
Alldata	Section	1.058786	0.243768	0.026135	Alldata	Section	1.058339	0.175769	0.018954	Alldata	Section	1.001814	0.152347	0.01624
			Section					Section					Section	
		Q1	0.912555				Q1	0.951535				Q1	0.925784	
		Q3	1.21674				Q3	1.140641				Q3	1.096573	
		IQR	0.304185				IQR	0.189106				IQR	0.170789	
		LAV	0.456278				LAV	0.667875				LAV	0.669601	
		UAV	1.673018				UAV	1.4243				UAV	1.352757	

5 ng/mL FGF2					10 ng/mL FGF2					50 ng/mL FGF2				
Total N #		9			Total N #		10			Total N #		8		
		Average	S.D.	S.E.			Average	S.D.	S.E.			Average	S.D.	S.E.
10.5-10.10	Section	1.100401	0.177971	0.025688	10.5-10.10	Section	1.016761	0.125186	0.018872	10.5-10.10	Section	1.046272	0.127845	0.023341
			Section					Section					Section	
		Q1	0.962269				Q1	0.925251				Q1	0.966665	
		Q3	1.226117				Q3	1.124658				Q3	1.129569	
		IQR	0.263848				IQR	0.199407				IQR	0.162904	
		LAV	0.566497				LAV	0.626139				LAV	0.722309	
		UAV	1.621888				UAV	1.423769				UAV	1.373924	
11.18-11.23		Average	S.D.	S.E.	11.18-11.23		Average	S.D.	S.E.	11.18-11.23		Average	S.D.	S.E.
	Section	1.288689	0.147194	0.033769		Section	1.213524	0.165926	0.040243		Section	1.216784	0.199732	0.049933
			Section					Section					Section	
		Q1	1.2137				Q1	1.059253				Q1	1.057338	
		Q3	1.356488				Q3	1.333637				Q3	1.389293	
		IQR	0.142788				IQR	0.274385				IQR	0.331955	
		LAV	0.999518				LAV	0.647675				LAV	0.559405	
		UAV	1.570671				UAV	1.745214				UAV	1.887225	
11.19-11.24		Average	S.D.	S.E.	11.19-11.24		Average	S.D.	S.E.	11.19-11.24		Average	S.D.	S.E.
	Section	1.22726	0.105459	0.024194		Section	1.133432	0.134857	0.033714		Section	1.093137	0.190322	0.04616
			Section					Section					Section	
		Q1	1.167139				Q1	1.028943				Q1	1.002012	
		Q3	1.288198				Q3	1.202826				Q3	1.241757	
		IQR	0.12106				IQR	0.173883				IQR	0.239745	
		LAV	0.985549				LAV	0.768118				LAV	0.642394	
		UAV	1.469788				UAV	1.463651				UAV	1.601375	
All data		Average	S.D.	S.E.	All data		Average	S.D.	S.E.	All data		Average	S.D.	S.E.
	Section	1.170026	0.176279	0.019009		Section	1.084445	0.158545	0.018068		Section	1.102223	0.177675	0.022385
			Section					Section					Section	
		Q1	1.049183				Q1	0.969918				Q1	0.98357	
		Q3	1.28199				Q3	1.180492				Q3	1.226389	
		IQR	0.232807				IQR	0.210574				IQR	0.242819	
		LAV	0.699973				LAV	0.654057				LAV	0.619342	
		UAV	1.631201				UAV	1.496354				UAV	1.590617	

One Way Analysis of Variance – 5 DAYS: FOLD INCREASE Friday, August 27, 2010, 3:40:27 PM

Data source: Data 1 in Notebook3

Normality Test (Shapiro-Wilk) Passed (P = 0.168)

Equal Variance Test: Failed (P < 0.050)

Test execution ended by user request, ANOVA on Ranks begun

Kruskal-Wallis One Way Analysis of Variance on Ranks Friday, August 27, 2010, 3:40:27 PM

Data source: Data 1 in Notebook3

Group	N	Missing	Median	25%	75%
none 5	87	0	1.109	0.902	1.224
edc 5	86	0	1.039	0.944	1.145
hep 5	88	0	1.003	0.923	1.099
5 ng 5	86	0	1.195	1.043	1.288
10 ng 5	77	0	1.072	0.967	1.184
50 ng 5	63	0	1.057	0.984	1.229

H = 40.281 with 5 degrees of freedom. (P = <0.001)

The differences in the median values among the treatment groups are greater than would be expected by chance; there is a statistically significant difference (P = <0.001)

To isolate the group or groups that differ from the others use a multiple comparison procedure.

All Pairwise Multiple Comparison Procedures (Dunn's Method) :

Comparison	**Diff of Ranks**	**Q**	**P<0.05**
5 ng 5 vs hep 5	131.629	6.169	Yes
5 ng 5 vs edc 5	89.767	4.183	Yes
5 ng 5 vs none 5	71.088	3.322	Yes
5 ng 5 vs 10 ng 5	68.129	3.086	Yes
5 ng 5 vs 50 ng 5	58.484	2.506	No
50 ng 5 vs hep 5	73.145	3.149	Yes
50 ng 5 vs edc 5	31.283	1.340	No
50 ng 5 vs none 5	12.604	0.541	Do Not Test
50 ng 5 vs 10 ng 5	9.645	0.403	Do Not Test
10 ng 5 vs hep 5	63.500	2.892	No
10 ng 5 vs edc 5	21.638	0.980	Do Not Test
10 ng 5 vs none 5	2.959	0.134	Do Not Test
none 5 vs hep 5	60.541	2.845	Do Not Test
none 5 vs edc 5	18.679	0.873	Do Not Test
edc 5 vs hep 5	41.862	1.962	Do Not Test

Note: The multiple comparisons on ranks do not include an adjustment for ties.

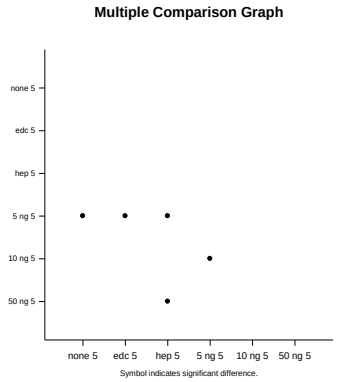

Appendix F.3: Total Cell Growth – 7 Days

NONE					EDC/NHS					EDC/NHS HEP				
Total N #		10			Total N #		9			Total N #		9		
		Average	S.D.	S.E.			Average	S.D.	S.E.			Average	S.D.	S.E.
10.5-10.12	Section	48510.26	7932.691	1209.724	10.5-10.12	Section	58356.67	6693.83	1243.013	10.5-10.12	Section	59991.73	12061.8	2279.467
			Section					Section					Section	
		Q1	43635.25				Q1	52815				Q1	53946.75	
		Q3	53318				Q3	62875				Q3	67842.13	
		IQR	9682.75				IQR	10060				IQR	13895.38	
		LAV	29111.13				LAV	37725				LAV	33103.69	
		UAV	67842.13				UAV	77965				UAV	88685.19	
11.18-11.25		Average	S.D.	S.E.	11.18-11.25		Average	S.D.	S.E.	11.18-11.25		Average	S.D.	S.E.
	Section	50086.23	7060.071	1578.68		Section	44301.73	5410.881	1209.91		Section	54324	7052.2	1470.485
			Section					Section					Section	
		Q1	46213.13				Q1	39674.13				Q1	48288	
		Q3	51431.75				Q3	47093.38				Q3	60234.25	
		IQR	5218.625				IQR	7419.25				IQR	11946.25	
		LAV	38385.19				LAV	28545.25				LAV	30368.63	
		UAV	59259.69				UAV	58222.25				UAV	78153.63	
11.19-11.26		Average	S.D.	S.E.	11.19-11.26		Average	S.D.	S.E.	11.19-11.26		Average	S.D.	S.E.
	Section	44361.81	8530.149	2010.575		Section	46808.59	5175.558	1255.257		Section	46834.89	5866.29	1382.698
			Section					Section					Section	
		Q1	38793.88				Q1	40994.5				Q1	43195.13	
		Q3	48225.13				Q3	51306				Q3	48728.13	
		IQR	9431.25				IQR	10311.5				IQR	5533	
		LAV	24647				LAV	25527.25				LAV	34895.63	
		UAV	62372				UAV	66773.25				UAV	57027.63	
Alldata		Average	S.D.	S.E.	Alldata		Average	S.D.	S.E.	Alldata		Average	S.D.	S.E.
	Section	47977.51	8033.867	892.6519		Section	51123.09	8774.048	1080.011		Section	54670.27	10507.74	1264.983
			Section					Section					Section	
		Q1	43761				Q1	45332.88				Q1	47030.5	
		Q3	52815				Q3	57593.5				Q3	61869	
		IQR	9054				IQR	12260.63				IQR	14838.5	
		LAV	30180				LAV	26941.94				LAV	24772.75	
		UAV	66396				UAV	75984.44				UAV	84126.75	

5 ng/mL FGF2					10 ng/mL FGF2					50 ng/mL FGF2				
Total N #		9			Total N #		10			Total N #		9		
		Average	S.D.	S.E.			Average	S.D.	S.E.			Average	S.D.	S.E.
10.5-10.12	Section	61994.75	10538.63	1862.985	10.5-10.12	Section	70307.26	11783.71	1547.276	10.5-10.12	Section	83269.36	10971.46	1654.01
			Section					Section					Section	
		Q1	54952.75				Q1	61366				Q1	76204.5	
		Q3	69602.63				Q3	75953				Q3	89345.38	
		IQR	14649.88				IQR	14587				IQR	13140.88	
		LAV	32977.94				LAV	39485.5				LAV	56493.19	
		UAV	91577.44				UAV	97833.5				UAV	109056.7	
11.18-11.25		Average	S.D.	S.E.	11.18-11.25		Average	S.D.	S.E.	11.18-11.25		Average	S.D.	S.E.
	Section	53431.18	4857.255	1086.115		Section	53145.92	4695.455	1077.211		Section	70231.38	5504.573	1230.86
			Section					Section					Section	
		Q1	49859.88				Q1	50425.75				Q1	66710.38	
		Q3	57593.5				Q3	56964.75				Q3	74695.5	
		IQR	7733.625				IQR	6539				IQR	7985.125	
		LAV	38259.44				LAV	40617.25				LAV	54732.69	
		UAV	69193.94				UAV	66773.25				UAV	86673.19	
11.19-11.26		Average	S.D.	S.E.	11.19-11.26		Average	S.D.	S.E.	11.19-11.26		Average	S.D.	S.E.
	Section	48106.36	5451.575	1284.949		Section	54645.36	11742.91	2767.83		Section	53751.14	6192.277	1459.534
			Section					Section					Section	
		Q1	45395.75				Q1	44704.13				Q1	51117.38	
		Q3	49985.63				Q3	57719.25				Q3	56021.63	
		IQR	4589.875				IQR	13015.13				IQR	4904.25	
		LAV	38510.94				LAV	25181.44				LAV	43761	
		UAV	56870.44				UAV	77241.94				UAV	63378	
All data		Average	S.D.	S.E.	All data		Average	S.D.	S.E.	All data		Average	S.D.	S.E.
	Section	55976.71	9927.23	1186.531		Section	63907.47	13359.17	1370.622		Section	73609.76	14839.05	1638.699
			Section					Section					Section	
		Q1	48853.88				Q1	53821				Q1	65201.38	
		Q3	61051.63				Q3	72809.25				Q3	82366.25	
		IQR	12197.75				IQR	18988.25				IQR	17164.88	
		LAV	30557.25				LAV	25338.63				LAV	39454.06	
		UAV	79348.25				UAV	101291.6				UAV	108113.6	

One Way Analysis of Variance – total cell growth: 7 days Friday, August 27, 2010, 4:03:39 PM

Data source: Data 1 in Notebook5

Normality Test (Shapiro-Wilk) Failed (P < 0.050)

Test execution ended by user request, ANOVA on Ranks begun

Kruskal-Wallis One Way Analysis of Variance on Ranks Friday, August 27, 2010, 4:03:39 PM

Data source: Data 1 in Notebook5

Group	N	Missing	Median	25%	75%
none 7	81	0	48036.500	43509.500	52940.750
edc 7	66	0	50677.250	45144.250	57845.000
hep 7	69	0	53066.500	47030.500	61994.750
5 ng 7	70	0	54324.000	48728.125	61366.000
10 ng 7	95	0	61114.500	53569.500	72935.000
50 ng 7	82	0	74695.500	64509.750	82743.500

H = 160.922 with 5 degrees of freedom. (P = <0.001)

The differences in the median values among the treatment groups are greater than would be expected by chance; there is a statistically significant difference (P = <0.001)

To isolate the group or groups that differ from the others use a multiple comparison procedure.

All Pairwise Multiple Comparison Procedures (Dunn's Method) :

Comparison	Diff of Ranks	Q	P<0.05
50 ng 7 vs none 7	230.303	10.987	Yes
50 ng 7 vs edc 7	195.916	8.854	Yes
50 ng 7 vs hep 7	158.301	7.242	Yes
50 ng 7 vs 5 ng 7	142.425	6.541	Yes
50 ng 7 vs 10 ng 7	71.139	3.527	Yes
10 ng 7 vs none 7	159.164	7.866	Yes
10 ng 7 vs edc 7	124.777	5.820	Yes
10 ng 7 vs hep 7	87.162	4.118	Yes
10 ng 7 vs 5 ng 7	71.286	3.382	Yes
5 ng 7 vs none 7	87.878	4.025	Yes
5 ng 7 vs edc 7	53.492	2.330	No
5 ng 7 vs hep 7	15.877	0.699	Do Not Test
hep 7 vs none 7	72.002	3.285	Yes
hep 7 vs edc 7	37.615	1.633	Do Not Test
edc 7 vs none 7	34.387	1.550	No

Note: The multiple comparisons on ranks do not include an adjustment for ties.

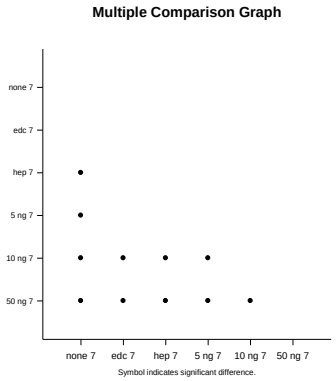

Appendix F.4: Increase over Attachment Data – 7 Days

NONE					EDC/NHS					EDC/NHS HEP				
Total N #		10			Total N #		9			Total N #		9		
		Average	S.D.	S.E.			Average	S.D.	S.E.			Average	S.D.	S.E.
10.5-10.12	Section	1.380526	0.225752	0.034427	10.5-10.12	Section	1.392989	0.159784	0.029671	10.5-10.12	Section	1.29331	0.26003	0.049141
			Section					Section					Section	
		Q1	1.241791				Q1	52815				Q1	1.162991	
		Q3	1.517347				Q3	62875				Q3	1.462549	
		IQR	0.275556				IQR	10060				IQR	0.299558	
		LAV	0.828457				LAV	37725				LAV	0.713654	
		UAV	1.930681				UAV	77965				UAV	1.911887	
		Average	S.D.	S.E.			Average	S.D.	S.E.			Average	S.D.	S.E.
11.18-11.25	Section	1.425376	0.200919	0.044927	11.18-11.25	Section	1.057494	0.129159	0.028881	11.18-11.25	Section	1.171124	0.152032	0.031701
			Section					Section					Section	
		Q1	1.315153				Q1	0.947032				Q1	1.040999	
		Q3	1.463667				Q3	1.124132				Q3	1.298538	
		IQR	0.148514				IQR	0.177099				IQR	0.257539	
		LAV	1.092382				LAV	0.681383				LAV	0.654691	
		UAV	1.686438				UAV	1.389781				UAV	1.684846	
		Average	S.D.	S.E.			Average	S.D.	S.E.			Average	S.D.	S.E.
11.19-11.26	Section	1.262468	0.242755	0.057218	11.19-11.26	Section	1.117334	0.123542	0.029963	11.19-11.26	Section	1.009673	0.126466	0.029808
			Section					Section					Section	
		Q1	1.104013				Q1	0.97855				Q1	0.931206	
		Q3	1.372412				Q3	1.224688				Q3	1.050487	
		IQR	0.268399				IQR	0.246138				IQR	0.119281	
		LAV	0.701415				LAV	0.609342				LAV	0.752284	
		UAV	1.77501				UAV	1.593895				UAV	1.229409	
		Average	S.D.	S.E.			Average	S.D.	S.E.			Average	S.D.	S.E.
All data	Section	1.365365	0.228631	0.025403	All data	Section	1.220322	0.209439	0.02578	All data	Section	1.178589	0.226527	0.027271
			Section					Section					Section	
		Q1	1.24537				Q1	1.082108				Q1	1.01389	
		Q3	1.503032				Q3	1.374772				Q3	1.33378	
		IQR	0.257663				IQR	0.292664				IQR	0.31989	
		LAV	0.858876				LAV	0.643111				LAV	0.534054	
		UAV	1.889526				UAV	1.813769				UAV	1.813616	

5 ng/mL FGF2					10 ng/mL FGF2					50 ng/mL FGF2				
Total N #		9			Total N #		10			Total N #		9		
		Average	S.D.	S.E.			Average	S.D.	S.E.			Average	S.D.	S.E.
10.5-10.12	Section	1.530318	0.260142	0.045987	10.5-10.12	Section	1.783831	0.298975	0.039257	10.5-10.12	Section	2.035319	0.268171	0.040428
			Section					Section					Section	
		Q1	1.356488				Q1	1.556974				Q1	1.862636	
		Q3	1.718115				Q3	1.927074				Q3	2.183833	
		IQR	0.361627				IQR	0.3701				IQR	0.321197	
		LAV	0.814048				LAV	1.001823				LAV	1.38084	
		UAV	2.260555				UAV	2.482224				UAV	2.665628	
11.18-11.25		Average	S.D.	S.E.	11.18-11.25		Average	S.D.	S.E.	11.18-11.25		Average	S.D.	S.E.
	Section	1.318929	0.1199	0.02681		Section	1.348414	0.119133	0.027331		Section	1.716637	0.134546	0.030085
			Section					Section					Section	
		Q1	1.230773				Q1	1.279398				Q1	1.630574	
		Q3	1.421674				Q3	1.445305				Q3	1.825752	
		IQR	0.190902				IQR	0.165907				IQR	0.195177	
		LAV	0.94442				LAV	1.030538				LAV	1.337809	
		UAV	1.708027				UAV	1.694166				UAV	2.118517	
11.19-11.26		Average	S.D.	S.E.	11.19-11.26		Average	S.D.	S.E.	11.19-11.26		Average	S.D.	S.E.
	Section	1.187488	0.13457	0.031718		Section	1.386458	0.29794	0.070225		Section	1.313817	0.151355	0.035675
			Section					Section					Section	
		Q1	1.120577				Q1	1.13423				Q1	1.249441	
		Q3	1.233877				Q3	1.464448				Q3	1.369314	
		IQR	0.113299				IQR	0.330219				IQR	0.119873	
		LAV	0.950628				LAV	0.638902				LAV	1.069632	
		UAV	1.403826				UAV	1.959777				UAV	1.549123	
All data		Average	S.D.	S.E.	All data		Average	S.D.	S.E.	All data		Average	S.D.	S.E.
	Section	1.381765	0.24505	0.029289		Section	1.621456	0.338948	0.034775		Section	1.799213	0.362705	0.040054
			Section					Section					Section	
		Q1	1.20594				Q1	1.365542				Q1	1.593691	
		Q3	1.507037				Q3	1.847311				Q3	2.013245	
		IQR	0.301097				IQR	0.481768				IQR	0.419554	
		LAV	0.754294				LAV	0.64289				LAV	0.96436	
		UAV	1.958682				UAV	2.569964				UAV	2.642576	

One Way Analysis of Variance – fold increase: 7 days Friday, August 27, 2010, 4:19:19 PM

Data source: Data 1 in Notebook6

Normality Test (Shapiro-Wilk) Failed (P < 0.050)

Test execution ended by user request, ANOVA on Ranks begun

Kruskal-Wallis One Way Analysis of Variance on Ranks Friday, August 27, 2010, 4:19:19 PM

Data source: Data 1 in Notebook6

Group	N	Missing	Median	25%	75%
none 7	81	0	1.367	1.238	1.507
edc 7	66	0	1.210	1.078	1.381
hep 7	69	0	1.144	1.014	1.336
5 ng 7	70	0	1.341	1.203	1.515
10 ng 7	95	0	1.551	1.359	1.851
50 ng 7	82	0	1.826	1.577	2.022

H = 171.189 with 5 degrees of freedom. (P = <0.001)

The differences in the median values among the treatment groups are greater than would be expected by chance; there is a statistically significant difference (P = <0.001)

To isolate the group or groups that differ from the others use a multiple comparison procedure.

All Pairwise Multiple Comparison Procedures (Dunn's Method) :

Comparison	Diff of Ranks	Q	P<0.05
50 ng 7 vs hep 7	230.010	10.523	Yes
50 ng 7 vs edc 7	211.237	9.547	Yes
50 ng 7 vs 5 ng 7	141.067	6.479	Yes
50 ng 7 vs none 7	140.444	6.700	Yes
50 ng 7 vs 10 ng 7	52.330	2.595	No
10 ng 7 vs hep 7	177.680	8.395	Yes
10 ng 7 vs edc 7	158.907	7.411	Yes
10 ng 7 vs 5 ng 7	88.738	4.210	Yes
10 ng 7 vs none 7	88.114	4.354	Yes
none 7 vs hep 7	89.566	4.086	Yes
none 7 vs edc 7	70.792	3.191	Yes
none 7 vs 5 ng 7	0.623	0.0285	No
5 ng 7 vs hep 7	88.943	3.918	Yes
5 ng 7 vs edc 7	70.169	3.057	Yes
edc 7 vs hep 7	18.773	0.815	No

Note: The multiple comparisons on ranks do not include an adjustment for ties.